PROTECTION AGAINST OXIDATIVE STRESS IN HEPATIC AND PANCREATIC CELLS BY SELECTED PLANT-DERIVED CHEMICALS

Amma Gyapomah Adomako-Bonsu, B.Pharm, MRes.

Thesis submitted to the University of Nottingham for the degree of Doctor of Philosophy

September 2016

Abstract

Persistent accumulation of free radicals in cells leads to oxidative stress, which plays a causative role in the induction and progression of various chronic diseases. Therapeutic focus has therefore shifted towards the use of antioxidants, with recent interest in those of plant origin. This study investigated radical scavenging and cytoprotective activities of phytochemicals (quercetin, curcumin, sulforaphane, rosmarinic acid, caffeic acid, danshensu (3,4-dihydroxyphenyllactic acid), ferulic acid and *m*-coumaric acid) against DPPH free radical in a non-cellular assay, and oxidative damage in hepatic (HepG2) and pancreatic (1.1B4) cells, elicited by an organic hydroperoxide (*tert*-butylhydroperoxide - *t*BHP) and a more physiologically relevant stressor (palmitate). Direct and indirect cytoprotective activities were assessed by neutral red viability assay after 5 h co-exposure and 20 h pre-exposure conditions, respectively.

Radical scavenging activities of three well-known phytochemicals - quercetin, curcumin and sulforaphane - were initially validated against DPPH (non-cellular assay), where quercetin was shown to be more potent than curcumin; sulforaphane was without effect. With quercetin as positive control, radical scavenging activities of rosmarinic acid and three of its principal metabolites (caffeic acid, danshensu and ferulic acid) were comparable, while *m*-coumaric acid lacked antiradical activity against DPPH radical.

Subsequently in HepG2 hepatoma cells, quercetin and curcumin were confirmed to possess direct and indirect cytoprotective acitivities against 0.5 mM *t*BHP while, sulforaphane only had indirect cytoprotective acitivities. Additionally, co-treatment of HepG2 cells with low concentrations of quercetin and curcumin (used together) exhibited direct cytoprotective activities against *t*BHP. However, direct cytoprotective potencies of rosmarinic acid and caffeic acid were less than quercetin. Similar pattern was observed for indirect cytoprotective activities; with danshensu, ferulic acid and *m*-coumaric acid lacking hepatoprotective activity in co-exposure and pre-exposure conditions. These results highlight the discrepancy between non-cellular and cellular antioxidant activities, which could be accounted to the poor lipophilicity profiles of rosmarinic acid and its principal metabolites.

Cytotoxicity assay in 1.1B4 human pancreatic β-cells revealed that these cells were more vulnerable to *t*BHP-induced oxidative damage than HepG2 cells. An investigation of selected phytochemicals in 1.1B4 cells produced novel findings, with quercetin exhibiting direct and indirect cytoprotective activities against *t*BHP (0.125 mM and 0.5 mM). Curcumin and caffeic acid were also cytoprotective against 0.125mM *t*BHP but only exhibited direct cytoprotection against 0.5mM *t*BHP. Sulforaphane lacked both direct and indirect cytoprotective activities in 1.1B4 cells, exhibiting marked cytotoxic effects in both conditions.

Further analysis in both HepG2 and 1.1B4 cells proved that indirect cytoprotective activities of selected phytochemicals were not dependent on pro-proliferative activities of quercetin, curcumin, caffeic acid and sulforaphane. Moreover, it was observed that high concentrations of curcumin and sulforaphane caused necrosis in both cell types, rather than apoptosis; caffeic acid also produced necrotic effect in 1.1B4 cells.

Whilst prolonged exposure of HepG2 and 1.1B4 cells to high glucose concentrations failed to elicit any evidence of glucotoxicity, sodium palmitate caused concentration-dependent cytotoxicity after short-term (5 h) and long-term (20 h) exposure to both cell types. Overall, selected phytochemicals caused additive cytotoxicity in the presence of palmitate, although quercetin demonstrated direct cytoprotection alone in HepG2 cells.

Using Western blot, curcumin, caffeic acid and sulforaphane did not upregulate NQO1, but 20 h exposure to 0.1 mM quercetin resulted in upregulation in HepG2 cells, amidst high basal levels of NQO1 in this cell type. However, both basal and inductive expression of NQO1 has not been observed in 1.1B4 cells.

Thus, although rosmarinic acid, danshensu, caffeic acid and ferulic acid may possess good intrinsic antioxidant properties, their physicochemical properties may limit pharmacological activities at the cellular level. Moreover, the additive cytotoxicity resulting from treatment with selected phytochemicals and sodium palmitate highlights a discrepancy between mechanisms of cytotoxicities by *t*BHP and palmitate.

List of publications

- **Abstracts**

1. ADOMAKO-BONSU, A., PRATTEN, M., FRY, J. & CHAN, S. 2014. Phytochemicals protect human pancreatic β-cells against oxidative damage. *Toxicology Letters***,** S135.
2. ADOMAKO-BONSU, A., PRATTEN, M., FRY, J. & CHAN, S. 2014. Hepatoprotection by curcumin and sulforaphane against tBHP-induced oxidative damage. *Planta Medica,* 80**,** P2Y20.
3. ADOMAKO-BONSU, A. G., FRY, J., CHAN, S., PRATTEN, M. & CLARKE, G. 2013. Protection against oxidative stress by rosmarinic acid and its major metabolites in hepatic cells. *Planta Med,* 79**,** PJ3.

- **Manuscript submitted**

ADOMAKO-BONSU, A[1]., PRATTEN M., CHAN S. L. F. & FRY J. 2016. Antioxidant activity of rosmarinic acid and its principal metabolites in chemical and cellular systems: importance of physico-chemical characteristics. *In Vitro* Toxicology.

Acknowledgement

Over the past four years, I have received enormous support from many people, without which my PhD program would not have been made possible.

I am immensely grateful to the University of Nottingham for the financial support I received to undertake this program, in the form of the Vice-Chancellor's Scholarship for Research Excellence (International). I also count it a privilege to have received financial assistance from the Schlumberger Foundation, and to be a fellow of the Faculty For The Future, a flagship program supported by the Schlumberger Foundation.

Without the guidance and patience of my supervisors, Dr Sue Chan, and Associate Professors Dr Jeffrey Fry and Dr Margaret Pratten, I would not have come this far in my PhD program. I must say that I have been overwhelmed by their dedication and mentorship. I am also very appreciative of their support and particularly thankful for their encouragement.

I am also very grateful to Dr Michael Garle, Mr Garry Clarke, Mr Liaque Latif and Mrs Monika Owen for their technical support with cell culture and Western blot experiments. Dr David Onion was also very helpful during the design and execution of flow cytometry experiments, and I am grateful to him. Also, proteomics studies would not have been possible without the kind support of Dr David Tooth and the University of Leicester Proteomics research team. I also appreciate my colleague PhD students at the School of Life Sciences for their contribution towards my research project.

A special thanks to my family for their immense support and love throughout my studies. To my parents for their prayers, encouragement and for believing that this great achievement, of successfully completing my studies, would be possible. Also to my best friend and loving husband Ernest, for his care and support during this program. I am also appreciative of the prayers and support from my church families and all my friends (both here in UK and in Ghana).

Abbreviations

.OH	-	Hydroxyl radical
8-OHdG	-	8-hydroxydeoxyguanosine
ABTS	-	2,2'-azino-bis(3-ethylbenzothiazoline-6-sulphonic acid)
ADP	-	Adenosine diphosphate
AGE	-	Advanced glycation end-product
AMPK/ACC	-	AMP-activated protein kinase /acetyl-CoA carboxylase
ARE	-	Antioxidant response element
ASK1	-	Apoptosis signal-regulating kinase 1
ATP	-	Adenosine triphosphate
Bax	-	Bcl-2–associated X protein
Bcl-2	-	B-cell lymphoma 2
BSA	-	Bovine serum albumin
BTB	-	Broad-Complex, Tramtrack, and Bric à brac dimerization domain
CA	-	Caffeic acid
CDK	-	Cyclin-dependent kinase
COMT	-	Cathechol-o-methyl transferases
COX	-	Cyclooxygenase enxzymes
Cul3	-	Cullin-3
CYP	-	Cytochrome P450
DMSO	-	Dimethylsulfoxide
DNA	-	Deoxyribonucleic acid
DPPH	-	2,2-diphenyl-1-picrylhydrazyl
DSU	-	Danshensu
EC_{50}	-	Effective concentration producing 50% response
EDTA	-	Ethylenediaminetetraacetic acid
ER	-	Endoplasmic reticulum
ERK	-	Extracellular-signal-regulated kinases
FA	-	Ferulic acid
FBS	-	Foetal bovine serum

FFA	-	Free fatty acid
FoxO1	-	Forkhead box other-1
FRAP	-	Ferric reducing ability of plasma
GCL	-	glutamate-cysteine ligase
GI	-	Gastrointestinal
GLUT	-	Glucose transporter
GP	-	Glutathione peroxidase
GR	-	Glutathione reductase
GSH	-	Glutathione (reduced form)
GSSG	-	Glutathione disulphide (oxidized form)
GST	-	Glutathione S-transferase
GSTP1	-	Glutathione S-transferase P 1
H_2O	-	Water molecule
HBSS	-	Hanks' Balanced Salt Solution
HepG2	-	Human hepatoma HepG2 cells
HLA	-	Human leukocyte antigen
HO-1	-	Haem oxygenase-1
$HO_2^{\cdot}$	-	Perhydroxyl radical
HPLC	-	High Performance Liquid Chromatography
IKBK	-	I kappa B kinase
IMAC	-	Immobilised metal ion affinity chromatography
IRS	-	Insulin receptor substrate
IVR	-	Intervening region
JNK	-	c-Jun N-terminal kinase
Keap-1	-	Kelch-like ECH-associated protein 1
LDL	-	Low-density lipoprotein
m-CoA	-	m-Coumaric acid
MCT	-	monocarboxylic acid transporter
MEM	-	Minimum essential medium
mRNA	-	messenger Ribonucleic acid

MRP	-	Multidrug resistance protein
MTT	-	3-(4,5-Dimethylthiazol-2-yl)-2,5-Diphenyltetrazolium Bromide
NADH	-	Nicotinamide adenine dinucleotide
NADP	-	Nicotinamide adenine dinucleotide phosphate,
NAFLD	-	Non-alcoholic fatty liver disease
NASH	-	Nonalcoholic steatohepatisis
NF-kappaβ	-	Nuclear factor-kappaβ
NO.	-	Nitric oxide
NQO1	-	Quinone reductase
Nrf2	-	Nuclear factor (erythroid-derived 2)-like 2
$O_2^{-\cdot}$	-	Superoxide anion
OATP	-	Organ anion transport polypeptides
OH	-	Hydroxyl group
ORAC	-	Oxygen radical absorbance capacity
OS	-	Oxidative stress
PDX-1	-	Pancreas duodenum homeobox-1
PI3K	-	Phosphatidylinositol 3-kinase
PKC	-	Protein kinase C
PPAR-α	-	Perixosome proliferation activator receptor–α
PVDF	-	Polyvinylidene fluoride
RA	-	Rosmarinic acid
RNA	-	Ribonucleic acid
RNS	-	Reactive nitrogen species
RO.	-	Alkoxyl radical
ROO.	-	Lipid-derived peroxyl radical
ROS	-	Reactive oxygen species
RP-SPE	-	Reversed-phase solid phase extraction
RSS	-	Reactive sulphur species
sMaf	-	small Maf

SULT	-	Sulfotransferase
T2DM	-	Type 2 diabetes mellitus
*t*BHP	-	*tert*-Butyl hydroperoxide
TC_{50}	-	Effective concentration producing 50% toxicity
TEAC	-	Trolox equivalent antioxidant capacity
ThR	-	thioredoxin reductase
TNF-α	-	Tumour necrosis factor-α
TRAIL	-	TNF-related apoptosis-inducing ligand
UCP-2	-	Uncoupling protein 2
UDPG	-	Uridine 5'-diphospho-glucuronosyltransferase

Table of contents

List of figures

List of Tables

CHAPTER 1

General introduction

CHAPTER 1 - General introduction

1.1 Cellular generation of reactive free radicals

Free radicals are highly reactive atoms, ions or molecules which bear unpaired electrons and are predominantly formed during various cellular metabolic activities; but can be induced by environmental factors such as radiation and heat. Free radicals can be classified as reactive oxygen species (ROS), reactive nitrogen species and reactive sulphur species. Reactive oxygen species include superoxide anion ($O_2^{\cdot-}$), perhydroxyl radical ($HO_2^{\cdot}$), hydroxyl radical (**.**OH), hydrogen peroxide (H_2O_2), singlet oxygen ($^1O_2$), hypochlorous acid (HOCl), lipid-derived peroxyl radical (ROO.), alkoxyl radical (RO.) and nitric oxide (NO.) (Singh, 2006; Lu et al., 2010).

During aerobic respiration, oxygen undergoes tetravalent reduction catalysed by cytochrome oxidase of complex IV (cytochrome c, oxidoreductase) in the electron transport chain, and this is vital for adenosine triphosphate (ATP) production (Cadenas and Davies, 2000) (Fig 1.1). In the electron transport chain, transfer of electrons between electron carriers is facilitated in the active mitochondrial respiratory state (state 3), when electron carriers are highly oxidized. Although the electron transport process is adequately efficient, it is associated with electron leakages and prone to ROS generation (Singh, 2006), (Fig 1.1). In the resting mitochondrial state (state 4), there is lack of adenine dinucleotide phosphate (ADP) and a decreased rate of respiration which could be due to the high reduction state of electron carriers (Cadenas and Davies, 2000). This also predisposes the electron transport process to univalent reduction of oxygen to generate $O_2^{\cdot-}$ and facilitates high ROS generation (Boveris and Chance, 1973; Boveris et al., 1999; Cadenas and Davies, 2000).

Monoamine oxidase located on the outer mitochondrial membrane also catalyses deamination of biogenic amines to produce H_2O_2, contributing to the amount of ROS in the mitochondrial matrix and cytosol. The mitochondria principally generate ROS from reactions involving NADH dehydrogenase (complex I) and ubiquinone-cytochrome C reductase (complex II) (Koek et al., 2011). In addition, $O_2^{\cdot-}$ and H_2O_2 are generated in

close proximity to redox-active atoms copper and iron, facilitating the Fenton reaction to form hydroxyl radical ($OH^{\cdot}$). This makes mitochondria and, hence, aerobic respiration major sources for cellular free radical generation, with an estimated 1 -2% of daily oxygen consumption forming $O_2^{\cdot-}$ (Cadenas and Davies, 2000). Cellular activities involving xanthine oxidase, cytochrome P450 and peroxisomes also make up common sources of endogenous ROS (Koek et al., 2011).

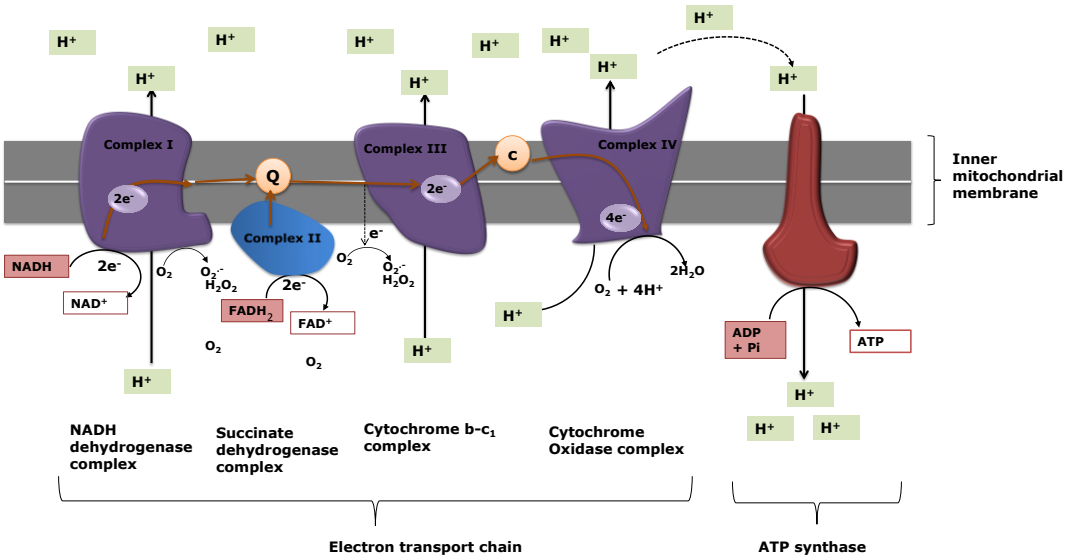

Figure 1.1 Pathway for electron transfer in mitochondrial electron transport chain. NADH generated by the tricyclic acid cycle donates electrons to the transport chain which are ferried individually from one complex to the other by ubiquinone (Q) and cytochrome c (Alberts et al., 2002). Succinate dehydrogenase complex also supplies ubiquinone (Q) with electrons from reduced flavin adenine dinucleotide ($FADH_2$). Electron transport by cytochrome oxidase complex commences when a total of four electrons have been received from cytochrome c. The electron transport chain, maintains proton gradient through proton pumping to power ATP synthesis from adenine dinucleotide phosphate (ADP) and phosphate (Pi). ROS are also generated during electron transport (Liu et al., 2002).

ROS are beneficial in mediating physiological responses, such as immune defences (Keisari et al., 1983; Lander et al., 1997; Droge, 2002), the cell proliferation cycle (Singh, 2006) and apoptosis (Slater et al., 1995; Dumont et al., 1999; Droge, 2002). $O_2^{\cdot-}$ and H_2O_2 also act as intracellular messengers during insulin signalling (Pi et al., 2007) and other cellular signalling cascades (Droge, 2002). However, ROS can react with cellular proteins, lipids, DNA and other macromolecules during redox imbalance leading to cell dysfunction, and ultimately cell death (Droge, 2002).

1.2 Oxidative stress and the cellular stress response mechanism

1.2.1 Oxidative stress

The presence of antioxidant enzymes: superoxide dismutase, catalase and glutathione peroxidase in the mitochondria, promotes redox homeostasis in aerobic organisms (Hauptmann et al., 1996). Superoxide anions are dismutated by the enzymatic activities of manganese superoxide dismutase to produce H_2O_2, which is readily neutralised by the peroxisome enzyme catalase to form water molecules, in a ferric-catalysed reaction (Fig 1.2). In addition to catalase, glutathione (GSH) is oxidized to glutathione disulphide (GSSG) as selenium-dependent glutathione peroxidase detoxifies H_2O_2 to form water. Subsequently, GSH levels are restored by glutathione reductase (GR) in a riboflavin-dependent process using reducing equivalent nicotinamide adenine dinucleotide phosphate (NADPH), as shown in Fig 1.2.

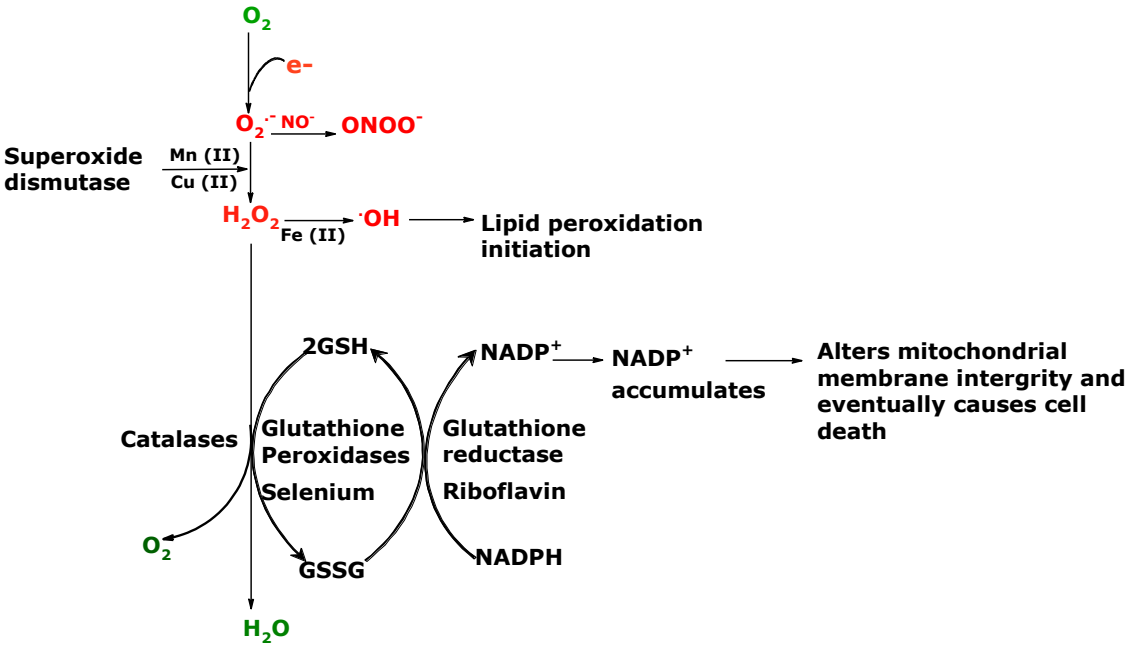

Figure 1.2 Schematic representation of ROS production and antioxidant activities which promote oxidative stress. Superoxide anions ($O_2^{\cdot-}$) are a primary source for generating other ROS when metabolised by superoxide dismutase to produce H_2O_2 (Singh, 2006).

During oxidative stress, cellular antioxidant defence is overwhelmed by persistent accumulation of ROS, leading to depletion of antioxidant enzymes and oxidative cell damage. Depletion of the cellular defence molecule GSH with the accumulation of GSSG levels indicate redox imbalance and this GSH/GSSG ratio is often used as a marker for oxidative stress (Koek et al., 2011). In response to oxidative stress, GSH levels are depleted, and the subsequent use of NADPH to restore the antioxidant system leads to a build-up of $NADP^+$ in the mitochondria (Fig 1.2). This disturbs respiratory activities of the electron transport chain as well as mitochondrial membrane integrity, resulting in calcium imbalance, cytochrome c release and activation of caspase signalling towards cell death (Alessio and Hagerman, 2006; Lima et al., 2006). In addition, hydrogen peroxide can undergo the Fenton reaction to produce the highly reactive hydroxide radicals ($^{\cdot}OH$), which attack lipid molecules to initiate and propagate lipid peroxidation (Singh, 2006), as shown in Fig 1.2.

Endogenous antioxidants such as superoxide dismutase, glutathione peroxidases and catalase are enzymatic in function, while GSH, thioredoxin, peroxiredoxin, metal-binding proteins and vitamins have non-enzymatic actions (Koek et al., 2011). In addition to endogenous antioxidants, exogenous antioxidant molecules usually obtained from diet may augment existing cellular defence mechanisms.

1.2.2 Redox homeostasis

Redox signalling triggers a cascade of antioxidant activities, where some cellular small molecules are utilized to reset other cellular antioxidants to their reduced state (see Fig 1.3). For example, vitamin C also restores GSH to its reduced state (Liu et al., 2002) in addition to its radical scavenging activities, and is referred to as a direct antioxidant. The terms direct and indirect antioxidants have been defined by the Food and Drinks Administration as radical scavenging agents and inducers of co-enzymes, respectively (Dinkova-Kostova and Talalay, 2008). Fig 1.3 shows the functional interplay between enzymatic and non-enzymatic antioxidants, as reviewed by Dinkova-Kostova and Talalay, (2008). Direct antioxidants (such as GSH, ubiquinol, ascorbate, tocopherols, lipoic acid, vitamin K) are redox-active low molecular weight compounds that are either modified or

used up during redox activities and need to be replenished, while indirect antioxidants are not always redox-active (Dinkova-Kostova and Talalay, 2008). In addition, a number of enzymes (the so-called "Phase II metabolising enzymes"), which play a key role in detoxification, catalyse regeneration of direct antioxidants leading to long-lasting antioxidant activities (Dinkova-Kostova and Talalay, 2008). For comprehensive reviews on cellular antioxidant systems, refer to Lui et al., (2002) and Dinkova-Kostova and Talalay, (2008).

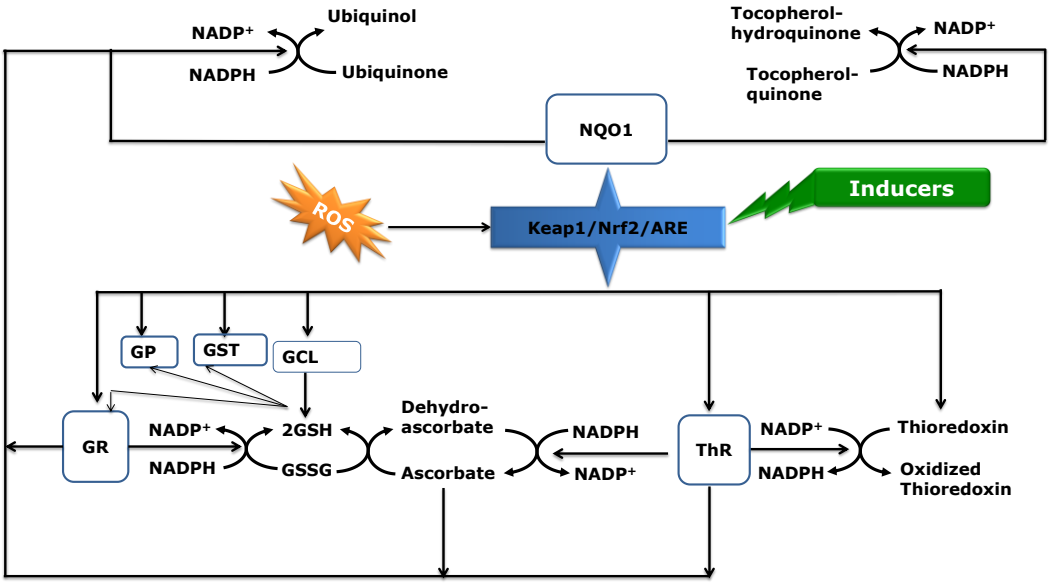

Figure 1.3 A schematic diagram showing the complex functional interplay between enzymatic and non-enzymatic antioxidant components of the cellular defence system. In this scheme, NADPH is used a cofactor to restore direct antioxidants GSH, ascorbate, thioredoxin, ubiquinol and tocopherol-hydroquinone to their reduced states. Thioredoxin is regenerated by thioredoxin reductase (ThR), while quinone reductase (NQO1) facilitates restoration of ubiquinol and tocopherol-hydroquinone. Also, glutamate-cysteine ligase (GCL) catalyses rate-limiting step in the biosynthesis of GSH, which is regenerated by glutathione reductase (GR). GSH is also used as a cofactor by glutathione S-transferase (GST) and glutathione peroxidase (GP). Adapted from Dinkova-Kostova and Talalay, (2008).

1.2.2.1 Phase II metabolising enzymes

In accordance with their cytoprotective activities, low expression of Phase II enzymes could present a risk for progression of diseases, where oxidative damage plays a key role (Talalay, 2000). Induction of cytoprotective enzymes in response to redox imbalance is dependent on three key cellular components, namely Kelch ECH associating protein 1 (Keap1), nuclear factor erythroid 2-related factor 2 (Nrf2) and antioxidant response

element (ARE), which together form the Keap1/Nrf2/ARE pathway (Motohashi and Yamamoto, 2004). The Keap1/Nrf2 complex is uniquely positioned in the cytosol to respond to inducers, playing a key role in adaption to environmental stressors. Keap1 is a cysteine-rich cytosolic protein that possess a BTB dimerization domain (Broad-Complex, Tramtrack, and Bric à brac), cysteine-rich IVR domain (Intervening region) and a Kelch domain, which contains 6 Kelch repeats and serves as an attachment point for binding Nrf2 (Baird and Dinkova-Kostova, 2011) (Fig 1.4A). Nrf2, which regulates effects of inducers on cytoprotective genes is a bZIP transcription factor belonging to the 'Cap and Collar' family of regulatory proteins such as NF-E2, Nrf1, Nrf3, Bach 1 and Bach 2 (Motohashi et al., 2002) (Fig 1.4B). Under basal conditions, Keap1 repression of Nrf2 promotes proteosomal degradation in the cytoplasm, facilitated by the BTB domain of Keap1 protein which serves as a substrate adaptor for Cullin-3 based E3 ubiquitin ligase (Cul3) (Zhang et al., 2004) (Fig 14A). Thus, Nrf2 is negatively regulated by the Keap1-Cul3-Rbx-1 E3 ubiquitin ligase which targets multiple lysine residues in the N-terminal Neh2 domain of Nrf2 for ubiquitination.

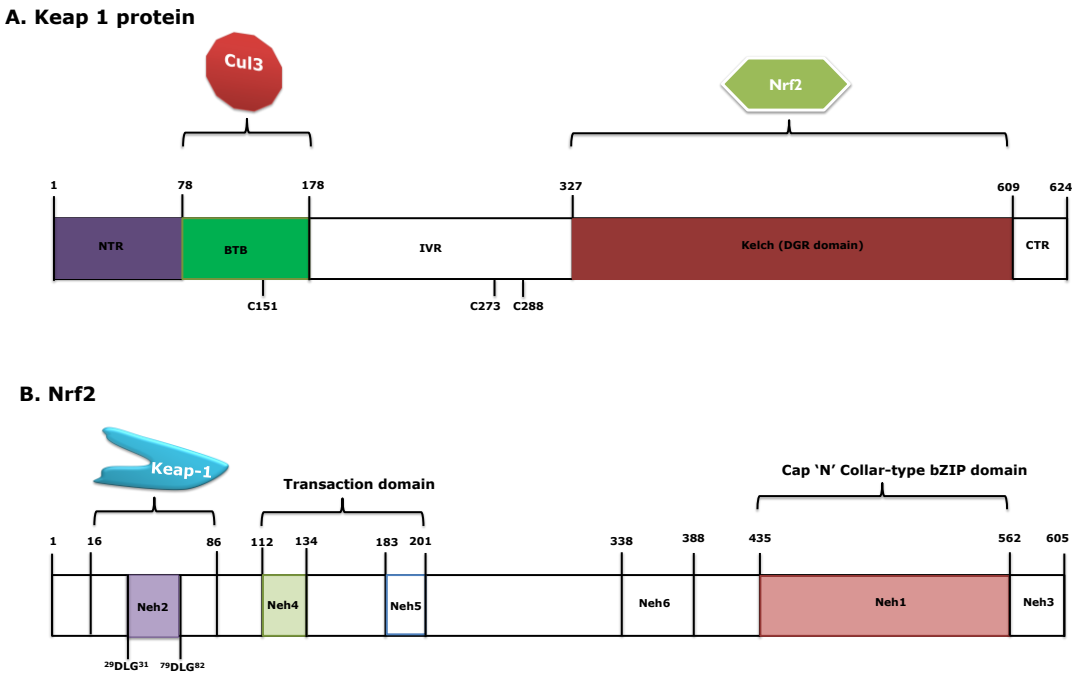

Figure 1.4 Domain structures of Keap1 and Nrf2. Figure shows (A) Keap1 domain for binding to Cullin-3 and Nrf2, as well as (B) Nrf2 domain for binding to Keap1 (Dinkova-Kostova and Wang, 2011).

During redox signalling, the Keap1 protein undergoes a conformational change following interaction with inducers at specific cysteine residues located on the IVR domain, stabilising Nrf2 which escapes ubiquitination and translocates to the nucleus (Fig 1.5). In the nucleus, Nrf2 partners with small Maf (sMaf) through the bZIP DNA binding and heterodimerisation domain to form a heterodimer (Nrf2/sMaf), and binds to the ARE promoter region to trigger transcriptional induction of cytoprotective genes (Itoh et al., 1995; Itoh et al., 1997; Marini et al., 1997), as illustrated in Fig 1.5.

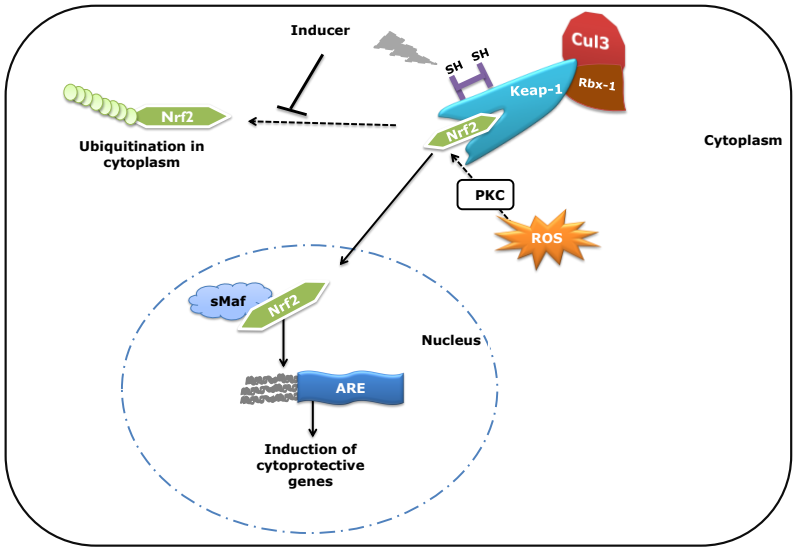

Figure 1.5 Transcriptional activation of Nrf2 from the Keap1/Cul3/Rbx-1 complex**.** Inducers of cytoprotective genes stabilize Nrf2 by interacting with cysteine residues on Keap1 protein in addition to phosphorylation by protein kinase C (PKC) (Dinkova-Kostova and Wang, 2011).

Three possible mechanisms have been proposed to mediate stabilization of Nrf2 based on correlation with evidence provided (Baird and Dinkova-Kostova, 2011). One proposal is interaction between inducer and the BTB domain of Keap1 via reacting with Cys 151 (located within BTB domain and surrounded by positively charged amino acid groups (Fourquet et al., 2010)). As a consequence, binding of Keap1 to Cullin-3 is altered, leading to inhibition of Nrf2 ubiquitination (Zhang et al., 2004; Rachakonda et al., 2008). It is also proposed that inducers, such as *tert*-butylhydroquinone, trigger Cul3-mediated ubiquitination of Keap1 by reacting with lysine-298 located on IVR domain of the Keap 1 protein (Hong et al., 2005; Zhang et al., 2005). Hence, there is less Keap1 to act as a

repressor of Nrf2. Lastly, in concert with Keap1 induction, Nrf2 becomes a target for phosphorylation at serine 40 (Ser40) site by protein kinase C, leading to its release from Keap1 repression and elevated ARE-dependent gene expression (Huang et al., 2002; Bloom and Jaiswal, 2003; Niture et al., 2009).

The list of over two hundred ARE-regulated genes is extensive and has recently been reviewed (Higgins and Hayes, 2011); however, Nrf2 modulates the activities of about half of these genes. Among the battery of Nrf2-regulated genes are genes which encode for GSH homeostasis, NADPH replenishing enzymes and other cytoprotective enzymes (Table 1.1), as reviewed by Dinkova-Kostova and Wang, (2011) and Higgins and Hayes, (2011).

Categories of Nrf2 regulated genes	**Some examples of Nrf2 regulated genes**	**References**
GSH homeostasis	glutathione peroxidase glutathione reductase-1 glutamate-cysteine ligase (GCL)	(Thimmulappa et al., 2002)
NADPH replenishing enzymes	6-phosphogluconate glucose 6-phosphate dehydrogenase malic enzyme	(Thimmulappa et al., 2002)
Other cytoprotective enzymes	quinone reductase (NQO1) haem oxygenase-1 (HO-1) peroxiredoxins thioredoxin thioredoxin reductase 1	(Ishii et al., 2000; Soriano et al., 2008; Dinkova-Kostova and Talalay, 2010; Dinkova-Kostova and Wang, 2011)
Metal-binding proteins	Metallothonein ferritin	(Dalton et al., 1994)

Table 1.1 Compilation of some ARE-associated genes regulated by Nrf2.

1.2.2.2 Inducers of cytoprotective enzymes

There are numerous inducers of Phase II enzymes, including cellular stresses (for example oxidative stress, endoplasmic reticulum stress) and chemically diverse small molecules of both endogenous and exogenous origins. However, small molecules have been classified into the following ten main groups: (i) oxidisable diphenols, phenylenediamines and quinones; (ii) Michael reaction acceptors (olefins or acetylenes with electrophilic groups); (iii) isothiocyanates and sulfoxythiocarbamates; (iv) thiocarbamates; (v) dithiolethiones; (vi) conjugated polyenes; (vii) hydroperoxides; (viii) trivalent arsenicals; (ix) heavy metals and (x) vicinal dimercaptans (Baird and Dinkova-Kostova, 2011).

In oxidative stress conditions, redox signalling also triggers cytoprotective response via the sMaf/Nrf2/ARE pathway. RNS and ROS display oxidative effect on Keap1 via intermolecular disulphide formation at Cys 151 residues of BTB domain leading to inhibition of Nrf2 ubiquitination (Fourquet et al., 2010), or facilitate Nrf2 phosphorylation by increasing activity of protein kinase C σ (PKCσ) (Konishi et al., 1997). Whilst transcriptional activation of Nrf2 by ROS induces cytoprotective genes, persistently high level of ROS could lead to depletion of antioxidant enzymes and then oxidative stress.

1.3 The role of oxidative damage in chronic diseases

In recent years, there has been increasing awareness of the role of oxidative stress in the onset and pathogenesis of disease conditions including atherosclerosis, diabetes, liver cirrhosis and neurodegenerative diseases. The causative role of oxidative stress is generally marked by indicators such as pro-oxidative shift in thiol/disulphide redox state (Droge, 2002), which signifies depletion of cellular antioxidant defence mechanisms. Cellular damage in such conditions is mediated by mitochondrial oxidative stress, inflammatory-mediated oxidative stress and endoplasmic reticulum stress (Droge, 2002).

1.3.1 Non-alcoholic steatohepatitis (NASH)

Non-alcoholic steatohepatitis (NASH) is pathologically rarely differentiated from non-alcoholic fatty liver disease (NAFLD), which encompasses a broad spectrum of hepatic modifications including hepatic steatosis (fat accumulation in liver exceeding 5-10% liver mass), fibrosis, cirrhosis, liver failure and hepatocellular carcinoma (Marra et al., 2008). NASH was first described in non-alcohol consuming patients who presented with liver cirrhosis, similar to observations in alcoholic cirrhosis; also liver biopsies showed lobular hepatitis, focal necrosis with inflammation and fibrosis among other findings (Ludwig et al., 1980). NASH is mainly associated with western lifestyle and has prevalence of 20–30% around the world, with 70-100% incidence in individuals with body mass index (BMI) greater than 30 (Fan et al., 2007). There is also increasing prevalence among the paediatric population (10%), which has been associated with rising childhood obesity (Manco et al., 2008). NASH is also associated with type 2 diabetes mellitus (T2DM) and metabolic syndrome (Thounaojam et al., 2012), and most patients show hyperglycaemia, hypertension, hypertriglyceridemia and low levels of high-density lipoprotein cholesterol (Charlton, 2004), in addition to general fatigue and malaise (Bacon et al., 1994; Thounaojam et al., 2012). Risk factors for NASH include high calorie consumption, sedentary lifestyle, genetic predisposition, metabolic syndrome, diabetes and cardiovascular disorder, in addition to exposure to drugs such as tetracyclines, nucleotide analogues and antimitotic agents (Thounaojam et al., 2012).

The aetiology of NASH is poorly understood, with a complex interplay of visceral adiposity, inflammation and liver fibrosis (Marra et al., 2008; Thounaojam et al., 2012). A number of reviewers have proposed that the pathogenesis of NASH can be distinctly categorised into steatosis and steatohepatitis (Day and James, 1998; Shifflet and Wu, 2009); however, Thounaojam et al., (2012) have included as the final stages of this metabolic disorder, cirrhosis and hepatocellular carcinoma, to propose a series of ‘three-hit’ stages (Fig 1.6). Nevertheless, it is important to mention that events identified in each of these ‘three-hit stages’ do not necessarily occur in any particular order, although some events may serve as triggers for others within the same stage or different stages.

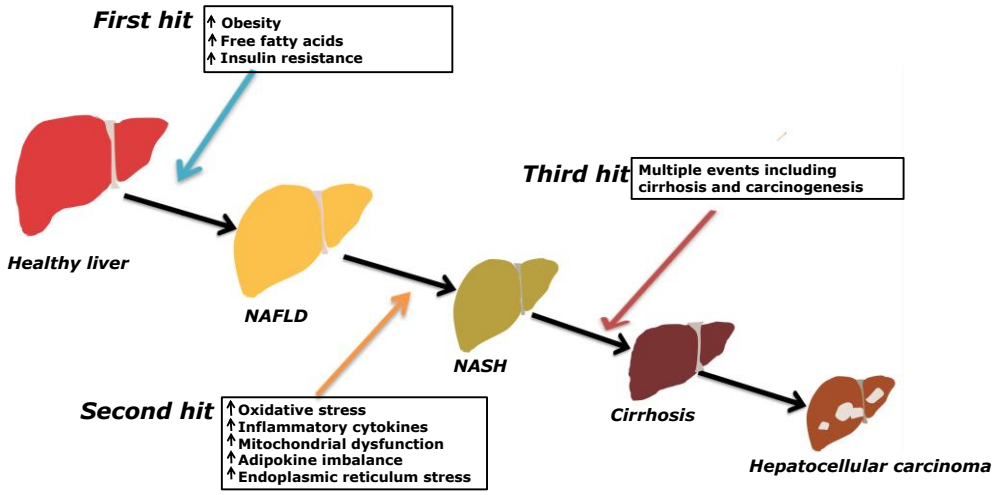

Figure 1.6 The 'three hit stage' model for pathogenesis of NASH. This figure was adapted from Asaokai et al., (Asaoka et al., 2013) and modified according to Thounaojam et al., (2012).

1.3.1.1 The three-hit stage of NASH

The 'first hit' stage is characterised by peripheral insulin resistance and steatosis (increased triglyceride accumulation), as a result of a complex network of events. High fat diet is a major source of elevated circulatory free fatty acids (FFA) and, together with increased *de novo* lipogenesis, could result in excessive hepatic FFA levels with subsequent accumulation of triglycerides (Shiota and Tsuchiya, 2006; Marra et al., 2008). Increasing circulatory FFA levels have also been linked to insulin resistance, where lipid-mediated desensitisation of insulin receptors interrupts insulin signalling (Marra et al., 2008). Insulin resistance, which is impaired glucose uptake in peripheral tissues (e.g. skeletal muscles), can lead to decreased anti-lipolytic effect of insulin on adipose tissues (Marra et al., 2008). Excessive free fatty acids can overwhelm the mitochondrial β-oxidation process, promoting electron leakage and aberration in mitochondrial function and structure (Marra et al., 2008; Koek et al., 2011). This in turn exacerbates ROS production, causing oxidative stress and mitochondrial DNA damage (Marra et al., 2008). This can disrupt lipid metabolism which may facilitate steatosis. FFA activates perixosome proliferation activator receptor–α (PPAR-α) to promote respiratory activities of the mitochondria and uncoupling protein 2 (UCP-2) in attempt to reduce rate of ROS generation (Lee et al., 2003; Koek et al., 2011). However, this adaptive mechanism promotes high ROS levels produced from increased fatty acid oxidation and upregulation

of UCP-2 levels, reducing the membrane proton gradient and ATP synthesis which promote necrosis (Serviddio et al., 2008).

Steatosis predisposes the liver to the 'second hit stage' which is characterised by complex interactions between hepatocytes, stellate cells, adipose cells, Kupffer cells, inflammatory mediators and ROS, and is driven by harmful adducts from FFA oxidation in mitochondria, perixosomes and microsomes which contribute to oxidative stress in NASH (Thounaojam et al., 2012). Again, this stage involves a combination of inter-related activities including inflammation and oxidative stress, which when put together can promote rapid decline in liver function from NAFLD to NASH. The role of stellate cells could involve activation of cellular lipid peroxidation and generation of high malondialdehyde and 4-hydroxynonenal levels, which prevent cytochrome c oxidase activity and could trigger fibrosis (Browning and Horton, 2004).

Fibrosis of the liver is also induced by escalating circulatory adipokines, oxidative stress, fat accrual in hepatocytes and metabolic syndrome (Marra et al., 2008), and is enhanced by leptin-mediated insulin resistance (Honda et al., 2002). The second phase of NASH is also marked by down-regulation of uncoupling proteins, increased ROS generation and activation of Kupffer cells (Thounaojam et al., 2012), and these can aggravate inflammation of the liver (Cai et al., 2005) and hepatocyte damage (Marra et al., 2008). While nuclear factor kappa B (NF-$_K$B) is active in maintaining survival of cells (Schwabe and Brenner, 2007), conditional activation by hepatic lipid accumulation can also induce sub-acute inflammation and steatosis in the liver, and insulin resistance (Cai et al., 2005). Inflammatory cytokines such as tumour necrosis factor-α (TNF-α) can also interfere with the mitochondrial respiratory chain as well as generate RNS and ROS via induction of nitric oxide synthase 2, and this aggravates mitochondrial dysfunction and hepatic injury (Pessayre et al., 2004). Expression of interleukin-8 and monocyte chemoattractant protein-1 are elevated in steatohepatitis patients and animal models (Haukeland et al., 2006). TNF-α and lipid peroxidation products decrease transport of electrons along the respiratory chain, promoting reduction of components of electron chain and increased mitochondrial ROS generation and mitochondrial DNA damage (Pessayre et al., 2002).

The final stage of NASH represents a multi-hit phase where impaired hepatocyte proliferation triggers progenitor cells towards hepatocyte differentiation, deepening fibrosis and leading to cirrhosis and carcinogenesis of the liver (Jou et al., 2008). In spite of the elaborate antioxidant system, hepatocyte damage is facilitated by oxidative stress and inflammation to cause apoptosis, marked by increased caspase-3 and -7 activities (Feldstein et al., 2003).

1.3.1.2 Evidence of oxidative damage in NASH

Oxidative stress in NASH is characterised by oxidative damage to lipids, proteins and DNA, producing high levels of thiobarbituric acid-reactive substances such as malonaldehyde, 4-hydroxynonenal, nitrotyrosine and 8-hydroxydeoxyguanosine (Marra et al., 2008). Development of steatosis and NASH was exacerbated by lack of GSH synthesis in mice, following deletion of the liver-specific enzyme GCL (Chen et al., 2007). In a recent study, mice lacking transcription factor Nrf2 showed increased progression to NASH and decreased GSH levels, which occurred concomitantly with increased oxidative stress and hepatic inflammation (Chowdhry et al., 2010). Furthermore, decreased levels of superoxide dismutase have been reported in NASH patients (Koruk et al., 2004).

1.3.1.3 Antioxidants as a treatment option for NASH

There are currently no pharmacological agents specified for the treatment of NASH, hence, lifestyle modification such as decreased caloric intake along with controlled weight loss remain the first-line for managing patient condition (Okita et al., 2001), since obesity and metabolic disorders are closely associated with NASH. However, insulin sensitizers such as metformin, glitazones and antihyperlipidaemic agents have shown promise in NASH treatment (Stein et al., 2009), considering the role of insulin resistance in disease onset and progression (Shifflet and Wu, 2009), although routine use is limited by adverse effects. There is also growing interest in the use of anti-inflammatory and antifibrotic agents, as well as probiotics and antioxidants (Thounaojam et al., 2012) to retard disease progression and potentially as preventative measures.

Although very few studies have been conducted, there are reports indicating high potential of herbal products in NASH treatment. Preclinical studies with the well-known hepatoprotective phytochemical silymarin, a flavonolignan isolated from *Silybum marianum,* showed reduction in alanine transaminase, aspartate transaminase levels and lipid markers of liver function in NASH patients, when used alone (Hajaghamohammadi et al., 2008) or in conjunction with vitamin E (Hajiani and Hashemi, 2009). The current status of herbal products in NASH treatment has been reviewed (Singal et al., 2011; Thounaojam et al., 2012). The plant-derived antioxidant compound epigallocatechin gallate (EGCG), which is abundant in green tea, also decreased serum and lipid markers of NASH, while increasing GSH levels in Sprague-Dawley rats fed on a high-fat diet (Kuzu et al., 2008).

1.3.2 Type 2 diabetes mellitus (T2DM)

Diabetes mellitus is a group of chronic metabolic disorders marked by prolonged hyperglycaemia and/or impaired insulin signalling, which causes secondary complications such as hypertension, nephropathy, retinopathy and neuropathy in a time-dependent manner. In 2016, the International Diabetes Federation estimates that one in 11 adults worldwide have diabetes, with more than 80% of diabetic patients living in low-income and middle income countries (International Diabetes Federation, 2015; Chan et al., 2016). In the UK alone the cost of diabetes treatment is a growing concern, with one in ten hospital admissions being due to diabetes and an annual death rate of 15% (Hex et al., 2012). Diabetes occurs in two main forms, type 1 and type 2. Onset of type 1 diabetes (HLA-related) typically occurs before age 30 and is reported in 5 – 15% of patients with diabetes depending on the population, a condition resulting from progressive autoimmune destruction of insulin-producing β-cells in the islet of Langerhans of the pancreas, leading to a lack of insulin production (Hex et al., 2012). T2DM accounts for the remaining 85 – 95% depending on population of cases of diabetes, caused by variable risk factors including obesity, smoking, genetic predisposition and aging (Hex et al., 2012).

In healthy individuals, plasma glucose levels (ranging from 4 to 7 mM) are maintained by controlled intestinal absorption, hepatic glucose synthesis, and uptake and metabolism by

peripheral tissues (Saltiel and Kahn, 2001). The pancreas remains at the centre of glucose homeostasis with hormonal activities of α- and β-cells of the islets of Langerhans. The β-cells, which make up about 50% of the islet cells in humans, serves as primary regulator for blood glucose levels by secreting insulin, while glucagon is secreted during hypoglycaemia by α-cells, which make up 40% of islets (Brissova et al., 2005; Steiner et al., 2010). Insulin is a 51 amino acid peptide hormone with plasma half-life of approximately 5 mins (Mincu and Ionescu-Tirgoviste, 1980). The main physiological regulator of insulin release is glucose. Glucose is taken up by glucose transporter-2 (GLUT-2) into β-cells by facilitated diffusion and metabolised to produce ATP (Pi et al., 2010). Increased ATP levels signal for cell depolarisation by closure of K_{ATP}-gated channels and increased Ca^{2+} influx via Ca^{2+} voltage-gated channels (Newgard and McGarry, 1995; Jensen et al., 2008). Insulin is subsequently released into the plasma through exocytosis; insulin promotes glucose uptake mainly into muscles and adipose tissues (Klip and Paquet, 1990). Thus, insulin lowers blood glucose levels. During fasting periods, low insulin levels also regulates blood glucose levels by promoting glycolysis and glycogenolysis and inhibiting glycogenesis.

1.3.2.1 Insulin resistance

Insulin receptor signalling on target cells is initiated by tyrosine phosphorylation of insulin receptor substrates (IRS-1 and IRS-2) by binding to insulin (Saltiel and Kahn, 2001). Subsequently, a series of secondary messenger pathways involving activation of phosphatidylinositol-3-phosphate and TC10, ras and the MAP kinase cascade promote glucose entry via GLUT-4 receptors, following their translocation from intracellular sites (in skeletal muscles and adipose tissues) to cell membrane (Saltiel and Kahn, 2001). However, insulin receptor signalling can be disabled by a negative feedback mechanism mediated by serine phosphorylation of insulin receptors and IRS, which reduces insulin-mediated tyrosine phosphorylation (Aguirre et al., 2002).

Attenuation of insulin signalling via this feedback pathway is mediated by hypertrophic adipocytes, which release TNF-α (Hotamisligil et al., 1996). Furthermore, continuous activation of protein kinase C and IkappaB kinase beta (IKKbeta) may contribute to

obesity-induced inhibition of insulin signalling (Kim et al., 2001; Yuan et al., 2001). Thus, increased plasma FFA levels, which predispose cells to mitochondrial ROS generation, could also be linked to increase in TNF-α activity. Nevertheless, as mentioned in Section 1.2.2, cellular redox-regulating proteins are induced to enhance adaptation to rising ROS levels. Activation of c-jun NH_2-terminal kinases (JNK), a TNF-α target could mediate ASK1-induced phosphorylation at serine 307 of IRS (Aguirre et al., 2000). Thus, the dimeric form of ASK1 is activated in the presence of ROS, which is also elevated by increased lipid oxidation in the presence of high FFA levels. Other signalling kinases that could mediate insulin resistance including phosphoinositide 3-kinase (PI3K), glycogen synthase kinase (GSK)-3, and mammalian target of rapamycin (mTOR) have been reviewed (Saltiel and Kahn, 2001). Insulin resistance consequently results in reduced insulin-stimulated glucose uptake in muscles, adipocytes and other peripheral tissues, leading to high plasma glucose levels.

1.3.2.2 Hyperglycaemia

Hyperglycaemia (persistent high plasma glucose levels) occurs as a consequence of impaired insulin signalling and impaired glucose tolerance. Hyperglycaemia occurs when blood glucose levels exceed 7 mM during fasting, or exceed 11.1 mM – 2 h after meals (Giugliano et al., 2008). It is unanimously accepted that hyperglycaemia is a precursor for the diverse secondary complications, such as nephropathy, neuropathy and hypertension, which develop in diabetes patients. Glucose metabolism in β-cells is regulated by glucokinase, a hexokinase analogue responsible for initiating the glycolytic pathway, to generate pyruvate for ATP production via the tricarboxylic acid cycle. However, compensatory activities of β-cells such as increased glucokinase activity, are activated to restore blood glucose levels to the normal range (Fridlyand and Philipson, 2004) leading to increased mitochondrial ROS levels. Emerging evidence indicates that minimal ROS levels may be beneficial to insulin signalling in β-cells, since H_2O_2 stimulated a surge in insulin release via increase in Ca^{2+} influx in rat islets (Janjic et al., 1999; Maechler and Wollheim, 1999).

However, high ROS levels cause β-cell dysfunction by initiating a series of debilitating activities on glucokinase gene expression, mitochondrial function and insulin secretory mechanism, via oxidative damage (Maechler and Wollheim, 1999; Butler et al., 2003). ROS can also impair glucose sensing in β-cells, which can result in decreased insulin output and consequently impaired inhibition of hepatic glucose production, lipolysis and decreased glycogen formation, so exacerbating hyperglycaemic condition (Fig 1.7).

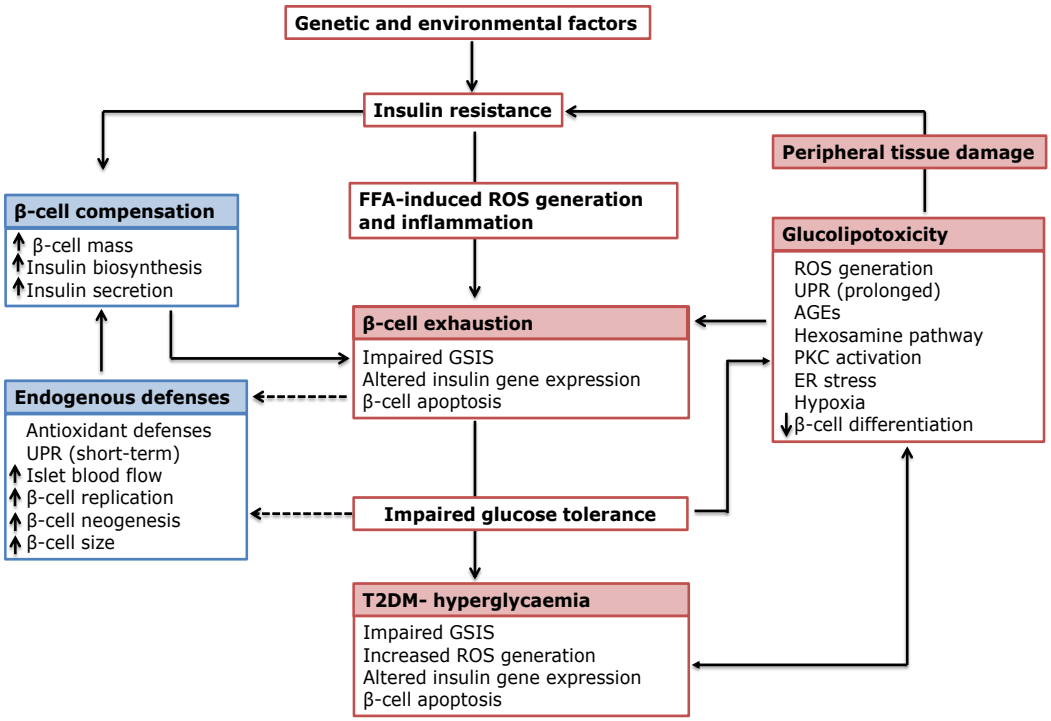

Figure 1.7 Scheme illustrating complex interplay of diverse mechanisms involved in β-cell damage in the pathophysiology of T2DM. This scheme which is adapted from Bensellam et al., (2012) summarises aetiology of T2DM (Henquin, 2000; Wollheim and Maechler, 2002; Cnop et al., 2005). Onset of T2DM is triggered by genetic and environmental factors that cause lack of insulin sensitivity, affecting insulin uptake. This initiates a series of mechanisms including high ROS levels and inflammatory mediators to result in impaired glucose tolerance; although transient β-cell regeneration serves as a compensatory mechanism. Also, increased demand for insulin synthesis puts a strain on the endoplasmaic reticulum (ER), which can be compensated in the short-term by activation of uncoupled protein response (UPR). Coupled to depletion of antioxidant defences, persistent elevation of ROS and impaired glucose-stimulated insulin secretion (GSIS) can lead to β-cell apoptosis.

Another compensatory mechanism is insulin hypersensitization, which results in enhanced insulin synthesis and release from β-cells (Fig 1.7). Thus, in the presence of high glucose levels, β-cells become more sensitive to glucose, increasing glucose metabolism, proinsulin biosynthesis and insulin secretion (Cnop et al., 2005). Evidence of

abnormal proinsulin synthesis has been found in T2DM, correlating with fasting hyperinsulinaemia (Sempoux et al., 2001), which could be facilitated by increased ATP synthesis and accumulation of calcium in the cytosol (Cnop et al., 2005). However, insulin hypersensitization may promote β-cell exhaustion due to depletion of insulin stores; subsequently, this could induce high mitochondrial ROS levels, which will deepen β-cell dysfunction and activate apoptotic mechanisms (Tanaka et al., 2002), leading to β-cell loss and disease progression.

1.3.2.3 Advanced glycation end products (AGEs)

As illustrated in Figure 1.7, hyperglycaemia can also cause reduced glucose-stimulated insulin-secretion (Cnop et al., 2005). Persistent hyperglycaemia enhances free radical generation via autoxidation of membrane proteins and plasma unsaturated fatty acids, in addition to autoxidation by sugars and sugar adducts (Baynes, 1991), and increased glyceraldehyde-3-phosphate or dihydroxacetate phosphate levels (Nishikawa et al., 2000). Also, activation of protein kinase C (PKC) during high glucose levels induces c-Myc via PKC beta 2 regulation (Kaneto et al., 2002); c-Myc supresses insulin gene transcription (Kaneto et al., 2002) and PKC activation, which contribute towards increased ROS levels. Increased ROS generation in hyperglycaemic conditions were also marked by GSH depletion in red blood cells (Mizukami et al., 2014).

1.3.2.4 Glucolipotoxicity in pathogenesis of T2DM

Elevated mitochondrial ROS generation induced by insulin resistance and hyperglycaemic conditions promote oxidative damage to pancreatic β-cells, this is exacerbated by glucolipotoxicity (cell damage caused by high glucose and lipid exposure). In β-cells, it has been suggested that lipotoxicity and glucotoxicity may be inter-dependent on each other (Jacqueminet et al., 2000), due to the ability of glucose to promote esterification of fatty acids into neutral lipids (Briaud et al., 2001). Although an earlier review proposed that glucotoxicity occurs prior to lipotoxicity (Poitout and Robertson, 2002), the complexity of both processes rather points towards an inter-relation, based on their association with increased ROS production and β-cell damage, as

reviewed by Newsholme et al., (2007). Following 72 h exposure to 2 mM FFA, cultured islets (isolated from pre-diabetic Zucker diabetic fatty rats, a rodent model of T2DM) showed increased ceramide formation, decreased insulin signalling, and increased nitric oxide (NO) levels which facilitated NO-mediated β-cell apoptosis (Shimabukuro et al., 1997). In addition, the endoplasmic reticulum (ER) which is responsible for esterification of FFA is overloaded in the presence of high lipid levels, causing impaired ER function and ER stress, leading to β-cell death (Cnop et al., 2005).

It has been suggested that low expression of antioxidant enzymes in β-cells is required to allow ROS–mediated insulin signalling (Lenzen et al., 1996; Pi et al., 2007); however, this works to the disadvantage of β-cells during prolonged exposure to high ROS levels. Thus, accumulation of increased ROS levels due to high glucose and high lipid load overwhelms the low antioxidant capacity, so causing apoptosis (Robertson and Harmon, 2007). In keeping with the proposal of ROS-mediated β-cell damage in diabetes, adenoviral overexpression of glutathione peroxidase in clonal hamster insulinoma HIT-T15 cells protected against glucose and ribose-induced oxidative stress, and promoted glucose-induced insulin release (Tanaka et al., 2002). Although β-cell deficit as a consequence of glucolipotoxicity is still debated, decreased β-cell volume correlated positively with increased glycated haemoglobin (Hb1Ac) levels in diabetic subjects (Mizukami et al., 2014). An increase in oxidative stress markers including 8-oxo-2'-deoxyguanosine and 4-hydroxynonenal have also been recorded during glucotoxicity in T2DM patients (Sakuraba et al., 2002; Mizukami et al., 2014). The complex interplay of insulin resistance, hyperglycaemia, ROS and β-cell apoptosis in the pathophysiology of T2DM has been debated further (Kahn, 2003; Robertson et al., 2003; Fridlyand and Philipson, 2004; Cnop et al., 2005; Pi et al., 2007). Therefore, it is proposed that the use of antioxidants could prevent oxidative stress and promote insulin secretion. Hence, upregulation of cellular antioxidant enzymes and use of radical scavengers may promote β-cell protection and repair, whilst relieving cell damage and low insulin secretion.

1.3.2.5 Antioxidants as a treatment option for T2DM

Although lifestyle modification is recommended as first-line in management of T2DM, pharmacological agents such as oral antihyperglycaemics, incretin-based therapies, and insulin are commonly used in sequential order as disease progresses (Kahn et al., 2014). However, current treatment options are not always effective and their use is often limited by adverse effects and contraindications. Therefore, more effective treatment options are needed to address the issue of β-cell dysfunction and loss of viability of β-cells, which play a fundamental role in the pathogenesis of diabetes. Hence, there is growing interest in the use of herbal medicinal products in diabetes treatment.

The use of medicinal plants such as *Momordica charantia*, *Blighia sapida* and *Vernonia amygdalinain*, in the treatment of diabetes dates back to many years and are common to various communities around the world (Rao M U. et al., 2010; Kibiti and Afolayan, 2015). Evidence in rodents also suggest that PPAR agonists could protect against insults by oxidative stress and inflammation in β-cells, see references within (Bonora, 2008). The link between antioxidant activities and preservation of β-cell function with improved glycaemic control has been established using the well-known antioxidant compound N-acetyl-L-cysteine (Kaneto et al., 1999; Takatori et al., 2004). In addition, antioxidant and anti-apoptotic activities of catalase (Chen et al., 2001), thioredoxin (Chen et al., 2005) and metallothionine (Kasono et al., 2004) recovered β-cells from streptozotocin-induced damage.

1.4 Phytochemicals as antioxidants

According to the US Food and Drugs Administration, an antioxidant is defined as “a substance for which there is scientific evidence that following absorption from gastrointestinal tract, the substance participates in physiological, biochemical and cellular processes that inactivate free radicals or that prevent free radical-initiated chemical reactions” (Dinkova-Kostova and Talalay, 2008). Interest in the importance of antioxidants was enhanced by the earlier discovery of vitamins E and C as reducing agents (Jacob, 1996; Wolf, 2005). Over the past decade, consumption of fruits and vegetables has

become the focus of public health campaigns. This is because most fruits and vegetables are believed to be a rich source of phytochemicals which can act as antioxidants, in addition to possessing diverse minerals and vitamins that form part of a healthy diet. Hence, it has been proposed that increased consumption of fruits and vegetables will provide preventative benefits against a wide range of diseases (Riboli and Norat, 2003). The search for plant-derived antioxidants has led to several reports of cytoprotection by dietary compounds such as polyphenols (Duvoix et al., 2005; Hamaguchi et al., 2009).

In this thesis, eight phytochemicals: quercetin, curcumin, sulforaphane, rosmarinic acid, caffeic acid, ferulic acid, *m*-coumaric acid and danshensu; were assessed for radical scavenging and cytoprotective activities against free radicals. Among the selected phytochemicals, quercetin, curcumin and sulforaphane were used as reference phytochemicals, owing to strong evidence of their antioxidant activities (Sections 1.5.1 – 1.5.3). Furthermore, there is compeling evidence from animal studies that rosmarinic acid exhibits antioxidant effects. Hence, there is the need to assess the contribution of activities by its principal metabolites towards *in vivo* effects of rosmarinic acid.

1.5 Review of metabolic and pharmacological profile of phytochemicals used in this study

This section presents metabolic profiles of quercetin, curcumin, sulforaphane, rosmarinic acid and its principal metabolites. Subsequently, evidence of pharmacological activities is highlighted, with focus on antioxidant activities.

1.5.1 Quercetin

Quercetin is a flavonoid widely distributed in nuts, fruits and vegetables (Harnly et al., 2006), such as onion, chilli pepper, tomato, broccoli, apple and cranberry (Rothwell et al., 2015), principally occurring as a glycoside (Yoo et al., 2010). Daily consumption of quercetin is by the order of 6 – 31 mg (Metodiewa et al., 1999), which is far less than the safety limit of 1000 mg/day or 756 mg/day following oral and intravenous administration

respectively (Harwood et al., 2007). Thus, among other phytochemicals, quercetin is considered relatively safe (Lamson and Brignall, 2000).

1.5.1.1 Metabolism and bioavailability

The presence of quercetin in plasma is influenced by metabolism prior to its absorption. Following incubation with quercetin 4'-glucoside, β-glycosidases in saliva cleave the attached glycosides to release quercetin (Walle et al., 2005), promoting buccal absorption of quercetin (Fig 1.8). Additionally, quercetin is also released by the β-glucosidase lactate phlorizin hydrolase (LPH, EC 3.2.1.62), resident on micro-villi of small intestinal epithelium (Németh et al., 2003), to facilitate passive diffusion in the small intestine (Day et al., 2003) (Fig 1.8).

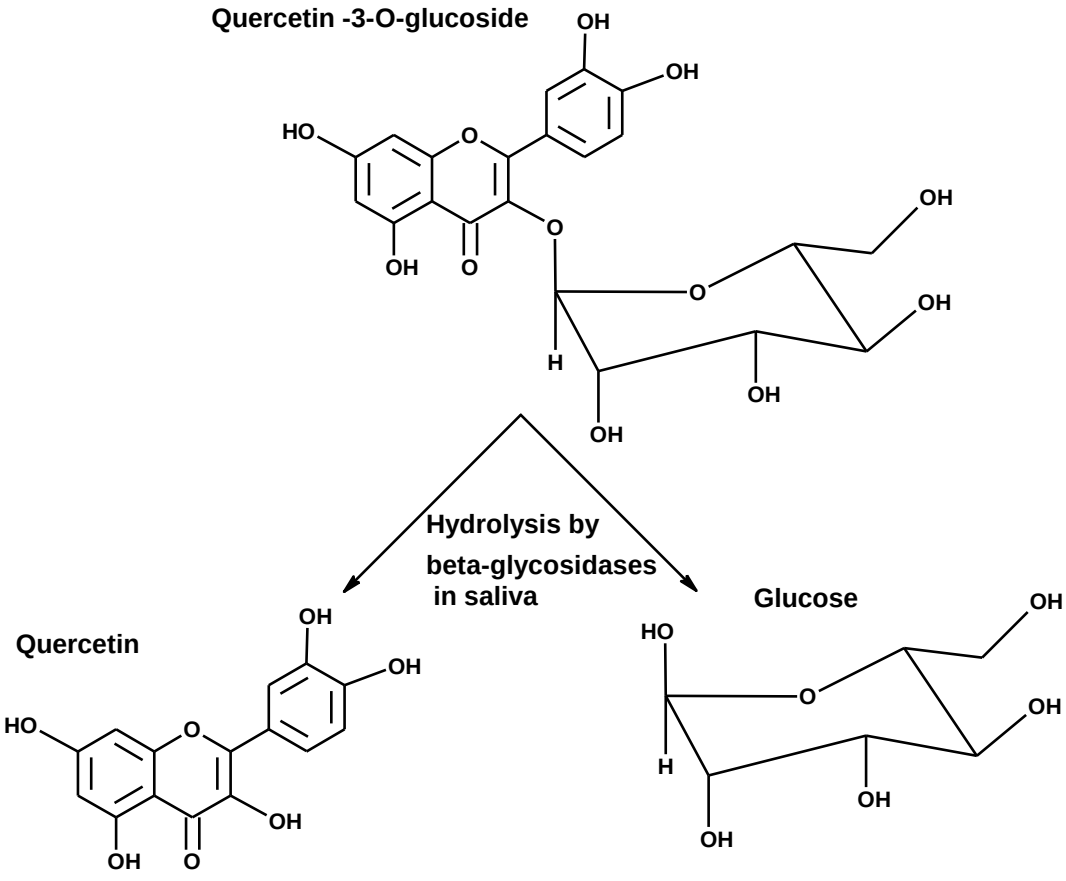

Figure 1.8 Hydrolysis of quercetin-glucoside in oral cavity by β-glycosidases to form quercetin and glucose.

Intestinal absorption of quercetin is also supported by organ anion transport polypeptides (OATP) (Nait et al., 2009). Enzymes within small intestinal epithelium are also involved in

degradation of quercetin to phenolic acids such as 3-hydroxyphenylacetic acid, benzoic acid, hippuric acid and CO_2 (Aura et al., 2002), which are excreted via urine and faeces (Mullen et al., 2008) (Fig 1.9). Thus, the integrity of gut microbiota plays a crucial role in the fate of quercetin and its metabolites following oral intake.

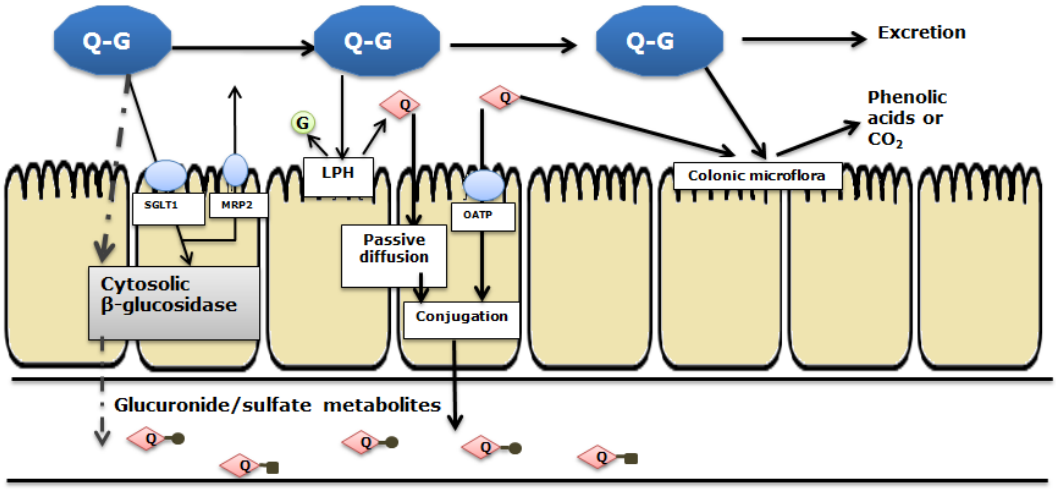

Figure 1.9 Intestinal metabolism of quercetin-glycoside following oral intake. Cleavage of remaining quercetin glycosides (Q-G) occurs partially due to cytosolic β-glycosidases and lactate phlorizin hydrolase (LPH) in the small intestines, causing release of quercetin (Q) for absorption and conjugation. Absorption of quercetin is facilitated by sodium-glucose linked transporter 1 (SGLT1) and organic anion-transporting polypeptide (OATP), while efflux is via multidrug resistance-associated protein 2 (MRP2). Adapted from Vargas and Burd, (2010).

Quercetin is metabolised to glucuronic acid, sulphate and methyl conjugates, catalysed by uridine 5'-diphosphoglucuronosyl transferase (UGT), phenosulfotransferase (sulfate conjugation- SULT) and catechol-O-methyltransferase (methylation - COMT) respectively (Walgren et al., 2000; Murota and Terao, 2003; van der Woude et al., 2004; Del Rio et al., 2013). A comprehensive list of Phase II metabolites has been provided by Guo et al., (2015). These metabolites enter the blood circulation reaching the liver via the portal vein, where passive diffusion and organ anion transport (OAT) and OATP-mediated transport account for uptake in hepatocytes (Wong et al., 2012).

Quercetin and its metabolites are distributed in various tissues, with free and methylated forms, ranging from 2 – 6 µM detected in porcine kidneys, liver and jejenum (Bieger et al., 2008). Studies in rats also confirmed 60 µM in plasma after feeding on quercetin 45 - 47 mg/day for 2 weeks (Silberberg et al., 2005). In human subjects receiving oral dose of

150 mg quercetin per day, plasma levels reached 380 nM after 2 weeks (Egert et al., 2008). A Phase I clinical trial in cancer patients recorded serum levels in the range of 200 – 400 µM within 30 min of intravenous administration of 945 mg/m^2 quercetin at a 3-week intervals, with 1 µM maintained in plasma up to 4 h after administration (Ferry et al., 1996). Thus, low plasma levels of quercetin are detected after oral intake in mammals.

The overall bioavailability of quercetin is influenced by a number of factors. The good lipid solubility of quercetin allows for absorption across small intestinal wall and hence increases bioavailability (Piskula and Terao, 1998); however this can be limited by extensive metabolism by Phase II enzymes in small intestinal epithelial cells and hepatocytes (van der Woude et al., 2004). Moreover, there is efflux of metabolites back into the intestinal lumen (Walgren et al., 1998; Crespy et al., 2001), whilst biliary excretion also channels compounds into the gut via multidrug resistance-associated protein 2 (O'Leary et al., 2003).

Quercetin is also metabolised in the liver by cytochrome P450 (Gradolatto et al., 2004), while some conjugates (quercetin 3'-glucuronide and quercetin 7'-glucuronide) are de-glucuronidated and subsequently sulfated to generate quercetin 3'-sulfate (O'Leary et al., 2003). Furthermore, daily supplementation with a higher dose of quercetin significantly increased the plasma quercetin concentration, despite relatively high inter-individual variability in plasma (Egert et al., 2008). Hence, the general understanding is that prolonged intake of quercetin will lead to tissue levels of quercetin similar to those in plasma (Vargas and Burd, 2010). There is also evidence to confirm that key *in vivo* metabolites such as 3'-O-methyl and 4'-O-methyl quercetin could exhibit similar pharmacological effects (Spencer et al., 2003).

1.5.1.2 Pharmacological activities

The benefits of flavonoids in humans are continuously being evaluated, since these compounds form a large part of human diet. Low intake of flavonoid-rich foods has been related to increased risks of coronary diseases in humans (Knekt et al., 1996). In an epidemiological study, hypertensive patients who received 730 mg quercetin as daily

supplement for 28 days recorded a reduction in blood pressure, by 7 mmHg (systolic) and 5 mmHg (diastolic) (Edwards et al., 2007).

A number of *in vivo* and *in vitro* studies have also reported a wide range of pharmacological activities by quercetin and its derivatives. Quercetin-3-O-β-D-glucuronide produced 20 – 28% inhibition against influenza A virus in mice after oral administration of 3 and 6 mg/kg for four days, and showed anti-inflammatory activity against dimethylbenzene at 8 - 20% more than aspirin (Fan et al., 2011). Following 5 h exposure to human macrophages and human adipocytes, 3 – 30 μM quercetin attenuated basal mRNA expression of TNF-α and interleukin-1 β by approximately 80%, with 60 – 70% decrease in COX-2, 37% and 63% decrease in induction of TNF-α and monocyte chemoattractant protein-1 (MCP-1), respectively (Overman et al., 2011).

Anticancer activities of quercetin were observed after 24 – 72 h treatment with 70 μM in human menaoma cells, with 40 – 60% inhibition of CDK2 activity and cell cycle block at G1 stage (Casagrande and Darbon, 2001). In Sprague-Dawley rats with colon cancer, oral intake of 43.35 g/kg quercetin led to 41% fewer high multiple abberant crypt foci and 88% increase in apoptotic cells in the distal colon, relative to untreated rats (Warren et al., 2009). These reports support the proposition that quercetin could be beneficial to humans.

In spite of its poor bioavailability, reports suggest that quercetin could be a potential therapeutic agent in the treatment of diabetes and NASH. Furthermore, the use of enhanced drug delivery methods such as nanocapsules (El-Gogary et al., 2014) and polymer-based carriers (Singhal et al., 2011; Chitkara et al., 2012) could overcome these challenges, leading to a promising outcome for quercetin in drug development. Chitkara et al., (2012) also observed increased bioavailability by approximately 523% and sustained plasma concentration of quercetin after dosing with poly(lactic-co-glycolic acid) quercetin nanoformulations, relative to quercetin suspension, with significant increase in antioxidant levels (superoxide dismutase and catalase) in pancreas and kidneys of diabtetic rats.

Earlier *in vitro* studies documented inhibition of haemoglobin glycosylation with increasing quercetin concentration (Asgary et al., 1999). In streptozotocin-induced diabetic rats, quercetin reduced plasma glucose levels, as well as plasma cholesterol and triglyceride levels, following intraperitoneal administration; these effects were not observed in non-diabetic animals (Vessal et al., 2003). In their study, quercetin also increased pancreatic islet mass in both normal and diabetic rats. In INS-1 rodent pancreatic β-cells, quercetin also exhibited antioxidant activities against hydrogen peroxide-induced oxidative damage and potentiated glucose-stimulated insulin secretion (Youl et al., 2010).

Quercetin has also been shown to reduce biomarkers of obesity such as plasma triglycerides, FFA, systolic blood pressure and insulin, which were increased in obese Zucker rats (Rivera et al., 2008). Although studies in human subjects are limited, a high number of *in vivo* (animal studies) and *in vitro* studies have reported quercetin activities against obesity (Nabavi et al., 2015). A high fat diet predisposes to insulin resistance and accumulation of FFA, and this is commonly used to induce NASH or fatty liver disease in animal models (Kucera and Cervinkova, 2014).

In experimental rats presenting with NASH, quercetin proved more protective than pioglitazone (antidiabetic) and hydroxyl citric acid (natural supplement for weight management), by reversing elevated serum levels of glucose and liver marker enzymes - alanine transaminase, aspartate transaminase and alkaline phosphatase (Surapaneni and Jainu, 2014). Also, quercetin demonstrated antioxidant, anti-inflammatory and antilipogenic activities via modulating the phosphatidylinositol 3-kinase (PI3K)/AKT pathway in the HUH-7 hepatocellular carcinoma cell line (Pisonero-Vaquero et al., 2015).

Quercetin exhibits a biphasic effect, in that antioxidant effects which have been reported at lower cellular concentrations (1 – 40 µM) are achievable in the human diet (Vargas and Burd, 2010), while cytotoxic activities *in vitro* are observed at concentrations above 40 µM (Metodiewa et al., 1999). Kim and Jang, (2009) reported pro-apoptotic effects following exposure of human hepatoma HepG2 cells to 100 µM quercetin for longer than 30 min, with antioxidant effects recorded at lower concentrations. Antioxidant effects of quercetin have been linked to the presence of a catechol group, which is involved in chelating

oxidizing metals (Murota and Terao, 2003) and could be required for inhibition of lipid peroxidation (Brown et al., 1998; Yamamoto et al., 1999). Antioxidant activities of quercetin have gained further interest in recent times due to its inductive effects on the Keap1/Nrf2/ARE pathways, resulting in upregulation of cytoprotective genes (Tanigawa et al., 2007).

1.5.2 Curcumin

Curcumin is obtained from turmeric, a rhizome of *Curcuma longa* of the family Zingiberacea, which has its historic use in Ayurvedic medicine - in cancer, inflammatory and other pathogenic conditions (Ammon and Wahl, 1991). There are numerous species of the *Curcuma*, with the most popular species (*Curcuma longa*) cultivated in Asia, largely produced in India (78% of global market) and exported for use as food spice (curry powder) and food colourant (E100) worldwide (Grynkiewicz and Slifirski, 2012). It is estimated that the average daily intake of turmeric (the anti-inflammatory agent (Aggarwal et al., 2003)) from an Indian diet is 60 – 100 mg per 60 kg individual (Casas-Grajales and Muriel, 2015).

Curcuma extracts usually consist of a mixture of three yellow-orange pigmented compounds: lesser amounts of dimethoxy-curcumin and bisdemethoxy-curcumin in addition to the major component curcumin (Grynkiewicz and Slifirski, 2012). Curcumin is a diarylheptanoid bearing the IUPAC name (1,7-bis-(4-hydroxy-3-methoxyphenyl)-1,6-heptadiene-3,5-dione), which is obtained in its stable form as a tautomeric ketone–enol mixture (Fig 1.10). Curcumin has been classified as GRAS (generally regarded as safe) by the US Food and Drug Administration for flavouring and colouring food varieties due to its lack of toxicity. This is backed by Phase I clinical studies where daily oral dosing with 12 g curcumin was well-tolerated (Cheng et al., 2001; Lao et al., 2006), suggesting its enormous potential as a therapeutic and chemopreventive agent.

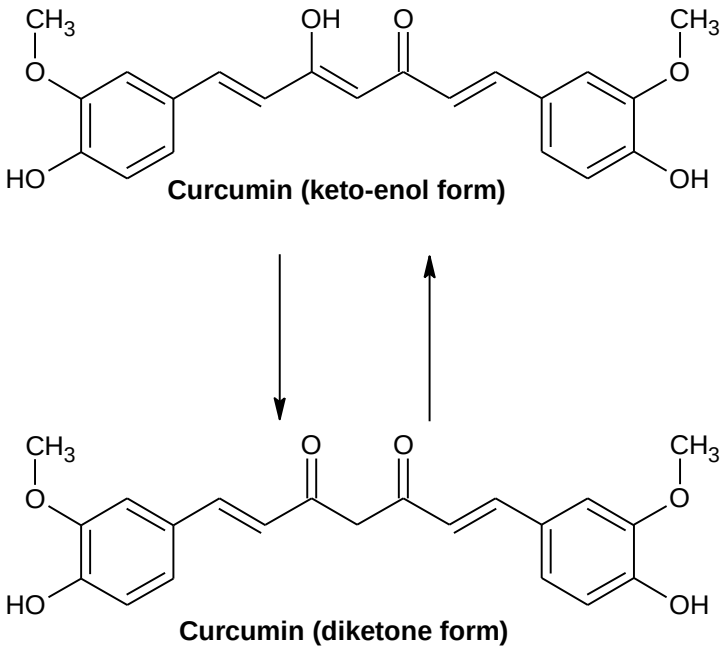

Figure 1.10 Structures of keto-enol tautomer of curcumin. Stable form of curcumin consists of both tautomeric forms (Tønnesen et al., 1982; Payton et al., 2007; Li et al., 2009).

1.5.2.1 Metabolism and bioavailability

Curcumin exhibits low systemic bioavailability, it is chemically unstable and has a strong yellow stain, all of which impede its progress in drug development. Although curcumin can be oxidized to ferulic acid and feruloylmethane (Wang et al., 1997), chemical stability can be achieved in the presence of foetal calf serum in aqueous medium, blood (Pfeiffer et al., 2003) and intestinal fluid, where pH is between 1 and 6 (Wang et al., 1997).

Poor systemic bioavailability results from extensive metabolism in the small intestines, inadequate intestinal absorption via paracellular diffusion and rapid elimination in urine (Ravindranath and Chandrasekhara, 1980; Anand et al., 2007). *In vivo* studies in both rats and humans have reported Phase I and II metabolism of orally administered curcumin (Sharma et al., 2007; Hoehle et al., 2006). Phase I metabolism was observed during incubation with intestinal and liver cytosolic enzymes, mainly as alcohol-dehydrogenase dependent (Hoehle et al., 2006), involving successive bio-reduction of the four double bonds in the olefenic heptanoid system (heptadiene-3,5-dione complex) to rather stable metabolites – dihydro, tetrahydro, hexahydro and octahydro-curcumin (Pan et al., 1999; Hoehle et al., 2006) (Fig 1.11).

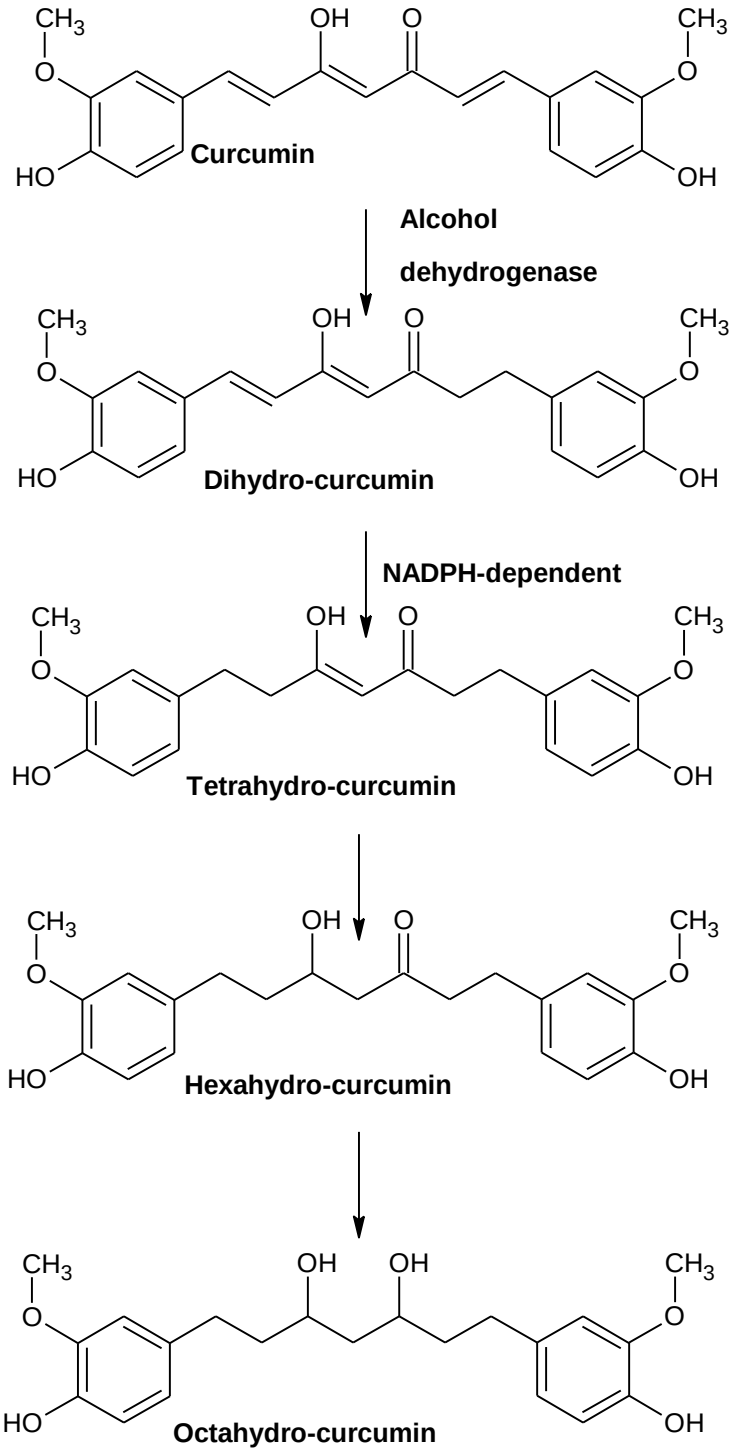

Figure 1.11 Metabolism pattern for orally administered curcumin. Adapted from Hoehle et al., (2006).

Metabolism of intermediate dihydrocurcumin occurs in an NADPH-dependent reaction to produce tetrahydrocurcumin (Fig 1.11), with hexahydro-curcumin glucuronide as the

predominant metabolite (Hoehle et al., 2006; Metzler et al., 2013). Both reduction and conjugation are initiated by intestinal enzymes but also occur in hepatic tissues of rats and humans (Ireson et al., 2002; Hoehle et al., 2006; Usta et al., 2007). The remaining parent compound and reductive metabolites are conjugated with sulfates and glucuronic acid (Ireson et al., 2001).

However, glucuronidation is the main route for conjugation and this generates two distinct and chemically reactive monoglucuronides, phenolic and alcoholic glucuronides as the major and minor metabolites, respectively (Pfeiffer et al., 2007; Fig 1.12). A number of sulfotransferases appear to be involved in the sulfation of curcumin and its metabolites in the liver and the gut (Hoehle et al., 2007; Pfeiffer et al., 2007).

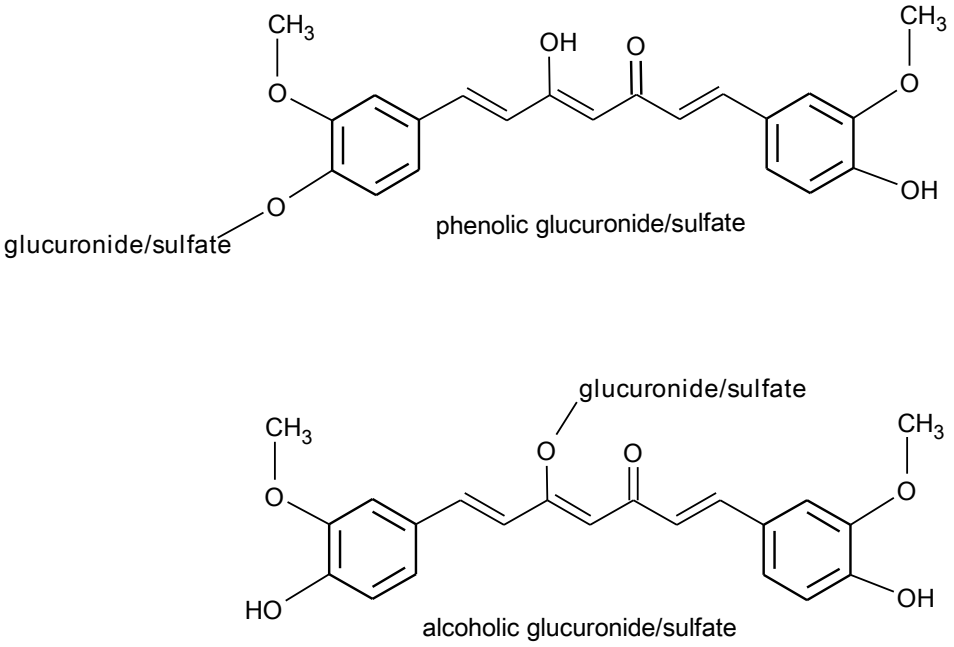

Figure 1.12 Phenolic (A) and alcoholic (B) glucuronide metabolites of curcumin. Adapted from Metzler et al., (2013).

Bioavailability studies following oral dosing in rodents and humans have reported inconsistent observations (Shoba et al., 1998; Anand et al., 2007). Intravenous administration of 10 mg/kg in rats produced peak levels of 1 μM, whereas 500 mg/kg oral intake reached 0.2 μM (Yang et al., 2007). However, oral doses of 4 – 8 g in humans

reached 0.41 – 1075 μM in plasma after 1 h (Cheng et al., 2001), while Sharma and colleagues, (2004) reported 11.1 nM following 1 h of intake of 3.6 g oral curcumin. After an oral dose of 3 g curcumin in human, both normal and malignant colorectal tissues recorded high levels at 12.7 nM and 7.7 nM curcumin, respectively (Garcea et al., 2004). Another study in colorectal cancer patients who received 3.6 g curcumin oral daily doses for 4 months revealed free curcumin, glucuronide and sulfate levels at 11 nM, 16 nM and 9 nM in plasma respectively, while urinary levels of conjugates were 1 nM and 500 nM respectively (Sharma et al., 2004).

In healthy humans however, only curcumin glucuronide and sulfates were detected in plasma at 3.7 μM and 2.2 μM respectively, 4 h after single oral dose of 10 g or 12 g (Vareed et al., 2008). These reports indicate that glucuronide and sulfate curcumin are present in plasma with glucuronide as the main metabolites.

Due to poor bioavailability of curcumin, it has been proposed that future research focus on the reduced metabolites such as hexahydro- or tetrahydro-curcumin (Sharma et al., 2005), since replicating biologically effective *in vitro* concentrations of curcumin *in vivo* seems rather unlikely (Dempe et al., 2013). However by improving drug delivery, the usefulness of curcumin could be enhanced.

1.5.2.2 Pharmacological activities

Curcumin has gained research popularity due to recent reports of its ability to modulate biological targets which are key in regulating homeostasis in mammals (Aggarwal et al., 2007; Aggarwal and Sung, 2009). Furthermore, biotechnological advances in drug delivery such as nanoparticles and liposomal encapsulation of curcumin have produced promising results to support its therapeutic potential (Li et al., 2005; Choudhury et al., 2016).

Anticancer and anti-inflammatory effects were observed in male athymic colon cancer-induced mice, where daily oral dose of 1 g/kg curcumin, given for four weeks, decreased expression of genes involved in metastasis (CXCR4 – 68%), invasion (MMP-9 – 64%) and inflammation (COX-2 - 49%) (Kunnumakkara et al., 2009). Curcumin also decreased

expression of anti-apoptotic proteins Bcl-xL and Bcl-2 in colon cancer cell lines – HCT 116, HT29 and SW620 (Kunnumakkara et al., 2009). Antioxidant activities of curcucum have been reported in an *in vitro* study, where 0.14 mM curcumin decreased the level of thiobarbituric acid reactive substances in platelet and plasma components by 35% (Kolodziejczyk et al., 2011).

A number of pharmacological activities by curcumin and its metabolites have also been reported in *in vivo* and *in vitro* studies, which could be related to antidiabetic and hepatoprotective effects. Curcumin exhibited a repressive effect on lipid metabolism, suggesting its lipid-lowering potential (Asai and Miyazawa, 2001). Evidence of therapeutic efficacy in diabetes was demonstrated by promoting skeletal muscle glucose uptake and AMPK/ACC (AMP-activated protein kinase/acetyl-CoA carboxylase) phosphorylation, in addition to induction of AMPK/ACC and PI3-kinase/Akt pathways during co-administration with insulin (Kang and Kim, 2010). Anti-diabetic effects have been related to activation of Nrf2 nuclear translocation, resulting in reduced ROS-mediated insulin resistance in human LO2 hepatocytes (Zhao et al., 2011).

Curcumin is a known antioxidant compound with strong antiradical activities. It has been reported that curcumin prevented ROS-induced oxidative damage by scavenging free radicals and preventing GSH depletion in hepatocytes (Zhao et al., 2011). Curcumin also belongs to the group of Michael acceptor compounds, which interact with intracellular sensors on cysteine-rich Keap1 protein, a negative regulator of Nrf2 (Dinkova-Kostova and Talalay, 1999). It is also reported that curcumin induces cellular ROS production, which could serve as a trigger for transcriptional activation of Nrf2 and MAP kinases to up-regulate haem-oxygenase 1 (HO-1) in liver cells (McNally et al., 2007). Thus, curcumin elicits antioxidant effect by directly scavenging free radicals and by up-regulating cytoprotective proteins. As a result of its strong antioxidant properties, pretreatment with 10 μM curcumin protected against streptozotocin-induced DNA damage in murine islets, and restored insulin levels and islet viability (Meghana et al., 2007).

1.5.3 Sulforaphane

Sulforaphane is an isothiocyanate produced from the hydrolysis of glucoraphanin, a plant-derived glucosinolate (Fig 1.13). Glucoraphanin is a 4-methylsulfinylbutyl glucosinolate found in several cruciferous vegetables such as cabbage, Brussels sprout, cauliflower, kale, cole crops and collards, but mainly obtained from broccoli (*Brassica oleracea*) and broccoli sprouts (Stoewsand, 1995; Tian et al., 2005). Glucoraphanin is an inducer of cytochrome P450 isoforms in the liver and produced pro-oxidant effects at concentrations above 120 mg/kg body weight in rats (Perocco et al., 2006).

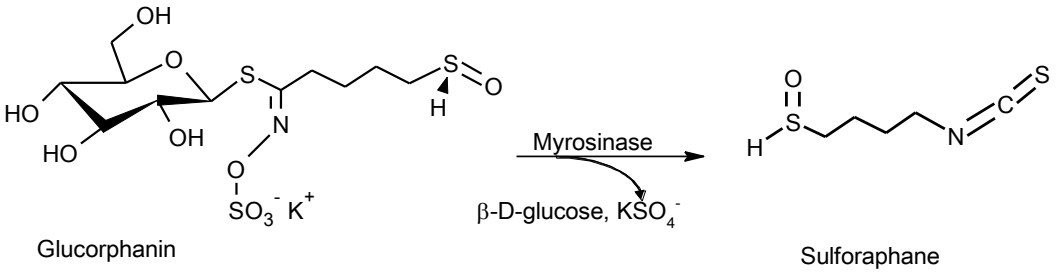

Figure 1.13 Enzymatic hydrolysis of glucoraphanin in the upper gastrointestinal tract to release sulforaphane.

1.5.3.1 Metabolism and bioavailability

Cleavage of glucoraphanin occurs in the upper gastrointestinal tract by endogenous plant-specific myrosinases (β-thioglucoside glucohydrolase enzymes) (Guerrero-Beltrán et al., 2012; Fig 1.13). Consequently, sulforaphane is absorbed by passive diffusion in the jejunum yielding high uptake due to its good lipid solubility (Petri et al., 2003). These authors also reported conjugation of sulforaphane during absorption and increase in mRNA levels of glutathione S-transferase in enterocytes, as well as efflux of sulforaphane-GSH back into the intestinal lumen which could be mediated by P-glycoproteins. Sulforaphane-GSH conjugates are also transported by multidrug resistant proteins 1 and 2 (MRP1 and 2), via the hepatic portal vein (Keppler et al., 1997; Harris and Jeffery, 2008). It has, however, been reported that metabolism of sulforaphane and its distribution, as well as that of its metabolites are not influenced by the presence of Nrf2 and glutathione S-transferase-P 1 (GSTP1) polymorphism (Clarke et al., 2011). The remaining intact glucoraphanin is hydrolysed by *Clostridia* and *Lactobacilli* in the lower

gut to produce isothiocyanates including sulforaphane, erucin and nitriles, in a pH-sensitive environment (Lai et al., 2010; Guerrero-Beltrán et al., 2012); also, see Fig 1.14.

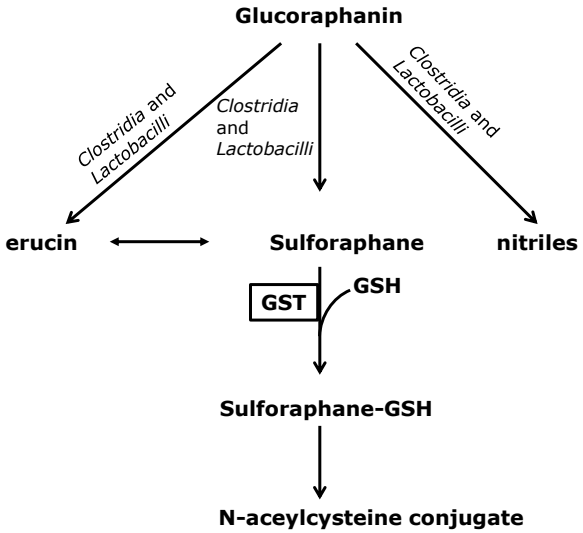

Figure 1.14 Enzymatic hydrolysis of glucoraphanin in the lower gastrointestinal tract to release sulforaphane, erucin and nitriles. As described in text, sulforaphane is subsequently metabolised to produce sulforaphane–GSH, which is later metabolised to N-acetylcysteine (Petri et al., 2003; Hwang and Jeffery, 2005; Lai et al., 2010).

The initial hydrolysis by plant myrosinase is essential to obtaining adequate plasma levels of sulforaphane, since colonic hydrolysis accounts for delayed peaks and lower plasma concentration (Clarke et al., 2011). Consumption of 40 g broccoli sprouts (containing 150 μmol and 71 μmol glucoraphanin and glucoerucin, respectively) by humans produced plasma levels of 2.5 μM and 1 μM euricin within 5 min of intake, but declined sharply within 10 min (Clarke et al., 2011). However when food is heated, plant endogenous myrosinase is deactivated and therefore it cannot cleave glucoraphanin to yield sulforaphane, sulforaphane will then not be absorbed (Conaway et al., 2000).

Sulforaphane is absorbed across both upper and lower gut walls but partly inter-converted by reduction of the sulfoxide moiety to a sulphide, forming a less bioactive compound erucin after intestinal absorption (Clarke et al., 2011). An analysis of mesenteric plasma revealed that sulforaphane was predominantly present as conjugates in rats (Wang et al., 2011). Sulforaphane cysteine-glycine (SFN-CG) was recorded as the

dominant metabolite in human plasma (82%), while sulforaphane-cysteine was barely detected (Clarke et al., 2011). Sulforaphane-cysteine was obtained from urine at 18%, 12 h after intake of broccoli sprouts (Clarke et al., 2011). The sulforaphane-glutathione conjugate is further metabolised to N-acetylcysteine conjugate which was found in urine (Hwang and Jeffery, 2005) (Fig 1.14). Clarke et al., (2011) recorded 72% and 83% of sulforaphane-N-acetylcycteine and erucin-N-acetylcysteine, respectively in urine.

1.5.3.2 Pharmacological activities

Consumption of sulforaphane-containing foods has been associated with several health benefits, mainly anticancer effect, which has been demonstrated in several carcinomas (Barcelo et al., 1996). Bioefficacy of sulforaphane and metabolites is determined by its bioavailability, with levels of intact and conjugated sulforaphane in plasma comparable levels to those in liver, kidney and lungs (Clarke et al., 2011). In Sprague Dawley rats, pre-treatment with 500 µg/kg/day for 3 days repressed post-ischaemic left ventricular end-diastolic pressure by 50% and increased coronary blood flow by 2 ml/min compared to control (Piao et al., 2010). In addition, Piao et al., (2010) observed sulforaphane-mediated reduction (27%) in infarct size and restored levels of catalase, HO-1 and SOD after repurfusion injury, partly via antioxidant mechanisms and mitochondrial K_{ATP} channels.

Lai et al., (2010) reported sulforaphane-mediated up-regulation of GCL via Nrf2 activation. Antioxidant effect of sulforaphane is mainly mediated through the induction of Phase II drug metabolising enzymes, which are ubiquitously present in various cell types, as well as through some Phase III transporters (Guerrero-Beltrán et al., 2012). While sulforaphane exists in R-S isomerism, it has been found in both liver and lung tissues that the R enantiomer is responsible for antioxidant potency in humans, acting as an inducer of cytoprotective enzymes (Abdull Razis et al., 2011).

Activation of Nrf2 activities by sulforaphane led to attenuation of oxidative cell damage and neutrophil proliferation in brain tissues subjected to intracerebral haemorrhage (Zhao et al., 2007), this by progressive up-regulation of HO-1 which inhibited cerebral

inflammation (Innamorato et al., 2008). It is also worth noting that pre-treatment of dopaminergic cells, CATH and SK-N-BE(2)C, with sulforaphane induced both mRNA and enzyme activity levels of quinone reductase, an ARE-driven target enzyme (Han et al., 2007). In retinal ARPE-19 cells, induction of Phase II enzymes prevented H_2O_2-mediated cell death caused by *tert*-butyl hydroperoxide (*t*BHP) (Cano et al., 2008). There are also reports on antidiabetic effects of sulforaphane, showing increased insulin levels which reduced hyperglycaemia and preserved function of pancreatic β-cells (Guerrero-Beltrán et al., 2012). In a randomised study on type 2 diabetic subjects receiving broccoli sprout powder supplements, insulin resistance declined after 4 weeks of treatment (Bahadoran et al., 2012). Sulforaphane is also reported to protect against streptozotocin-induced β-cell damage *in vitro*, by attenuating NF-KB pathway a concentration-dependent manner (Song et al., 2009).

1.5.4 Rosmarinic acid

Rosmarinic acid (α-O-caffeoyl-3, 4-dihydroxyphenyl lactic acid; Fig 1.15) is a secondary metabolite in herbs of the Lamiaceae family such as *Perilla frutescens* (beefsteak plant), *Silvia officinalis* (sage), *Melissa officinalis* (mint), *Ocimum canum* (basil), *Origanum vulgare* (oregano), *Rosmarinus officinalis* (rosemary) and *Thymus vulgaris* (thyme) (Petersen and Simmonds, 2003).

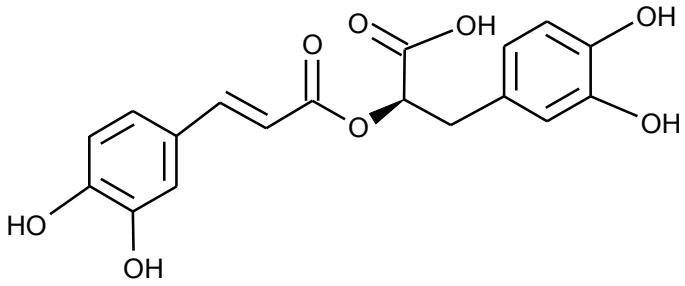

Figure 1.15 Chemical structure of rosmarinic acid.

Most of these plants are used traditionally against infectious diseases, inflammatory and neurological conditions (Youn et al., 2003). Rosmarinic acid is an acid ester of caffeic acid and 3,4-(dihydroxyphenyl)lactic acid, and is known to inhibit inflammatory effects

through decreasing expression of COX-2 enzymes and prostaglandin levels (Youn et al., 2003; Osakabe et al., 2004). Anti-inflammatory activities have been demonstrated in various skin models, 48 h treatment with 25 μM rosmarinic acid led to 23% radioprotection in human lymphocytes (Sánchez-Campillo et al., 2009), while using cream with 0.3% rosmarinic acid improved symptoms of atopical dermatitis in human subjects (Lee et al., 2008). Thus, indicating its potential therapeutic and protective use in topical disorders.

There is substantial evidence confirming the free-radical scavenging and lipid-lowering effects of rosmarinic acid (Al-Musayeib et al., 2011; Brosková et al., 2012; De Oliveira et al., 2012), in addition to anti-apoptotic activities via blocking caspase-3 activity (Gao et al., 2005). Antioxidant properties of several plants have been linked to their high rosmarinic acid content (Lee et al., 2013). *Ocimum canum* Sims (Ghanaian plant known as Akokobesa) a regular kitchen spice, is used traditionally as an antidiabetic in Ghana (Berhow et al., 2012). Following HPLC analysis of its extracts, Berhow et al., (2012) identified rosmarinic acid as a prominent constituent of *Ocimum canum* Sims and proposed that rosmarinic acid could account for the alleged antidiabetic effect of this herbs. Antidiabetic effects could be supported by improved insulin sensitivity and decreased plasma lipid levels, oxidative damage and cardiac hypertrophy in fructose-fed hypertensive rats following supplementation with 10 mg/kg rosmarinic acid for 44 days (Karthik et al., 2011). An *in vitro* study also reported protection against sorbitol-induced free radical-damage following 1 h pre-incubation with 25 μM rosmarinic acid (Salimei et al., 2007), suggesting that antidiabetic effects could be linked to its antioxidant properties.

Lima et al., (2006) reported a direct antioxidant effect of rosmarinic acid which led to increased basal levels of cellular GSH and decreased lipid peroxidation in HepG2 hepatoma cells. This report correlated positively with a subsequent study, where sage extracts protected against *t*BHP-induced GSH depletion in the same *in vitro* model (Lima et al., 2007). Both ethanolic and water-based extracts of sage, which were rich in phenolic compounds including rosmarinic acid, also reversed liver fibrosis, indicating potential in protecting against oxidative stress in liver diseases (Lima et al., 2007). The principal evidence of antioxidant potential has been reported with plant extracts and *in*

vivo models; however, cytoprotective mechanism of rosmarinic acid still remains to be explored. Nevertheless, the above evidence suggests that rosmarinic acid is primarily an antioxidant compound and may be of interest in diseases for which oxidative stress plays a key role.

What is becoming apparent in studies involving plant chemicals is that whilst chemicals have been identified as antioxidants, there is very good evidence, that in many instances a low amount of the parent compound can be identified in plasma after oral administration. This may be due to substantial extreme pre-systemic metabolism, hence the metabolism of rosmarinic acid needs to be appreciated – this is discussed in detail in the following section.

1.5.4.1 Metabolic pattern of rosmarinic acid

Rosmarinic acid is metabolised to derivatives of ferulic acid, *m*-coumaric acid, 3,4-(dihydroxyphenyl)lactic acid and caffeic acid by gastrointestinal enzymes (Baba et al., 2004). Orally-administered rosmarinic acid is rapidly but poorly absorbed into the abdominal aorta via paracellular diffusion in the upper gut, yielding very low amounts of rosmarinic acid in plasma (Konishi et al., 2005). In the liver, rosmarinic acid is conjugated to methyl derivatives and glucuronides by catechol-O-methyl transferases (COMT) and UDP-glucuronosyltransferases respectively, and occurs as conjugates in plasma (Baba et al., 2004, 2005). An LC-MS (liquid chromatography-mass spectrometry) analysis of plasma levels obtained from male Sprague-Dawley rats, following oral intake of rosmarinic acid at a dose of 50 mg/kg body weight, indicated that most of intact rosmarinic acid absorbed from the upper gastrointestinal tract (4.63 μM) is methylated by COMT to methyl-rosmarinic acid (Baba et al., 2004). Methyl-rosmarinic acid was subsequently obtained as conjugate and free forms in urine (Baba et al., 2004).

Moreover, following a single oral dose of *Perilla fructescens* extract which contained 200 mg rosmarinic acid in human subjects, about 50% of rosmarinic acid was absorbed from the gut with peak levels of total methyl-rosmarinic acid at 1.15 μM (Baba et al., 2005), urinary detection was similar to the profile obtained with an earlier study in rats (Baba et

al., 2004). The remaining rosmarinic acid is degraded by esterases of the colonic microflora in the lower gut to 3,4-(dihydroxyphenyl)lactic acid and caffeic acid (Nakazawa and Ohsawa, 1998; Bel-Rhlid et al., 2009) (Fig 1.16).

Bel-Rhlid et al., (2009) identified *Lactobacillus jonhsonii* as the main microorganism responsible for this cleavage of rosmarinic acid. These colonic bacteria are also found in humans (Couteau et al., 2001) and could be responsible for colonic hydrolysis of the phenolic ester in humans. Thus, the abundance and function of colonic bacteria could influence the bioavailability as well as bioefficacy of rosmarinic acid metabolites, since absorption of parent compound in the colon remains to be elucidated.

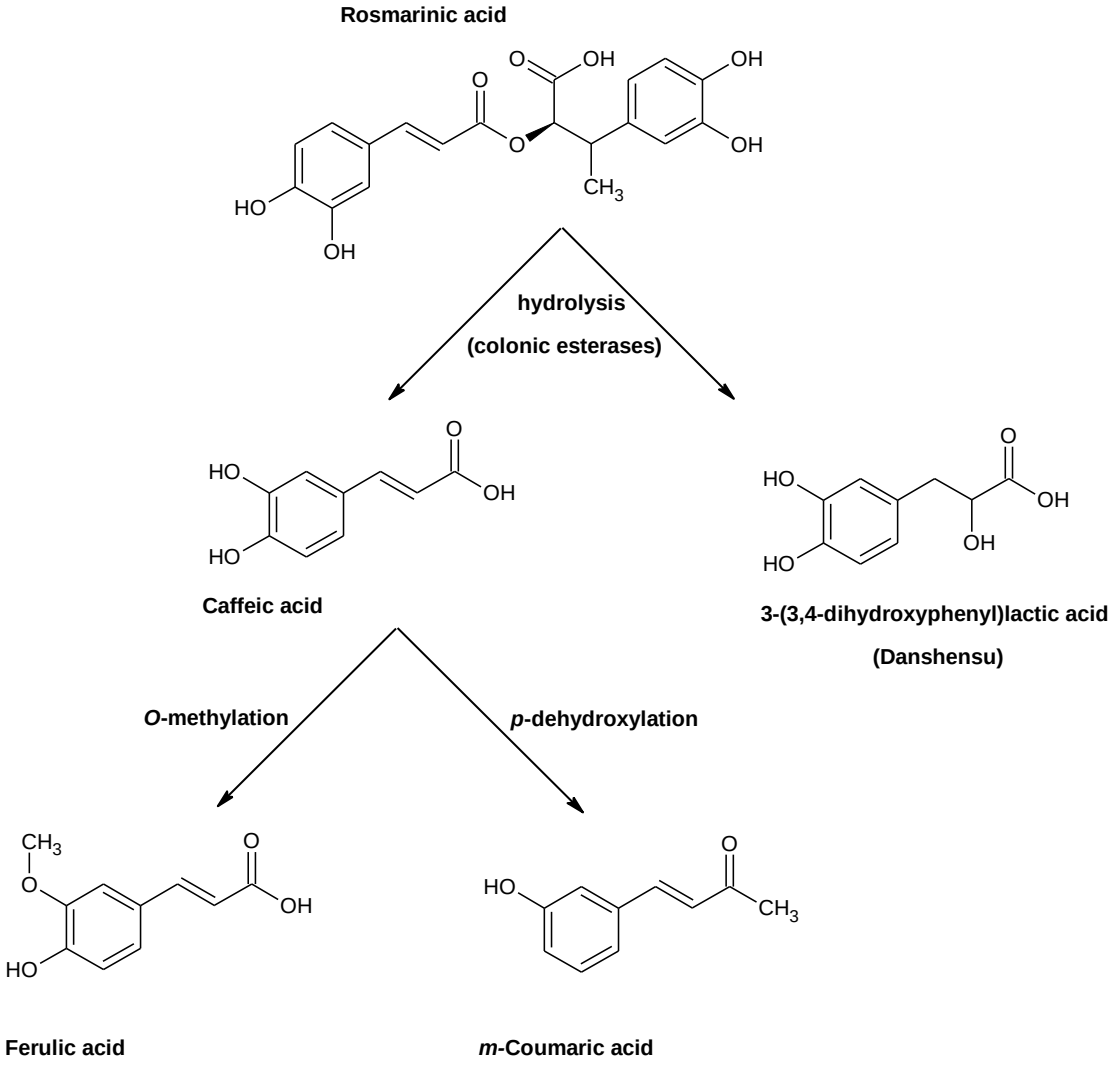

Figure 1.16 Metabolic pathway of rosmarinic acid after oral intake. Hydrolysis of rosmarinic acid occurs in the gastrointestinal tract leading to subsequent metabolism of caffeic acid to ferulic acid and *m*-coumaric acid in the lower gut.

Caffeic acid is predominantly absorbed from the gut by paracellular diffusion but also has low affinity for monocarboxylic acid transporters, which contributed to higher plasma levels of caffeic acid than rosmarinic acid in rats (Konishi et al., 2005). This suggestion was in accordance with the observation that the area under the curve ($AUC_{abdominal}$) for caffeic acid was approximately 7-fold greater than rosmarinic acid (Konishi et al., 2005). In the same study, greater intestinal absorption of caffeic acid also correlated with higher plasma concentration (11.2 ±2.3 μM) compared to rosmarinic acid (1.4 ±0.1 μM), following a dose of 100 μmol/kg body weight (Konishi et al., 2005). Thus, structural modification of monocarboxylic acid transporter substrates hinders affinity of compounds (such as rosmarinic acid) for the transporter (Konishi et al., 2005).

1.5.5 Caffeic acid

The polyphenol caffeic acid (3,4-dihydroxycinnamic acid), is a constituent in herbs such as *Eucalyptus globulus* (Santos et al., 2011) and *Salvinia molesta* (Choudhary et al., 2008). Caffeic acid can also be obtained from honey (Jaganathan et al., 2010), coffee beverage, ciders, blueberries and apples, in conjugate forms with quinnic acid to produce chlorogenic acids such as 5-O-caffeoyl-quinic acid and caffeoylquinic acid, and di-esters, tri-esters and tetra-esters of caffeoylquinic acid (Clifford, 1999). *Caffea canephora* (Alonso-Salces et al., 2009) and *Gardenia jasminiodes* (Nishizawa et al., 1987; Clifford, 1999) of the family Rubiaceae, also contain mixed di-esters of caffeic acid and ferulic acid (3-caffeoyl-4-feruloylquinic acid) and sinapic acid (caffeoylsinapoylquinic acid).

The supply of chlorogenic acid, a major constituent in roast coffee, is largely dependent on type of roast, with up to 675 mg consumed from 200 ml strong brew yielding approximately 338 mg caffeic acid; regular coffee consumers take 500 – 1000 mg/day (Clifford, 1999). Herbs such as rosemary and basil are rich in rosmarinic acid but they are consumed in minimal amounts hence, regarded as a poor source of conjugated caffeic acid (Clifford, 1999).

.

1.5.5.1 Metabolic pattern

Caffeic acid is also a prominent product from *in vivo* metabolism of rosmarinic acid after oral intake by humans (and rats) (Rubio et al., 2012). Caffeic acid is metabolised by gut microbiota, by mechanisms other than esterification (Gonthier et al., 2006). Caffeic acid could also be partly metabolised into its *O*-methylated derivatives, ferulic and isoferulic acid, by the small intestinal epithelium during absorption across the gut epithelium (Kern et al., 2003; Lafay et al., 2006) (Figs 1.17 and 18).

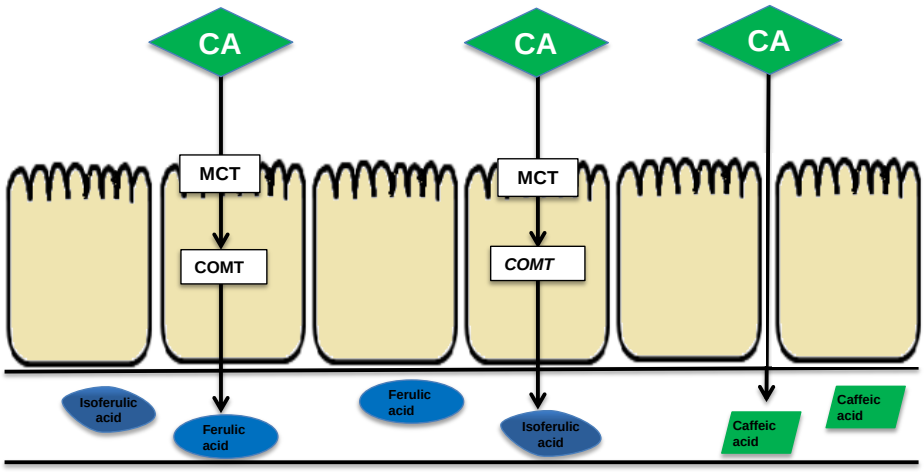

Figure 1.17 Intracelluar metabolism of caffeic acid by the small intestinal epithelium. Caffeic acid is partly absorbed intact in the small intestines by passive dissufion, while cathecol-O-methyl transferases (COMT) in the epithelium metabolise caffeic acid to ferulic and isoferulic acid.

Regarding the detection of ferulic acid (in either free or conjugate forms) in plasma, earlier research conducted in rats has provided contradictory reports after oral intake of rosmarinic acid or caffeic acid. Whilst conjugates of ferulic acid were detected in rat urine after oral dosing with rosmarinic acid (Nakazawa and Ohsawa, 1998; Baba et al., 2004) and caffeic acid (Camarasa et al., 1988), Konishi et al., (2005) could not detect either the metabolite or its conjugates. However, both free and conjugate forms of ferulic acid were detected in human plasma, within 30 min of administering an extract of *Perilla fructesens* (containing 200 mg rosmarinic acid; Baba et al., 2005). This then highlights species variation in models used to evaluate pharmacokinetic profile of experimental compounds.

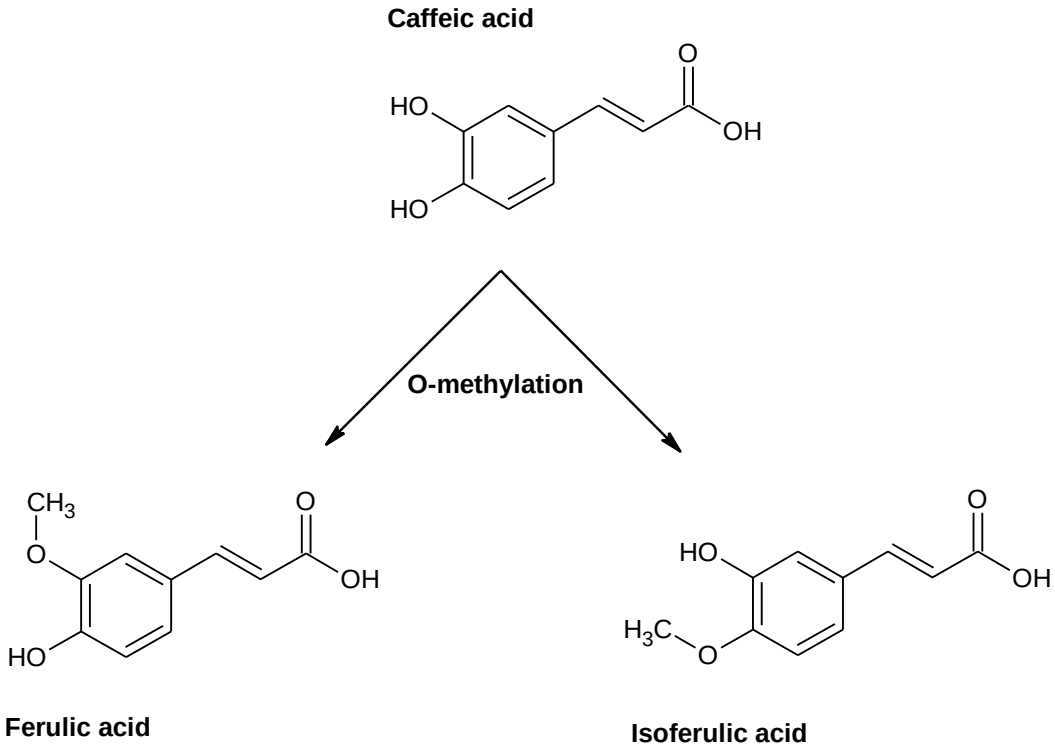

Figure 1.18 *O*-methylation of caffeic acid in the small intestine, following oral intake.

The actual site of *m*-coumaric acid production has not been elucidated although, *m*-coumaric acid was detected in rats, 8 h after oral administration of rosmarinic acid (Baba et al., 2004). Also, Baba et al., (2005) detected trace amounts of *m*-coumaric acid in urine 24 – 48 h after administering *Perilla fructescens* to humans. The most likely reaction for production of *m*-coumaric acid in the lower gut is *para*-dehydroxylation, which could either result from a series of metabolic reactions or possibly a single double de-hydroxylation reaction. However, an earlier report in rats suggests that gut microflora are responsible for generating *m*-coumaric acid following reduction and then *para*-dehydroxylation of caffeic acid in rats (Goodwin et al., 1994) (Fig 1.16). Additionally, *m*-hydroxyphenylpropionic acid was detected as a plasma metabolite of *Perilla fructescens* extract following oral intake in rats (Nakazawa and Ohsawa, 2000).

Metabolism by Phase I and II enzymes, which occurs during and after absorption, influences the bioefficacy of hydroxycinnamic acids such as caffeic acid and *m*-coumaric acid (Lafay et al., 2006). Caffeic acid, ferulic and *m*-coumaric acid are transported to the

liver, where glucuronidation, methylation and sulfation occur (Nakazawa and Ohsawa, 1998; Baba et al., 2004, 2005). Also, studies have shown that sulfation occurs during absorption into the abdominal aorta (Kern et al., 2003; Baba et al., 2005) with subsequent glucuronidation in the liver (Kern et al., 2003).

Caffeic acid and ferulic acid, undergo sulfation by sulfotransferase 1A1 (SULT1A1) at the 3-hydroxyl position, which has been found to contribute positively towards their antioxidant potencies (Wong et al., 2010). Some key metabolites of caffeic acid, including glucuronide and sulfate derivatives, retain their antioxidant properties *in vitro* (Piazzon et al., 2012). A brief review on the two main derivatives of caffeic acid, ferulic acid and *m*-coumaric acid is presented in Sections 1.5.6 and 1.5.7.

1.5.5.2 Pharmacological activities

Caffeic acid is also reported to have antioxidant, anticancer and antimutagenic effects (Okutan et al., 2005). In a concentration-dependent manner, caffeic acid (0.05 – 1 mM) repressed tumour invasiveness and angiogenesis via decreasing TNF-α, IL-1β and IL-8 levels by 67%, 45% and 31%, respectively at 1 mM, while increasing anti-inflammatory cytokine IL-10 levels after 72 h incubation in hepatocellular carcinoma cells (Guerriero et al., 2011). Caffeic acid also enhanced concentrations of endogenous antioxidants, as well as increased lipoprotein resistance to oxidation *ex vivo* (Lafay et al., 2006).

In diabetic Wistar rats, administration of an extract of *Cyamposis tetragonoloba* enhanced glucose uptake and insulin secretion, with antidiabetic effects attributed to protective activities of its polyphenol constituents, caffeic acid and gallic acid (Gandhi et al., 2014). Caffeic acid (0.02% of diet), after 5-weeks supplementation in diabetic mice, improved β-cell viability and structure, and increased plasma insulin levels by 64%, leading to 15 mmol/L reduction in blood glucose (Jung et al., 2006). In addition, Jung et al., (2006) observed improved glucose uptake by adipose cells as well as decreased insulin resistance in the liver.

It is also reported in adult male Wistar rats that intact caffeic acid in the small intestines (administered orally at 250 mg/kg body weight, 15 and 120 min after single intraperitoneal

dose of cisplatin - 6 mg/kg body weight) restored intestinal enzymes to control levels (Arivarasu et al., 2013). In the same study, caffeic acid restored basal activities of endogenous antioxidants – catalase, glutathione peroxidase, glutathione reductase and thioredoxin; thus, could be of therapeutic importance against gastrointestinal toxicity.

In *Perilla frutescens* extract, caffeic acid was the constituent responsible for increase in GCL levels, yielding 1.4 – 1.8–fold increase in activity and 1.7 - 2.7-fold surge in GSH levels, following 72 h treatment with 0.56 - 2.78 mM caffeic acid in HepG2 hepatoma cells (Park et al., 2010). Protection against cerebral ischaemia in rats was displayed via inhibition of 5-lipooxygyenase activity (Zhou et al., 2006). Cytoprotective activities of rosmarinic acid have also been linked to antioxidant effects of its metabolite, caffeic acid (Yang et al., 2013).

1.5.6 Ferulic acid

Ferulic acid (4-hydroxy-3-methoxycinnamic acid) is present in fruits and vegetables such as bananas, tomatoes, carrots, coffee, cereals, (D'Archivio et al., 2007; Mancuso and Santangelo, 2014) and Chinese herbs including *Angelica sinensis* and *Cimicifuga racemose* (Ou and Kwok, 2004). Ferulic acid does not exist as a free form, but as conjugates via ester-linkages with mono-, di- and poly-saccharides in the cell wall (for example, 5-O-ferouloyl-2-arabinofuranose and 5-O-ferouloylarabinoxylane are the most common forms of ferulic acid in cereals) (Saulnier et al., 1995; Clifford, 1999). Also, ferulic acid conjugates with hydroxyl fatty acids, suberin and cutin, glycoproteins, liginin and polyamines (Bourne and Rice-Evans, 1998; Mancuso and Santangelo, 2014). These conjugates are hydrolysed by colonic microbial cinnamoyl esterases (Couteau et al., 2001), xylanase and ferulic acid esterases (Kroon et al., 1997).

The free ferulic acid, which either results from its conjugates or as a derivative of caffeic acid, is predominantly absorbed by passive diffusion, with a small proportion absorbed by monocarboxylic acid transporters (Poquet et al., 2008), with peak levels recorded under 15 min (Zhao et al., 2003). Earlier studies in Wistar rats observed that 50% ferulic acid was absorbed after gastric perfusion with 250 µM ferulic acid, this was available to

tissues, although it was rapidly eliminated accounting for plasma levels of 7.6 μM (Adam et al., 2002).

Ferulic acid is metabolised by 1A1 and 2B7 isoforms of UDP-glucuronosyltransferase (Li et al., 2011) and sulfotransferases, mostly by SULT1E (Wong et al., 2010), to produce sulfoglucuronide conjugates as predominant forms in plasma; a small percentage of glucuronide and free forms of ferulic acid are also present in plasma (Bourne and Rice-Evans, 1998; Zhao et al., 2004). Conjugation of ferulic acid occurs mainly in the liver (Zhao et al., 2004) and to a lesser extent in the intestinal mucosa and kidney (Kern et al., 2003; Zhao et al., 2003). However, conjugation does not affect bioavailability of ferulic acid.

Low levels of ferulic acid also undergo β-oxidation in the liver to 4-hydroxy derivatives (Chesson et al., 1999). Additional plasma and urinary metabolites detected in rats were vanillic acid, vanilloylglycine, feruloylglycine, *m*-hydroxyphenylpropionic acid and dihydroferulic acid (Zhao et al., 2003; Zhao and Moghadasian, 2008; Choudhury et al., 1999). As far as can be ascertained, there is currently no report on the methylation of ferulic acid in the gastrointestinal tract or liver.

Studies in rats and humans have shown that conjugates of ferulic acid, as found in plants, affect its pharmacokinetic parameters such as increasing the time for achieving peak plasma levels, increasing half-life and decreasing peak plasma levels (Zhao et al., 2004; Mancuso and Santangelo, 2014). For example, amount of ferulic acid recorded in rat plasma was after single oral dose of ferulic acid and 5-O-feruloyl-$_L$-arabinofuranose (equimolar amounts of 70 μmol ferulic acid/kg body weight) were 23.0 μM at 30 min and 109.5 μM at 15 min, respectively after ingestion (Zhao et al., 2003).

Additionally, total ferulic acid was detected in rat plasma at 240 min after administration of ferulic acid ester compared to rats given ferulic acid alone, which recorded no amount of the total compound (Zhao et al., 2003). As a metabolite of RA, both modified and unmodified forms of ferulic acid are excreted in urine (Bourne and Rice-Evans, 1998). Adam et al., (2002) observed biliary excretion of up to 7% of ferulic acid from

supplements, while food matrix of diet rich in ferulic acid showed impaired absorption, with significant levels of ferulic acid in faeces.

1.5.6.1 Pharmacological activities

It is reported that ferulic acid shows promising therapeutic potential in several conditions including cancers, diabetes, Alzheimer's and cardiovascular diseases (Mancuso and Santangelo, 2014). In streptozotocin-induced diabetic rats, blood glucose levels were reduced by 145 – 169 mg/dl after 21 days of receiving oral dose of 10 mg/kg ferulic acid per body weight (Prabhakar et al., 2013). These authors also observed synergistic hypoglycaemic effects when ferulic acid was administered in concert with oral hypoglycaemic agents – metformin (50 mg/kg) and thiazolidone - resulting in increased islet size, while decreasing occurrence of side-effects observed after administration of thiazolidinedione alone (Prabhakar et al., 2013). Ferulic acid also improved insulin secretion, which occurred concomitantly with decreased blood glucose levels, total cholesterol and low-density lipoprotein concentrations in type 2 diabetic mice, as well as increased hepatic glycogenesis (Jung et al., 2007).

Ferulic acid possesses strong antioxidant properties, which are defined by the presence of electron-donating groups on its benzene ring (4-hydro and 3-methoxy groups) and carboxylic group on the ferulic acid structure (Kanski et al., 2002). These functional groups enhance its free radical scavenging and anti-lipid peroxidation activities. The antioxidant potential of ferulic acid was evaluated in carbon tetrachloride-induced hepatotoxicity in female rats, daily oral dose of 20 mg/kg ferulic acid for 90 days reduced TBARS in liver and kidney tissues by approximately 35%, and increased GSH levels by 29% (Srinivasan et al., 2005). These reports promote the notion that intake of ferulic acid could provide cytoprotection against oxidative stress.

1.5.7 *m*-Coumaric acid

m-Coumaric acid, a microbial metabolite of caffeic acid, is dissimilar to ferulic acid in the sense that, as far as can be ascertained, there are currently no reports on its natural

occurrence in fruits and vegetables. The *m*-hydroxycinnamic acid is, however, present in vinegar (Gálvez et al., 1994). In addition to rosmarinic acid and caffeic acid, *m*-coumaric acid is also a microbial metabolite detected after oral intake of chlorogenic acid in rats (Gonthier et al., 2003).

m-Coumaric acid, as the last major metabolite produced from caffeic acid in the gut, was detected in plasma, and accumulated slowly in urine 18 h after rosmarinic acid administration in rats (Nakazawa and Ohsawa, 1998). However, *m*-coumaric acid has high affinity for mono-carboxylic acid transporters (Konishi and Kobayashi, 2004), due to the presence of the monocarboxylic group, and an aromatic hydrophobic moiety which facilitate its absorption (Rahman et al., 1999).

There is currently limited literature on the pharmacological benefits of *m*-coumaric acid. However, antioxidant activity of *m*-coumaric acid was determined as 1.7 μM Trolox equivalent (Gomez-Ruiz et al., 2007). This suggests that the caffeic acid metabolite may retain antioxidant properties of its parent compound.

1.5.8 3,4-(dihyroxyphenyl)lactic acid

Danshensu (3,4-dihyroxyphenyllactic acid), a product obtained from hydrolysis of rosmarinic acid, is also present in aqueous extracts of *Salvia miltiorrhiza* (Zhou et al., 2006), a perennial Chinese plant known generally as Danshen or red sage. Intestinal absorption of danshensu is facilitated by P-glycoprotein transporter (Zhou et al., 2006), promoting good plasma distribution of the plant compound (Zhang et al., 2011). Although the mechanism involved has not been reported, danshensu is metabolised to isopropyl 3-(3,4-dihydroxyphenyl)-2-hydroxypropanoate, a vasodilator (perhaps via esterification, Fig 1.18), which is rapidly eliminated after oral ingestion in rats (Zhang et al., 2008).

3-(3,4-dihydroxyphenyl)lactic acid

(Danshensu)

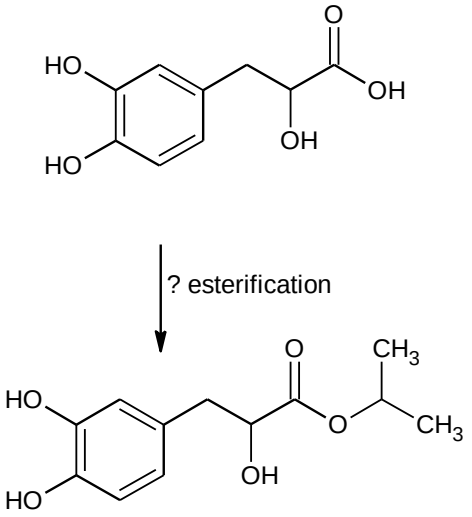

Isopropyl 3-(3,4-dihydroxyphenyl)-2-hydroxypropanoate

Figure 1.19 Metabolism of danshensu to isopropyl 3-(3, 4-dihydroxyphenyl)-2-hydroxypropanoate in rats, after oral intake.

1.5.8.1 Pharmacological activities

As with most phenolic acids, the presence of the tri-hydroxyl group on its structure could account for antioxidant effects (Han et al., 2009), as well as radical scavenging against 2,2-diphenyl-1-picrylhydrazyl ($DPPH^{\cdot}$) radical and superoxide anions (Zhao et al., 2008).

In hepatic stellate cells, 62.5 – 250 mM danshensu mediated anti-proliferative activity and reduction of type I collagen after 24 h exposure, via repressing c-Jun N-terminal kinases and NF-kappaB signalling (Yu et al., 2009). Co-exposure of hepatic stellate cells to 200 μM acetaldehyde and 150 μM danshensu repressed mRNA expression of transforming growth factor –β1 and plasmogen activator inhibitor-1, which were both up-regulated by treatment with acetaldehyde alone (Zhang et al., 2012).

In addition, 8 h treatment with danshensu induced apoptosis in fibroblasts (Jiang et al., 2001). Anti-inflammatory and antifibrotic activities suggest that danshensu could be investigated further for potential benefits in liver fibrosis and other forms of liver injury such as NASH, where inflammation plays a major role in its pathogenesis. The cardioprotective effect of danshensu, following oral intake of 160 mg/kg in rats for 21

days, was mediated by accentuating Nrf2 signalling (20% increase in protein levels) and anti-apoptotic gene Bcl-2, while decreasing Bax and caspase-3 protein levels (Li et al., 2012). Thus, danshensu could be of interest as an inducer of Phase II enzymes against oxidative damage. By stimulating mRNA expression of pregnane X receptor and potentially regulating cytochrome P450 enzymes, danshensu as a cytoprotective phytochemical and inducer of xenobiotic metabolism could augment disease prevention and possibly treatment (Liu et al., 2011).

1.6 Screening of antioxidant compounds

The antioxidant efficiency of any compound depends on its ability to donate an electron or hydrogen to stabilize free radical species (Fig 1.19). Thus, an antioxidant molecule can either be oxidized to a less reactive free radical or delocalise its structure to regain inert status. The use of *in vitro* assay methods are very popular for determining antioxidant efficiency of compounds (Karadag et al., 2009), as they enable direct chemical interaction between reductant and oxidant being assessed, to define radical scavenging properties of the compound.

Dietary phytochemicals exhibit either free-radical scavenging activities (i.e., attenuating free radical chain reactions) or preventative antioxidant activities (inhibiting reactive oxidation reactions) (Karadag et al., 2009).

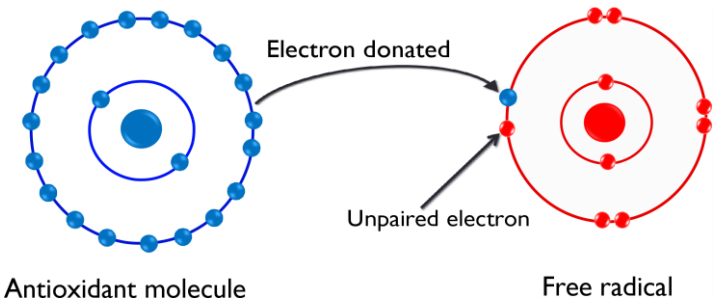

Figure 1.17 Antioxidant molecule stabilizes a free radical species in a reduction reaction.

Preventative antioxidant activities are accurately determined in a cellular environment, where cytoprotection is observed. Hence, not all reductants can act as antioxidants (Karadag et al., 2009).

1.6.1 Chemical-based antioxidant activity assays

There are various *in vitro* chemical-based methods used to determine antioxidant activity of compounds. These methods have been classified based on the ability of antioxidant compounds to engage in either electron transfer or hydrogen atom transfer, as determined by bond dissociation and ionisation potentials (Karadag et al., 2009).

Although hydrogen atom transfer methods such as oxygen radical absorption capacity assay (ORAC) are very rapid, they involve a synthetic free radical generator such as 2,2'-azino-bis(3-ethylbenzothiazoline-6-sulphonic acid) ABTS, antioxidant compound and an oxidizable molecular probe such as fluorescein (Moore et al., 2006; Karadag et al., 2009); therefore, the use of multiple variables could influence accuracy of these methods.

Electron transfer methods include Trolox equivalent antioxidant capacity (TEAC), 2,2-diphenyl-1-picrylhydrazyl (DPPH) and ferric reduction activity potential (FRAP) assays. Electron transfer methods involve a reaction mixture of reductant and oxidant, which also acts as a probe. During electron transfer, the oxidant receives an electron from the reductant causing a change in colour of the oxidant, which is proportional to the amount of reductant present in the mixture (Karadag et al., 2009) and serves as a marker for terminating the reaction. Extrapolation of effective concentration (denoted as EC_{50}) from linear curve defines the reducing capacity, also called antioxidant capacity or efficiency (Karadag et al., 2009).

The $DPPH^{\cdot}$ (2,2-diphenyl-1-picrylhydrazyl) radical is a purple organic nitrogen which is reduced to produce yellow hydrazine species, the stable form of DPPH (Fig 1.20). Classification of the DPPH scavenging assay as one based on electron transfer or hydrogen atom transfer is still debated (Magalhães et al., 2008; Karadag et al., 2009). However, DPPH scavenging is strongly influenced by pH and solvent of the reaction mixture, as is the case for electron transfer-based assays (Magalhães et al., 2007). Thus,

in strong hydrogen bond-accepting solvents such as methanol and ethanol, electron transfer is more dominant than hydrogen atom abstraction, which is minimal (Foti et al., 2004).

The DPPH· radical scavenging assay first reported by Brand-Williams et al., (1995) is widely used as a more reliable method than FRAP, for determining antioxidant activity of plant extracts (Clarke et al., 2013). This rapid method was used in this project to evaluate antioxidant activity of phytochemicals.

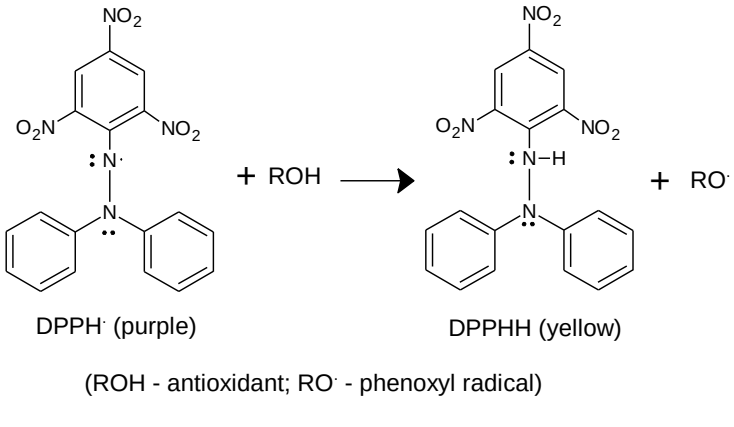

Figure 1.20 Radical scavenging of DPPH· free radical in methanolic and ethanolic solvents. This reaction was described by (Foti et al., 2004). During electron transfer, an antioxidant molecule (ROH) stabilizes a DPPH· radical which becomes 2,2-diphenyl-1-picrylhydrazine hydrogen (DPPHH).

Cytoprotection was assessed using two distinct methods against cytotoxicity resulting from oxidative damage; (i) direct cytoprotection: evaluated the ability of phytochemicals to alleviate high ROS levels in a cellular environment and (ii) indirect cytoprotection: evaluated the ability of phytochemicals to boost cellular cytoprotective enzymes against ROS-mediated oxidative damage. The direct cytoprotection model is more reminiscent of chemical-based radical scavenging and, therefore, indicates antioxidant activity, unlike indirect cytoprotection model which is taken to signify preventive activity. In accordance with their involvement in the pathology of NASH and T2DM, human hepatoma HepG2 cells and human pancreatic 1.1B4 β-cells were used as cellular models.

1.7 Research interest

As detailed in earlier sections, minimal ROS levels may be required for signalling during cellular activities however, persistent increase in ROS results in oxidative stress, leading to cell damage. Since NASH and T2DM are currently difficult to treat and incidence rates are likely to double in the next decade, the use of antioxidants, particularly of plant origin, to both prevent and treat such diseases has become of great interest. In addition, the expectation exists that phytochemicals present a safer alternative in disease treatment, due to constant exposure to the human body through diets.

A number of plant-derived antioxidants appear to exert their cytoprotective effects by one or both of two actions - a direct and an indirect effect. The direct effect is mediated via radical scavenging properties whilst the indirect effect is mediated via up-regulation of a variety of cellular antioxidant enzymes, many of which are involved in metabolism of redox-active species and in maintenance of intracellular redox homeostasis. Evidence also suggests that phytochemicals are able to modulate cellular antioxidant enzymes without oxidant challenge, see Section 1.5.

1.7.1 Rational of thesis

Based on the pharmacological activities of selected phytochemicals, it was proposed that quercetin, curcumin and sulforaphane could exhibit direct and indirect cytoprotective activities. Hence, they were used as reference phytochmeicals for evaluating the cytoprotective activities of rosmarinic acid and its principal metabolites. Evidence of cytoprotective activities by rosmarinic acid alongside its principal metabolites, in *in vitro* models, is currently lacking. Therefore this thesis presents a new approach in assessing their cytoprotective activities, to better understand their *in vivo* effects, following continuous intake of foods rich in rosmarinic acid.

Thus, experimental conditions used in this study were intended to evaluate the cytoprotective effects of dietary phytochemicals against oxidative stress *in vitro,* mimicking an *in vivo* scenario of their prolonged exposure to hepatocytes and pancreatic β-cells.

The following terminologies were also used to describe findings in this thesis:

- Additive effect: the sum of pharmacological effect of individual phytochemicals.
- Potentiative effect: the pharmacological effect of one phytochemical enhanced by another phytochemical to produce response greater than the sum of indivivial responses.
- Synergistic effect: the enhanced pharmacological effect resulting from an interaction between two phytochemicals with dissimilar individual effects.

1.7.2 Objectives of the study

This study was intended to investigate antioxidant and cytoprotective activities of phytochemicals against free radicals in cellular and non-cellular experimental models.

Specific objectives of this study were:

- To confrim radical scavenging activities of reference phytochemicals – quercetin, curcumin and sulforaphane - , and rosmarinic acid and its principal metabolites against DPPH free radical in a non-cellular assay. This work is presented in Chapter 2.
- To confirm direct and indirect cytoprotective activities of reference phytochemicals against *t*BHP (free radical generator) in human hepatoma HepG2 cells. This work is presented in Chapter 2.
- Subsequently, direct and indirect cytoprotective activities of rosmarinic acid alongside its principal metabolites, against *t*BHP, would be evaluated in HepG2 cells. This is a new approach to investigate the contribution of these principal metabolites towards cytoprotective activities of rosmarinic acid, in comparison with radical scavenging activities. This is work is presented in Chapter 2.
- To investigate cytoprotective activities of chosen phytochemicals (quercetin, curcumin, caffeic acid and sulforaphane) against *t*BHP in human pancreatic 1.1B4 β-cells. This novel study investigates the antioxidant potential of these phytochemicals in novel human pancreatic 1.1 B4 β-cells. This work is also presented in Chapter 2.

- To investigate the effects of selected phytochemicals on cell viability in HepG2 cells and 1.1B4 β-cells. This work is presented in Chapter 3.
- To assess vulnerability of HepG2 cells and 1.1B4 β-cells to cytotoxicity following high glucose and high lipid exposure. This work is presented in Chapter 4.
- A novel investigation of the cytoprotective effects of selected phytochemicals against lipotoxicity (by sodium palmitate) is presented in Chapter 4.
- To evaluate the role of NQO1 and other cellular proteomes in mediating indirect cytoprotective activities. This is a new approach to establish the ability of selected phytochemicals to upregulate cellular proteomes in pre-exposure conditions, to produce indirect cytoprotective activities against subsequent oxidative damage. This work is presented in Chapter 5.

1.7.3 Hypothesis

Based on the understanding of the oxidative stress theory of disease and antioxidant properties of phytochemicals, it was expected that;

- Phytochemicals will exhibit radical scavenging and cytoprotective activities against free radicals $DPPH^{\cdot}$ and *t*BHP, respectively; cytoprotective activities in HepG2 cells and 1.1B4 β-cells. This is the first report on cytoprotective acitivities of selected phytochemicals in 1.1B4 β-cells, as presented in Chapter 2.
- Furthermore, a novel comparison of the cytoprotective activities of selected phytochemicals, against *t*BHP-induced cytotoxicity and lipotoxicity, was made in Chapter 4. Thus, with the observation of cytoprotective acitivities against *t*BHP, it was proposed that selected phytochemicals would protect against more physiological stressors such as exposure to high levels of sodium palmitate.
- It was also proposed that indirect cytoprotection against *t*BHP will result from upregulation of cellular cytoprotective proteins by selected phytochemicals, in pre-exposure pre-condition; rather than by increasing cell number. This idea is partly investigated in Chapter 3, with in-depth work presented in Chapter 5.

CHAPTER 2

Direct and indirect cytoprotective activities of selected phytochemicals in HepG2 and 1.1B4 cells

CHAPTER 2 - Direct and indirect cytoprotective activities of selected phytochemicals in HepG2 and 1.1B4 cells

This chapter describes evaluation of the cytoprotective activities of selected phytochemicals, in human hepatoma HepG2 cells and novel human pancreatic 1.1B4 β-cells; with accompanying critical analysis and discussion of the results.

2.1 Introduction

Phytochemicals exhibit diverse therapeutic effects as a result of their ability to influence multiple cellular targets (Zhang et al., 2006). Therefore, there is the need to distinguish beween direct and indirect/inductive cytoprotective activities of phytochemicals. Ahmed Hamed (thesis, 2009) and Fadzelly Abu Bakar (thesis, 2010) identified regulatory effects of quercetin, curcumin and sulforaphane on cellular defence mechanisms, acting as potent inducers of antioxidant enzymes and heat shock proteins; HSP 70 and 90 in hepatocytes (Hamed, 2009; Abu Bakar, 2010). These reports suggest that pleiotropic agents quercetin, curcumin and sulforaphane could exhibit cytoprotective effects via modulating endogenous antioxidant enzymes against oxidative stress; hence their use in this study as reference phytochemicals, for investigating cytoprotective acitvities of rosmarinic acid and its principal metabolites.

Due to inconsistent reports on their benefits in humans, there are controversies surrounding the use of dietary supplements in humans, (Omenn et al., 1996; Stephens et al., 1996; Yusuf et al., 2000). Furthermore, it is argued that pharmacological activities reported in *in vitro* studies may not reflect *in vivo* conditions (Liu, 2004). Liu, (2004) also argues that activities of individual antioxidants compounds are incomparable to mixtures of phytochemicals, which are responsible for the beneficial effects of fruit- and vegetable-rich diets (Chu et al., 2002; Sun et al., 2002). Therefore cytoprotective effects resulting from co-treatment with quercetin and curcumin (used together) were investigated in the current study, using HepG2 cells.

While direct cytoprotection by the selected phytochemicals has been reported in HepG2 cells (Lima et al., 2006), this observation remains novel in the 1.1B4 human pancreatic β-cells. Moreover, the benefits of phytochemicals in prophylactic use against chronic diseases has not been thoroughly examined in *in vitro* studies. Thus, indirect cytoprotection by selected phytochemicals, against oxidative challenge, has not been clearly defined.

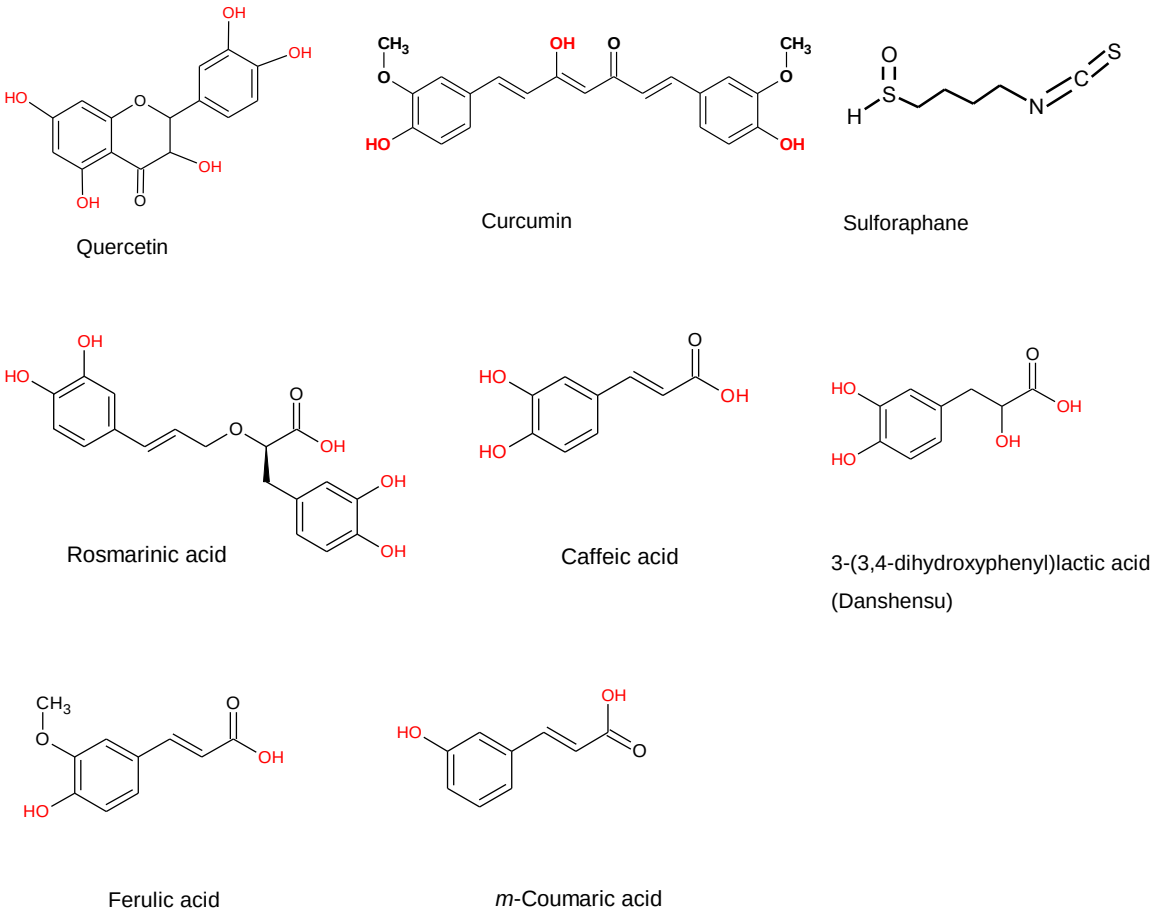

Figure 2.1 Chemical structures of phytochemicals used in the current study, showing hydroxyl groups in red.

2.1.1 Cellular models for evaluating cytoprotective activities of phytochemicals

Whilst the argument persists that cell-based *in vitro* models do not always provide evidence of *in vivo* situations, they are often a readily available experimental tool which continues to provide meaningful scientific results in drug discovery. Also, the use of other

mammals (e.g. rodents) in toxicity studies is limited due to animal rights issues and species differences when compared to human scenarios, as can be deduced from pharmacokinetic profiles of plant-derived compounds (Section 1.5). Since stability of primary cells in experimental situations cannot always be guaranteed, as is reproducibility of data obtained using primary cells (Madan et al., 2003), the availability of human cell lines remains an asset to drug discovery.

2.1.1.1 HepG2 cells

Human hepatoma HepG2 cells are an established experimental model *in vitro* for metabolic and toxicological studies (Alía et al., 2006; Mateos et al., 2006). Albeit being obtained from hepatocellular carcinoma (of a fourteen-year-old Caucasian boy), HepG2 cells retain principal functional characteristics of normal hepatocytes as well as Phase I, II and antioxidant enzymes, making them suitable for studies on drug metabolism enzymes and hepatotoxicity (Knasmüller et al., 2004; Lima et al., 2006). Primary hepatocytes display typical cubic cell shape while HepG2 cells are rather epithelial-like, contrasting primary hepatocytes (Wilkening et al., 2003). However, HepG2 cells are readily accessible and consistent in various cytotoxicity (Sermeus et al., 2012; Cannito et al., 2015) and metabolic assessments (Lima et al., 2006). Cytoprotective activities of selected phytochemicals were evaluated using this cellular model, as these cells have proved reliable in similar investigations involving several medicinal plant extracts and phytochemicals (Lima et al., 2006; Kim et al., 2013; Salla et al., 2016).

2.1.1.2 Pancreatic β-cells

In pancreatic β-cells, the increase in ATP/ADP ratio following carbohydrate and fat metabolism causes closure of ATP-sensitive K^+ channels, resulting in membrane depolarisation, increased influx of Ca^{2+} ions and activation of protein kinases to mediate exocytosis of insulin (Newsholme et al., 2007). While elevated plasma glucose and fatty acid levels initially increase ATP production, persistently high glucose and lipid load increases superoxide anion production and alters transmembrane gradient in pancreatic

β-cells, decreasing free ADP levels with subsequent decrease in ATP synthesis (Fridlyand and Philipson, 2004).

Recent studies have reported a direct relation between redox imbalance, impaired glucose uptake, β-cell dysfunction and antioxidants, see references within (Fridlyand and Philipson, 2004). In patients with T2DM, islet β-cell volume reduced to 40 - 60% as a result of increased apoptosis, while neogenesis was unaffected (Butler et al., 2003). Thus, preservation of β-cell viability (and ultimately β-cell volume) is vital in preventing or delaying onset and deterioration of disease, to alleviate hyperglycaemia and insulin resistance under diabetic and pre-diabetic conditions.

2.1.1.2 Novel human pancreatic β-cell line

The foundation for pancreatic β-cell research has been previously established with rodent β-cells (Finegood et al., 1995; Ihara et al., 1999; Kulkarni et al., 2012). However inconsistencies due to species variation in drug discovery (Eizirik et al., 1994) highlight the need for suitable human pancreatic β-cell models, which are not readily accessible (McCluskey et al., 2011). NES2Y, Blox 5 and other immortalised human β-cell lines which were previously developed, demonstrated good potential in restoring normoglycaemia via K_{ATP} channels and *Pdx-1* genes (Soldevila et al., 1991; MacFarlane et al., 1999; De la Tour D et al., 2001; Zalzman et al., 2005). Nevertheless, experimental results obtained with these β-cell lines were not reproducible, and β-cell function and signalling was found to be different from primary human β-cells (McCluskey et al., 2011).

McCluskey et al., (2011) have recently developed the novel 1.1B4 human pancreatic β-cells by electrofusion of fresh human β-cells with PANC-1 epithelial cells. Ultimately, this procedure resulted in three hybrid cell lines (1.1E7, 1.4E7 and 1.1B4 human βcells), which displayed epithelial growth pattern as monolayers, patterned in a pavement “cobble-stone effect”. Among these hybrid cell lines, the 1.1B4 β-cells were most sensitive to glucose-stimulated insulin secretion, as they recorded highest insulin levels, GLUT-1 expression and glucokinase enzyme activity. The 1.1B4 β-cells, which are also enriched in genes of pancreatic β-cells, have a stable growth rate and share several

functional features and signalling pathways of human insulin-secreting cells (McCluskey et al., 2011), making them closely related to human primary β-cells. Vasu et al., (2013), reported that 1.1B4 β-cells were sucesptible to H_2O_2-mediated apoptosis, hence they could be a useful research tool in pancreatic disorders such as diabetes. However, the suitability of these β-cells as a model for antioxidant research remains to be established.

2.1.2 Aim

The various experimental approaches used in this chapter were intended to define the correlation between radical scavenging and direct cytoprotective activities of phytochemicals in non-cellular and cellular models respectively. Indirect cytoprotection assessed cytoprotective activities of selected phytochemicals, following prophylactic exposure, against subsequent oxidative damage. Direct cytoprotection (5 h co-exposure with phytochemicals) and indirect cytoprotection (20 h pre-incubation with phytochemicals then, 5 h exposure to *t*BHP) were investigated against *t*BHP; followed by cell viability assessment via uptake of the neutral red dye.

The aim of the current study was to validate radical scavenging activities of reference phytochemicals - quercetin, curcumin and sulforaphane -, and rosmarinic acid and its principal metabolites against DPPH free radical in a non-cellular assay. Subsequently, direct and indirect cytoprotective activities of reference phytochemicals, against *t*BHP, were confirmed using HepG2 cells as cellular model.

Considering that rosmarinic acid has shown poor bioavailability (Konishi et al., 2005), it is imperative to predict that its principal metabolites could contribute towards *in vivo* evidence of antioxidant activities by rosmarinic acid. Therefore, quercetin was used as a positive control to evaluate direct and indirect cytoprotective activities of rosmarinic acid alongside its principal metabolites in HepG2 cells.

Furthermore, cytotoxic effect of *t*BHP was also investigated in 1.1B4 β-cells, as a human pancreatic β-cell model. Direct and indirect cytoprotective activities of quercetin, caffeic acid, curcumin and sulforpahane, against *t*BHP-induced cytotoxicity, were also investigated using 1.1B4 β-cells.

The scheme presented in Fig 2.2 was used as a guide to predict antioxidant properties of the phytochemicals, influenced by radical scavenging and/or cytoprotective activities observed.

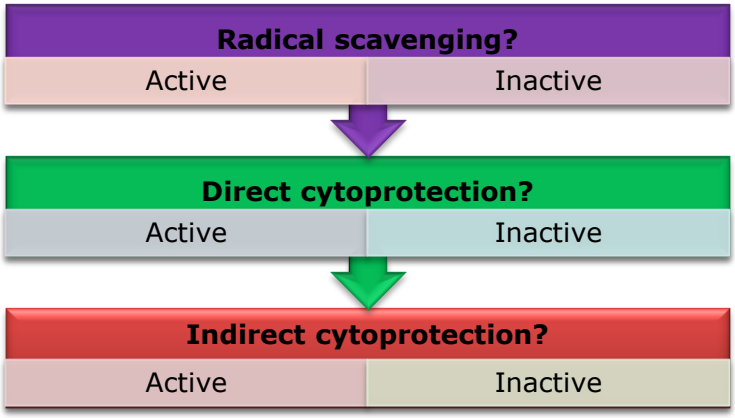

Figure 2.2 Schematic representation of hypothesis for assessing antioxidant activities of phytochemicals. Phytochemicals were initially screened in non-cellular assay for antiradical activities, followed by cellular cytoprotection assay in both co-exposure (with oxidant stressor) and pre-exposure conditions. In all screening models, phytochemicals were either classified as active or inactive antioxidant compounds based on their response to oxidant challenge.

2.2 Materials and Methods

2.2.1 Materials and experimental models

List of all chemicals used and their suppliers can be obtained from Appendix I. List of instruments used in the current study can also be obtained from Appendix I.

2.2.1.1 Experimental models

Human Hepatoma HepG2 cells and human pancreatic 1.1B4 β-cells were obtained from ECACC (Salisbury, UK).

2.2.1.2 Preparation of solutions

❖ **Phytochemicals**: Stock solutions and serial dilutions of selected phytochemicals were prepared with DMSO as vehicle. Range of concentrations used in non-cellular and cellular assays are detailed in Table 2.1. Solutions were stored at -20^{o}C. Final concentrations of phytochemicals in cellular assays were obtained by 1 part in 100 dilutions of stocks using culture medium; final DMSO was therefore at 1%($^{v}/_{v}$) in incubation/culture medium.

Phytochemicals	DPPH assay solutions (mM)	Cellular assay solutions (mM)
Quercetin	0.03 - 1.06	0.02 - 0.33
Curcumin	0.03 - 0.36	0.02 - 0.27
Sulforaphane	0.06 - 1.80	0.04 - 0.56
Rosmarinic acid	0.03 - 0.89	0.02 - 2.78
Caffeic acid	0.06 - 1.78	0.03 - 2.22
Danshensu	0.05 - 1.61	0.03 - 2.02
Ferulic acid	0.05 - 1.65	0.03 - 2.06
m-Coumaric acid	0.06 - 1.95	0.04 - 2.44

Table 2.1 Concentration range of selected phytochemicals used in DPPH and cellular assays.

❖ **DPPH stock solution in methanol***:* A stock solution of DPPH (1 mg/ml) was prepared and stored at -20^{o}C in a foil-covered universal bottle.

❖ **Neutral red working solution**: 1 part in 100 of 3.3 mg/ml stock solution supplied by Sigma (Dorset, UK) was freshly prepared in culture medium (containing 2%($^{v}/_{v}$) foetal bovine serum - FBS) under sterile conditions and pre-warmed for each experiment. Final working solution contained 33 ug/ml of the neutral red dye. Remaining solution was discarded after use.

❖ **Fixative** was made of glacial acetic acid (5%($^{v}/_{v}$)) in a 50%($^{v}/_{v}$) aqueous ethanol solution.

2.2.1.3 Preparation of culture media

2.2.1.3.1 HepG2 culture media components and solutions

MEM Eagle complete medium (10%($^{v}/_{v}$)) comprised of MEM Eagle with Earle's salts (500 ml) supplemented with gentamicin (0.1%($^{v}/_{v}$)), MEM non-essential amino acid solution (1%($^{v}/_{v}$)), amphotericin B (1%($^{v}/_{v}$)), L-glutamine (1%($^{v}/_{v}$)) and FBS (10%($^{v}/_{v}$)).

MEM Eagle complete medium (2%($^{v}/_{v}$)) comprised of MEM Eagle with Earle's salts (500 ml) supplemented with gentamicin (0.1%($^{v}/_{v}$)), MEM non-essential amino acid solution (1%($^{v}/_{v}$)), amphotericin B (1%($^{v}/_{v}$)), L-glutamine (1%($^{v}/_{v}$)) and FBS (2%($^{v}/_{v}$)).

2.2.1.3.2 1.1B4 β-cell Culture Media components and solutions

RPMI-1640 complete medium (10%($^{v}/_{v}$)) comprised of RPMI-1640 solution (500 ml), penicillin/streptomycin (0.125 IU/ml and 0.125 µg/ml), L-glutamine (1%($^{v}/_{v}$)) and FBS (10%($^{v}/_{v}$)).

RPMI-1640 complete medium (2%($^{v}/_{v}$)) comprised of, RPMI-1640 solution (500 ml), penicillin/streptomycin (0.125 iu/ml and 0.125 µg/ml), L-glutamine (1%($^{v}/_{v}$)) and FBS (2%($^{v}/_{v}$).

2.2.2 DPPH radical scavenging assay

In a 96-well plate, 20 µl each of DMSO (solvent) as well as selected phytochemicals was pipetted to separate wells in triplicate. To each well, 0.4%($^{v}/_{v}$) DPPH working solution (in

methanol) was added to make 200 µl as final volume. Vehicle control consisted of 20 µl DMSO and 180 µl methanol (A_{-DPPH}). Wells which contained DMSO (20 µl) and DPPH (180 µl) only were also made in triplicate, denoted as DPPH only – (A_0). Absorbance of pigmented phytochemical (curcumin) was determined from triplicate wells containing 20 µl of each concentration and 180 µl methanol, to eliminate interference with antiradical activities. Samples were kept in the dark for 15 min to allow radical scavenging of DPPH prior to measurement of absorbance values. Samples were then shaken for 1 min to ensure homogeneity. Absorbances were measured at 540 nm due to specificity of filters of the spectrophotometer used. However, lambda max for DPPH is 517 nm. Following blank subtraction (mean absorbance of vehicle control), mean absorbance of test samples (A_{+DPPH}) were normalised to A_0 (mean absorbance of DPPH only). Absorbance of pigmented compound (curcumin) was subtracted from A_{+DPPH} values to obtain actual absorbance (Amic et al., 2003; Nara et al., 2006).

2.2.3 Basic cell culture techniques

Cells were maintained in 5% CO_2-in-air atmosphere at 37°C in a humidified SANYO CO_2 incubator. Cell culture was conducted in a Nuaire class II cell culture cabinet. All media and solutions used for cellular assays and cultures were incubated at 37^oC prior to use.

2.2.3.1 Human hepatoma HepG2 cells

Subculturing HepG2 cells: Upon ensuring that cells were healthy and approximately 80% confluent (using Olympus microscope), culture medium was discarded and cells washed with 15 - 20 ml of warm Hanks Balanced Salts solution (HBSS) without Ca^{2+} and Mg^{2+}. HBSS was discarded and 10 ml of warm Trypsin-EDTA (1X) solution added to culture and the flask incubated for 5 – 10 min at 37^oC. Trypsinisation reaction was stopped by the addition of 10 ml of 10%($^v/_v$) MEM Eagle complete medium. The cell suspension was centrifuged at 700 rpm for 5 min. The supernatant was discarded and the cell pellet suspended in 10 ml medium and passed through a 25-gauge needle and syringe twice to break up clumps of cells. Cell suspension was diluted in 20 ml medium. From the final cell suspension obtained (30 ml), 2.5 ml (approximately 5 x10^6 cells) was

seeded in 40 ml warm medium in a T175 cm^2 flask and incubated at 37^oC. Thus, in routine subcultures, cells were split 1:8 when they reached 80% confluence one week later. Medium was changed every 3 - 4 days. Passage numbers used for subsequent experiments were between 20 and 37.

For cellular experiments, HepG2 cells were seeded at a density of approximately 1.2 x 10^6 cells/ml of 10%($^v/_v$) MEM Eagle complete medium. Cells were cultured at this high density in each well to ensure that cells were confluent and not dividing any further during cytoprotection experiments. For treatment of cells and assays, MEM Eagle medium supplemented with 10%($^v/_v$) FBS or 2%($^v/_v$) FBS was used where appropriate.

2.2.3.2 1.1B4 human pancreatic β-cells

Subculturing 1.1B4 cells: Flasks were observed under an Olympus microscope to ensure that cells were confluent and healthy. When cells reached approximately 80% confluence, culture medium was discarded and cells washed with 5 ml of warm Dulbecco's Phosphate Buffered Saline solution (PBS) without Ca^{2+} and Mg^{2+}. PBS was discarded and cells were incubated with 2 ml warm Trypsin-EDTA solution (10X) for 2 - 5 min at 37^oC. The trypsinisation reaction was stopped by adding 10 ml of 10%($^v/_v$) RPMI-1640 complete medium. Cell suspension was then centrifuged at 1000 rpm for 5 min. Supernatant was discarded; cells were suspended in 10 ml medium and counted using the trypan blue exclusion assay described in section 2.2.3.3. For routine maintenance in T75 cm^2 flask (Corning Incorporated New York, USA), 3 ml of cell suspension was cultured in 10 ml of warm 10%($^v/_v$) RPMI-1640 complete medium. Thus, cells were split 1:3 when they reached 80% confluence 2 - 3 days later.

For cellular experiments, 1.1B4 cells were seeded at a density of approximately 1.3 x 10^5 cells/ml in 10%($^v/_v$) RPMI-1640 complete medium. Cells used were within passages 32 – 39. For cell treatment or assays, RPMI-1640 medium supplemented with 10%($^v/_v$) FBS or 2%($^v/_v$) FBS was used where appropriate.

2.2.3.3 Cell counting

In a 0.5 ml microfuge tube, 10 µl cell suspension was mixed with 10 µl($^{v}/_{v}$) trypan blue (a cell viability indicator). The mixture was then carefully transferred into a cell counting slide. The number of cells per ml was obtained by reading through an automatic cell counter. Viable cells exclude trypan blue, while the dye is taken up into the nucleus of non-viable cells.

2.2.4 *t*BHP-induced cytotoxicity in human cell lines

After approximately 48 h, culture medium was replaced with fresh media supplemented with 2%($^{v}/_{v}$) FBS, containing varying concentrations of *t*BHP (0.0625 – 1.0 mM). Cells treated with culture medium only acted as negative control. Cells were then incubated at 37^{o}C for 5 h prior to neutral red viability assay (outlined in Section 2.2.5.3).

2.2.5 Cytoprotection against *t*BHP-induced oxidative damage

Cultures at approximately 80% confluent were exposed to *t*BHP. Cells were treated with 1%($^{v}/_{v}$) DMSO as vehicle control.

2.2.5.1 5 h co-exposure with selected phytochemicals and *t*BHP

After approximately 48 h of plating, culture medium was replaced with 1 ml culture medium (2%($^{v}/_{v}$) FBS complete) containing phytochemicals with or without 0.5 mM *t*BHP (aqueous) in duplicate wells. After incubation at 37^{o}C for 5 h, cell viability assay was performed.

A similar procedure was applied to co-treatment conditions, where HepG2 cells were exposed to 2%($^{v}/_{v}$) MEM Eagle complete medium containing quercetin (0.01 mM), curcumin (0.03 mM) or both quercetin (0.01 mM) and curcumin (0.03 mM) used together, with or without 0.5 mM *t*BHP. Thus, in co-treatment experiments, cells in each well were treated with both phytochemicals (used together) at the same time, with or without *t*BHP, after which cell viability was assessed via the neutral red uptake assay.

2.2.5.2 20 h pre-exposure to selected phytochemicals

After approximately 28 h of plating, culture medium was replaced with 1 ml medium (supplemented with 10%($^{v}/_{v}$) FBS) containing varying concentrations of selected phytochemicals in quadruplicate wells. Following approximately 20 h exposure to phytochemicals, medium in duplicate wells of each concentration was replaced with 0.5 mM *t*BHP (aqueous) in 1 ml culture medium supplemented with 2%($^{v}/_{v}$) FBS and incubated for 5 h at 37^{o}C. Cells in remaining wells were exposed to culture medium supplemented with 2%($^{v}/_{v}$) FBS only. Cell viability assay was subsequently performed.

For co-treatment experiments, HepG2 cells were pre-exposed to 10%($^{v}/_{v}$) MEM Eagle complete medium containing quercetin (0.01 mM), curcumin (0.01 mM), or quercetin (0.01 mM) and curcumin (0.01 mM) used together. HepG2 cells were cultured for approximately 20 h with the phytochemicals (used singularly or together) prior to oxidative challenge. Cell viability was assessed using neutral red uptake assay.

2.2.5.3 Cell viability assay

Live cells were defined by their ability to take up neutral red by passive diffusion and incorporate the dye in their lysosomes. The neutral red assay has been established as a rapid and simple assay which yields reproducible assessment of cell viability (Fautz et al., 1991; Repetto et al., 2008). Following treatment, culture medium was replaced with 33 µg/ml neutral red dye (1 part in 100 of 3.3 mg/ml neutral red stock solution) in 400 µl medium (supplemented with 2%($^{v}/_{v}$) FBS), including a blank well (well without cells). After 1 h incubation at 37^{o}C, unabsorbed stain was removed by aspirating neutral red medium and washing cells with 400 µl Dulbecco's PBS. Dulbecco's PBS was immediately aspirated, then 400 µl chilled fixative was pipetted into each well to extract the absorbed red dye from the cells. Plates were shaken gently for about 2 min to achieve efficient dye extraction and uniformity. Samples in the 24 well plate could be kept overnight at -20^{o}C at this stage.

2.2.5.4 Sample reading

Samples in each of the 24 wells were transferred to a 96 well plate in triplicate (3 x 100 µl) including blank wells (no-cell). The absorbance of neutral red dye retained by live cells was measured at 540 nm. Upon blank subtraction, actual absorbance per well was obtained for data analysis.

2.2.6 Data analysis

❖ **Presentation of concentrations:** Cytoprotection data were deduced from percentage cell viability data for ease of comparing antioxidant efficiencies among selected phytochemicals compounds.

❖ Unless stated otherwise, data were obtained from at least six independent experiments for each phytochemical, in both chemical and cellular conditions. For co-treatment studies, data were obtained from four independent experiments.

❖ Data were analysed using GraphPad Prism 6 to obtain EC_{50} ± 95% CIs (Confidence Intervals) and maximal response values using the equation below; where Y represents percentage response

$$Y=Bottom + (Top-Bottom)/1+10^{((LogEC_{50}-X)*HillSlope))}$$

However, within the confines of the above equation, EC_{50} and ± 95% CIs obtained were not accurate for some data sets. In such instances, $Y=100/(1+10^{((LogEC50-X)*HillSlope))}$ was used.

Line of best fit was defined by closeness of R^2 values to 1.0 (perfect fit) and this influenced the choice of equation for any data set analysed by nonlinear regression.

GraphPad Prism was used to define EC_{50} as the concentration of phytochemical that yields a response halfway between the minimum and maximum thresholds. Maximal response was defined as maximum percentage protection produced by each phytochemical.

❖ For cytotoxicity data, TC_{50} ± 95% CI values were obtained using the equation below, where Y represents percentage response

$$Y=100/(1+10^{((LogTC_{50}-X)*HillSlope)})$$

GraphPad Prism was also used to define TC_{50} as the toxic concentration that yields a response halfway between the minimum and maximum thresholds.

2.2.6.1 Radical scavenging

Radical scavenging activity was calculated using the equation:

$$\% \ Scavenging = 100 \times [A_0 - (A_{+DPPH} - A_{-DPPH})]/A_0.$$

Where (A_0): Absorbance of DMSO plus DPPH; (A_{-DPPH}) Absorbance of pigmented samples plus methanol; (A_{+DPPH}) Absorbance of samples plus DPPH.

EC_{50} value was obtained from a graph of percentage scavenging against concentration (mM) as described above.

For multiple comparisons of antiradical activities against DPPH (EC_{50} values), one-way ANOVA was used and Bonferroni's test as post hoc test, with ($P<0.05$) being set as evidence for significant statistical reasoning.

2.2.6.2 Cytoprotection

Cell viability: Percentage viability was calculated as ratio of the mean absorbance of two wells (with the same treatment condition) to that of the vehicle control (DMSO) taken as 100% as shown in the equation below:

$$\% \text{ cell viability} = \left[\frac{\text{mean absorbance at sample (phytochemicals)}}{\text{Mean absorbance at control (DMSO treated cells)}} \right] \text{X } 100\%$$

Percentage cytoprotection: This was an indicator of the cytoprotective activity of selected phytochemicals against *t*BHP, relative to toxicities by plant compounds, as described in the equation below:

$$\% \text{ protection} = \left[100 - \left[\frac{\text{mean absorbance (-}t\text{BHP) – mean absorbance (+}t\text{BHP) sample}}{\text{mean absorbance (-}t\text{BHP) – mean absorbance (+}t\text{BHP) DMSO}} \right] \right] \text{X } 100\%$$

Absorbance of cells treated without *t*BHP was taken as –*t*BHP and absorbance of cells treated with *t*BHP as +*t*BHP.

2.6.2.3 Criteria for statistical tool used

For percentage viability obtained in the absence of *t*BHP, statistical significance was determined using Friedman test and post hoc analysis by Dunn's multiple comparisons test. Due to data distribution pattern, non-compliance with Gaussian distribution was assumed.

Statistical analysis for percentage viability obtained in the presence of *t*BHP was conducted using one-way ANOVA with Dunnett's multiple comparisons test. Data obtained generally followed Gaussian distribution, with low percentage viability recorded at lowest and highest concentrations of most phytochemicals. Since sample size was too small to perform test for normality, normality was assumed.

For data obtained with 1.1B4 cells, potencies (mean EC_{50} values) of selected phytochemicals were analysed by one-way ANOVA, with post hoc analysis by Dunnett's multiple comparison tests.

For statistical analysis of percentage cytoprotection data obtained during co-treatment conditions, one-way ANOVA was used with post hoc analysis by Bonferroni's multiple comparisons test. Where confidence intervals across data set are within the same range, statistical analysis was not performed.

2.3 Results

2.3.1 Radical scavenging against DPPH

Radical scavenging activities of selelcted phytochemicals were characterised by the visible discolouration from purple ($DPPH^{\cdot}$) to yellow (DPPHH), as a function of phytochemical concentration. Radical scavenging activities were observed in a concentration-dependent manner, with quercetin, rosmarinic acid, caffeic acid and danshensu recording comparable potencies (Table 2.2). Curcumin was significantly less potent than rosmarinic acid, caffeic acid and danshensu, approximately 1.9-fold less than quercetin. Ferulic acid was approximately 3.1-fold less potent than quercetin, rosmarinic acid, caffeic acid and dansehsu. Sulforaphane (0.06 – 1.80 mM) and *m*-coumaric acid (0.03 – 1.95 mM) lacked radical scavenging activity within the concentration range used.

Overall, selected phytochemicals were in the range of approximately 4- to 7-fold less potent compared to existing reports of radical scavenging activities at lambda max - 517 nm (Table 2.2). This observation is discussed further in Section 2.4.1.

Phytochemical	**Radical scavenging**	
	Mean EC_{50} values; CI (mM) at 540 nm	**Mean EC_{50} values mM (existing reports) at 515[a], 516[b] or 517[c] nm**
Quercetin	0.21 (0.20, 0.22)	0.03 (Nimmi and George, 2012)[c]
Curcumin	0.39 (0.32, 0.47) *#∞γ	0.09 (Ak and Gulcin, 2008)[c]
Sulforaphane	No effect (>0.2)	< 0.01 µM – less than 40% scavenging (Farag and Motaal, 2010) - at 550 nm
Rosmarinic acid	0.24 (0.24, 0.25)	0.07 (Erkan et al., 2008)[a]
Caffeic acid	0.26 (0.22, 0.30)	0.02 – 51.5% activity (Chen and Ho, 1997)[c, d]
Danshensu	0.22 (0.21, 0.23)	<0.01 (Zhao et al., 2088)
Ferulic acid	0.67 (0.32, 1.02) *#∞γ	0.11 (Shimoji et al., 2002)[c]
m-Coumaric acid	No effect (>0.2)	At 0.04, <2% activity (Nenadis and Tsimidou, 2002)[b, d]

Table 2.2 Compilation of potencies of radical scavenging against DPPH free radical. Values are mean EC_{50} confidence intervals (CI) of six independent experiments; n = 8 for quercetin. Statistical analysis was performed using one-way ANOVA and post hoc analysis by Bonferroni's multiple comparisons test. Statistical significance is defined as P <0.05 (*) compared with positive control (quercetin), P<0.001 (#) compared with rosmarinic acid, P<0.001 (∞) compared with caffeic acid and P<0.001 (γ) compared with danshensu. Due to lack on evidence of EC_{50} values, % DPPH inhibition is quoted (d).

2.3.2 Cytoprotection in HepG2 hepatoma cells

Having demonstrated radical scavenging activity against $DPPH^{\cdot}$, cytoprotective activities of selected phytochemicals were evaluated against *t*BHP-induced cytotoxicity in co-exposure and pre-exposure conditions.

2.3.2.1 *t*BHP-induced cytotoxicity

After 5 h exposure, *t*BHP caused HepG2 hepatoma cells to appear rounded and separated from neighbouring cells (Fig 2.3). In accordance with these morphological changes, cell viability decreased with increasing concentration of *t*BHP (0.0625 – 1.0 mM), which resulted in approximately 40% cell death at 0.25 mM ($P<0.05$, $n = 6$).

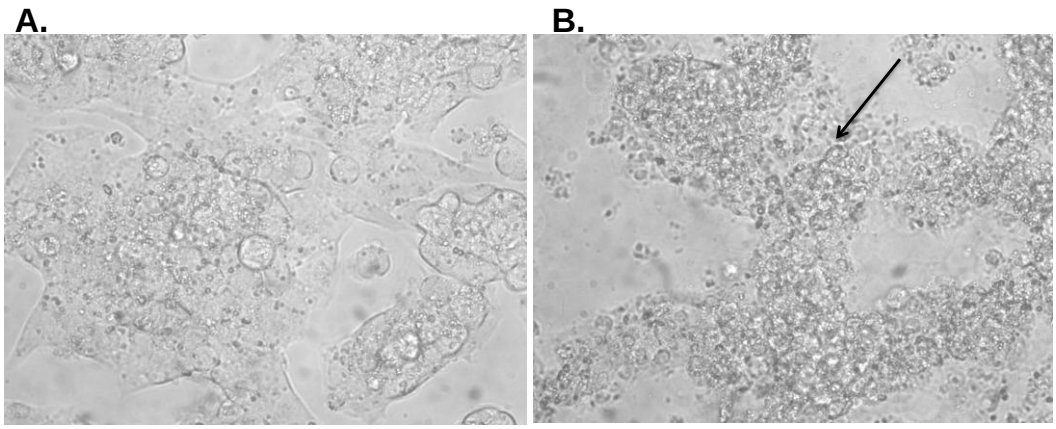

Figure 2.3 Photographic representation of HepG2 cells treated with 0.5 mM *t*BHP for 5 h. Images show cells looking healthy after treatment with culture medium only (A), while cells are more rounded and detached from neighbouring cells (indicated by black arrows) following *t*BHP treatment (B). Images were obtained at 40X magnification using the CMEX-18PRO camera with the Olympus Ck2 microscope.

Cell viability recorded beyond this concentration was not greater than approximately 7% (Fig 2.4). Although cytotoxicity caused by mean TC_{50} value (0.20 mM, CI: 0.15 – 0.26) was comparable to that obtained at 0.25 mM, loss in cell viability recorded at the latter concentration was not significantly different from 0.5 mM ($P>0.05$). Results obtained agree with earlier reports of approximately 95% cytotoxicity following incubation with 0.5 mM *t*BHP (Alia et al., 2005). Hence, 0.5 mM was used to evaluate the cytoprotective properties of phytochemicals used in this study.

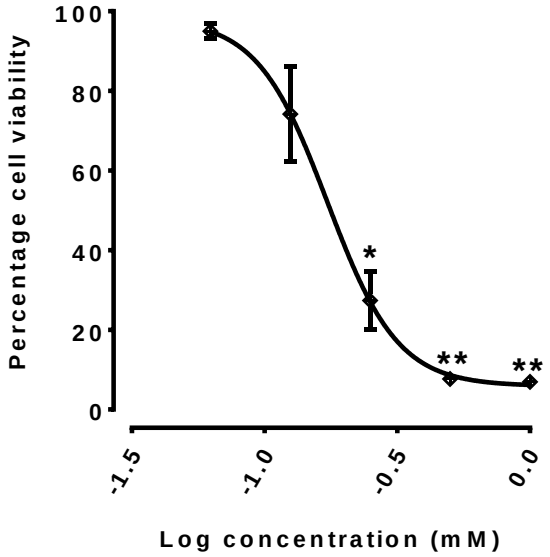

Figure 2.4 Concentration-response curve of *t*BHP-induced cytotoxicity in HepG2 human hepatoma cells. Cells were exposed to varying concentrations of *t*BHP, represented in logarithm as Log [chemical] vs. response-variable slope. Each data point represents mean of duplicate wells from six independent experiments normalised to mean absorbance untreated cells to obtain percentage cell viability ± SEM. Statistical analysis was performed using one-way ANOVA and post hoc by Dunnett's multiple comparison test. Where indicated, values were significantly different from control (MEM Eagle medium (supplemented with 2%($^{v}/_{v}$) FBS)), which was taken to be 100% viability, at $P<0.05$ (*) and $P<0.01$ (**).

2.3.2.2 Cytoprotection by reference phytochemicals in HepG2 cells

Direct cytoprotection observed in co-exposure experiments represented direct interaction between phytochemicals and high intracellular ROS induced by 0.5 mM *t*BHP. On the other hand, indirect cytoprotection was recorded following 20 h pre-exposure to phytochemicals, cells were then treated with *t*BHP alone. Without phytochemical intervention, *t*BHP caused approximately 90% cell damage in both exposure conditions. Cells treated with DMSO alone were taken to be 100% viable.

2.3.2.2.1 Direct cytoprotection

Quercetin was nontoxic and showed a concentration-dependent cytoprotection against 0.5 mM *t*BHP (Fig 2.5A). In the presence of *t*BHP, quercetin (0.02 mM) produced approximately 41% viability, which increased to about 100% at 0.08 mM quercetin. Subsequently, a marginal drop in cell viability (20%) was recorded after co-exposure to 0.33 mM quercetin and *t*BHP.

When cells were treated with curcumin, there was a sharp rise in percentage cell survival from 10.1 ±4.27% to 71.8 ±2.83 ($P<0.05$, n = 6) at 0.03 mM and 0.07 mM curcumin, respectively (Fig 2.5B). Beyond this concentration, cell viability declined dramatically due to cytotoxicity, which was also recorded in the absence of *t*BHP.

Sulforaphane was without cytoprotective activity under the conditions tested however, cell viability decreased at concentrations above 0.07 mM sulforaphane (Fig 2.5C).

Quercetin, with mean EC_{50} value of 0.02 mM (0.01, 0.04), was more potent than curcumin 0.80 mM (1.0, 16.7) in 5 h co-exposure conditions.

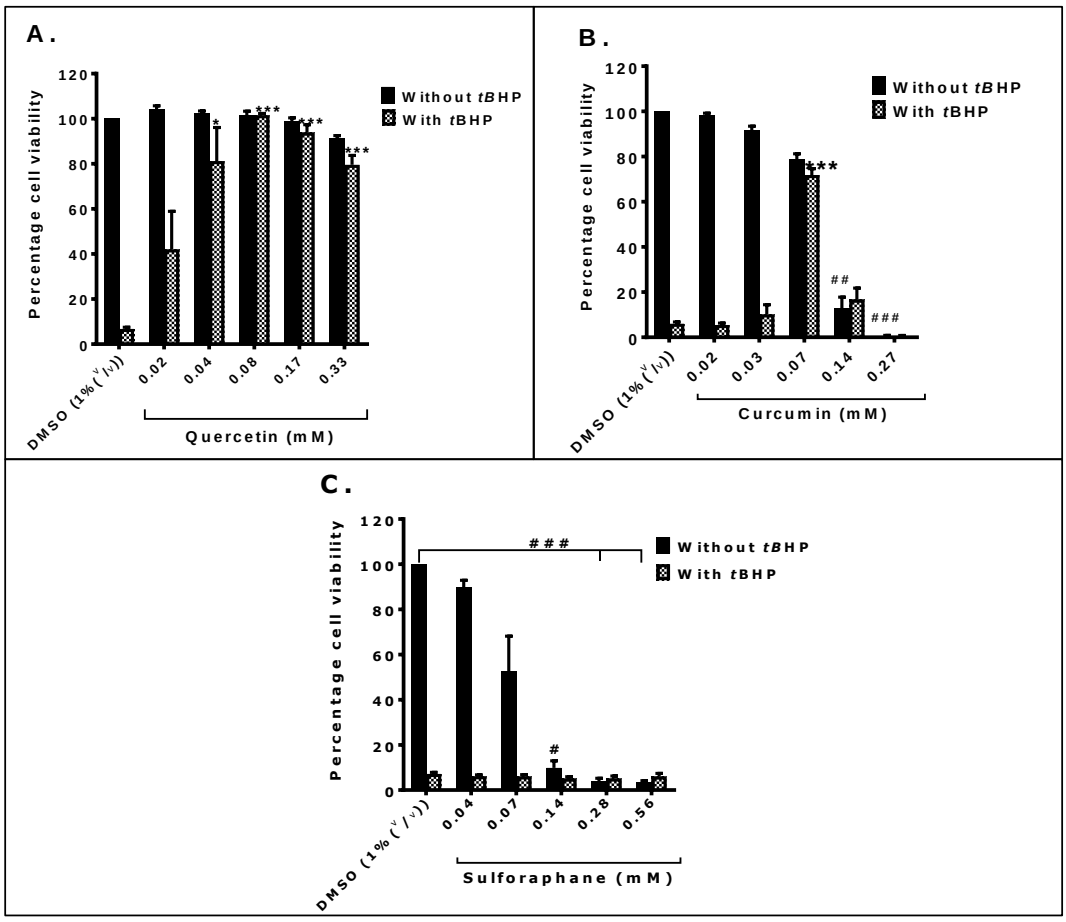

Figure 2.5 Protection by reference plant-derived chemicals against *t*BHP-induced cytotoxicity after 5 h co-exposure. HepG2 cells were co-incubated with varying concentrations of quercetin (A), curcumin (B) and sulforaphane (C). Each data point represents mean percentage viability of six independent experiments ± SEM, from duplicate wells for each concentration. Statistical analysis was performed using Friedman test, where values were significantly different from control (DMSO alone) at $P<0.05$ (#), $P<0.01$ (##) and $P<0.001$(###). Also, one-way ANOVA and post hoc analysis – Dunnett's multiple comparisons test were conducted and statistical significance denoted as $P<0.05$ (*) and $P<0.001$ (***) when compared with *t*BHP control.

2.3.2.2.2 Indirect cytoprotection

Following pre-treatment, quercetin produced concentration-dependent protection against *t*BHP-induced oxidative challenge, with cell viability increasing from approximately 50% at 0.04 mM ($P<0.05$, $n = 6$) to 87% at 0.33 mM quercetin ($P<0.001$, $n = 6$) respectively (Fig 2.6A). Again, quercetin alone showed no significant toxicity in HepG2 cells.

However, curcumin was toxic to the HepG2 cells at high concentrations (Fig 2.6B) as was observed in 5 h experiments, showing a bell-shaped concentration-response effect which is characteristic of Michael acceptor compounds (Magesh et al., 2012). Following pre-exposure, curcumin produced was a sharp increase in cell survival from approximately 55% to 90% at 0.02 mM and 0.03 mM curcumin, respectively. However, cytoprotective activity recorded at 0.07 mM curcumin was limited by about 20% toxicity, which was also observed in the absence of *t*BHP.

Although sulforaphane showed cytotoxicity with increasing concentration, cytoprotective activity was observed at 0.04 mM sulforaphane only, with percentage viability of approximately 57% ($P<0.05$, $n = 6$) (Fig 2.6C). Again, protective effect of sulforaphane was markedly limited by its cytotoxicity at concentrations above 0.07 mM ($P<0.05$), causing greater than 60% cell death (Fig 2.6C).

Curcumin (mean EC_{50} value: 0.02 mM; 0.01, 0.02) was more potent than quercetin (0.08 mM (0.05, 0.10)) in 20 h conditions. Due to marked cytotoxicity by sulforaphane, a cytoprotective index could not be determined.

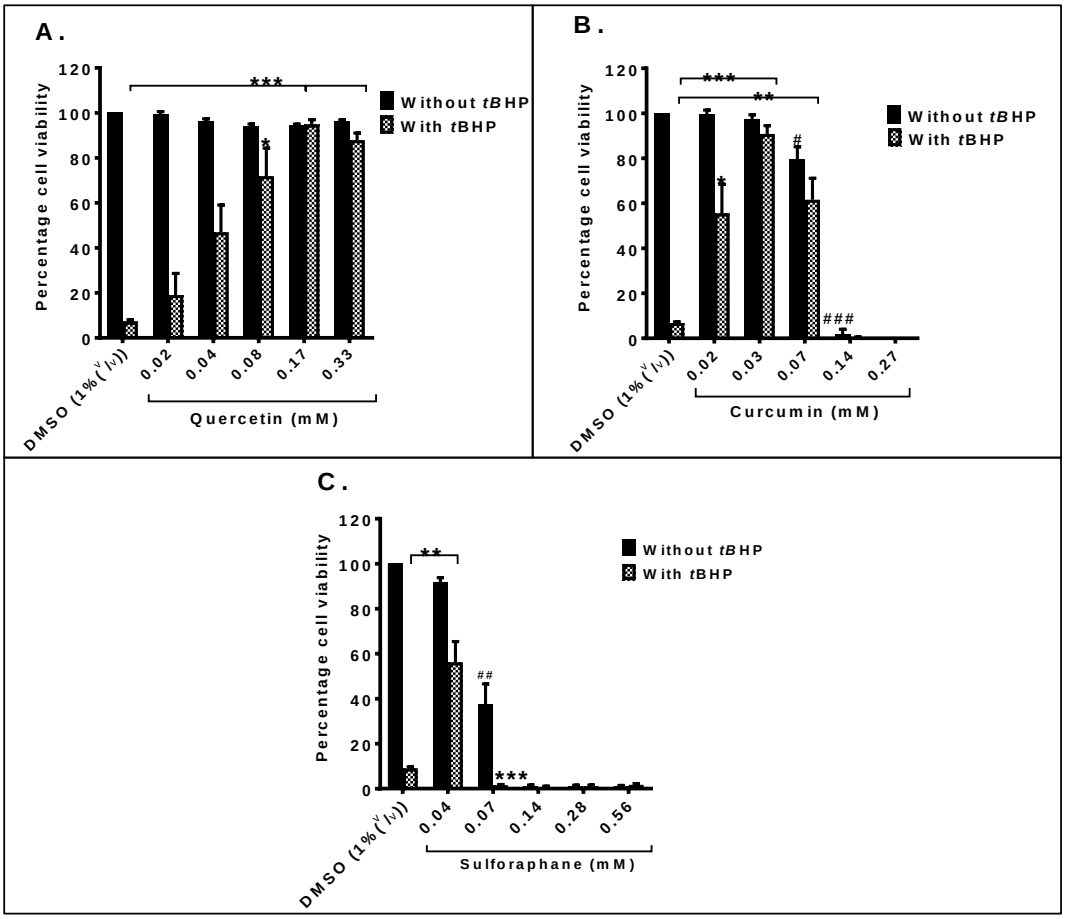

Figure 2.6 Protection by reference plant-derived chemicals against subsequent cytotoxicity by *t*BHP. HepG2 cells were co-incubated with varying concentrations of quercetin (A), curcumin (B) and sulforaphane (C) for 20 h prior to oxidative challenge. Each data point represents mean percentage viability of six independent experiments ± SEM, from duplicate wells for each concentration. Statistical analysis was performed using Friedman test, where values were significantly different from control (DMSO alone) at P<0.05 (#) and P<0.01 (##). Also, one-way ANOVA and post hoc analysis – Dunnett's multiple comparisons test were conducted and statistical significance denoted as P<0.05 (*), P<0.01 (**) and P<0.001 (***) when compared with *t*BHP control.

2.3.2.3 Cytoprotection by co-treatment with quercetin and curcumin (used together)

Since quercetin and curcumin demonstrated strong cytoprotective activities against *t*BHP; similar effects were assessed using very low concentrations (EC_{10}) of both plant compounds used together, - quercetin (0.01 mM) and curcumin (0.03 mM and 0.01 mM) for 5 h and pre-exposure conditions, respectively. In the following set of experiments, HepG2 cells were co-exposed with 0.5 mM *t*BHP and both phytochemicals (singularly or together) or pre-exposed to both phytochemicals alone (again, singularly or together) for 20 h prior to oxidative challenge with 0.5mM *t*BHP.

After 5 h co-exposure with *t*BHP in HepG2 cells, quercetin and curcumin alone; at their "EC_{10}" concentrations were without cytoprotective effect. However, when cells were co-treated with quercetin and curcumin, approximately 64% viability was obtained (Fig 2.7A). Neither quercetin nor curcumin was cytotoxic when treated alone, although marginal toxicity was recorded in co-treated cells. Percentage cytoprotection recorded after co-treatment with quercetin and curcumin was 75.9 ±5.34% ($P<0.01$, n = 4; Fig 2.7B).

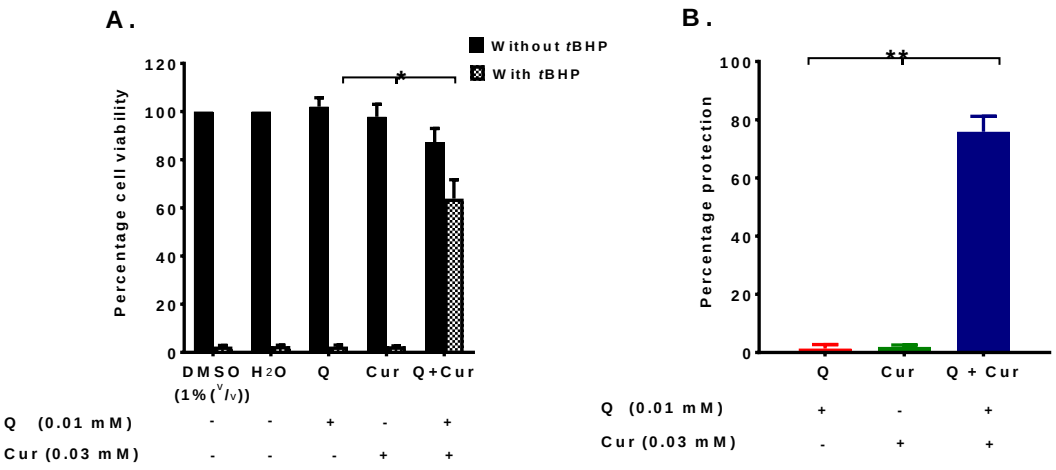

Figure 2.7 Cytoprotective activities by co-treatment with quercetin and curcumin (used together) after 5 h co-exposure with *t*BHP. Cells were also pre-incubated with same concentrations of quercetin (0.01 mM) and curcumin (0.03 mM) alone as controls. This figure shows percentage cell viability (A) and (B) percentage protection data, with each data point representing mean percentage viability of four independent experiments ± SEM, performed in duplicate wells for each treatment condition. Statistical analysis was performed using one-way ANOVA, post hoc analysis – Bonferroni's multiple comparisons test. When compared with quercetin or curcumin (used singularly) pre-treated cells significant difference was denoted as $P<0.05$ (*) and $P<0.01$ (**).

Furthermore, pre-exposure to "EC_{10}" concentrations of quercetin or curcumin did not produce protection against subsequent oxidative challenge, although marginal increase in cell viability was recorded for quercetin alone (Fig 2.8A). In co-treated cells, there was no increase in cell survival as quercetin and curcumin (used singularly or together) were without cytoprotective response against *t*BHP-induced damage (Fig 2.8B). There was also no cytotoxic effect when cells were pre-exposed to quercetin or curcumin alone, or together.

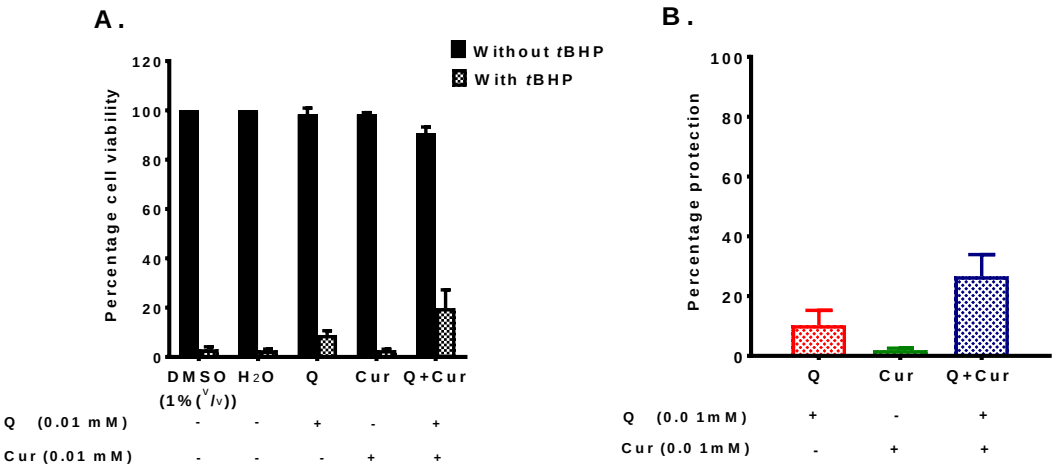

Figure 2.8 Effect of pre-incubation with quercetin and curcumin (together) against oxidative damage. HepG2 cells were also pre-exposed to quercetin (0.01 mM) and curcumin (0.01 mM) alone for approximately 20 h as controls. This figure shows percentage cell viability (A) and (B) percentage protection data, with each data point representing mean percentage viability of four independent experiments ± SEM, performed in duplicate wells for each treatment condition. Statistical analysis of percentage viability data was performed using one-way ANOVA, post hoc analysis – Bonferroni's multiple comparisons test.

2.3.2.4 Direct cytoprotection by rosmarinic acid and its principal metabolites

Whereas radical scavenging activities of rosmarinic acid and three of its metabolites were comparable to quercetin, cytoprotective activities observed in HepG2 cells did not occur within the same concentration range as the positive control (0.02 – 0.33 mM). Therefore, rosmarinic acid and its principal metabolites were evaluated further at higher concentrations (Fig 2.9).

Quercetin as positive control was essentially non-toxic but effective in preventing oxidative damage, recording peak viable count of approximately 95% at 0.08 mM ($P<0.001$, $n = 8$), although marginal decrease to about 80% viability was recorded at 0.33 mM quercetin (Figure 2.9A).

In cells treated with rosmarinic acid alone, cell viability declined at concentrations above 1.39 mM, with approximately 20% toxicity was observed at 2.78 mM rosmarinic acid ($P<0.01$, $n = 6$; Fig 2.9B). Nevertheless, rosmarinic acid demonstrated a concentration-dependent increase in survival of HepG2 cells against oxidative damage, with

approximately 69% viability at 1.39 mM rosmarinic acid, and no further increase beyond this concentration.

Caffeic acid was without toxicity in the absence of *t*BHP (Fig 2.9C). Nevertheless, in the presence of *t*BHP, cell viability increased in a concentration-dependent pattern, producing a maximum effect of about 70% viability at 2.2 mM caffeic acid ($P<0.001$, $n = 6$).

Approximately 20% decrease in cell viability was recorded after 5 h incubation with 2.02 mM danshensu alone ($P<0.01$, $n = 6$), however no protection was observed against *t*BHP-induced cytotoxicity, within the concentration range 0.03 – 0.50 mM (Fig 2.9D). Finally, ferulic acid and *m*-coumaric acid were without cytotoxic effect and showed no increase in cell viability during 5 h co-exposure conditions (Figs 2.9E and F).

At the range of concentrations used, danshensu, ferulic acid and *m*-coumaric acid were without cytoprotective activity during 5 h co-exposure with 0.5 mM *t*BHP (Fig 2.10). Cytoprotective efficiencies of rosmarinic acid and caffeic acid were not comparable to quercetin, rosmarinic acid was about 20-fold less effective than quercetin (mean EC_{50} value: 0.03 mM; 0.03, 0.04). However, maximum effects of both phytochemicals were comparable. Furthermore, maximum protection obtained after co-exposure with quercetin was approximately 20% greater than caffeic acid, which was about 19.3-fold less effective than quercetin.

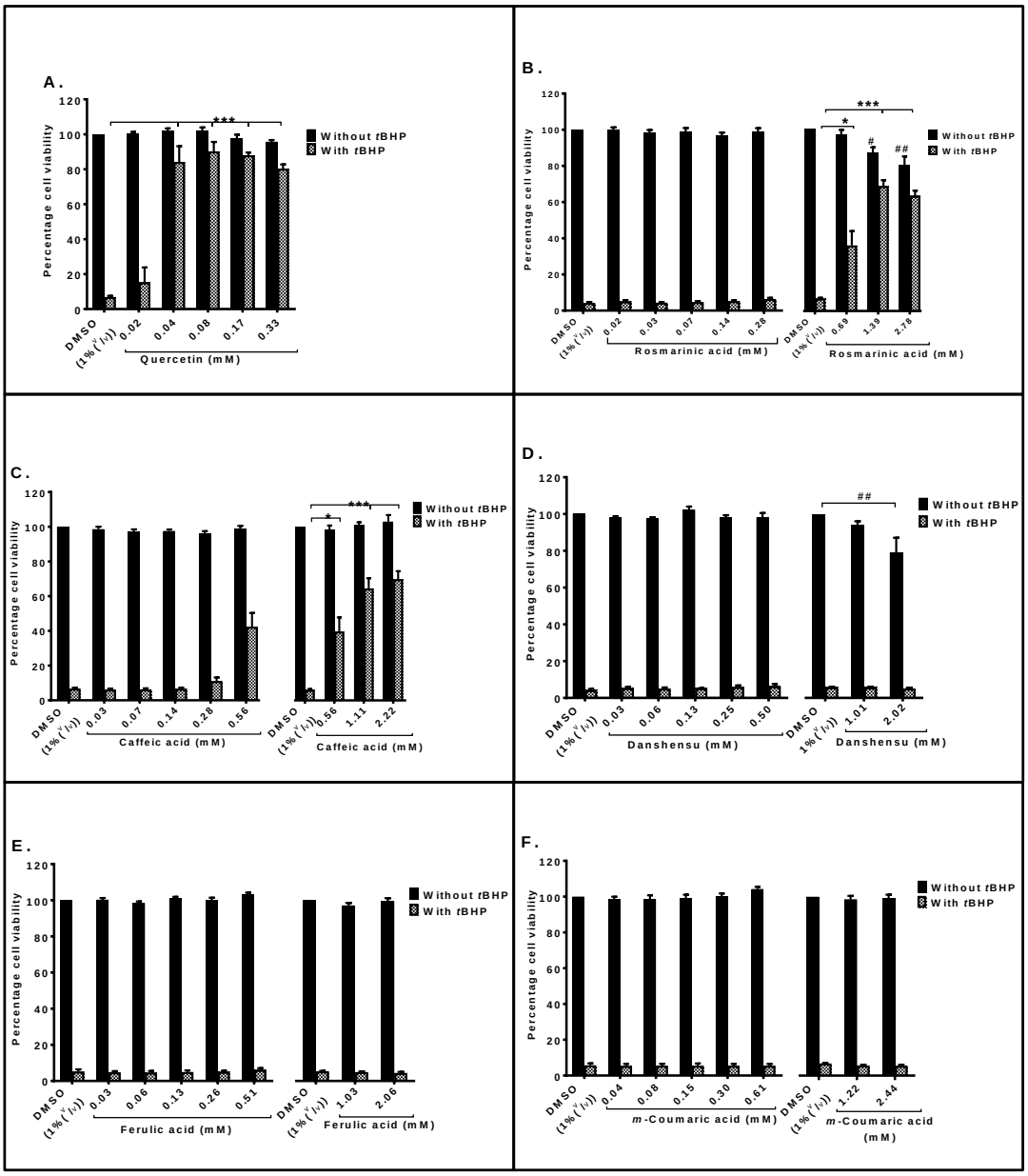

Figure 2.9 Protection against *t*BHP-induced oxidative damage in HepG2 hepatoma cells following 5 h co-exposure to rosmarinic acid and its principal metabolites. Cells were exposed to varying concentrations of (B) rosmarinic acid, caffeic acid (C) danshensu (D), ferulic acid (E) and *m*-coumaric acid (F), in the absence and presence of *t*BHP. Quercetin (A) and 1%($^{v}/_{v}$) DMSO were used as positive and vehicle controls respectively. Each data point represents mean percentage viability of six independent experiments ± SEM performed in duplicate wells for each concentration, for quercetin; n = 8. Statistical significance was performed using one-way ANOVA and post hoc analysis by Dunnett's multiple comparisons test, where values were significantly different from DMSO control at p<0.05 (#) and P<0.01 (##). Data obtained in the presence of *t*BHP were analysed using Friedman test (-*t*BHP), with significance denoted as P<0.05 (*) and P<0.001 (***).

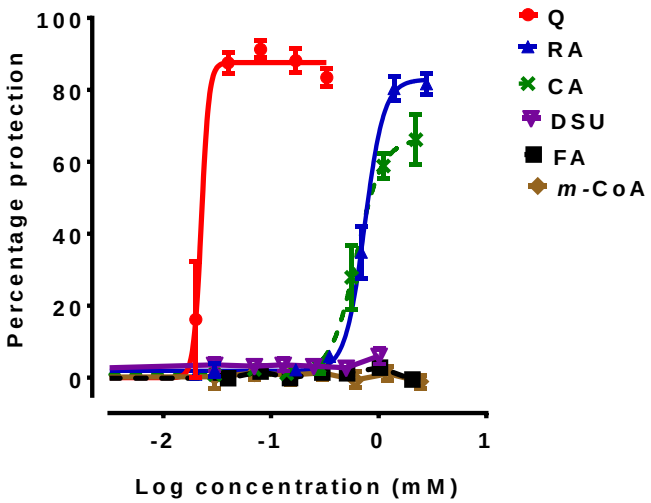

Figure 2.10 Concentration-response curves for direct cytoprotection by rosmarinic acid and its principal metabolites. Curve represents data from Fig 2.9 summarised as Log [chemical] vs. response-variable slope of rosmarinic acid (RA), caffeic acid (CA), danshensu (DSU), ferulic acid (FA) and *m*-coumaric acid (*m*-CoA) at concentration range 0.02 – 3 mM and represented on horizontal axis in logarithm. Quercetin (Q) was used as positive control. Each data point represents six independent experiments expressed as percentage protection ± SEM, for quercetin; n = 8.

2.3.2.5 Indirect cytoprotection by rosmarinic acid and its principal metabolites

Pre-treatment with quercetin alone showed no significant toxicity in HepG2 cells but produced a concentration-dependent protection against *t*BHP-induced oxidative challenge, with cell viability increasing from approximately 37% at 0.08 mM ($P<0.05$, n = 6) to 87% at 0.33 mM quercetin ($P<0.001$, n = 6) respectively (Fig 2.11A).

Similar to 5 h conditions, rosmarinic acid alone decreased cell viability at high concentrations to approximately 80% at 2.78 mM rosmarinic acid ($P<0.01$, n = 6; Fig 2.11B). Rosmarinic acid preserved the viability of HepG2 cells in a concentration-dependent manner, recording approximately 88% at 1.39 mM rosmarinic acid, although viability decreased beyond this concentration. Reduction in cell viability observed at the highest concentration of rosmarinic acid could be due to cytotoxicity recorded in the absence of *t*BHP. Caffeic acid was however non-toxic within the range of concentrations used (Fig 2.11C). Cytoprotection was also demonstrated in increasing concentrations of caffeic acid, yielding approximately 91% viability at 2.22 mM caffeic acid ($P<0.001$, n =6).

Unlike caffeic acid, 2.02 mM danshensu showed about 27% toxicity but was without cytoprotection against *t*BHP (Fig 2.11D). Furthermore, cells retained 100% viability when treated with ferulic acid and *m*-coumaric acid, which did not preserve cell viability against subsequent oxidative challenge (Figs 2.11E and F).

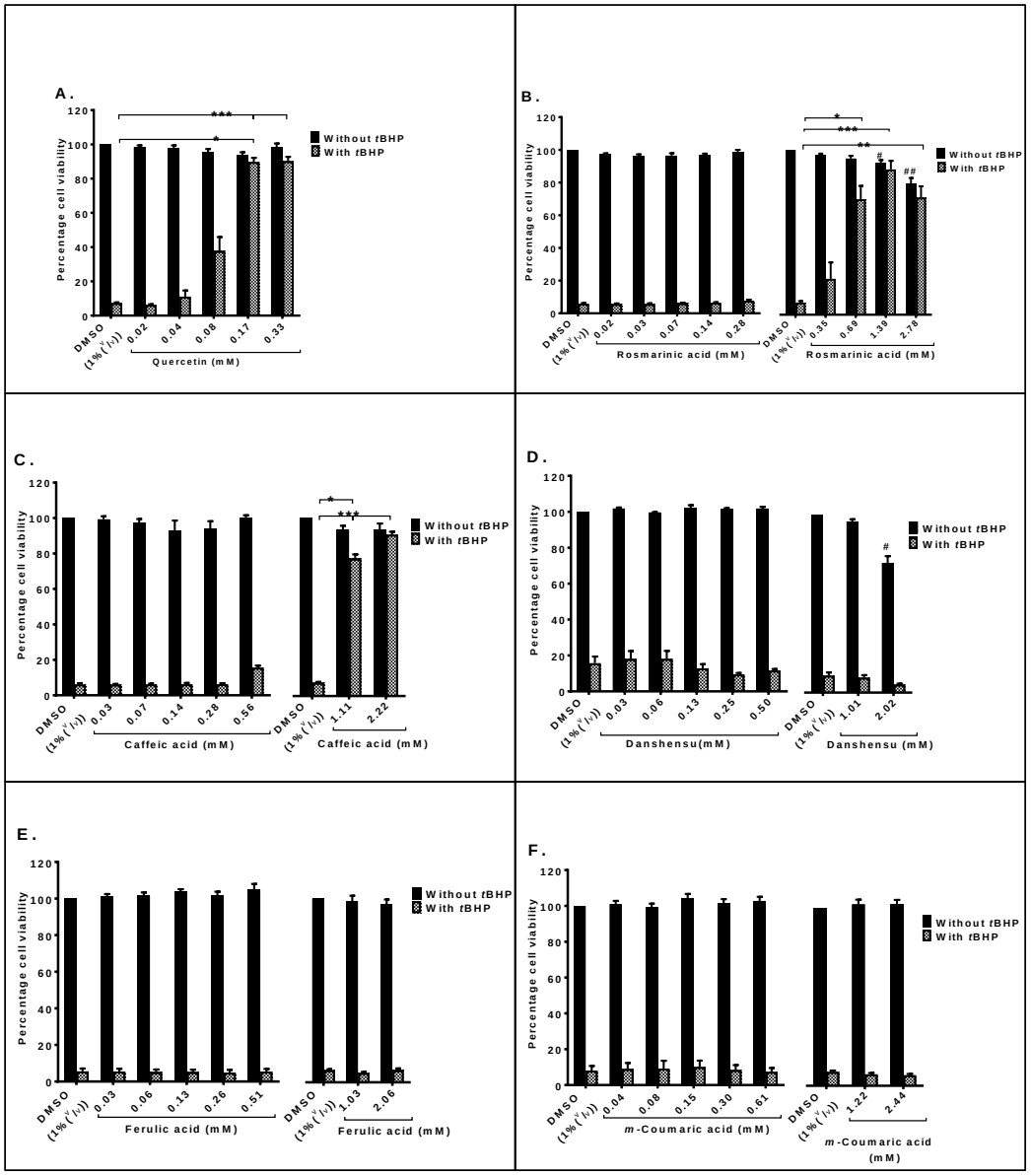

Figure 2.11 Protection against *t*BHP-induced oxidative damage in HepG2 hepatoma cells after 20 h pre-exposure to rosmarinic acid and its principal metabolites. Cells were exposed to varying concentrations of (B) rosmarinic acid, caffeic acid (C) danshensu (D), ferulic acid (E) and *m*-coumaric acid (F), in the absence and presence of *t*BHP. Quercetin (A) and 1%($^{v}/_{v}$) DMSO were used as positive and vehicle controls respectively. Each data point represents mean percentage viability of six independent experiments ± SEM performed in duplicate wells for each concentration, for quercetin; n = 8. Statistical significance was performed using one-way ANOVA and post hoc analysis by Dunnett's multiple comparisons test, where values were significantly different from DMSO control at P<0.05 (#) and P<0.01 (##). Data obtained in the presence of *t*BHP were analysed using Friedman test (-*t*BHP), with significance denoted as P<0.05 (*), P<0.01 (**) and P<0.001 (***).

Nevertheless Fig 2.13 indicates that, rosmarinic acid (mean EC_{50}: 0.75 mM; 0.57, 0.94) and caffeic acid (mean EC_{50}: 0.77 mM; 0.64, 0.94) were about 8.5-fold less potent than quercetin (mean $EC_{50:}$ 0.09 mM; 0.06, 0.12). Danshensu, ferulic acid and *m*-coumaric acid did not show indirect cytoprotective activity against oxidative challenge within the range of concentrations used (Fig 2.12).

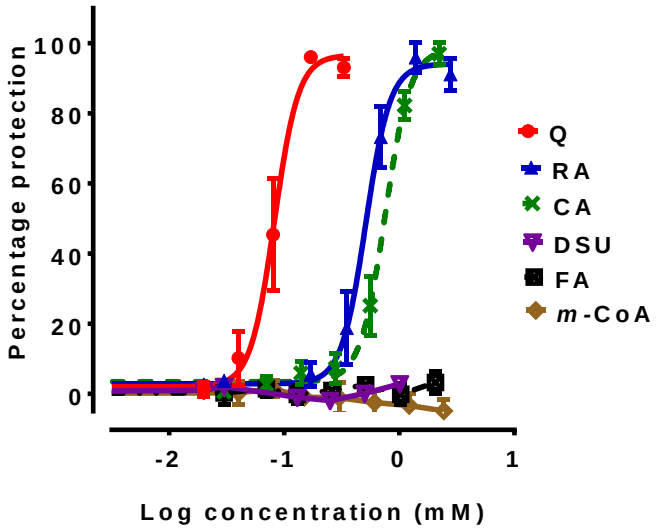

Figure 2.12 Concentration-response curves for indirect cytoprotection by rosmarinic acid and its principal metabolites. Curve represents data from Fig 2.11 summarised as Log [chemical] vs. response-variable slope of rosmarinic acid (RA), caffeic acid (CA), danshensu (DSU), ferulic acid (FA) and *m*-coumaric acid (*m*-CoA) at concentration range 0.02 – 3mM and represented on horizontal axis in logarithm. Quercetin (Q) was used as positive control. Each data point represents six independent experiments expressed as percentage protection ± SEM, for quercetin; n = 8.

2.3.3 Cytoprotection by selected phytochemicals in 1.1B4 pancreatic β-cells

2.3.3.1 *t*BHP-induced cytotoxicity in 1.1B4 cells

The 1.1B4 β-cells were treated with varying concentrations of *t*BHP (0.0625 – 1.0 mM) for 5 h, prior to neutral red viability assay. Morphological changes observed included 1.1B4 cells appearing rounded and separated from each other, with increasing *t*BHP concentrations from 0.25 mM – 1.0 mM *t*BHP, as shown with 0.5 mM *t*BHP in Fig 2.13B.

In accordance with morphological changes, cell numbers reduced to approximately 60% after 5 h exposure to 0.0625 mM *t*BHP (Fig 2.14), with marked reduction in cell viability at

concentrations above 0.125 mM (P<0.001, n = 6). Mean TC_{50} was calculated as 0.07 mM (0.04, 0.10 mM). However, as antioxidant efficiencies of phytochemicals were assessed with 0.5 mM *t*BHP in HepG2, similar conditions were used with the 1.1B4 β-cells.

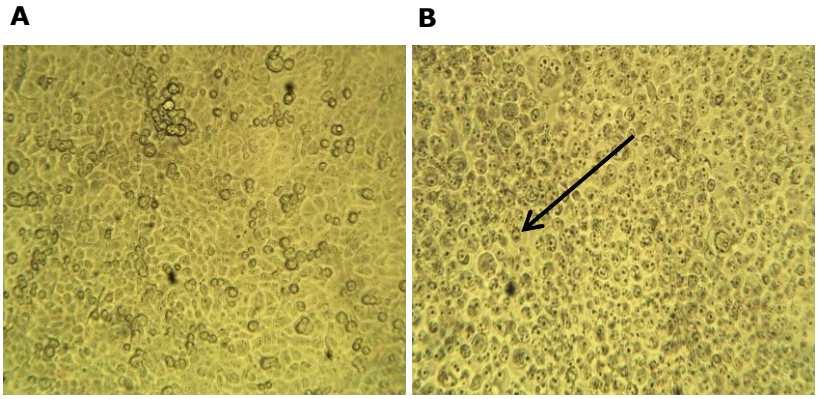

Figure 2.13 Photographic representation of 1.1B4 human pancreatic β-cells treated with or without 0.5 mM *t*BHP for 5 h. Image shows β-cells growing well in culture medium alone (A), while cells appear rounded and separated from neighbouring cells after treatment with *t*BHP, indicated by black arrow. Images were obtained at 10X magnification with the Olympus camera, using the Olympus Ck2 microscope.

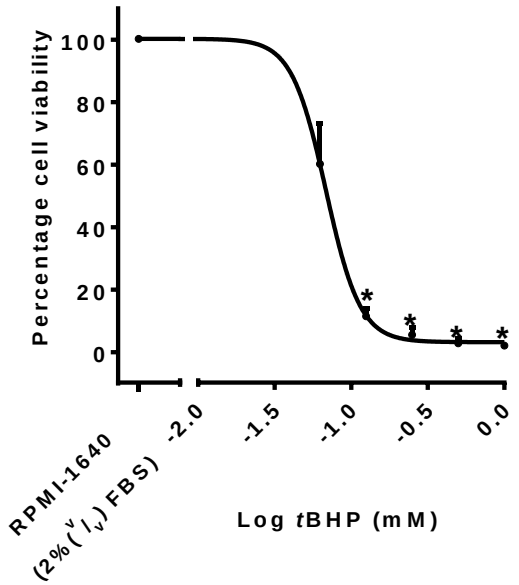

Figure 2.14 Concentration response curve of *t*BHP-induced cytotoxicity in 1.1B4 pancreatic β-cells. Curve shows Log [*t*BHP] vs. response-variable slope at concentration range 0.0625 – 1.0 mM *t*BHP, represented on horizontal axis. Each data point represents mean percentage cell viability of duplicate wells from six independent experiments ± SEM, R^2>0.9. Statistical analysis performed using one-way ANOVA and post hoc by Dunnett's multiple comparisons test. Compared to RPMI-1640 (2%($^v/_v$) FBS) control, significance is denoted as different P<0.001(*).

2.3.3.2 Establishing quercetin as a positive control in 1.1B4 β-cells

Since quercetin proved a reliable positive control for investigating cytoprotective activities of rosmarinic acid and its principal metabolites in HepG2 cells (Fig 2.7A and 2.9A), its ability to emulate such consisitent results was evaluated in human pancreatic 1.1B4 β-cells.

Quercetin protected against 0.5 mM *t*BHP, which caused approximately 98% toxicity after 5 h treatment in both co-exposure and pre-exposure conditions in 1.1B4 cells. In co-exposure experiments, quercetin was essentially non-toxic in absence of *t*BHP (Fig 2.15A). However in the presence of *t*BHP, quercetin produced 71.9 ±8.9% viability at 0.04 mM ($P<0.01$, n = 6) with higher concentrations of quercetin yielding greater cell viability. Similar responses were observed in 20 h pre-exposure conditions, where viable count increased significantly at 0.17 mM and 0.33 mM quercetin, approximately 50% and 60% respectively (Fig 2.15B). However after 20 h exposure, cytotoxicity was recorded at 0.33 mM quercetin, with approximately 23% loss in cell viability ($P<0.05$, n = 6).

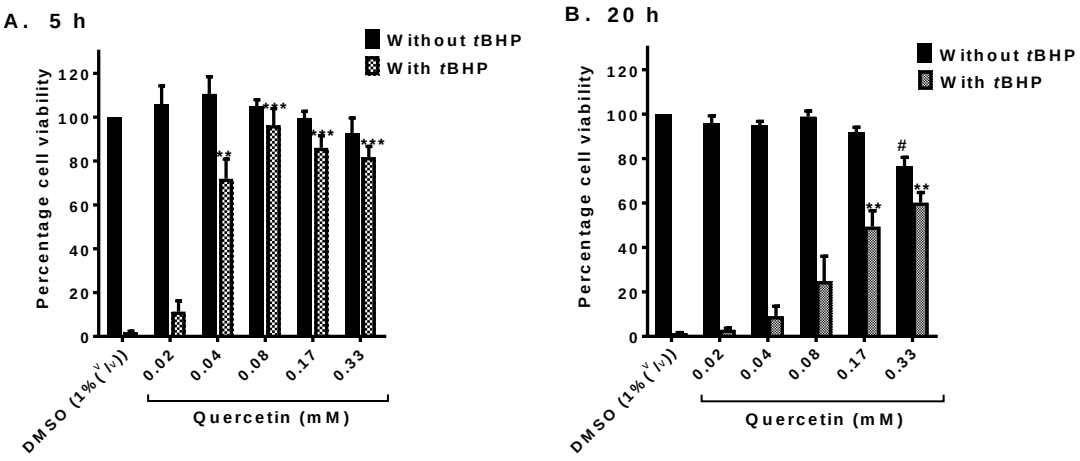

Figure 2.15 Quercetin protects against *t*BHP-induced toxicity in 1.1B4 pancreatic β-cells. Cells were treated with varying concentrations of quercetin for 5 h in the presence and absence of 0.5 mM *t*BHP (A) and 20 h pre-exposure with and without subsequent oxidative challenge by 0.5 mM *t*BHP (B). Each data point represents mean percentage viability of six independent experiments ± SEM, performed in duplicate wells for each concentration. Statistical analysis was performed using one-way ANOVA and post hoc analysis by Dunnett's multiple comparisons test, where values were significantly different from *t*BHP control at $P<0.05$ (*), $P<0.01$ (**) and $P<0.001$ (***). When analysed with Friedman's test, values were significantly different from DMSO control at $P<0.05$ (#).

Similar to earlier results obtained in HepG2 cells (Sections 2.3.2.2, 2.3.2.4 and 2.3.2.5), quercetin displayed concentration-dependent protection and was approximately 3.2-fold more potent in co-exposure experiments (mean EC_{50} value: 0.05 mM; 0.02, 0.07), than in 20 h pre-exposure experiments (mean EC_{50} value: 0.16 mM; 0.11, 0.21) ($P<0.05$, n = 6).

2.3.3.3 Cytoprotection against 0.5 mM tBHP by selected phytochemicals

2.3.3.3.1 Direct cytoprotection against 0.5 mM tBHP

Amidst marginal data variability, quercetin exhibited concentration-dependent direct cytoprotection similar to Fig 2.15A. Caffeic acid being the only metabolite of rosmarinic acid to produce cytoprotection in HpeG2 cells was assessed in 1.1B4 cells, together with quercetin, curcumin and sulforaphane.

However, curcumin alone was cytotoxic at concentrations above 0.07 mM curcumin (Fig 2.16B), and this overlapped with significant protection observed at 0.07 mM (45.8 ±9.9%), in the presence of *t*BHP ($P<0.05$, n = 6).

In a similar pattern, significant cytotoxicity was recorded after 5 h incubation with caffeic acid alone, yielding about 36% toxicity at 1.11 mM caffeic acid (Fig 2.16C). Nevertheless, protection by caffeic acid against *t*BHP was concentration-dependent, with *t*BHP causing approximately 20% added cytotoxicity after 5 h co-exposure with 2.22 mM caffeic acid. Cytotoxicity increased with increasing concentration of sulforaphane alone, without protection against 0.5 mM *t*BHP (Fig 2.16D).

As presented in Fig 2.17, antioxidant potency of quercetin (mean EC_{50}: 0.04 mM; 0.03, 0.04) was comparable to curcumin (mean EC_{50} value: 0.04 mM; 0.08, 0.16), but both phytochemicals were approximately 25-fold more potent than caffeic acid. However, maximum cytoprotective response by quercetin (approximately 80%) was about 0.6-fold more than curcumin and caffeic.

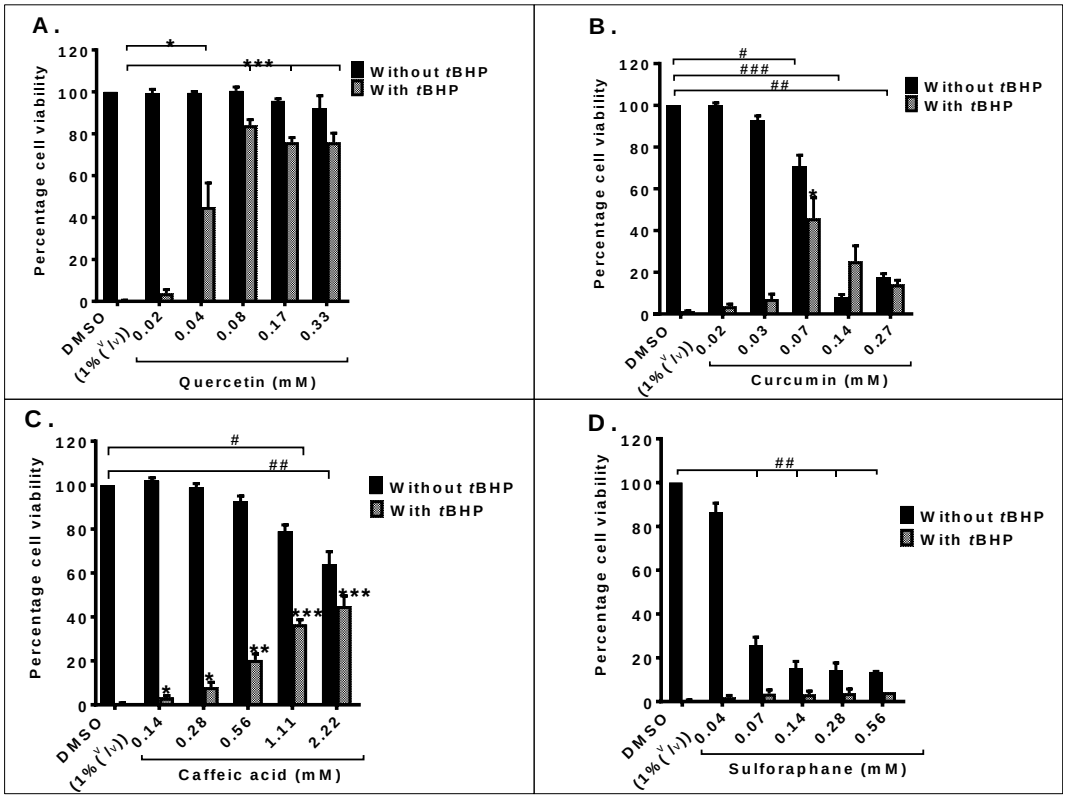

Figure 2.16 Protection against 0.5 mM *t*BHP-induced toxicity in 1.1B4 pancreatic β-cells after 5 h co-exposure to phytochemicals. Cells were treated with quercetin (A), curcumin (B), caffeic acid (C), and sulforaphane (D) and 0.5 mM *t*BHP for 5 h. Each data point represents mean percentage viability of six independent experiments ± SEM, performed in duplicate wells, for quercetin; n = 7. Statistical analysis was performed using one-way ANOVA and post hoc analysis by Dunnett's multiple comparisons test, with values significantly different from DMSO at P<0.05 (#), P<0.01 (##) and P<0.001 (###). For comparison with *t*BHP control, Friedman test was used, with significant difference at P<0.05 (*), P<0.01 (**) and P<0.001 (***).

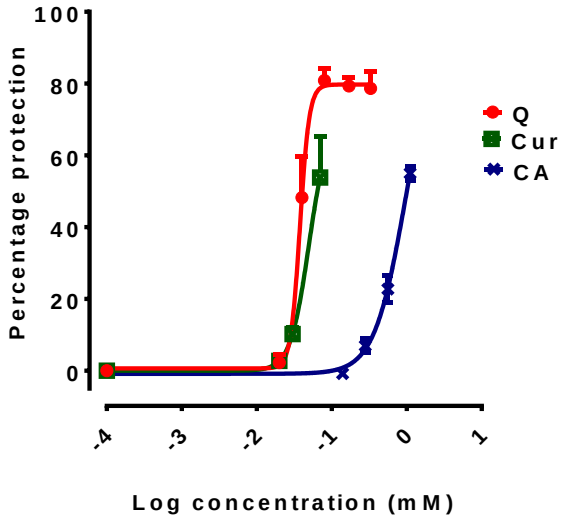

Figure 2.17 Concentration-response cytoprotection curves for quercetin (Q), caffeic acid (CA) and curcumin (Cur) after 5 h co-exposure with 0.5mM *t*BHP in 1.1B4 pancreatic β-cells. Data from Figs 2.16A – D summarised as Log [phytochemical] vs. response-variable slope at concentration range 0.02 – 2.22 mM.

Quercetin (Q) used as positive control. Each data point represents five independent experiments; for quercetin, n = 7, expressed as mean percentage protection ± SEM. R^2>0.8 for all three curves. Less than 4 data points were used for curcumin and caffeic acid due to cytotoxicities at high concentrations.

2.3.3.3.2 Indirect cytoprotection against 0.5 mM tBHP

Quercetin exhibited concentration-dependent cytoprotection, not dissimilar from Fig 2.15B; mean EC_{50} value obtained was 0.26 mM (0.22, 0.29). However, curcumin, sulforaphane and caffeic acid lacked indirect cytoprotective activities against 0.5 mM *t*BHP, whilst producing cytotoxic effects in the absence of *t*BHP.

2.3.3.4 Phytochemicals exhibit cytoprotective activities against 0.125 mM *t*BHP

The lack of indirect cytoprotection by curcumin and caffeic acid in 1.1B4 cells was rather unexpected, considering that these phytochemicals previously demonstrated strong cytoprotection against 0.5 mM *t*BHP in HepG2 cells. Therefore, to enable observation of enhanced cytoprotection, quercetin, caffeic acid and curcumin were evaluated for cytoprotective activities against 0.125 mM *t*BHP. However, due to the lack of cytoprotective effect against 0.5 mM *t*BHP, sulforaphane was not evaluated against 0.125 mM *t*BHP.

2.3.3.4.1 Direct cytoprotection against 0.125 mM tBHP

Overall, direct cytoprotective activities by quercetin, curcumin and caffeic acid were enhanced in the current study compared to Fig 2.16. Although curcumin and caffeic acid were cytotoxic, as observed in Figs 2.16B and C, quercetin showed significant decrease in viability at 0.33 mM quercetin (data not shown).

As presented in Table 2.3, cytoprotective potencies of quercetin and curcumin were comparable, but not dissimilar to Fig 2.17. Caffeic acid was approximately 1.5-fold more potent against 0.125 mM *t*BHP but was about 66-fold and 22-fold less potent than quercetin and curcumin respectively (P<0.001).

Phytochemical	Direct cytoprotection against 0.125 mM *t*BHP Mean EC_{50} values; CI (mM)
Quercetin	0.01 (0.0, 0.03)
Curcumin	0.03 (0.02, 0.05)
Caffeic acid	0.66 (0.30, 1.01)*$^{\alpha}$

Table 2.3 Comparison of direct cytoprotective activities of selected phytochemicals against 0.125 mM *t*BHP. Data are mean EC_{50} and confidence interval (CI) values from five independent experiments; for quercetin, n = 7. Statistical analysis was performed using one-way ANOVA and post hoc analysis by Bonferonni multiple comparisons test. Where indicated, values were significantly different from quercetin at P<0.001 (*) and curcumin at P<0.001 ($^{\alpha}$).

2.3.3.4.2 Indirect cytoprotection against 0.125 mM tBHP

Without phytochemical intervention, 0.125 mM *t*BHP caused an average of 89% cytotoxicity with larger variability compared to the 0.5 mM *t*BHP. With 20 h treatment, cell viability was not affected by quercetin, until 0.33 mM quercetin was used, which caused a reduction of cell viability to approximately 75% (Fig 2.18A). Quercetin significantly increased survival in a concentration-dependent manner to about 73% at 0.17 mM quercetin, with no further increase in viability beyond this concentration.

Pre-treatment with curcumin and caffeic acid alone caused cytotoxicity in 1.1B4 cells. However, significant protection was observed against 0.125 mM *t*BHP, following pre-exposure to 0.07 mM curcumin, which yielded 33.9 ±7.4% increase in viability (P<0.05, n = 6; Fig 2.18B), relative to earlier observations (against 0.5 mM *t*BHP – data not shown). In pre-treated cells, 1.11 mM caffeic acid produced approximately 40% viability against 0.125 mM *t*BHP (P<0.05, n = 6; Fig 2.18C).

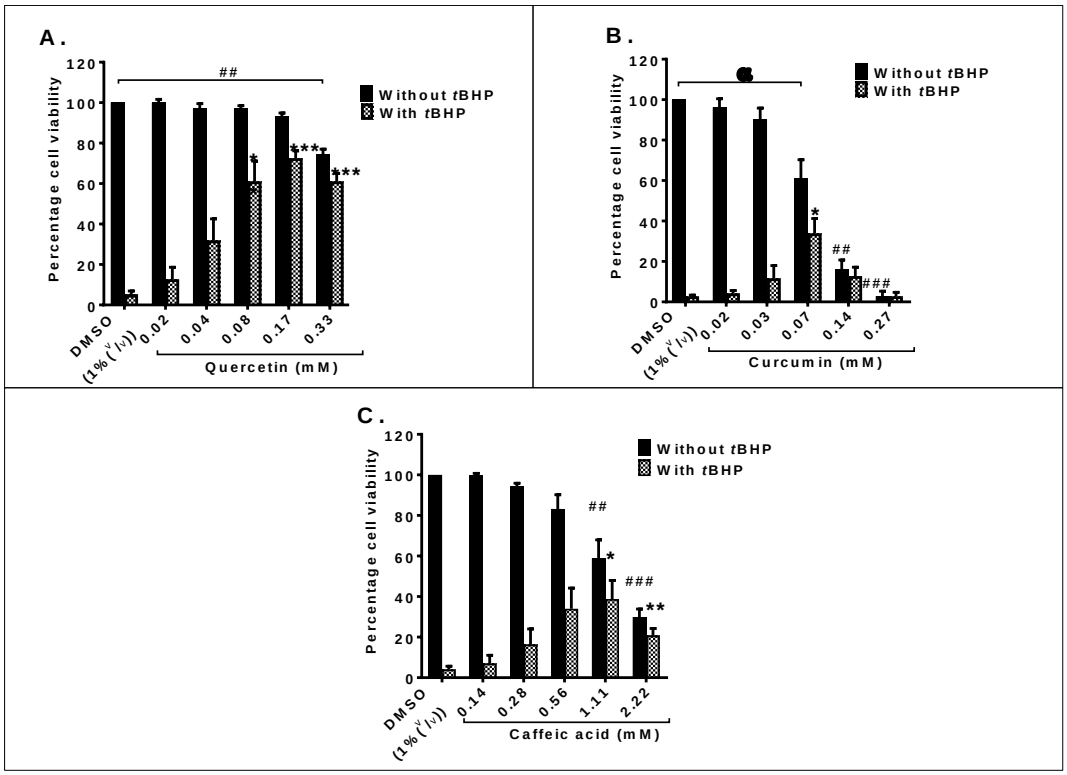

Figure 2.18 Protection against 0.125mM *t*BHP-induced toxicity in 1.1B4 pancreatic β-cells following 20 h pre-exposure to phytochemicals. Cells were treated with quercetin (A), curcumin (B) and caffeic acid (C) for 20 h, then with 0.125 mM *t*BHP for 5 h. Each data point represents mean percentage viability of six independent experiments ± SEM, performed in duplicate wells; for quercetin, n = 7. Statistical analysis was performed using one-way ANOVA and post hoc analysis by Dunnett's multiple comparisons test, with values significantly different from DMSO at P<0.05 (#), P<0.01 (##) and P<0.001 (###). Also, analysis with paired Student's t-test produced statistical significance at P<0.05 (α). For comparison with *t*BHP control, Friedman test was used, with significant difference at P<0.05 (*), P<0.01 (**) and P<0.001 (***).

As presented in Fig 2.19, maximum cytoprotective response by curcumin was less than 25%, as a result of its cytotoxic effects. However, given the data available, mean EC_{50} value obtained was 0.04 mM (0.01, 0.07), and this was comparable to quercetin. The maximum cytoprotective response of caffeic acid was also limited by cytotoxic activities, producing 70.8±7.2%, which was significantly less than quercetin. Also quercetin was about 4.3-fold more potent than caffeic acid (P<0.05, n = 6).

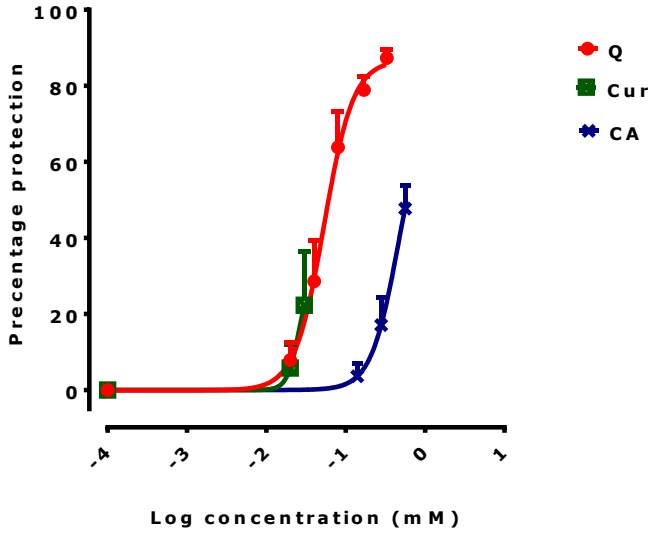

Figure 2.19 Concentration-response cytoprotection by quercetin (Q) and caffeic acid (CA) following 20 h pre-exposure conditions against 0.125 mM *t*BHP in 1.1B4 pancreatic β-cells. Data from Figs 2.18A – D summarised as Log [phytochemical] vs. response-variable slope at concentration range 0.02 – 2.22 mM, with quercetin (Q) used as positive control. Each data point represents five independent experiments; for quercetin, n = 7, expressed as mean percentage protection ± SEM. R^2>0.8 for all three curves. Less than four data points were used for curcumin and caffeic acid due to cytotoxicities at high concentrations.

Phytochemical	**Mean EC_{50} mM (CI)**	
	Cytoprotective activities in HepG2 cells	
	5 h co-exposure	**20 h pre-exposure**
Quercetin	0.03 (0.03, 0.04)	0.09 (0.06, 0.12)
Rosmarinic acid	0.62 (0.58, 0.66)$^{\Psi}$	0.75 (0.57, 0.94)$^{\beta}$
Caffeic acid	0.58 (0.38, 0.72)$^{\Psi}$	0.77 (0.64, 0.94)$^{\beta}$
Danshensu	No effect (>2.02)	No effect (>2.02)
Ferulic acid	No effect (>2.06)	No effect (>2.06)
m-Coumaric acid	No effect (>2.44)	No effect (>2.44)

Table 2.4 Summary of potencies of cytoprotective activities by rosmarinic acid and its principal metabolites. Values are mean EC_{50}, CI of six independent assays; for quercetin, n = 8. Statistical analysis was performed using one-way ANOVA and post hoc analysis by Bonferroni's multiple comparisons test. Statistical significance when compared with quercetin was denoted as P <0.001($^{\Psi}$) in 5 h co-exposure and P<0.001 ($^{\beta}$) in 20 h pre-exposure conditions.

Phytochemical	Mean EC_{50} mM (CI) – cytoprotective activities in 1.1B4 cells			
	Against 0.5mM *t*BHP		Against 0.125mM *t*BHP	
	Direct cytoprotection (5 h)	**Indirect cytoprotection (20 h)**	**Direct cytoprotection (5 h)**	**Indirect cytoprotection (20 h)**
Quercetin	0.04 (0.03, 0.04)	0.26 (0.21, 0.29)	0.01 (0, 0.03)	0.07 (0.03, 0.11)
Curcumin	0.04 (-0.08, 0.16)	No effect >2.22	0.03 (0.02, 0.05)	0.04 (0.01, 0.07)
Caffeic acid	1.0 (0.70, 1.31)$^{\Psi}$	No effect >0.27	0.66 (0.30, 1.01)*$^{\alpha}$	0.30 (0.16, 0.53)*$^{\alpha}$
Sulforaphane	No effect >0.56	No effect >0.56	Not tested	Not tested

Table 2.5 Comparison of cytoprotective activities of quercetin, caffeic acid and curcumin. Data are mean EC_{50} and confidence interval (CI) values obtained from cytoprotection studies in 1.1B4 cells. Statistical analysis was performed using one-way ANOVA and post hoc analysis by Dunnett's multiple comparisons test. Where indicated, values were significantly different from quercetin at $P<0.05$ ($^{\Psi}$) and from curcumin at $P<0.001$ ($^{\alpha}$) and quercetin at $P<0.001$ (*).

2.4 Discussion

The current study aimed to assess radical scaveniging activities of selected phytochemicals in a non-cellular model, and direct and indirect cytoprotective activities in hepatic- and pancreatic β- cells. While HepG2 hepatoma cells were used to establish the robustness of methodology used (amidst interesting findings), cytoprotective activities of the selected phytochemicals, against oxidative stress, are novel findings in the recently developed human-derived pancreatic β-cell line, 1.1B4.

2.4.1 Radical scavenging activities in non-cellular model

In the current study, selected phytochemicals exhibited radical scavenging against DPPH· ranked in a decreasing order of potency: caffeic acid = danshensu = quercetin = rosmarinic acid > curcumin > ferulic acid > m-coumaric acid = sulforaphane. Although Mean EC_{50} values obtained were higher than exisiting reports at 517 nm (Table 2.1), it is important to highlight the different experimental conditions used by earlier studies. Whilst DPPH scavenging activities were generally determined after at least 30 min of incubation (Ak and Gulcin, 2008; Erkan et al., 2008) with phytochemicals, the assay was also conducted using DPPH/ethanolic solvents (Nimmi and George, 2012) and lower concentrations of DPPH (Nimmi and George, 2012), relative to the current study. These assay conditions could have influenced the higher radical scavenging activities recorded. Nevertheless, results obtained from the current study were reproducible, and indicate an interesting trend with structural properties of the selected phytochemicals.

During radical scavenging, antioxidant molecules could form intermediate antoxidant radicals with low reduction potential (Choe and Min, 2005), which are also stabilised by resonance delocalization in their phenolic structures (Choe and Min, 2006) due to formation of C=O bonds from C-OH (Choe and Min, 2009). Furthermore, the presence of adjacent hydroxyl groups results in increased radical scavenging activity (Gavin et al., 2006).

Radical scavenging activities of quercetin have been linked to its phenolic polyhydroxyl groups (Bors et al., 1990; Rice-Evans et al., 1996; Brown et al., 1998). The presence of a

catechol group also enhances radical scavenging activities of quercetin, and confers metal chelating properties (Terao et al., 1994).

It has also been reported that, the phenolic structures of curcumin act as the preferred site for initial radical scavenging activities, although donating a hydrogen atom on the β-diketone CH_2 group forms an essential part of its antioxidant activities (Jovanovic et al., 1999; Jovanovic et al., 2001). This potential bi-targeted reaction with free radicals stems from its keto-enol tautomerism (Sharma et al., 2005) but is influenced by the type of radical encountered. The lack of DPPH scavenging activity by sulforaphane agrees with the absence of hydroxyl groups on its chemical structure (Fig 2.1).

The order of radical scavenging against DPPH contradicts earlier reports which suggested that rosmarinic acid was more potent than quercetin and caffeic acid, (Lima et al., 2006). DPPH scavenging activities of rosmarinic acid, caffeic acid and danshesu could be due to the presence of catechol groups on their chemical structures, while quercetin has two hydroxyl groups in addition to its catechol group (Fig 2.1). DPPH scavenging activities observed following co-incubation with danshensu have been reported (Zhao et al., 2008), and this phytochemical has also shown activity against superoxide anion (Guo et al., 2008) and hydrogen peroxide (Xing et al., 2005; Guo et al., 2008), which could explain its cardioprotective effect (Tang et al., 2011). Thus, it is expected that caffeic acid and danshensu, products from hydrolysis of rosmarinic acid, share equal antiradical potencies with the parent compound. An earlier report by Nakamura et al., (1998) linked superoxide scavenging property of rosmarinic acid to similar activities by caffeic acid and danshensu. Hence, metabolites of rosmarinic acid could retain intrinsic antioxidant properties following biotransformation of rosmarinic acid after oral intake.

Within the confines of the concentration range used, *m*-coumaric acid demonstrated no antiradical activities, suggesting its lack of intrinsic antioxidant potential in accordance with lack of hydroxyl groups, although earlier reports indicated that metabolites of caffeic acid retain antioxidant properties of the parent compound (Gomez-Ruiz et al., 2007). In contrast to earlier reports, methoxy substitution of caffeic acid (to produce ferulic acid)

negatively influenced its antiradical activity (Natella et al., 1999; Cai et al., 2006). The 3-methoxy and 4-hydroxyl groups on its benzene ring, together with its carboxylic acid group are the structural components which mediate antiradical activities of ferulic acid (Graf, 1992), which was least potent against $DPPH^{\cdot}$ radical (Table 2.2). It has also been reported that methylation of hydroxyl groups reduced antioxidant properties of natural phenolic compounds, such as caffeic acid (Simic et al., 2007).

Therefore, it can be inferred that the number and position of hydroxyl groups influence radical scavenging effects of hydroxycinnamics used (Natella et al., 1999). Thus, the lack of polyhydroxyl groups on the structure of *m*-coumaric acid fits with this idea. Results obtained from the DPPH assay may imply that substitution at the *p*-OH removes radical scavenging activity of hydroxycinnamic acids such as caffeic acid metabolite (*m*-coumaric acid). Furthermore, radical scavenging activities of rosmarinic acid and its principal metabolites were used to predict their cytoprotective activities against oxidative damage in HepG2 hepatoma cells.

2.4.2 *t*BHP-induced oxidative damage

*t*BHP caused concentration-dependent cytotoxicity, marked by loss of morphological integrity and viability of HepG2- and 1.1B4 β-cells (Figs 2.3 and 2.4; 2.13 and 2.14 respectively). Here, the β-cells were markedly sensitive to *t*BHP-induced oxidative damage (mean value TC_{50}: 0.068 mM; 0.04, 0.10) compared to HepG2 cells (0.20 mM: 0.15, 0.26). This suggests cell-specific sensitivity to oxidative damage. Presumably, the role of hepatocytes in detoxification in multicellular organisms could be the reason for a higher threshold to oxidative damage.

Experimental conditions such as concentration and exposure duration, used to evaluate cytotoxicity by *t*BHP are similar to protocols used in earlier reports, which have established oxidative stress as a mediator of *t*BHP-induced damage (Piret et al., 2004; Alia et al., 2005; Prasad et al., 2007). Similar to observations by Alia et al., (2005), 0.5 mM *t*BHP caused cells to appear rounded and detached from neighbouring cells (Figs 2.3 and 2.13), resulting in more than 90% cell death in this study. These authors also

observed high cellular ROS levels, lipid peroxidation and high malonaldehyde levels in HepG2 cells after treatment with *t*BHP, which undergoes Fenton reaction to generate high levels of ROS (Prasad et al., 2007).

As far as can be ascertained, this is the first time *t*BHP has been used as an oxidant stressor to model oxidative stress in human pancreatic β-cells. Earlier studies on oxidative stress-mediated damage in β-cell have used streptozotocin and alloxan, β-specific diabetogenic agents which react with intracellular thiols to generate high ROS levels (Lenzen, 2008). Pancreatic β-cells express low basal levels of redox-regulating enzymes such as superoxide dismutase, catalase, glutathione peroxidase and thioredoxin (Lenzen et al., 1996). Hence, such cells are at high risk of redox imbalance and ultimately oxidative damage, as observed in this study.

The low abundance of antioxidant enzymes in pancreatic β-cells remains a controversial topic. It is argued that, ROS such as H_2O_2 contribute to glucose-stimulated insulin signalling and this justifies observation of limited radical scavengers in β-cells (Lenzen et al., 1996; Pi et al., 2010). It has also been reported that minimal levels of mitochondrial ROS is part of the signalling cascade required for hypothalamic glucose sensing (Leloup et al., 2006) and glucose-stimulated insulin secretion (Leloup et al., 2009). The role of H_2O_2 in insulin signalling could be dependent on mitochondrial Ca^{2+} influx (Pi et al., 2007). However, the need to protect pancreatic β-cells against oxidative stress remains vital in alleviating β-cell dysfunction, which exercebates diabetes.

In various cell types including hepatocytes, *t*BHP induced apoptosis via processes which involved calcium influx (Kim et al., 1998) and reduced cellular antioxidant enzyme activity (Alia et al., 2005).

2.4.3 Cytoprotective activities by phytochemicals in HepG2 hepatoma cells

The current study confirms quercetin, curcumin, rosmarinic acid and caffeic acid as both direct and indirect cytoprotective phytochemicals in HepG2 cells, while sulforaphane demonstrated indirect cytoprotection.

2.4.3.1 Direct cytoprotection against oxidative damage

The ability of phytochemicals to mimic radical scavenging activities observed against $DPPH^{\cdot}$ radical was investigated by co-incubation with *t*BHP in HepG2 cells. For reference phytochemicals, the rank order for radical scavenging potencies in non-cellular assay - quercetin > curcumin - was similar to direct cytoprotection recorded against *t*BHP. The lack of direct cytoprotection by sulforaphane also correlated positively with absence of DPPH scavenging activity and hydroxyl group on its chemical structure. Therefore, it can be inferred that radical scavenging activities of these phytochemicals contributed greatly to direct cytoprotection observed.

It was rather unexpected that direct cytoprotective activities by rosmarinic acid and its major metabolites were not in concert with $DPPH^{\cdot}$ scavenging activities; with danshensu and ferulic acid lacking effect in HepG2 cells (Table 2.4). These results suggest either extensive metabolism of phytochemicals to inactive metabolites in HepG2 cells or limitations in cellular uptake of phytochemicals. It is however not expected that extensive metabolism of ferulic acid will occur in HepG2 cells since Mateos et al., (2006) identified conjugates of caffeic acid not ferulic acid, after exposure of both phytochemicals to these hepatocytes (Mateos et al., 2006). Methylation of rosmarinic acid to methyl-rosmarinic acid was also reported in the humans following oral intake of rosmarinic acid (Baba et al., 2005). The discrepancy between radical scavenging and direct cytoprotection potencies is discussed further in Section 2.4.4, in the context of lipophilicity profiles. With the lack of $DPPH^{\cdot}$ scavenging activities, it was not surprising that *m*-coumaric acid showed no protection against oxidative damage in HepG2 cells.

The presence of a catechol group is known to account for quercetin effects against lipid peroxidation and copper-induced damage in human low-density lipoprotein (LDL) (Terao et al., 1994). The presence of reducing groups such as polyhydroxyl substituents (OH), which are efficient in radical scavenging (Choe and Min, 2009), could also account for direct cytoprotective activities against *t*BHP-induced oxidative stress.

In addition to the presence of polyhydroxyl groups, direct cytoprotection could also depend on the ability of phytochemicals to disengage GSH from conjugating with *t*BHP as

proposed by Lima et al., (2006). This was reported in isolated hepatocytes, where caffeic acid-GSH conjugates were observed (Moridani et al., 2001). Although the exact mechanism is not known, it is expected that following good cellular uptake, antioxidant compounds will demonstrate radical scavenging activities against high ROS levels generated *in situ*. This could ultimately prevent *t*BHP-GSH conjugation.

Since rosmarinic acid possesses two catechol groups, which are responsible for metal chelating properties (Brown et al., 1998), it was presumed that this phytochemical would exhibit stronger direct cytoprotection than quercetin or even caffeic acid with one catechol group. This rank order was not observed in the current study although, Lima et al., (2006) reported, that rosmarinic acid (mean EC_{50} 69.2 ±5.3 µM) was more potent than caffeic acid (114.1 ±11.5 µM) in direct cytoprotection against 2 mM *t*BHP in HepG2 cells, both phenolic acids being less potent than quercetin. However, the current study found both phenolic acids to be equi-potent. Furthermore, cytoprotective efficacy of rosmarinic acid was comparable to quercetin, unlike caffeic acid (approximately 70%) which could have been limited by poor cellular uptake following short-term exposure (Mateos et al., 2006).

2.4.3.2 Indirect cytoprotection against oxidative damage

Potency of indirect cytoprotection was observed as: curcumin > quercetin > sulforaphane, rosmarinic acid and caffeic acid, in decreasing rank order. Since HepG2 cells were pre-exposed to selected phytochemicals prior to oxidative challenge, it can be inferred that phytochemicals augmented cellular antioxidant systems against subsequent *t*BHP-induced damage. However, the underlying mechanism for indirect cytoprotection is not clear at this point.

There are reports to suggest that ARE-targeted antioxidant enzymes could be upregulated following phytochemical treatment (Guerrero-Beltrán et al., 2012). Indirect cytoprotective activities of curcumin have be linked to its electrophilic acetylene group, which can interact with highly-reactive cysteine residues located on Keap1 to annul its repressive effect on Nrf2 and subsequently lead to induction of these enzymes, as mentioned in Section 1.2.2.1. Furthermore, cytochrome P450 can metabolize the

catechol group on the structure of quercetin to quinone species (Prochaska et al., 1985; Wang et al., 2010), which disengage Nrf2 from the Keap1/Nrf2 complex (Dinkova-Kostova and Wang, 2011). Indirect cytoprotective activities by sulforaphane reported in the current study is consistent with previous studies in ARPE-19 retinal cells following 24 h pre-exposure to 4 μM sulforaphane, where the role of cytoprotective enzymes was highlighted (Cano et al., 2008). Sulforaphane is also a known inducer of Nrf2 translocation due to its electrophilic central carbon (-N=C=S) (Halkier and Gershenzon, 2006).

Similar to direct cytoprotective activities, poor cellular uptake could have contributed to quercetin being more potent than rosmarinic acid and caffeic acid. Although, maximum responses of caffeic acid, quercetin and rosmarinic acid suggest comparable efficacies, mean EC_{50} values of rosmarinic acid and caffeic acid were approximately 8-fold less than quercetin (Table 2.4). One may argue that cells accumulate phytochemicals during long-term exposure and this is responsible for potencies recorded in indirect cytoprotection. Thus, only limited residual amounts of rosmarinic acid and its metabolites persisted in cells after long-term exposure, producing less cytoprotection against oxidative challenge. However, it is important to highlight that the cellular model used, HepG2 cells, are of hepatic origin and are known to retain their metabolising capacity *in vitro* experiments, unlike primary hepatocytes (Wilkening et al., 2003). However, metabolism of rosmarinic acid in the liver excludes hydrolysis of the polyphenol ester, which is rather conducted by colonic microbiota; see Section 1.5.4.1.

Pre-tretatment (5 h) of Male Sprague–Dawley rats with rosmarinic acid and caffeic acid restored GSH, catalase and glutathione peroxidase levels against oxidative damage by *t*BHP (0.5 mmol/kg body weight). In human HaCaT cells, pre-treatment with rosmarinic acid led to cytoprotection against UVB-irradiation damage, via upregulation of HO-1, an Nrf2-targeted gene (Fernando et al., 2016). Caffeic acid also reduced expression of the Keap1 protein against APAP-induced hepatic damage in mice and following 7-day pre-treatment in HepG2 cells (Pang et al., 2016). Also, Pang et al., (2016) observed increased hepatic GSH expression and decreased ROS levels in caffeic acid pre-treated

mice. Caffeic acid increased cellular glutathione levels via promoting GCL activities (Park et al., 2010; Yang et al., 2013).

Indirect cytoprotection by rosmarinic acid and caffeic acid could be linked to the presence of both nucleophilic (catechol group) and electrophilic (Michael acceptor) moieties on their structures, which cause to transcriptional activation of Nrf2 (Sirota et al., 2015). Thus, pre-exposure of cells could promote oxidization of catechol groups by cellular H_2O_2 to generate quinones, which act as electrophiles against cysteine residues of Keap1 (Dinkova-Kostova and Wang, 2011). Although danshensu (Li et al., 2012) and ferulic acid (Fetoni et al., 2010) are said to accentuate Nrf2 signalling and anti-apoptotic genes, no cytoprotective activities were observed following 20 h pre-exposure.

2.4.4 Limitation of cytoprotective activities of rosmarinic acid and its metabolites by physicochemical properties

With cell membranes mediating exchange of molecules between the intracellular and extracellular environments, the lipophilicity profiles of extracellular molecules could be an important variable for cellular uptake. Hence, phytochemicals were examined for their lipophilicity profiles (Log P), which changes as a function of pH (Log D values preferred at physiological pH; Table 2.6).

Chemicals	Log P	Log D at pH 7.4
Quercetin	1.70	1.63
Rosmarinic acid	1.42	-2.45
Caffeic acid	1.64	-1.78
Danshensu	1.83	-3.46
Ferulic acid	-0.29	-1.23
m-Coumaric acid	2.07	-1.34

Table 2.6 Log P and Log D (pH7.4) values of rosmarinic acid and its principal metabolites. Values were determined by testing structures of quercetin, rosmarinic acid and its principal metabolites in ACD/I-Lab resources.

The unexpected lack of good correlation between intrinsic and antioxidant effects could result from poor lipophilicity profiles of rosmarinic acid and its principal metabolites. As far as can be ascertained, this is the first *in vitro* report on the impact of poor cellular uptake on cytoprotective activities of rosmarinic acid and its principal metabolites. In both 5 h and 20 h conditions, decreasing lipophilicity - quercetin > caffeic acid > rosmarinic acid – showed a good correlation with the rank order for decreasing cytoprotective potencies, and could account for lower potencies of caffeic and rosmarinic acid, relative to quercetin. The influence of cell permeability on cytoprotective reponses has been observed with most plant compounds (Rice-Evans et al., 1996; Spencer et al., 2004).

Rosmarinic acid has demonstrated poor bioavailability in several pharmacokinetic models (see metabolic pattern of rosmarinic acid, Section 1.5.4.1), where *in vivo* levels were dependent on paracellular diffusion across gastrointestinal walls (Konishi et al., 2005). Considering the narrow margin of their lipophilicity profiles, studies in HepG2 cells showed that intracellular amount of ferulic acid was 10% higher than caffeic acid, following an 18 h incubation period (Mateos et al., 2006). Nevertheless, caffeic acid has a poor lipophilicity profile relative to ferulic acid (Table 2.6). Among the principal metabolites of rosmarinic acid, danshensu is least lipophilic confirmed by its uptake via P-gycoprotein transporter-mediated active transport in Caco-2 monolayer model (Zhu et al., 2006; Zhang et al., 2011).

Nonetheless, ferulic acid and *m*-coumaric acid being the most lipid-soluble principal metabolites of rosmarinic acid exhibited no hepatoprotection under the experimental conditions used. Whilst *m*-coumaric acid lacked radical scavenging activity against $DPPH^{\cdot}$, glucuronide and sulfate conjugates of ferulic acid were obtained from the liver after injection of ferulic acid (8 µmol/kg body weight, into the stomach) in rats (Zhao et al., 2004). Therefore it is proposed that, low lipophilic profiles could account for the discrepancy between intrinsic and cellular antioxidant activities of rosmarinic acid and its major metabolites. This is crucial to progression in drug development, since pharmacological activities of rosmarinic acid and its *in vivo* metabolites will ultimately depend on cellular uptake.

2.4.5 Quercetin potentiates curcumin effect during co-treatment

Quercetin or curcumin (singularly) at EC_{10} values lacked cytoprotection against *t*BHP in co-exposure and pre-exposure conditions in HepG2 cells, but co-treatment (both phytochemicals used together) produced direct cytoprotection against *t*BHP. The results obtained from the current study suggest that a mixture of phytochemicals, which may be present in meals and at low levels, could display potent antioxidant activities. The absence of cytoprotective activities by the phytochemicals individually negates the idea that results obtained resulted from synergistic effect; rather, direct cytoprotection was potentiated by the presence of both phytochmeicals.

Quercetin is reported to promote curcumin uptake both *in vivo* and *in vitro* (Kim et al., 2012); plasma levels of curcumin were enhanced after intravenous co-infusion with quercetin in rodents, as wells as cellular uptake in WiDr human colon carcinoma cells. This resulted from competitive albumin binding by quercetin, which shares the same albumin-binding site (subdomain IIA) as curcumin (Kim et al., 2012), suggesting that quercetin could boost pharmacological activities of curcumin during co-treatment. Thus, it can be inferred that radical scavenging activities of low amount of curcumin was dependent on quercetin in co-treatment experiments, quercetin potentiating radical scavenging by curcumin.

This highlights the potential to boost anticancer properties of curcumin, which has poor bioavailability (Anand et al., 2007; Kim et al., 2012); although cytotoxicity observed in the current study was only marginal (Figs 2.7A and 2.8A). This was demonstrated in colorectal cancer patients, where co-treatment with 20 mg quercetin and 480 mg curcumin for 6 months (three times daily) produced a decline in the number and size of polyps by 60.4% and 50.9% respectively (Cruz–Correa et al., 2006). Co-administration of curcumin and quercetin could also be particularly useful in liver diseases, since albumin is largely synthesised in hepatocytes (Kim et al., 2012).

2.4.6 Direct and indirect cytoprotection by selected phytochemicals in 1.1B4 pancreatic β-cells

In the 1.1B4 β-cells, direct cytoprotective activities against *t*BHP (0.125 mM and 0.5 mM) were observed as quercetin = curcumin > caffeic acid, in decreasing rank order. However, caffeic acid showed about 1.5-fold increase in potency against low *t*BHP concentration (Table 2.5). A similar rank order was observed for indirect cytoprotection against 0.125 mM *t*BHP. With the concentrations used, sulforaphane lacked direct and indirect cytoprotective activities. Quercetin was also about 4-fold more cytoprotective than caffeic acid but comparable to curcumin, although maximum protective responses achieved by test phytochemicals (curcumin and caffeic acid) were significantly less than the positive control (quercetin).

Quercetin was more potent as direct cytoprotective chemical, relative to indirect cytoprotection; in keeping with findings in HepG2 hepatoma cells where quercetin served as a reputable standard for evaluating antioxidant activities of rosmarinic acid and its main metabolites. Similar observation was made in rat INS-1 β-cells, where quercetin was more potent during simultaneous incubation with H_2O_2 than in pre-treatment conditions (Kim et al., 2010). Quercetin also protected β-TC1 and HIT β-cells against H_2O_2-mediated oxidative stress during co-exposure conditions (Lapidot et al., 2002). In a report by Youl et al., (2010), 20μM quercetin potentiated glucose-stimulated insulin secretion and extracellular signal-regulated kinase (ERK) 1/2 phosphorylation, inducing a 2.5-fold increase in insulin levels in INS-1 β-cells. Furthermore, quercetin also protected against H_2O_2-induced oxidative damage, while similar concentrations of N-acetyl-L-cysteine and resveratrol were ineffective in 1 h co-exposure conditions (Youl et al., 2010). In addition to these reports, findings of the current study suggest that quercetin has enormous potential in preserving β-cell integrity, as well as protecting against further oxidative damage.

The patterns of direct and indirect cytoprotection by curcumin and caffeic acid are similar to previous findings in HepG2 cells, where curcumin was more potent than caffeic acid. Again, impaired cellular permeability of caffeic acid (Log D value of -1.78) could account for its low cytoprotective activities, relative to curcumin (Log D value of 2.73). Generally,

there is paucity of information on the cytoprotective activities of caffeic acid and curcumin in human β-cells; however, application of phytochemicals in diabetic secondary complications such as retinopathy (Kowluru and Kanwar, 2007), wound healing (Panchatcharam et al., 2006) and nephropathy/renal lesions (Sharma et al., 2006) are well documented. Likewise, evidence of indirect cytoprotection in pancreatic β-cells is currently lacking in the literature. Whilst some studies have been conducted in animals, findings obtained using *in vitro* β-cell models (and certainly human β-cells) is very limited. Currently, this study is the first report on cytoprotective activities of selected phytochemicals against oxidative stress in the human pancreatic 1.1B4 β-cells.

In recent studies, caffeic acid and quercetin improved β-cell survival and function under glucotoxic conditions (Bhattacharya et al., 2013). Taken together, results of direct cytoprotection obtained imply that simultaneous administration of quercetin, curcumin or caffeic acid, under conditions of high cellular ROS levels, can provide protection against oxidative damage via radical scavenging. This has been shown using phytochemicals - quercetin, naringenin and caffeic acid (Bhattacharya et al., 2013) -; nevertheless, further investigations using more physiologically relevant conditions could influence therapeutic management of diabetes mellitus. Following 5-week supplementation with 0.02% caffeic acid, islet architecture and insulin signalling were preserved in *db*/*db* diabetic mice, as well as increased hepatic and erythrocyte antioxidant levels (Jung et al., 2006). Improved insulin signalling has been linked to the preservation of β-cell mass and integrity, considering that β-cell apoptosis correlated positively with impaired glucose tolerance (Butler et al., 2003).

Indirect cytoprotection against streptozotocin was observed in concert with restored insulin secretion, following 24 h pre-exposure to 10 μM curcumin in murine islets (Meghana et al., 2007). In the current study, curcumin showed minimal protection against oxidative damage by 0.125 mM *t*BHP in 1.1B4 human pancreatic β-cells (Fig 2.18B), probably due to marked cytotoxic effects at cytoprotective concentrations. However sulforaphane, which was without cytoprotective activity in this study, is reported to activate nuclear translocation of Nrf2, resulting in upregulation of cytoprotective enzymes as well as inhibition of ROS production and cyclooxygenase expression in rat RINm5F

insulinoma cells (Song et al., 2009). Nevertheless, findings in this study (loss of β-cell viability by sulforaphane) could support recent report by Fu et al., (2013) that sulforaphane suppressed insulin signalling in β-cells; since reduction in β-cell mass has been related to decreased insulin secretion.

Although quercetin, caffeic acid, and to a lesser extent curcumin, exhibited indirect cytoprotective activities, their direct cytoprotective activities may take precedence under high ROS conditions. Further investigations are needed to explore the ability of phytochemicals to potentially upregulate antioxidant enzymes in β-cells, in pre-exposure conditions.

2.4.7 Phytochemicals induce cytotoxicity

In both HepG2 and 1.1B4 cells, curcumin and sulforaphane produced cytotoxic effects after short-term (5 h) and long-term (20 h) exposure, limiting their cytoprotective activities. Sulforaphane lacked direct cytoprotective activities and was not cytoprotective in 1.1B4 cells. Cytotoxic effects of curcumin and sulforaphane could be mediated by increased ROS production (Singh et al., 2005). Sulforaphane also elicited cytotoxicity in hepatomas and adenocarcinomas at higher concentrations (Barcelo et al., 1996). Similar cytotoxic effects have been reported in HepG2 cells following treatment with high concentrations of curcumin, which activated apoptotic mechanisms (Cao et al., 2007; Pledgie-Tracy et al., 2007).

Cytoprotective activities of caffeic acid were limited by their pro-oxidant activities in both 5 h and 20 h conditions. Similarly, quercetin, the most potent cytoprotective agent tested showed marginal cytotoxicity at concentrations above 0.33 mM quercetin (Fig2.4B, Fig 2.10A and 2.12A). Cytotoxicity by quercetin was reported earlier in other β-cell types (Lapidot et al., 2002), albeit shown at lower quercetin concentration than that used in this study. The apoptotic effects of caffeic acid, curcumin and sulforaphane are investigated further in Chapter 3.

Rosmarinic acid and danshensu showed toxicity at high concentrations in HepG2 cells, suggesting a fairly narrow therapeutic index for the phenolic ester in future applications,

unlike caffeic acid. Anticancer effects of rosmarinic acid have also been reported in various cell types as concentration-dependent (Ngo et al., 2011), with anti-proliferative (Tao et al., 2014) and apoptotic (Xavier et al., 2009) activities emerging as potential mechanisms. These reports indicate anticancer potential of rosmarinic acid and danshensu, which has also gained recent research interest (Tao et al., 2014; Gonzalez-Vallinas et al., 2015).

The reason for reduced efficacy (direct cytoprotection) observed at concentrations above 1.11mM caffeic acid, is currently undefined. However, this could be due to either competitive cellualr uptake with *t*BHP or cytotoxicity in the presence of *t*BHP. Nevertheless, this observation could not result from cytotoxicity by caffeic acid, since cytotoxicity was not recorded in the absence of *t*BHP, in HepG2 cells, (Fig 2.5C). Earlier evidence of caffeic acid metabolism shows formation of cytotoxic intermediate species such as quinoids and o-quinones in hepatocytes, following oxidation by hydrogen peroxide (Moridani et al., 2001). Caffeic acid-GSH conjugate formation has also been reported in HepG2 cells and could enhance cellular damage (Lima et al., 2006). Hence, it is presumed that radical scavenging activities promote availability of GSH within the cells, which could then conjugate with quinoid and o-quinone intermediates of caffeic acid. This can lead to cells being deficient in GSH levels and hence more susceptible to cytotoxicity of o-quinone species (O'Brien, 1991). Thus, the initial surge in reactive intermediate of caffeic acid could overwhelm cellular defence mechanism resulting in about 30% toxicity observed in the presence of *t*BHP. Nevertheless, on account of its strong intrinsic antioxidant properties, oxidative damage could have been exceptionally minimised (Fig 2.9C). In the absence of further experimental evidence, this phenomenon which is common among most phyto-antioxidant compounds such as quercetin and kaempferol (Galati et al., 2001), presents interesting ideas worth deliberating.

2.5 Conclusion

From the present study, quercetin and curcumin displayed direct cytoprotective activities against *t*BHP, with quercetin being more potent; while sulforaphane was not effective.

However, sulforaphane showed indirect cytoprotective activities but was less effective than quercetin and curcumin, in order of increasing potencies. Thus, curcumin was the most potent indirect cytoprotective phytochemical. In co-treated cells, quercetin potentiated direct cytoprotective activities of curcumin against oxidative damage, when both phytochemicals were used together at low concentrations.

Although rosmarinic acid and three of its principal metabolites (caffeic acid, danshensu and ferulic acid) possess potent intrinsic antioxidant properties comparable to quercetin, lack of good correlation with direct cytoprotective activities in HepG2 cells highlights poor cellular uptake, as influenced by their lipophilicities profiles. Nevertheless, rosmarinic acid and caffeic acid exhibited both direct and indirect cytoprotective activities, albeit less potent than quercetin.

In 1.1B4 β-cells, direct cytoprotective activities of quercetin and curcumin were comparable against *t*BHP-induced cytotoxicity, but were both more potent than caffeic acid. A similar order of potency was observed for indirect cytoprotection against 0.125 mM *t*BHP, although quercetin alone exhibited indirect cytoprotective activities against 0.5 mM *t*BHP. However sulforaphane lacked both direct and indirect cytoprotective activities against 0.5 mM *t*BHP in 1.1B4 β-cells. The cytoprotective activities of curcumin and caffeic acid were limited by narrow margin between their cytoprotective and cytotoxic activities in β-cells.

With evidence of indirect cytoprotective activities by quercetin, curcumin, sulforaphane and caffeic acid, the role of pro-proliferative activities in mediating these effects was evaluated, in addition to effects of phytochemicals on apoptotic events in HepG2- and 1.1B4 β-cells.

CHAPTER 3

Pro-proliferative and cytotoxic effects of selected phytochemicals in HepG2 and 1.1B4 cells

CHAPTER 3 - Pro-proliferative and cytotoxic effects of selected phytochemicals in HepG2 and 1.1B4 cells

Having shown cytoprotective activities in previous studies, selected phytochemicals were assessed for their effects on cell growth in the context of pre-exposure conditions. In addition, this chapter describes the effects of selected phytochemicals on apoptotic events in HepG2 and 1.1B4 β-cells.

3.1 Introduction

3.1.1 Cell division

Balance of cell number in an organ or organism is dependent on proliferation and cell loss. All cells, being the fundamental living structures of a multicellular organism, divide from a quiescent state (G_o) to produce two daughter cells. In eukaryotic cells, cell division involves interphase, mitosis and cytokinesis modulated by a complex interplay of intracellular signalling transduction, growth factors, enzyme-linked and protein-degradation dependent receptors (Go et al., 2011), with mitogen-activated protein kinases (MAPK), phosphatidylinositol 3-kinase (PI3K) and tyrosine kinase playing a major role (Zhang and Liu, 2002).

Prior to division, cells remain in a quiescent state G_o, a period of zero growth and energy conservation for cell division, but re-enter the cell cycle when growth factors are induced as an essential trigger for the cell division cycle (Cooper, 2000). Cell cycle division consists of two main stages: interphase, comprising of G_1 (dividing cell prepares for DNA synthesis), S (DNA replicates with chromatid formation, resulting in DNA doubling)and G_2 phases (formation of cellular organelles), and mitotic phase (DNA synthesis). A dividing cell could return to G_0 in the absence of growth factors, until the cell passes the restriction point (R) (Fig 3.1), beyond which it commits to the remaining stages of the cell division cycle (Cooper, 2000). Specific CDK-cyclin complexes (such as CDK2, CDK4 and CDK6) are required during interphase, while CDK1 (also known as cell division control protein 2), cyclin A, B, D and E are actively involved in cellular activities towards division in mitosis,

the role of cyclins and CDK in cell division has recently been reviewed (Malumbres and Barbacid, 2009). At the end of the cycle, cells are divided to 2 identical halves.

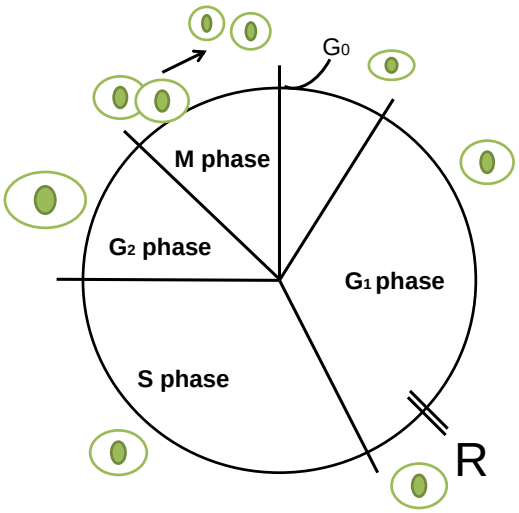

Figure 3.1 The various phases of cell cycle division. Adapted from Cooper, (2000). Induction of growth factors propels a quiescent cell (G_0) into cell growth, with generation of cellular organelles through G_1 to the M phase where mitotic activities result in cell doubling.

Whereas various biomarkers peculiar to cell cycle are commonly used to assess cell proliferation, the resultant increase in cell numbers remains the ultimate confirmation of enhanced proliferation. Therefore, an increase in viable cell count is a more definitive method of assessing increased proliferation, while evaluation of biomarkers remains vital for predicting signalling pathways used by pro- and anti-proliferative agents to increase or decrease cell growth, respectively.

3.1.1.1 Liver regeneration

The liver, which is the largest organ in the body responsible for detoxification and metabolism of xenobiotics, is known to recover anatomy and function of lost tissue after partial hepatectomy via regeneration (Morales-Gonzalez et al., 2015). This is driven by cell proliferation of remnant lobules to reinstate functional tissues to previous states (Michalopoulos, 1990; Fausto and Webber, 1993) and directed by mature cell populations, such as hepatocytes, biliary epithelial cells, endothelial cells, Kupffer cells, and Ito cells, which are able to proliferate to regenerate their individual cell populations (Kang et al., 2012). Hepatocyte proliferation commences 10 – 14 h after partial

hepatectomy, with initial DNA synthesis, peaking at 24 h with subsequent small peaks at 36 – 48 h, until 7 – 10 days when proliferation is completed (Kang et al., 2012).

Liver regeneration is elaborate due to regulation by intracellular signalling cascades, which coordinate regeneration kinetics via a number of growth factors (Morales-Gonzalez et al., 2015). Therefore, an in-depth understanding of these processes will enhance their application in chronic liver diseases, where proliferation is dysregulated (Kang et al., 2012). Using Nrf-2-null mice with partial hepatectomy, it has been suggested that Nrf2 modulates Cyclin A2 and the Wee1/Cdc2/Cyclin B1 pathway, and could be essential for timely replication of hepatocytes (Zou et al., 2015). In addition Nrf2 modulates the augmenter of liver regeneration, which acts as an antioxidant and liver regeneration protein (Dayoub et al., 2013); thus, the ability of exogenous antioxidant compounds to enhance cell proliferation could present novel interest in liver transplantation and regeneration.

3.1.1.2 β-cell regeneration

β-cell replication or regeneration has attracted a great deal of attention in the treatment of diabetes (both type 1 and 2), due to substantial evidence pointing towards loss of β-cell mass in diabetes. Thus, clinical intervention in early stages of T2DM, such as administration of insulin, could enhance regeneration of new β-cells and produce better disease outcome in patients (Weyer et al., 1999). In T2DM, β-cell mass is markedly influenced by unbalanced β-cell replication, apoptosis and new islet formation (Finegood et al., 1995; Bonner-Weir, 2000). However, replication of adult human β-cells is restricted by lack of adequate response to growth factor, nutrition and mitogens such as insulin, lactogen and glucagon-like peptide-1, that have been successful in rodent models (Kulkarni et al., 2012). Differences in signalling of β-cell replication cycle between rodents and humans have been reviewed by Kulkarni et al., (2012).

Human β-cell proliferation was significantly induced following adenoviral overexpression of cell cycle markers such as c-Myc, cdks and cyclin D & E (Karslioglu et al., 2011; Kulkarni et al., 2012), indicating that lack of β-cell replication is due to lack of cell cycle induction by relevant upstream signals (Kulkarni et al., 2012). However, the use of islet

transplantation to restore β-cell mass in T2DM has not always been successful and is inadequate to meet the increasing demand from larger number of T2DM patients. Hence, recent interest has shifted towards *in vivo* β-cell regeneration via the use of therapeutic agents such as phytochemicals.

3.1.2 Hepatocellular and pancreatic cancers

Hepatocellular carcinoma is the second most common cause of cancer-related deaths (Jemal et al., 2011), presenting with high mortality rate due to its poor treatment (Bruix and Sherman, 2011). Early diagnosis could be linked to the occurance of NASH, hepatitis B and C which lead to hepatocellular carcinomas (Johnson, 2013). However, hepatic dysfunction resulting from cirrhosis could affect pharmacokinetic profiles of anticancer drugs, and their therapeutic outcomes (Montella et al., 2016). The challenges of treating hepatocellular carcinomas has been reviewed (Montella et al., 2016).

Pancreatic cancers, generally formed from pancreatic ductal cells, are the ninth most deadly cancer worldwide, have a low survival rate and are unresponsive to conventional chemotherapies and radiotherapies, and recur even after surgery (Warshaw and Fernandez-del Castillo, 1992; Magee et al., 2002). Surgical resection is only effective in about 20% of patients, leading to poor prognosis of the disease (Yeo et al., 2002). In addition to risk factors such as cigarette smoking (Iodice et al., 2008), diabetes could cause or be a secondary complication of pancreatic malignancy (Magruder et al., 2011). Obesity alone presents 1.19 to 1.47 risk of developing pancreatic cancer (Preziosi et al., 2014). The low incidence of pancreatic cancers have been linked to consumption of cruciferous vegetables (Srivastava et al., 2011) hence, phytochemicals have gained interest in prevention and treatment of pancreatic cancers.

3.1.2.1 Apoptosis as a mechanism of cytotoxicity

Generally, cell death could occur via mitochondrial fatality, regulated necrosis, autophagy, apoptosis in both caspase-dependent and –independent modes (Galluzzi et al., 2012). Necrosis is a more haphazard mode of cell death characterised by swelling and inflammation which attacks neighbouring cells upon rupture, while apoptosis occurs in a

regulated manner, thus often called “programmed-cell death” (Fink and Cookson, 2005). Apoptosis is a spontaneous biological means by which cell numbers in an organ are regulated in a controlled manner, characterised by morphological changes such as cell shrinkage, membrane blebbing, increased cytoplasmic granularity, chromatin condensation and formation of nuclear bodies (Kerr et al., 1972; Wyllie, 1992; Wilkins et al., 2002). In addition to its role in removing superfluous cells or those which have become deviant in function, apoptosis is a key phenomenon used to coordinate cell growth in tissue and organ development (Wyllie, 1992).

Apoptosis can be induced by endogenous or exogenous stimuli: the endogenous stimuli can include ROS and DNA damage; while exogenous stimuli include these such as drugs, viruses, cytokines and external stress (Fink and Cookson, 2005; Galluzzi et al., 2012). Exogenous stimuli trigger apoptosis via the extrinsic pathways, which involve signalling death receptors (Fas ligand, TRAIL, TNF-alpha) localised to plasma membrane to activate caspase-mediated events (Schafer and Kornbluth, 2006). The intrinsic pathway is activated by endogenous stimuli via signalling mitochondrial membrane-bound pro-apoptotic proteins (Bax and Bad) and down-regulating anti-apoptotic proteins (Bcl-2 and Bcl-$_X$L) (Kim et al., 2006). This alters mitochondrial membrane potential which is associated with increased calcium influx and cytochrome C release, which activates Apaf-1 (a caspase-9 associated protein) to initiate caspase activation (Kim et al., 2002) (Fig 3.2).

Upon activation, caspase-9 in turn mediates subsequent activation of pro-caspases such as capsase-3 and -7, to initiate a cascade of events in the execution phase (Fig 3.2). In particular, caspase-3 is notorious for its ferocious attack on the cell membrane which destroys its symmetry and results in externalisation of phosphatidylserine to the outer leaflet (Fink and Cookson, 2005). In normal cells, phosphatidylserine and phosphatidylcholine are located on the inner and outer leaflets of the plasma membrane respectively and this ‘flipping’ of phosphatidylserine could be used to investigate apoptosis-mediated cell death. This signals macrophages for phagocytosis, to prevent potential damage to the tissue by cell lysis (Fadok et al., 1992). Hence, phosphatidylserine translocation has been used as a marker for apoptotic events by its

adsorption to annexin V (Andree et al., 1990), as annexin V-positive cells showed nuclear condensation and internucleosomal DNA cleavage (Koopman et al., 1994).

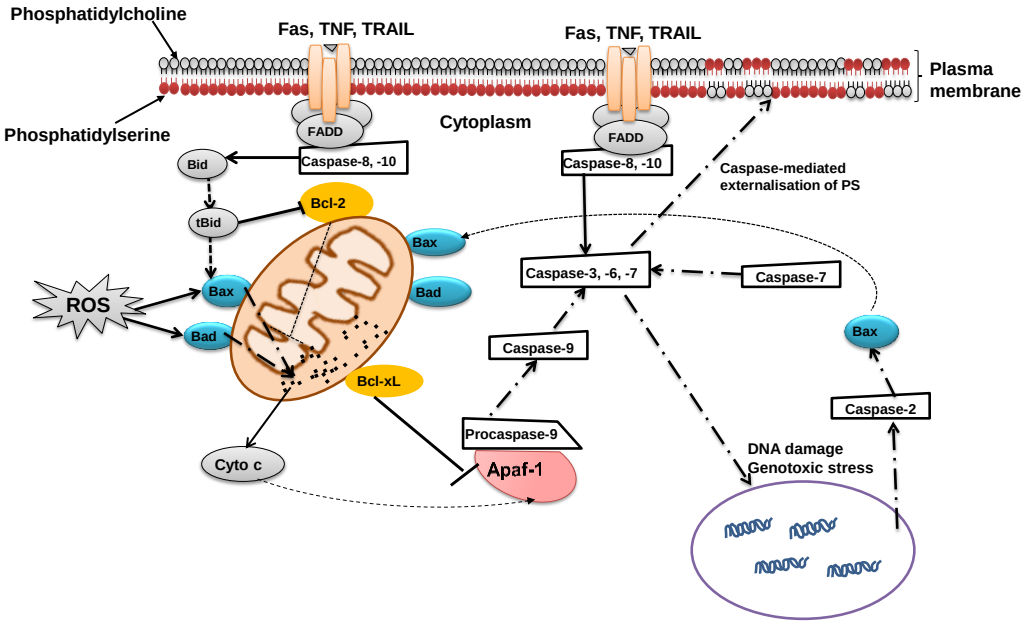

Figure 3.2 An abridged diagram on apoptosis signalling showing intrinsic and extrinsic apoptotic pathway. External stimuli such as viruses bind membrane-bound ligands Fas, TNF-alpha and TRAIL to induce caspase-8 activation via FADD. Intrinsic signalling involves activation of pro-apoptotic proteins Bad and Bax to cause mitochondrial release of Cytochrome c which activates Apaf-1(a procaspase-9 associated protein) to initiate a cascade of caspase-mediated events (Galluzzi et al., 2012). Diagram also highlights the role of pro-apoptotic (Bad, Bax, Bid, tBid) and anti-apoptotic (Bcl-2, Bcl-$_X$L) proteins during apoptosis signalling.

3.1.2.2 Phytochemicals as anticancer agents

Epidemiological studies have shown that regular intake of fruits and vegetable inhibit cancer progression (Riboli and Norat, 2003), with evidence that phytochemicals could potentiate anticancer effects in chemotherapy (Duarte et al., 2010), owing to their ability to modulate cell growth. Hence, research interest has shifted towards apoptotic effects of existing and new chemotherapeutic agents.

Anticancer properties of phytochemicals have attracted considerable attention with interest in their prophylactic as well as curative potentials. Curcumin (Aggarwal et al., 2003; Duvoix et al., 2005) and sulforaphane (Singh et al., 2005) have shown good potential as drugs in cancer therapy or adjuvants of conventional chemotherapy, due to their apoptosis-inducing effects. Additionally, curcumin increased mitochondrial

membrane potential and calcium influx in HepG2 cells (Wang et al., 2011) while, sulforaphane induced caspase-3 activation and ROS levels as part of its apoptotic effects in cancer cells (Park et al., 2007; Singh et al., 2005). *In vivo* studies indicate that caffeic acid could also demonstrate anti-proliferative effects in cancer treatments (Rajendra et al., 2011; Rosendahl et al., 2015). Therefore, there is the need to investigate the mechanisms involved in cytotoxic effects of these phytochemicals.

3.1.3 Aim

Pro-proliferative studies: The current study was conducted to investigate the pro-proliferative effects of quercetin, curcumin, caffeic acid and sulforaphane in HepG2 cells, using cytoprotective concentrations previously identified from results of indirect cytoprotection against *t*BHP. With the exception of sulforaphane which did not demonstrate cytoprotection, pro-proliferative effects of quercetin, curcumin and caffeic acid were also evaluated in 1.1B4 cells. Increase in cell number was assessed by neutral red uptake into the lysosomes of viable cells.

Cytotoxicity studies: In Chapter 2, curcumin and sulforaphane (0.07 mM and 0.14 mM) exhibited cytotoxic effects in HepG2 cells after 5 h treatment; for 1.1B4 cells similar observations were made after 5 h exposure to curcumin and sulforaphane, and caffeic acid (1.10 mM and 2.20 mM). Therefore in this chapter, the mechanism(s) of cytotoxicity was investigated following 2 h treatment with selected phytochemicals, since it was proposed that by reducing the treatment duration (to 2 h), apoptotic events could be observed.

3.2. Materials and methods

3.2.1 Chemicals

List of all chemicals used and their suppliers can be obtained from Appendix I. For apoptosis assay, Alexa Fluor 488 annexin V, propidium iodide and 5X annexin V binding buffer were purchased from Life technologies, UK.

3.2.2 Methods

3.2.2.1 Preparation of solutions

Stock solutions of phytochemicals in DMSO were prepared for quercetin, caffeic acid, curcumin and sulforaphane, as detailed in Section 2.2.1.2.

3.2.2.2 Cell culture techniques

HepG2 cells and 1.1B4 cells were maintained in T175 cm^2 and T75 cm^2 flasks respectively, as detailed in Section 2.2.3.

3.2.2.3 Investigating effect of phytochemicals on cell growth

HepG2 cells were cultured in wells of 24-well plates at high seeding density, approximately 1.2 x 10^6 cells/ml in 10%($^v/_v$) MEM complete medium as described in Section 2.2.5.

The 1.1B4 human β-cells were harvested cultured in 24-well plates at 1.3 x 10^5 cells/ml in 10%($^v/_v$) RPMI-1640 complete medium as described in Section 2.2.5.

Phytochemical concentrations used were obtained from cytoprotection curves as concentrations which produced least protection (baseline of protection curve), between 30 - 60% protection (along the slope of curve) and maximum protection (>70%). These were quercetin (0.02 mM, 0.04 mM, 0.08 mM and 0.17 mM), curcumin (0.02 mM, 0.03 mM and 0.07 mM), caffeic acid (0.14 mM, 1.11 mM and 2.22 mM) and sulforaphane (0.04 mM).

Basal cell growth rate: After the initial 28 h (i.e., before addition of test phytochemical), medium was aspirated and cell viability assessed via neutral red uptake (see below).

❖ **Cell viability after 20hrs treatment:** After culturing for 28 h, HepG2 and 1.1B4 cells were treated with chosen concentrations of phytochemicals for 20 h prior to neural red viability assay.

❖ **Cytoprotection against *t*BHP**: Cytoprotection experiment was conducted simultaneously with cell viability experiments as a control for each cell type, as mentioned in Section 2.2.5. Cell viability was performed as described in Section 2.2.5.3.

3.2.2.4 Investigating cytotoxic effects of phytochemicals

After 28 h of culture, media were replaced with 1 ml fresh culture medium (10%($^{v}/_{v}$) complete) containing phytochemicals or DMSO (1%$^{v}/_{v}$) and cells were treated in triplicate wells, prior to incubation at 37^{0}C. After the 2 h incubation period, cells were assayed for cytotoxicity as described below.

3.2.2.4.1 Assessing cytotoxicity via neutral red assay in attached cells

Following 2 h exposure to phytochemicals, the neutral red viability assay was used to assess cytotoxicity in attached cells as described in Section 2.2.5.3.

3.2.2.4.2 Evaluating effect of selected phytochemicals on early and late apoptosis events in HepG2 cells

After 2 h treatment with phytochemicals, culture media from triplicate wells were collected into sterile 5 ml FACS tubes, for each treatment. The culture medium was then centrifuged at 500 x g for 5 min, to include detached cells in subsequent procedure of this experiment. Cells were washed with 400 µl HBSS (for HepG2 cells) or PBS (for 1.1B4 cells) and solutions was collected in respective FACS tubes containing cell pellet (obtained from initial centrifugation stage) and centrifuged for 5 min at 500 x g. Cells were detached from wells using 100 µl trypsin EDTA (appropriate for each cell type) at 37^{o}C for approximately 5 min. Trypsinisation was then neutralised using 1 ml 10%($^{v}/_{v}$) complete

medium per well. Cell suspension from triplicate wells for each treatment condition was collected into corresponding FACS tube (containing pelleted cells) and centrifuged at 500 x g for 5 min. The supernatant was discarded and cell pellet was suspended in 2 ml ice cold PBS. Cell suspensions were kept on ice to minimise the rate of cell death. Cells were then mixed by pipetting cell suspension a few times to produce single-cell suspensions for each treatment, and were re-centrifuged at 500 x g for 5 min. After washing cells in ice-cold PBS, cell suspensions were centrifuged at 500 x g for 5 min.

Subsequently, cell pellets were resuspended in 100 µl 1x annexin-binding buffer (prepared by adding 1 ml 5X annexin binding buffer to 4 ml deionized water) at this stage. The annexin-binding buffer contains Ca^{2+} ions which facilitate adsorption of annexin V to phosphatidylserine on the outer cell membrane (Fig 3.3).

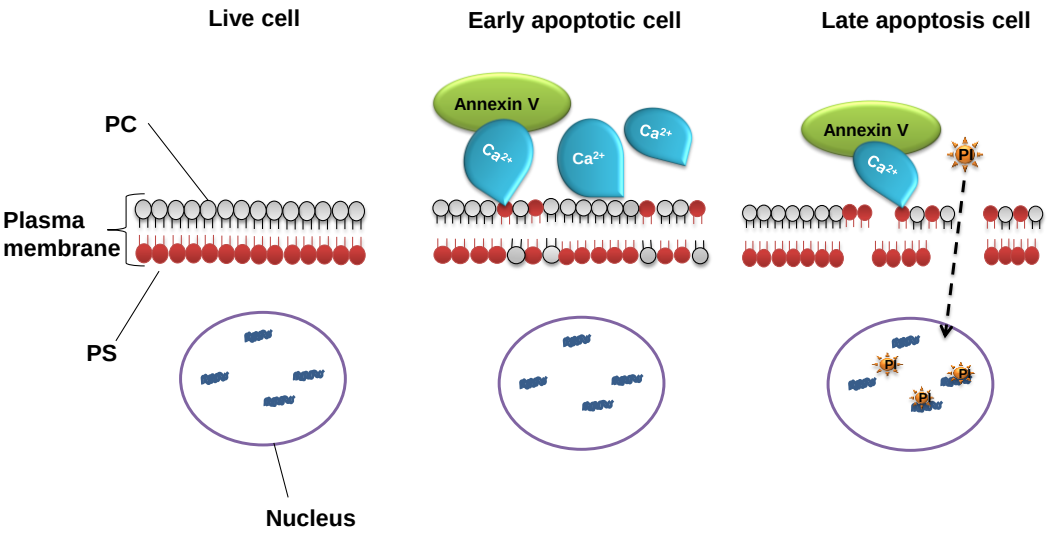

Figure 3.3 A cross-section of an intact cell undergoing early and late apoptosis. This diagram also highlights the events associated with mechanism of the annexin V apoptosis assay. Live cells display phospholipid asymmetry, with a large proportion of phosphatidylserine on the inner leaflet, and sphingomyelin and phosphatidylcholine on outer membrane. Phospholipid asymmetry is lost upon entry of cells into apoptosis (early apoptotic stage) with externalisation of phosphatidylserine (PS) to outer membrane (Fadok et al., 1992), which is adsorbed to anticoagulant protein (annexin V) in the presence of Ca^{2+} ions (Andre et al 1990). Cationic requirement for adsorption to PS is highly specific to the presence rather than concentration of Ca^{2+} (Andree et al., 1990). As apoptosis progresses to the late stage, propidium iodide (PI) gains access to DNA via porous cell membrane.

After adding 5 µl Alexa Fluor 488 annexin V to each suspension, cells were incubated in the dark at room temperature for 10 min. After 10 min, 1 µl of 100 µg/ml propidium iodide

working solution (5 µl of 1 mg/ml propidium iodide stock solution in 45 µl 1X annexin-binding buffer) was pipetted per sample and incubated further for 5 min. After the final incubation period, 400 µl 1X annexin-binding buffer was added to each sample and mixed gently prior to flow cytometry. Stained cells could be kept on ice and analysed by flow cytometry (Beckman Coulter FC500) within 1 h of staining. Flow cytometry was conducted by measuring fluorescence emission at 530 nm and 575 nm, using 488 nm excitation. Data obtained from 10,000 events were analysed using Weasel software version 3.1 (developed by The Walter and Eliza Hall Institute of Medical Research Melbourne, Australia) as shown in Section 3.2.3.

3.2.2.4.3 Cytotoxicity assessment in detached cells using neutral red assay

Cells were treated with cytotoxic concentrations of curcumin and sulforaphane as detailed in Section 3.2.2.4. Both attached and detached cells were collected in a single cell suspension using methodology outlined in Section 3.2.2.4.2. After washing with ice-cold PBS cell suspension was centrifuged, the supernatant was discarded and cell pellet was suspended in 1.2 ml neutral red-containing medium (2%($^{v}/_{v}$) complete medium) in sterile 1.5 ml microfuge tubes, representing 400 µl per well as described in section 2.2.5.3. Neutral red assay was conducted at room temperature for 1 h, with microfuge tubes placed in a petri dish shaking gently at approximately 37 revs/min. Afterwards, cells were centrifuged at 500 x g for 5 min to remove unabsorbed neutral red dye. Cell pellet was resuspended in 1.2 ml warm PBS and centrifuged at 500 x g for 5 min. Fixative (1.2 ml) was pipetted in each microfuge tube and shaken to achieve efficient dye extraction and distribution. Samples in each microfuge tubes were transferred to 96-well plate (9 x 100 µl) and neutral red absorbances measured at 540 nm. Actual absorbance of viable cells was determined after deducting absorbance of no-cell samples.

3.2.3 Data analysis

Data analysis, statistical analysis and data presentation were performed using GraphPad Prism 6.0, as described in Chapter 2.2.6.

❖ Percentage cytotoxicity by neutral red assay was determined using the equation below:

$$\% \text{ cytotoxicity} = \left[\frac{\text{mean absorbance at control} - \text{mean absorbance at sample}}{\text{Mean absorbance at control}} \right] X\ 100\%$$

Data obtained followed Guassian distribution, hence statistical analysis was performed using one-way ANOVA and post hoc by Dunnett's multiple comparison.

❖ Cells stained with Alexa Flour® 488 annexin V and propidium iodide were gated and analysed in a bivariate manner using dot plots of side scatter (SS –PI) versus forward scatter (FS - annexin V) intensity in a four region cytogram as illustrated in Fig 3.4A and B. The gated region represents approximately of 10000 cells enclosed in a polygon to include live, apoptotic and necrotic or dead cells. Cells were categorised as illustrated in Fig 3.4B. Results are presented as means of four different experiments for each treatment from cells of triplicate wells (data represents means of three different experiments for sulforaphane – 0.14mM), with error bars representing standard error of the mean (SEM).

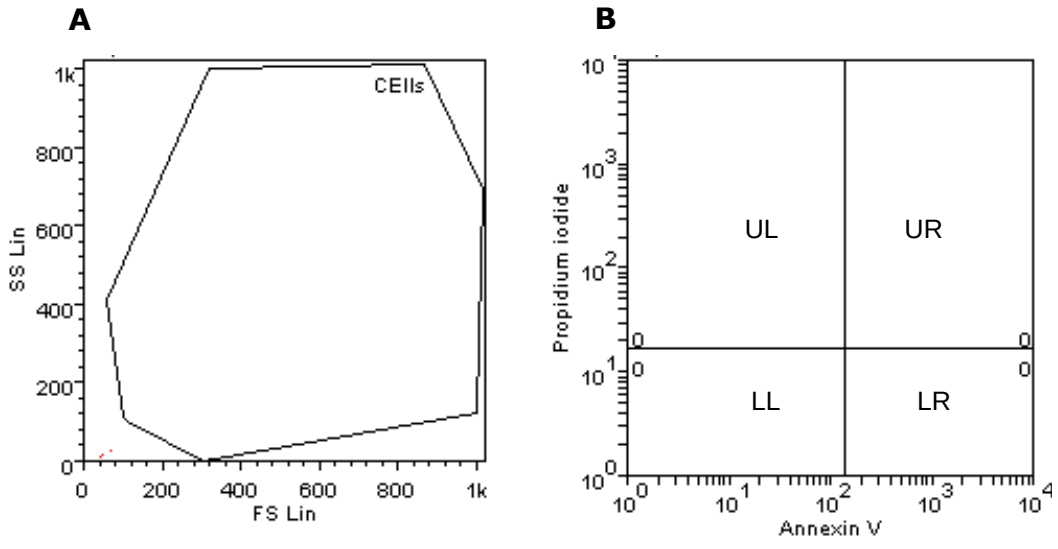

Figure 3.4 Diagrams showing (A) gated cells, (B) cytogram for analysis of gated cells. Cytogram showing quadrant of gated cells (B) defined as LL-Live/undamaged cells (Annexin V and PI negative), LR-early apoptotic cells (Annexin V positive /PI –negative), UR-late apoptotic cells (Annexin V positive /PI positive) and UL dead or necrotic cells (Annexin V negative /PI positive) as defined by Wilkins et al., (2002).

3.3. Results

3.3.1 Pro-proliferative effects of phytochemicals in HepG2 hepatoma cells

3.3.1.1 Basal growth rate of untreated HepG2 cells

After 28 h of seeding at approximately 1.2 x10^6 cells/ml per well, basal cell count of approximately 0.7 (absorbance) was recorded, and this was maintained after culturing for additional 20 h in 10%($^v/_v$) MEM Eagle complete medium (Fig 3.5). Exposure to vehicle control (1%($^v/_v$) DMSO) for 20 h showed no effect.

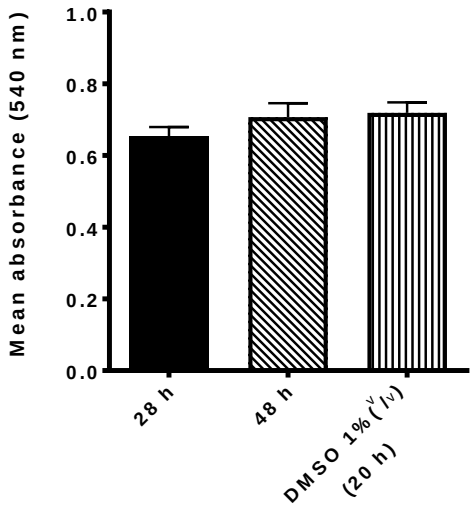

Figure 3.5 Viability of HepG2 hepatoma cells (seeded at high density) after culturing for 28 h and 48 h. Cells were seeded at 1.2x10^6 cells/ml/well in a 24-well plate and cultured for 28 h and 48 h in 10%($^v/_v$) MEM Eagle complete medium. Cells were also treated with 1%($^v/_v$) DMSO as vehicle control for 20 h, prior to neutral red assay. Each data point represents mean absorbance from duplicate wells of six independent experiments ± SEM.

3.3.1.2 Indirect cytoprotection is independent of pro-proliferative effects

Approximately 100% viability was assumed (representing mean absorbance value of 0.65 ±0.07) with DMSO causing a minimal effect. In Fig 3.6A, percentage cell viability recorded after treatment with quercetin did not change with increasing concentration, as was

observed with caffeic acid (0.28 mM, 0.56 mM, 2.22 mM) and curcumin (0.02 mM, 0.03 mM and 0.07 mM). Similar observation was made following 20 h exposure to 0.07 mM sulforaphane.

Whilst *t*BHP caused greater than 90% toxicity in this study, significant cytoprotective activities observed in this study were recorded at high concentrations of quercetin (0.08 mM and 0.17 mM), curcumin (0.03 mM and 0.07 mM) and caffeic acid (2.2 mM) against oxidative damage (Fig 3.6B). These concentrations have previously shown maximum cytoprotection against *t*BHP as essentially greater than 80%, with the exception of 0.08 mM quercetin and 0.03 mM curcumin, which recorded approximately 80% protection (Sections 2.3.2.2.2 and 2.3.2.5). However, significant cytoprotection obtained with quercetin, caffeic acid and curcumin support the use of the various concentrations in this study. Together, Fig 3.6 shows that indirect cytoprotective activities against oxidative damage were not influenced by increase in cell number by selected phytochemicals.

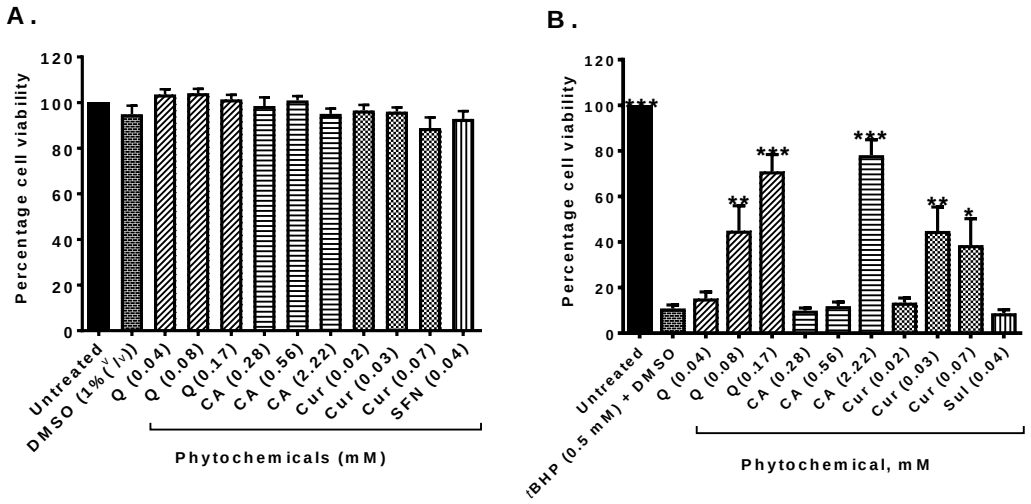

Figure 3.6 Effects of cytoprotective phytochemicals on cell viability of HepG2 hepatoma cells. After 28 h of plating, cells were treated with varying concentrations of quercetin (Q), curcumin (Cur), caffeic acid (CA) and sulforaphane (SFN) in 10%($^{v}/_{v}$) MEM Eagle complete medium for 20 h. Cell viability was assessed after treatment with phytochemicals (A) and after subsequent oxidative challenge (B). Cells were also incubated with 10%($^{v}/_{v}$) MEM Eagle complete medium and 1%($^{v}/_{v}$) DMSO as controls. Data point represents mean percentage viability from duplicate wells of six independent experiments from duplicate wells ± SEM. Statistical analysis was performed (B) using one-way ANOVA and post hoc analysis by Dunnett's multiple comparisons test. Where indicated, values were significantly different from *t*BHP/DMSO control at P<0.05 (*), P<0.01 (**) and P<0.001 (***).

3.3.2 Pro-proliferative effect of phytochemicals in 1.1B4 pancreatic β-cells

3.3.2.1 Basal growth rate in untreated 1.1B4 cells

Mean absorbance obtained after 28 h and 48 h were 0.40 ±0.05 and 0.56 ±0.02 respectively, accounting for approximately 16% increase in cell count ($P<0.05$, n = 6). Further to this, 1%($^{v}/_{v}$) DMSO (approximately 0.58 absorbance) did not enhance cell growth over 20 h exposure (Fig 3.7).

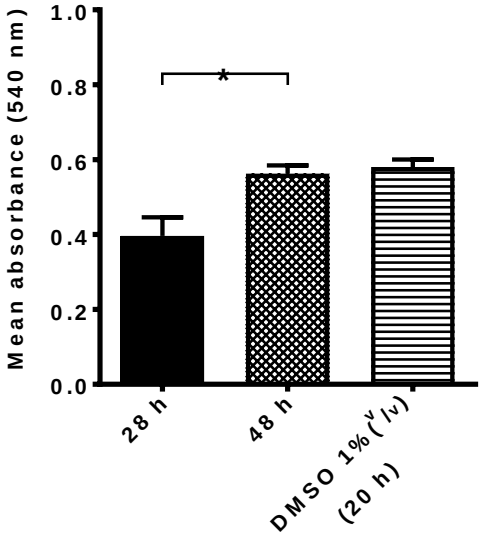

Figure 3.7 Viability of 1.1B4 human pancreatic β-cells was assessed after culturing for 24 h and 48 h. Each data point represents six independent experiments ± SEM obtained from duplicates wells for each experiment. Statistical analysis was performed Kruskal-Wallis test and post hoc by Dunn's multiple comparison test, where mean absorbance at 28 h was used as control. Where indicated, values were significantly different from control (28 h) at $P<0.05$ (*).

3.3.2.2 Effect of selected phytochemicals on β-cell viability

Quercetin exhibited no effect on cell viability, relative to DMSO which was taken to be 100% viability (Fig 3.8A). Likewise increasing concentration of caffeic acid, and curcumin at 0.02 mM and 0.03 mM, had no effect on cell viability; although treatment with curcumin (0.07 mM) led to a decline in cell viability, to 62.92 ±5.61% ($P<0.05$, n = 6).

Exposure of cells led to drastic fall to approximately 4% cell viability ($P<0.001$, relative to absence of *t*BHP – untreated) following 5 h exposure to 0.125 mM *t*BHP ($P<0.05$, Fig

3.8B). Quercetin preserved cell viability against 0.125 mM *t*BHP in a concentration-dependent manner, with significant increase at 0.08 mM and 0.17 mM quercetin (Fig 3.8B). In pre-treated cells, 0.56 mM caffeic acid protected against oxidative damage whilst, cell viability increased with increasing concentration of curcumin, resulting significant effect of 32.1 ±8.24% at 0.07 mM ($P<0.05$, n = 6).

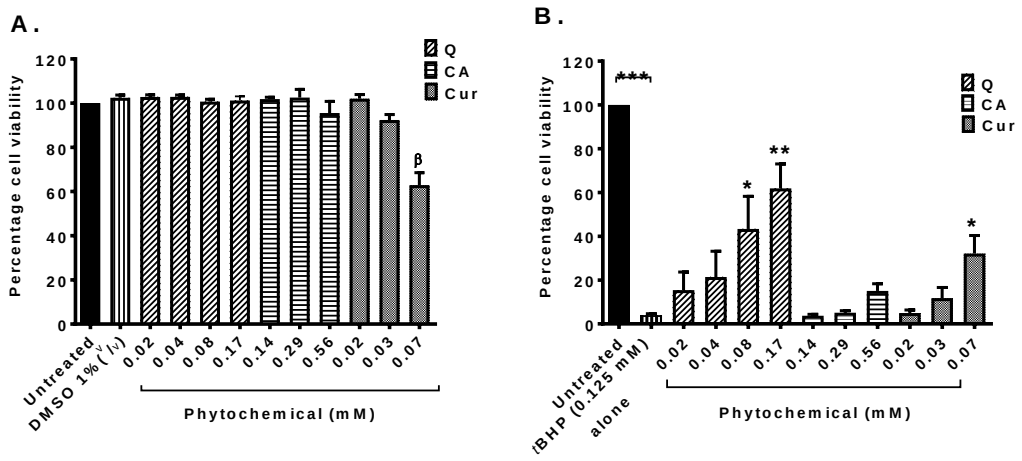

Figure 3.8 Effects of cytoprotective concentrations of phytochemicals on cell viability of 1.1B4 pancreatic β-cells. After culturing for 28 h, cells were treated with varying concentration of quercetin (Q), caffeic acid (CA) and curcumin (Cur) in 10%($^{v}/_{v}$) RPMI-1640 complete medium for 20 h and cells viability assessed (A). Also, indirect cytoprotection was evaluated after phytochemical treatment (B). Cells were also exposed to 10%($^{v}/_{v}$) RPMI-1640 complete medium (untreated) and 1%($^{v}/_{v}$) DMSO as controls for the effect of DMSO and phytochemicals respectively. Each data point was obtained from six independent experiments ± SEM, from duplicate wells. Statistical analysis was performed (A) using Friedman's test and post hoc by Dunn's multiple comparisons test, where values were significantly different from DMSO control at $P<0.01$ (β). One-way ANOVA and post hoc by Dunnett's for multiple comparisons test were used (B), where values were significantly different from *t*BHP control at $P<0.05$ (*), $P<0.01$ (**) and $P<0.001$ (***).

3.3.3 Cytotoxic effects of curcumin and sulforaphane in HepG2 hepatoma cells

3.3.3.1 Cytotoxicity assay in attached cells

After 2 h treatment with curcumin and sulforaphane in HepG2 cells, cytotoxicity was assessed using the neutral red assay (Fig 3.9). For cells treated with DMSO alone, cytotoxicity was on average 6%, and this was not significantly changed by treatment with 0.07 mM and 0.14 mM curcumin. Viability of cells after curcumin exposure was not greatly affected, unlike toxicity previously recorded after 5 h exposure (Section 2.3.2.2.1).

This served as a good marker for further assessment on the effect of phytochemicals on apoptotic events at this time point. However, cytotoxicity increased significantly with increasing concentration of sulforaphane, producing approximately 68% cell death at 0.14 mM sulforaphane ($P<0.01$, $n = 4$).

Although sulforaphane was largely cytotoxic, viable cells remaining after exposure to both concentrations indicated that 2 h exposure could be an appropriate time to investigate underlying mechanism of cytotoxicity.

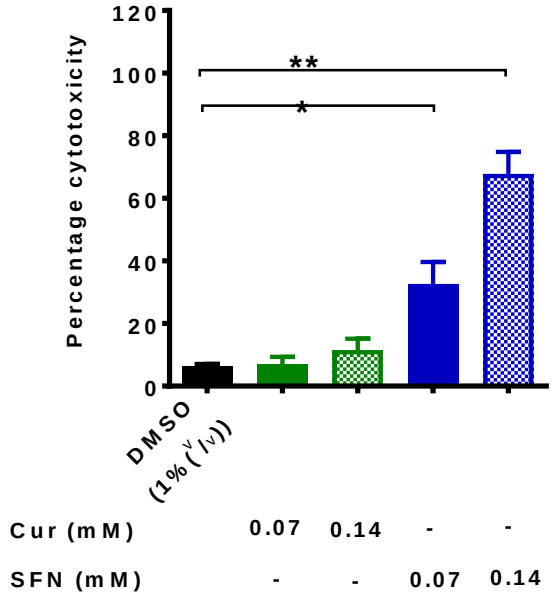

Figure 3.9 Cytotoxicity of curcumin and sulforaphane in HepG2 hepatoma cells (attached cells). Cells were treated for 2 h with 10%($^{v}/_{v}$) MEM Eagle complete medium containing varying concentrations of curcumin (Cur), and sulforaphane (SFN) that were previously shown to be cytotoxic (Section 2.3.2.2.1) and subsequently assayed for neutral red uptake. Each data point represents mean percentage toxicity values from six independent experiments ± SEM from triplicate wells for each treatment. Statistical analysis was determined using one-way ANOVA and post hoc by Dunnett's correction for multiple comparisons test, with significance indicated as $P<0.05$ (*) and $P<0.01$ (**).

3.3.3.2 Effects of plant compounds on early and late apoptosis in HepG2 cells

The Alexa Fluor 488 apoptosis assay detects early and late apoptosis on a per-cell basis using flow cytometry, through adsorption of vascular anticoagulant protein (annexin V) to phosphatidylserine, which is manifested at the plasma membrane surface during apoptosis (Fig 3.10).

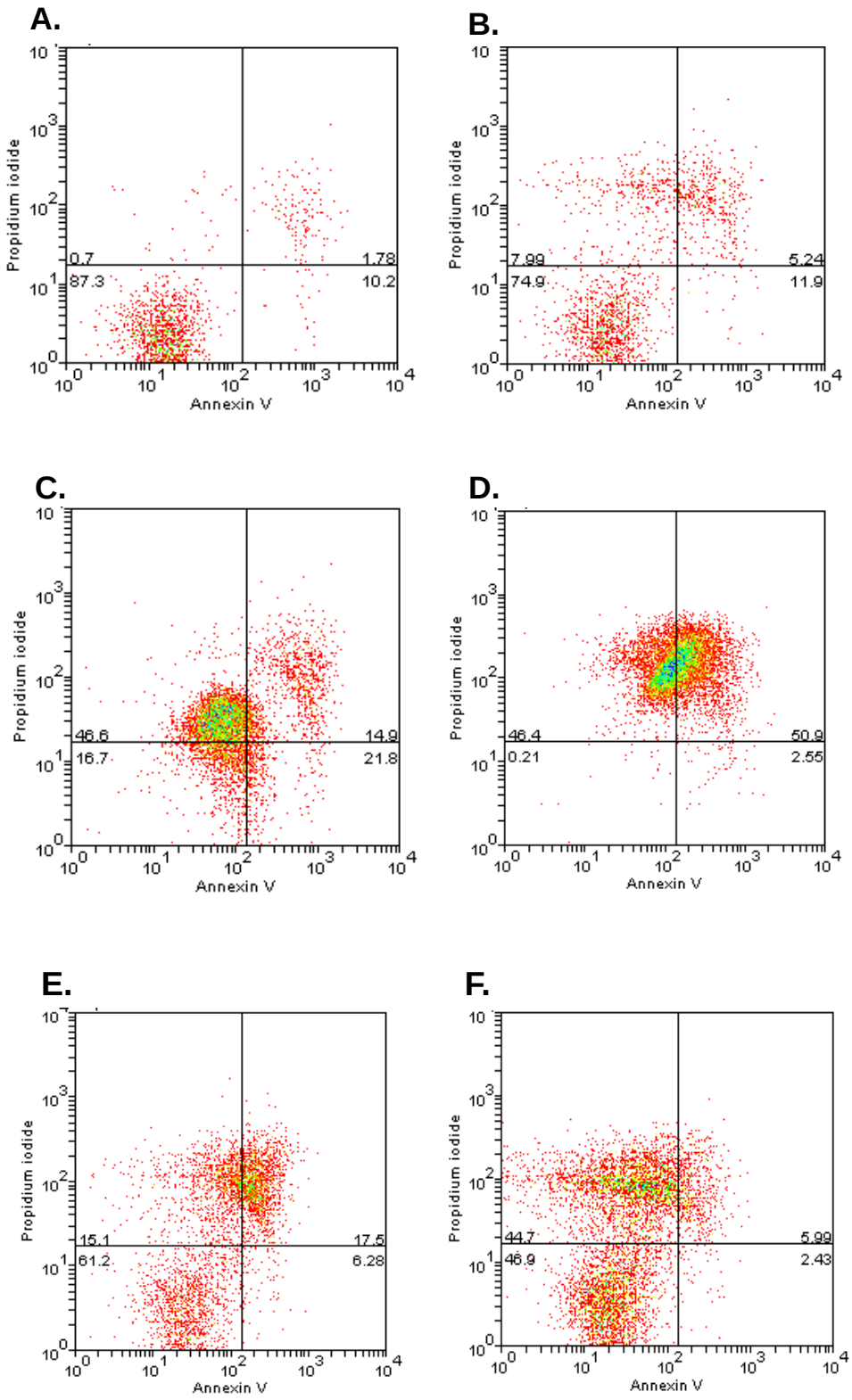

Figure 3.10 Flow cytometry analysis of early and late apoptosis in HepG2 hepatoma cells following 2 h treatment with phytochemicals. Scans are representative of one experiment, showing forward scatter (annexin V) and side scatter (propidium iodide) of gated cells treated with 10%($^{v}/_{v}$) MEM Eagle complete medium alone (A), 1%($^{v}/_{v}$) DMSO (B), curcumin (0.07 mM) (C) and 0.14 mM (D), sulforaphane (0.07 mM) (E) and 0.14 mM (F). Cell populations were categorised as annexin V/PI negative (LL: lower left quadrant), annexin V positive/PI negative (early apoptotic, LR: lower right quadrant), annexin V/PI positive (late apoptotic, UR: upper right quadrant) or annexin V negative/PI positive (necrotic, UL: upper left quadrant).

By conjugating annexin V to a fluorchrome, apoptotic cells in heterogeneous cell population can be distinguished as annexin V-positive with flow cytometry. The role of apoptosis in cytotoxicities by curcumin and sulforaphane was investigated using Alexa Fluor annexin V and propidium iodide, where cells were also labelled with the nonvital dye propidium iodide (PI), which binds to DNA through disrupted cell membrane in late apoptosis, as annexin V/PI positive. Also, PI-positive cells were classified as necrotic or dead (Matteucci et al., 1999).

As shown in Figs 3.10 and 3.11, percentage of live cells recorded in untreated and DMSO-treated cells, approximately 82% and 77% respectively, were not significantly different. Also, the proportions of early and late apoptotic cells were about 10% and 5% respectively, in untreated and DMSO-treated cells. Although, the proportion of necrotic cells recorded in cells treated with DMSO alone (9%) was higher than that for untreated cells (2%), this was not statistically significant.

However, the proportion of live cells decreased markedly with increasing curcumin concentration, this was consistent with increase in early and late apoptotic cells as well as necrotic cells (Fig 3.11B). In cells treated with 0.07 mM curcumin, there was significant increase in late apoptotic cells (approximately 15%) and necrotic cells (approximately 65%), ($P<0.05$, $n = 4$). Moreover, 2 h incubation with 0.14 mM curcumin resulted in 56% necrosis and a further increase in late apoptosis, approximately 27%, compared to 0.07 mM curcumin.

Sulforaphane also decreased the proportion of live cells at both concentrations tested (0.07 mM and 0.14 mM), albeit not significant compared to DMSO, as presented in Fig 3.11C. Furthermore, there was significant increase in necrosis, showing 31.4 ±5.19% ($P<0.05$) after treatment with 0.14 mM, although marginal increase in necrosis was recorded after incubation with 0.07 mM sulforaphane.

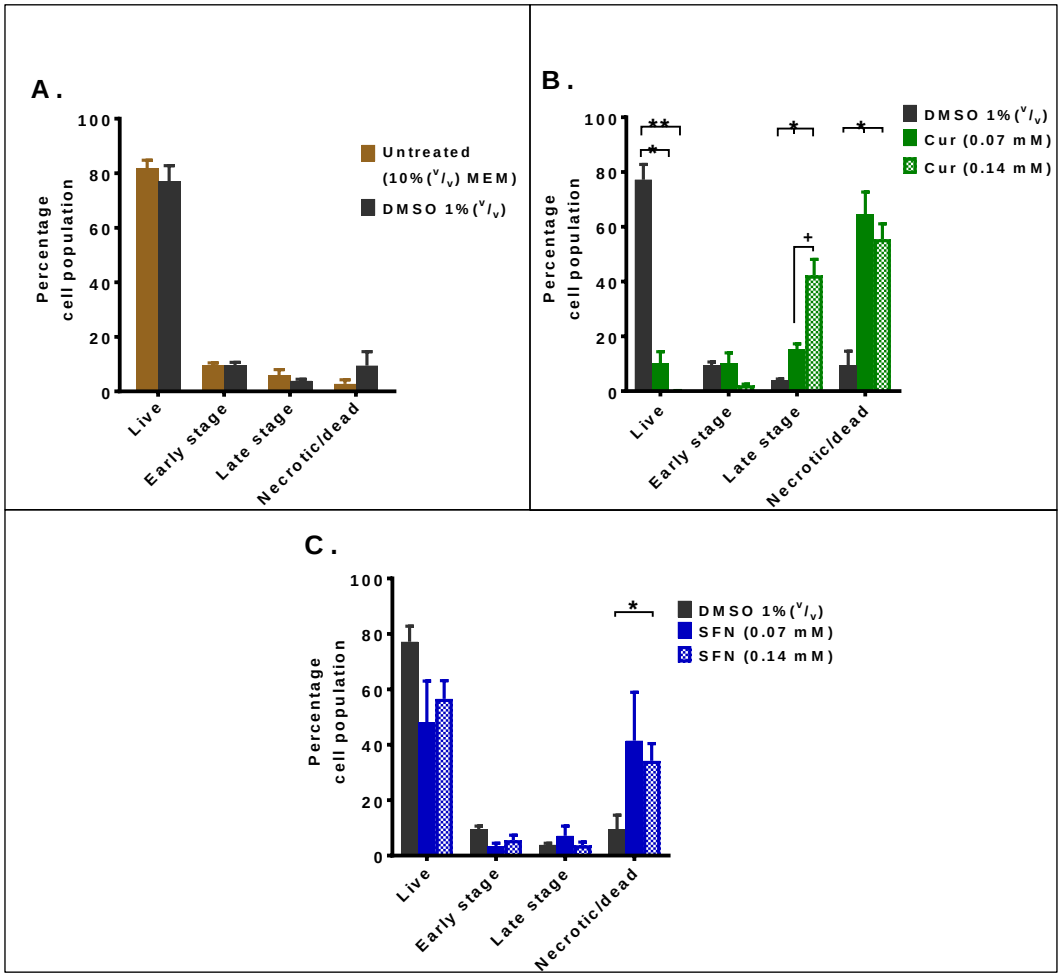

Figure 3.11 Assessment of early and late apoptosis events in HepG2 hepatoma cells. Cultured cells were incubated in 10%($^{v}/_{v}$) MEM Eagle complete medium, also referred to as untreated (A) and 1%($^{v}/_{v}$) DMSO, (B) with curcumin (0.07 mM and 0.14 mM) and (C) with sulforaphane (0.07 mM and 0.14 mM) for 2 h. After staining, cells were categorised as shown in Fig 3.4. Data for DMSO presented in A is repeated in B and C for ease of comparison with curcumin and sulforaphane. Each data point represents percentage cell population from four independent experiments ± SEM but from three independent experiments ± SEM for sulforaphane (0.14 mM), obtained from triplicate wells in each experiment. Statistical analysis was performed using one-way ANOVA and post hoc by Dunnett's multiple comparisons test. Statistical significance, compared to DMSO control is indicated as P<0.05 (*) and P<0.01 (**). Also, values were significantly different from 0.07 mM curcumin at P<0.05 (+).

3.3.3.3 Effect of mechanical stress on phytochemical-mediated cytotoxicity (detached HepG2 cells)

As described in the previous section, most of the cells treated with cytotoxic concentrations of curcumin and sulforaphane were classified as being predominantly late apoptotic or necrotic. Therefore, the effect of mechanical stress on cell viability was investigated.

Cytotoxicity by DMSO treatment was approximately 3%, this was not significantly less than approximately 13% and 27% recorded at 0.07 mM and 0.14 mM curcumin, as well as 0.07 mM sulforaphane (Fig 3.12). However, 0.14 mM sulforaphane produced approximately 30-fold toxicity compared to DMSO ($P<0.05$, n =4).

Compared to cytotoxicity recorded in attached cells (Fig 3.9), there was consistent increase in cytotoxicity, ranging between 7- to 30-fold, recorded in detached cells. Significant effect was only recorded at 0.14 mM sulforaphane, which was higher than the 10-fold increase in toxicity recorded in attached cells. Thus, mechanical stress did not contribute much towards necrotic events observed in Figs 3.10 and 3.11.

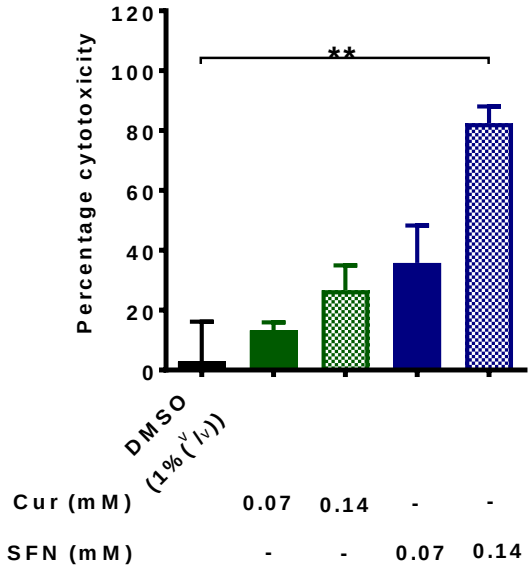

Figure 3.12 Effect of mechanical stress on HepG2 hepatoma cells after treatment with curcumin and sulforaphane. Cells were treated with cytotoxic concentrations of curcumin (Cur), and sulforaphane (SFN) in 10%($^{v}/_{v}$) MEM Eagle complete medium for 2 h and detached to obtain cell suspensions, which were assayed for neutral red uptake. Each data point represents at least four independent experiments ± SEM from triplicate wells. Statistical analysis was performed using one-way ANOVA and post hoc by Dunnett's correction for multiple comparisons test. Where indicated, values were significantly different from DMSO control at $P<0.01$ (**).

3.3.4. Cytotoxic effects of phytochemicals in 1.1B4 pancreatic β-cells

3.3.4.1 Cytotoxicity in attached cells

While DMSO lacked effect, approximately 20% was observed after 2 h incubation with 1.10 mM and 2.22 mM caffeic acid ($P<0.05$, n = 5). Curcumin was also cytotoxic, with approximately 4.5-fold increase in toxicity at 0.07 mM curcumin (Fig 3.13). Additionally, cytotoxicity by curcumin increased markedly from 16.9 ±2.36% to 75.8 ±7.49% at 0.07 mM and 0.14 mM curcumin, respectively ($P<0.05$). A similar behaviour was observed when cells were treated with sulforaphane at 0.07 mM (29.7 ±3.84%) and 0.14 mM (49.7 ±4.94%).

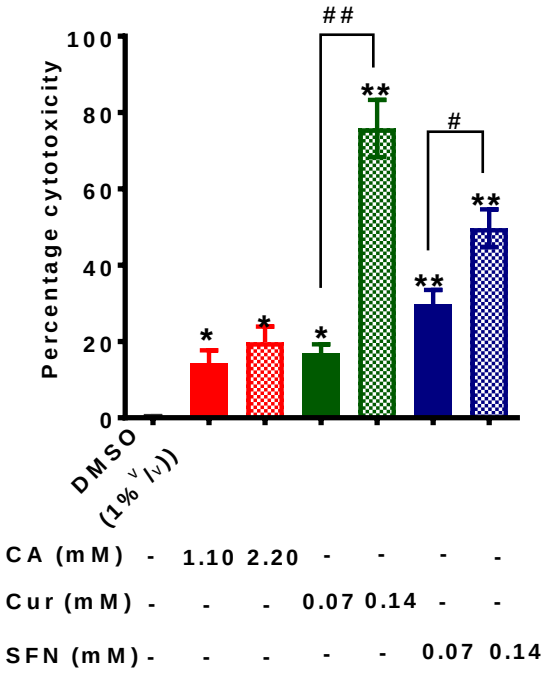

Figure 3.13 Cytotoxicity by caffeic acid, curcumin and sulforaphane in 1.1B4 pancreatic β-cells (attached cells). Cells were treated for 2 h with 10%($^{v}/_{v}$) RPMI-1640 complete medium containing concentrations of caffeic acid (CA), curcumin (Cur), and sulforaphane (SFN) that were previously shown to be cytotoxic (Chapter 2). Cells were also treated with vehicle control and DMSO for curcumin and sulforaphane. Each data point represents mean percentage toxicity values from five independent experiments ± SEM from triplicate wells for each treatment. Statistical analysis was performed using one-way ANOVA and post hoc by Dunnett's multiple comparisons test, where values were significantly different from DMSO control at $P<0.05$ (*) and $P<0.01$ (**). Also, values were significantly different from 0.07mM curcumin at $P<0.01$ (##) and from 0.07mM sulforaphane at $P<0.05$ (#).

3.3.4.2 Effect of phytochemicals on early and late apoptosis events in 1.1B4 cells

Subsequent to phytochemical treatment, cells were labelled as annexin V positive (early apoptotic), annexin V/PI positive (late apoptotic), PI positive (necrotic cells) and annexin V/PI negative (live cells) as presented in Fig 3.14.

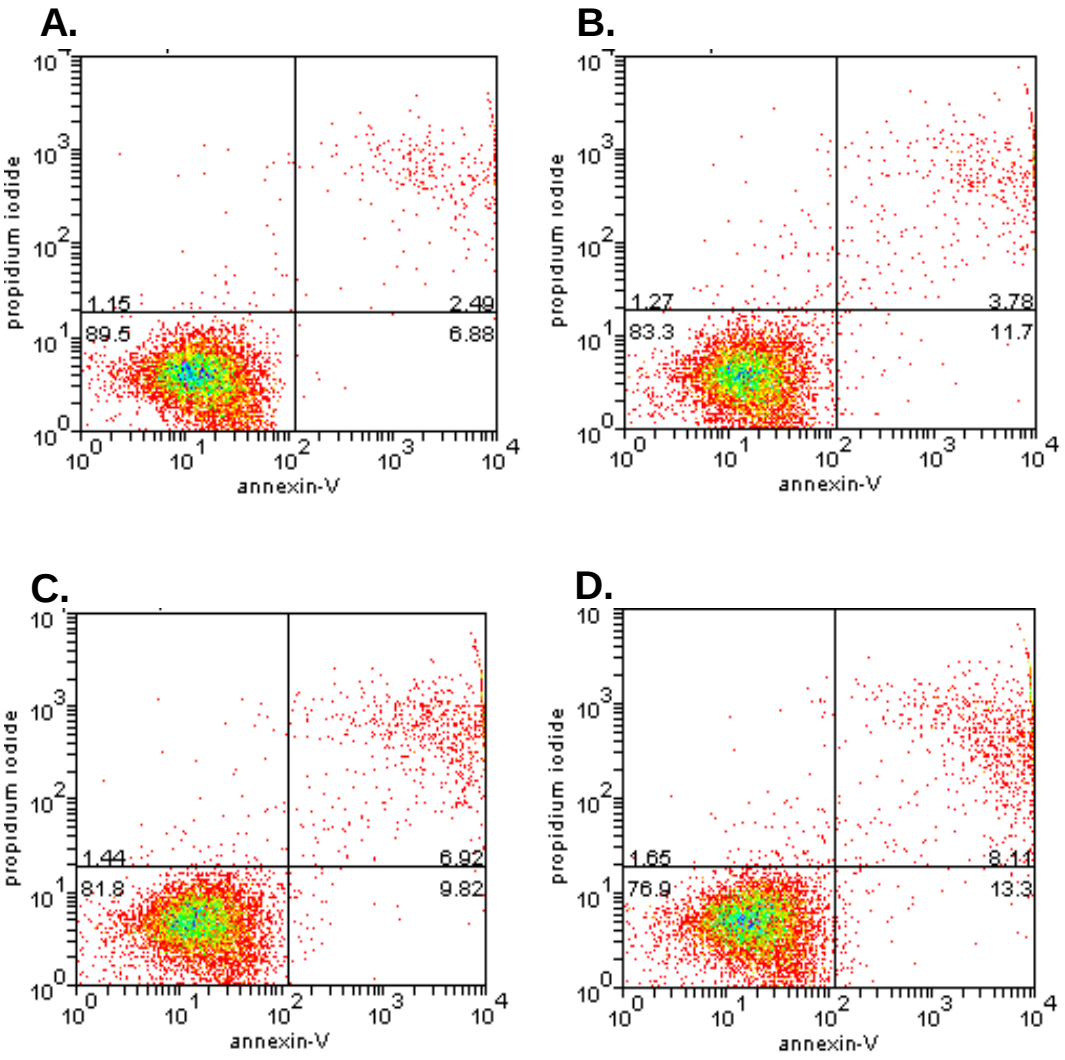

Figure 3.14 Flow cytometry analysis of early and late apoptosis in 1.1B4 pancreatic β-cells following 2 h treatment with DMSO and caffeic acid. Scans, which are representative of one experiment, show forward scatter (annexin V) and side scatter (propidium iodide) of gated cells treated with 10%($^{v}/_{v}$) RPMI-1640 complete medium alone (A); DMSO (B); caffeic acid 1.11 mM (C) and 2.22 mM (D). Cell populations were categorised as annexin V/PI negative (LL: lower left quadrant), annexin V positive/PI negative (early apoptotic, LR: lower right quadrant), annexin V/PI positive (late apoptotic, UR: upper right quadrant) or annexin V negative/PI positive (necrotic, UL: upper left quadrant).

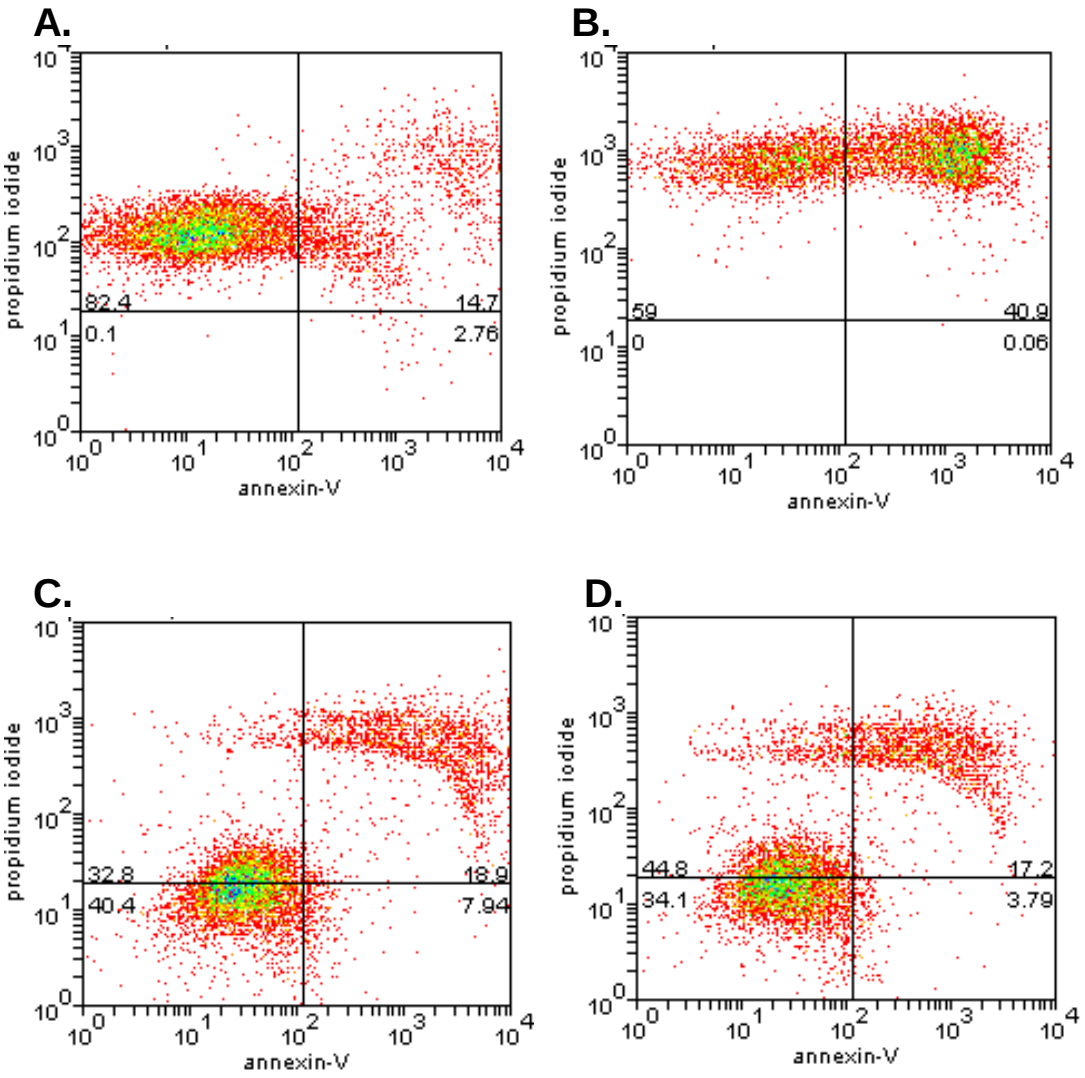

Figure 3.15 Flow cytometry analysis of early and late apoptosis in 1.1B4 pancreatic β-cells following 2 h treatment with curcumin and sulforaphane. Scans, which are representative of one experiment, show forward scatter (annexin V) and side scatter (propidium iodide) of gated cells treated with (A); curcumin (0.07 mM) (E) and 0.14 mM (F); sulforaphane (0.07 mM) (G) and 0.14 mM (H). Cell populations were categorised as annexin V/PI negative (LL: lower left quadrant), annexin V positive/PI negative (early apoptotic, LR: lower right quadrant), annexin V/PI positive (late apoptotic, UR: upper right quadrant) or annexin V negative/PI positive (necrotic, UL: upper left quadrant).

After 2 h incubation with 1%($^{v}/_{v}$) DMSO, there was no significant reduction in the proportion of live cells, compared to 10%($^{v}/_{v}$) RPMI-1640 control; also, 1%($^{v}/_{v}$) DMSO did not increase the percentage of total apoptotic cells (early and late apoptosis). Similar observation was made in terms of necrotic cells (Fig 3.16A).

Caffeic acid produced a concentration-dependent decrease in the proportion of live cells with significant effect at 2.22 mM caffeic acid ($P<0.05$, Fig 3.16B). However, there was no significant increase in early or late apoptotic cells when compared with DMSO control,

and total apoptosis (about 12%) was also not higher than DMSO (about 10%). Nevertheless, cells treated with 2.22 mM caffeic acid recorded approximately 4% increase in necrotic cells, which was significantly higher than observation in DMSO ($P<0.05$, $n = 4$).

There was a drastic reduction in proportion of live cells following 2 h exposure to curcumin ($P<0.001$, $n = 4$; Fig 3.16C). While both concentrations of curcumin, did not demonstrate any effect on early apoptosis, significant increase in late apoptotic cells was recorded relative to DMSO, with a further increase of approximately 60% at 0.14 mM curcumin ($P<0.05$). The low proportion of late apoptotic cells observed after treatment with 0.07 mM was in accordance with the marked proportion of necrotic cells (87.0 ±3.83%) recorded at this concentration. Compared to DMSO, 0.14 mM curcumin produced approximately 7.5-fold increase in necrotic events.

Although live cell population decreased with increasing concentration, 62.1 ±9.52% and 49.4 ±8.28% at 0.07 mM and 0.14 mM sulforaphane respectively, this was not significantly different from DMSO (Fig 3.16D). There was also no significant difference between early and late apoptosis compared to DMSO. Sulforaphane, at both concentrations, increased the apoptotic population significantly by about 35%, relative to DMSO. Nevertheless, the percentage of necrotic cells increased in a concentration-dependent pattern, recording significant effect of 14.9 ±1.30% at 0.14 mM sulforaphane ($P<0.05$, $n = 4$).

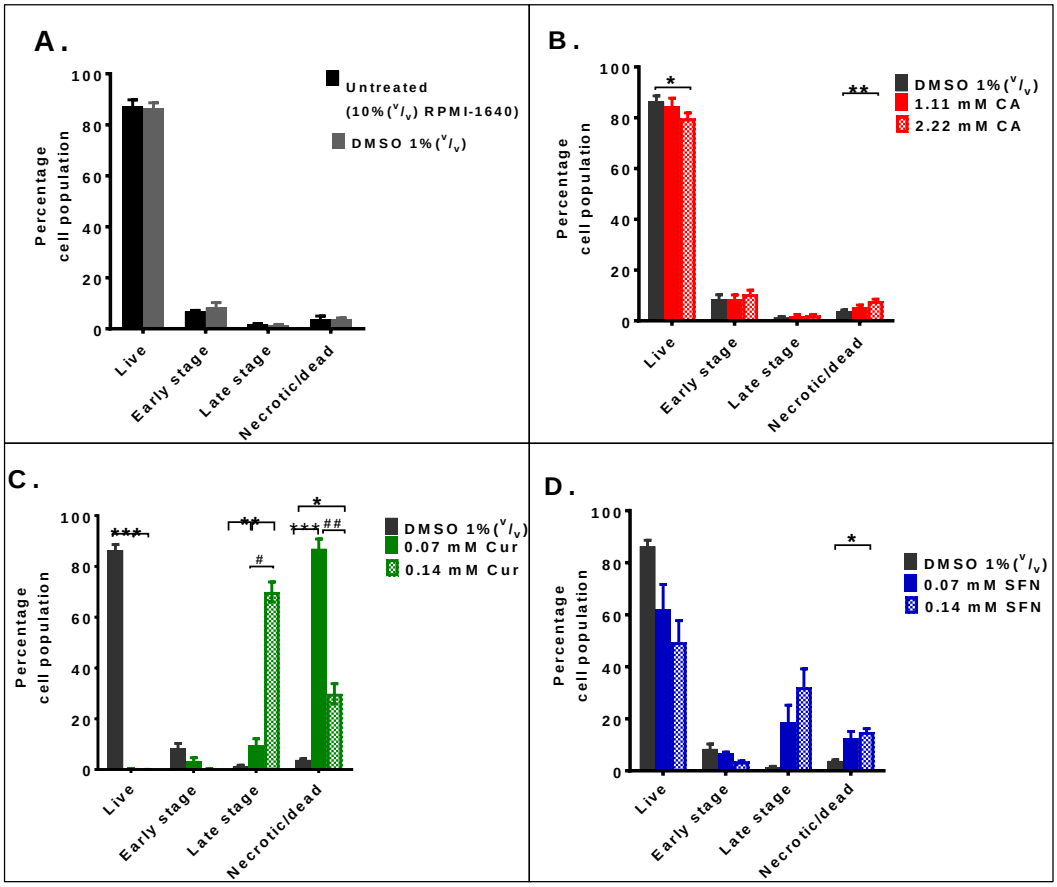

Figure 3.16 Assessment of early and late apoptosis events in 1.1B4 pancreatic β-cells. Cultured cells were treated with 10%($^{v}/_{v}$) RPMI-1640 complete medium (A – untreated (10%($^{v}/_{v}$) RPMI-1640 complete medium) and 1%($^{v}/_{v}$) DMSO as controls, (B) caffeic acid (1.11 mM and 2.22 mM), (C) curcumin (0.07 mM and 0.14 mM) and (D) sulforaphane (0.07 mM and 0.14 mM) for 2 h. Data for DMSO presented in A is repeated in B,C and D for ease of comparison with caffeic acid, curcumin and sulforaphane respectively. Each data point represents percentage cell population obtained from triplicate wells of four independent experiments ± SEM. Statistical significance was determined using one-way ANOVA and post hoc by Dunnett's multiple comparisons test, where values were significantly different from DMSO control at P<0.05 (*), P< 0.01 (**) and P<0.001 (***). Also, values were significantly different from 0.07 mM curcumin at P<0.05 (#) and P<0.01 (##).

3.3.4.3 Effect of mechanical stress on toxicity assay in 1.1B4 cells

The cytotoxicity data obtained in detached β-cells was not significantly higher than results from attached cells (Fig 3.13). Therefore, as presented in Fig 3.17, the supposed 'mechanical stress' which may have been exerted on the 1.1B4 cells by the use of trypsin did not influence apoptosis data illustrated in Figs 3.14 – 3.16.

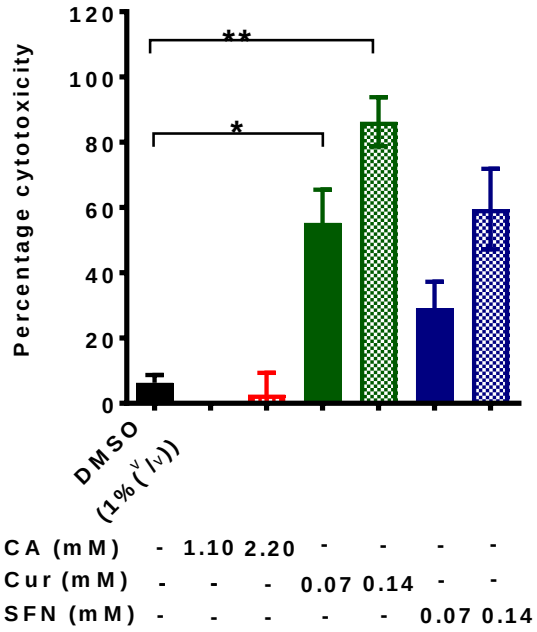

Figure 3.17 Effect of mechanical stress on cytotoxicity by phytochemicals in 1.1B4 pancreatic β-cells. Each data point represents at least N = 4 ± SEM independent experiments from triplicate wells for each treatment. Statistical analysis was performed using one-way ANOVA and post hoc by Dunnett's correction for multiple comparisons test. Where indicated, values were significantly different from DMSO control at $P<0.05$ (*) and $P<0.01$ (**).

3.4 Discussion

3.4.1 Cytoprotection is not mediated by pro-proliferative activities of phytochemicals

Whilst phytochemicals could be useful in promoting cell growth, it may be essential to characterise antioxidant, pro-oxidant and pro-proliferative activities for optimal therapeutic benefits, although these effects could be inter-related in multicellular organisms. Results obtained from the current study indicate that indirect cytoprotective activities exhibited by quercetin, caffeic acid, curcumin and sulforaphane were independent of enhanced cell growth (over the duration of pre-exposure experiments – 20 h) in HepG2 and 1.1B4 cells. Thus, cytoprotective concentrations of the chosen phytochemicals did not produce any significant effect on cell viability, although cytoprotection was recorded.

3.4.1.1 Lack of pro-proliferative effects by phytochemicals in HepG2 and 1.1B4 cells

The lack of significant growth, when HepG2 cells were cultured for additional 20 h ($P>0.05$), could result from high cell seeding density (1.2×10^6 cells/ml), making cells fairly confluent prior to phytochemical treatment. Thus, cytoprotection experiments were designed to limit any significant increase in cell proliferation over the 48 h experimental period. This could serve as an alternative method to staging cells by serum starvation, which is commonly used in *in vitro* studies.

In 1.1B4 cells, significant increase in cell number was recorded ($P<0.05$, $n = 6$) between 28 h to 48 h culture period (Fig 3.7). However, no increase in cell number was observed following exposure to varying concentrations of quercetin and caffeic acid; curcumin (0.07 mM) caused a reduction in cell viability.

The lack of pro-proliferative effect by phytochemicals suggests that indirect cytoprotection was produced by an alternate mechanism, possibly via upregulation of cytoprotective proteins. These results contradict some reports of pro-proliferative effects by the selected phytochemicals. In a report by Woude et al., (2003), quercetin stimulated cell cycle progression at low concentrations. Using HCT-116, HT29 and MCF-7 carcinoma cells, these authors observed pro-proliferative effect of quercetin at concentrations <20 µM, 30

- 40 µM and 20 – 40 µM, respectively. Also, Li et al., (2013) recently reported that quercetin repressed leptin signalling and Akt/Forkhead box O1 (Akt/FoxO1) activation to preserve β-cell mass under high fructose levels in rat islets (Li et al., 2013). Furthermore, quercetin enhanced pancreatic islet regeneration, while reducing plasma glucose levels in streptozocin-induced diabetic rats (Vessal et al., 2003). Thus, while quercetin may demonstrate biphasic effect on cell cycle progression, these effects are remarkably influenced by cell type, flavonoid concentration and, possibly, cell density. Hence, it can be inferred that the cytoprotective range of quercetin may be well distinct from cytotoxic range.

Although caffeic acid showed no effect in HepG2 cells, marginal decline in viability was observed in 1.1B4 cells. This could be consistent with concentration-dependent decrease in cell proliferation and increase in sub-G_1 arrest, as well as increase in ROS levels after 48 h exposure to HCT 15 colon cancer cells (Jaganathan, 2012). However, an earlier study in human monocytic U937 cells, reported no proliferative effect after 18 h treatment with 500 µM caffeic acid (Nardini et al., 1998); however, a recent report suggested that the caffeoyl moiety drives high hepatocyte growth factor levels in human dermal fibroblasts (Kurisu et al., 2013). In the current study, approximately 35% cytotoxicity recorded at 0.07 mM curcumin in 1.1B4 cells (Fig 3.8) could have resulted from curcumin-induced ROS generation. While ROS induced by curcumin causes cellular damage (Gupta et al., 2011), this may influence indirect cytoprotective activities by curcumin.

It is important to mention that the neutral red assay is more suitable for end-point determination of effects on cell growth (viable cell count), compared to relatively up-stream molecular targets determined by cell cycle analysis and other techniques, which provide more definite details of modulatory effects on cell growth factors and signalling.

3.4.2 Cytotoxic effects of phytochemicals

In the present study, curcumin and sulforaphane caused significant cytotoxicity after 2 h exposure in HepG2 cells. Also, both phytochemicals caused necrosis, with a small proportion of HepG2 cells in early and late apoptosis stages (Fig 3.10 and 3.11). Similar results were obtained in 1.1B4 cells, following 2 h treatment with caffeic acid, curcumin

and sulforaphane (Fig 3.14 - 3.16). This could imply that either cells may have already been necrotic at the time of the apoptosis assay or that concentrations used were too high to enable detection of early apoptotic events, such as externalisation of phosphatidylserine. These results are not consistent with evidence of apoptotic effects induction by curcumin and sulforaphane, although evidence of necrosis by curcumin, via mitochondrial– and caspase-mediated p53-independent pathway, has been reported in human lung cancer cell line H1299 (Li et al., 2015). However, necrotic events by these phytochemicals is a novel observation in both cell types.

Chang et al., (2014) observed apoptosis via increase in cytochrome c and caspase 3 activities at 80 µM curcumin, using osteosarcoma MG63 cells. In human pancreatic cancer BxPC-3 and PANC-1 cell lines, 3-day treatment with curcumin led to down-regulation of apoptosis inhibitory proteins Notch-1, Hes-1, Cyclin D1 and Bcl-$_X$L while inducing apoptosis (Wang et al., 2006). In PANC-1 and MIA PaCa-2 human pancreatic cancer cell lines, sulforaphane activated caspase-8 and caused loss of mitochondrial membrane potential as well as loss of plasma membrane integrity (Pham et al., 2004). However, percentages of early and late apoptotic events in 1.1B4 β-cells, were not significantly different from the vehicle control (Fig 3.16C). Recent studies also reported ROS-mediated induction of apoptosis following treatment with 0.8 mM caffeic acid in HCT 15 colon cancer cells (Jaganathan, 2012). Results of the current study suggest that upstream markers in apoptosis signalling are required to enhance our understanding of the mechanism involved in cytotoxic effects observed.

3.4.2.1 Inconsistencies in interpreting apoptosis data in HepG2 cells

The lack of significant evidence of apoptotic events in the current study highlights the complexities in detecting various apoptotic events and the disadvantages of different experimental techniques in confirming various stages of this process. The concentrations and exposure duration used in this study vary from earlier reports of apoptosis induction by curcumin (Wang et al., 2011) and sulforaphane (Park et al., 2007).

For HepG2 cells, the trend for cell population distribution towards the upper right quadrant (Fig 3.10C and D) after curcumin exposure is reminiscent of the results of Wang et al., (2011) where increasing concentration of curcumin induced apoptosis after 1 h treatment in HepG2 cells. In fact, they recorded similar proximity between late apoptotic and necrotic cells, as was observed in the current study. Cao et al., (2007) also reported similar effects using annexin V apoptosis assay. While subsequent research on apoptosis by curcumin have rightly proceeded from the findings of Wang et al., (2011, about 58 citations) and Cao et al., (2007, about 125 citations), their classification of cell populations by the use of the cytogram (as shown in Fig 3.4) highlights the subjectivity in gating and interpreting flow cytograms (Janatpour et al., 2002; Wilkins et al., 2002), particularly in the case of Cao et al., (2007).

3.4.2.2 Effect of mechanical stress on apoptotic events

With the neutral red assay, percentage toxicity in detached cells was marginally higher than in attached cells, possibly due to the added traumatic effect of detaching cells and multiple pipetting to produce single cell suspensions. Although cytotoxic agents may have compounded this effect, critical analysis of control samples (untreated and DSMO-treated cells) presents a good reflection of damaging effects caused by sample preparation and its effect on data accuracy. Koopman et al., (1994) also reported adsorption of annexin V to internalised phosphatidylserine in B cells which were also ethidium bromide positive. Thus, while such cells may register as double positive (annexin and PI, in this study) and be classified as late apoptotic, they may well be necrotic. Clarity on this topic could also be obtained from intensities of annexin V and PI stains on cytograms (see Fig 3.10, 3.11 , 3.14 and 3.15) as was also highlighted by Wilkins et al., (2002). Nevertheless, this method of sample preparation is commonly used and reflects a credible approach to flow cytometry (Wang et al., 2011).

Several reports on apoptosis, induced by curcumin and sulforaphane, have employed supporting results such as DNA damage, mitochondrial dysfunction, upregulation and downregulation of anti- and pro-apoptotic proteins respectively, in addition to exposure of phosphatidylserine on outer cell membrane (Syng-ai et al., 2004; Cao et al., 2007; Wang

et al., 2011). Thus, additional results are needed to confirm data obtained in this study. Nevertheless, the neutral red viability assay remains a credible colorimetric method of evaluating cytotoxic effects of compounds (Repetto et al., 2008) and in this study, it was effective in both attached and detached cells.

3.5 Conclusion

Results from the current investigation negate the influence of increased cell numbers in mediating indirect cytoprotective activities by selected phytochemicals against *t*BHP, suggesting that other cellular activities by phytochemicals may have produced cytoprotection.

The role of apoptosis in mediating cytotoxicity induced by curcumin and sulforaphane could not be confirmed, since cells were predominantly necrotic at the time of apoptosis assay. Nevertheless, caffeic acid did not demonstrate effect on apoptotic events in the 1.1B4 β-cells. Hence cytotoxic activities could be mediated by other mechanisms, but require further studies at different exposure conditions.

CHAPTER 4

Glucotoxicity and lipotoxicity in human hepatoma and pancreatic β-cells

CHAPTER 4 - Glucotoxicity and lipotoxicity in human hepatoma and pancreatic β-cells

This chapter investigates the effects of high glucose and high lipid load on the viability of human pancreatic 1.1B4 β-cells and human hepatoma HepG2 cells. Subsequently, cytoprotective activities of phytochemicals were investigated against high lipid exposure.

4.1 Introduction

The synergistic effects of both chronic hyperglycaemia and elevated FFA on impairment of β-cell function have led to the concept of glucolipotoxicity, which has been accepted as a major event in the pathogenesis of T2DM (Fridlyand and Philipson, 2004). It has also been established that both high glucose and high FFA levels cause apoptosis and loss of β-cell viability; although the exact mechanism remains to be elucidated, oxidative stress is known to play a key role (reviewed in Section 1.3.2). Furthermore, increase in circulating FFA levels is a predisposing factor for insulin resistance, and accumulation of FFA in the liver plays a causative role in induction and progression of NASH (reviewed in Section 1.3.1).

4.1.1 The role of glucose toxicity in pathogenesis of diabetes

Chronic exposure to supraphysiological glucose concentrations causes time-dependent irreversible damage to insulin synthesis and exocytosis, as well as β-cell components, and this is referred to as glucose toxicity (or glucotoxicity) (Robertson et al., 2003). Additional effects of glucotoxicity include decreased mitochondrial activity and glucokinase gene expression, reduced binding of pancreas duodenum homeobox-1 (Pdx-1) to insulin promoter, as well as accelerated apoptosis (Kajimoto et al., 1999; Butler et al., 2003). Glucotoxicity is different from glucose desensitization which is a reversible state of β-cell exhaustion caused by short-term exposure to elevated glucose levels (Kaiser et al., 1991). The underlying mechanism of glucotoxicity involves a complex

interplay of events including glucose metabolism by hexosamine pathway, formation of advanced glycation end-products (AGE), inflammation, ER stress hypoxia, and oxidative stress, leading to β-cell dysfunction and apoptosis, as reviewed by Bensellam et al., (2012; also shown in Fig 4.1).

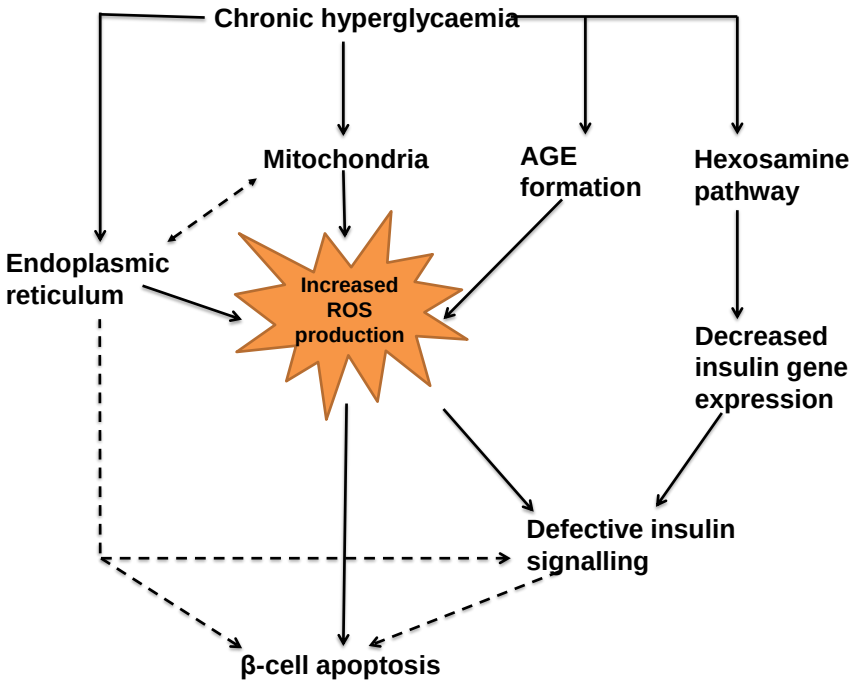

Figure 4.1 Schematic representation of pathways involved in β-cell apoptosis during chronic hyperglycaemia as reviewed by Bensallam et al., (2012). Chronic hyperglycaemia causes β-cell dysfunction and apoptosis via a complex interplay of events.

Flux of glucose through the hexosamine pathway eventually leads to increased activity of O-linked β-N-acetylglucosamine transferase, an enzyme that facilitates post-translational modification of Pdx-1 (Gao et al., 2003) and forkhead box other-1 (FoxO1) (Kuo et al., 2008), causing β-cell dysfunction (Bensellam et al., 2012). Treatment of rat INS-1 cells with AGEs decreased insulin stores, glucose-stimulated insulin secretion and ATP synthesis, and impaired mitochondrial function (Zhao et al., 2009). It has been reported that oxidative stress could play a role in AGE-mediated glucotoxicity since both N-acetyl cysteine and aminoguanidine (inhibitor of AGE formation) prevented decrease in insulin gene promoter activity, insulin mRNA and insulin secretion (Tanaka et al., 1999).

The role of oxidative stress in glucotoxicity is supported by evidence of β-cell protection by antioxidant use or overexpression (Tanaka et al., 2002; Robertson et al., 2003). Persistent exposure to high ROS levels has been shown to impair binding of Pdx-1 to insulin promoter via stimulating c-Jun N-terminal kinase (Kaneto et al., 2002). Oxidative stress also facilitates loss of MafA protein levels which affects endogenous insulin gene expression (Harmon et al., 2005); in addition, upregulation of c-Myc expression suppresses insulin gene transcription (Kaneto et al., 2002); c-Myc is required for β-cell dysfunction and apoptosis (Cheung et al., 2010).

A recent study in glucose-infused rats has established relation between ER stress and oxidative stress pathways (Tang et al., 2012). The ER, which is at the centre of lipid and protein synthesis, is important to β-cell function due to its role in proinsulin synthesis and secretion. As illustrated in Fig 1.7 (Chapter 1), increased demand for ER response such as can occur during chronic hyperglycaemia (requiring high levels of insulin) or glucotoxicity (requiring repair of damaged proteins) can lead to ER stress. Moreover, failure of adaptive response by the ER (activation of Unfolded Protein Response) prolongs ER stress and triggers apoptosis, which involves a cascade of events including Ca^{2+} imbalance (Bensellam et al., 2012).

4.1.1.1 Glucose-mediated apoptosis in hepatocytes

The liver also plays a regulatory role in glucose metabolism via inhibition of gluconeogenesis and activation of glycogenesis. Impaired insulin signalling promotes increased gluconeogenesis, which could exacerbate hyperglycaemic conditions in T2DM patients. Hyperglycaemia has been shown to trigger serine or threonine phosphorylation of IRS-1, leading to insulin resistance (Aguirre et al., 2002). High glucose exposure in HepG2 hepatoma cells elevated upstream stimulatory factors 1 and 2, increasing hepatic lipase expression and could also promote dyslipidaemia, which is characteristic of T2DM patients (van Deursen et al., 2008). It has also been reported that high glucose exposure resulted in oxidative stress-mediated apoptosis and activation of caspase-3 activity in HepG2 cells (Chandrasekaran et al., 2010).

Since glucotoxicity remains at the centre of T2DM, effect of hyperglycaemia on viability of human β-cells and HepG2 hepatoma cells was investigated.

4.1.2 Lipotoxicity in pathogenesis of diabetes and NASH

Lipotoxicity results from cellular damage caused by dysregulated accumulation of fatty acids. Elevated free fatty acid levels and adiposity have been associated with β-cell dysfunction in T2DM, whilst contributing to insulin resistance. Circulating saturated FFA include palmitic acid, oleic acid and stearic acid (Marra et al., 2008). Chronic exposure to high levels of these saturated FFA has been related to the occurrence of apoptosis in β-cells (Maechler and Wollheim, 1999). Palmitate metabolism has been related to increased ceramide production, which is involved in signalling of ROS-mediated apoptosis (Cacicedo et al., 2005) and also causes β-cell dysfunction (Newsholme et al., 2007). High free fatty acid levels have several effects including increased FFA oxidation and esterification (Marra et al., 2008), oxidative stress (Inoguchi et al., 2000) and decreased insulin promoter gene activity (Gremlich et al., 1997).

As reviewed in Section 1.3.1, hepatic steatosis resulting from increased FFA circulation and *de novo* lipogenesis is a hallmark of NASH. An assessment of the lipid profile of NASH patients showed high levels of oleic acid and palmitic acid (de Almeida et al., 2002). Lipoapotosis (cell death due to lipid accumulation) is also a characteristic feature of the pathogenesis and loss of structural integrity in NASH (Feldstein et al., 2003; Malhi and Gores, 2008). It has also been proposed that the ER, which also regulates cellular Ca^{2+} homeostasis, contributes to lipotoxicity via activation of ER stress by FFA-mediated depletion of calcium stores and subsequent apoptosis (Araki et al., 2003).

4.1.3 Aim

Having established the effect of *t*BHP on viability of human hepatoma HepG2 cells and 1.1B4 human pancreatic β-cells, this study was intended to investigate effects of high glucose and high palmitate exposures in these two cell types. Subsequently, cytoprotective activities of phytochemicals (quercetin, curcumin and caffeic acid) were

evaluated against palmitate toxicity, a novel approach to evaluate effects of phytochemicals on lipotoxicity, illustrated in Figure 4.2.

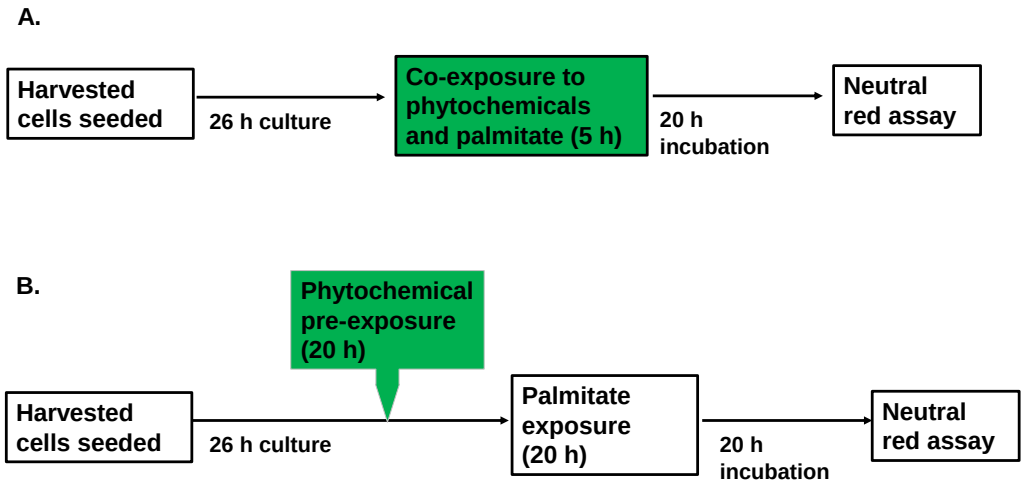

Figure 4.2 Experimental models for investigating cytoprotective activities of phytochemicals against palmitate toxicity. Figure shows (A) 5 h co-exposure with palmitate and (B) 20 h pre-exposure to phytochemicals, then 20 h palmitate treatment models.

4.2 Materials and methods

List of chemicals used and their suppliers is provided in Appendix I.

4.2.1 Methods

4.2.1.1 Solutions for cytotoxicity assays

MTT [3-(4,5-Dimethylthiazol-2-yl)-2,5-Diphenyltetrazolium Bromide] solution (5 mg/ml) was prepared by dissolving 5 mg MTT dye in 1 ml sterile water. The solution was freshly made each time and kept in a sterile tube, away from light. Unused solution was discarded.

Annexin binding buffer (1X) and propidium iodide working solution (100 µg/ml) were prepared as described in Section 3.2.2.4.2.

4.2.1.2 Stock solutions for glucotoxicity experiments

A stock solution of 1 M glucose was prepared by dissolving 3.60 g D-glucose in 20 ml sterile water. When dissolved, this solution was filtered through a 0.22 µm filter in a sterile cabinet and stored at -20^{o}C.

Stock solution of 1 M mannitol was made by dissolving 3.64 g of D-mannitol in 20 ml sterile water at 37^{o}C. The stock solution was filtered through a 0.22 µm filter in a sterile cabinet and stored at -20^{o}C.

4.2.1.3 Stock solution of palmitate for lipotoxicity assays

Stock solution of 100 mM palmitate was made by dissolving 278.4 mg sodium palmitate in 10 ml of 50%($^{v}/_{v}$) ethanol at 70^{o}C as described by Vasu et al., (2013). Also 5 g of bovine serum albumin (BSA) was dissolved in 50 ml sterile water at room temperature to make 10%($^{w}/_{v}$) BSA. To facilitate dissolution, 5 g BSA was divided into three parts and was spread onto the 50 ml sterile water in a beaker, as a thin film, and then placed on a magnetic stirrer at low speed. This was repeated until the required amount of BSA was dissolved and then filtered using 0.45 µm filter. The desired concentration of palmitate complexed to BSA was produced by combining fixed proportions of both solutions (Rho et

al., 2007), to allow adsorption of palmitate unto BSA, for facilitated uptake of palmitate. For example, for 5 ml of 16 mM palmitate/10%($^{w}/_{v}$) BSA solution, 0.8 ml of 100 mM palmitate was added dropwise to 4.2 ml 10%($^{w}/_{v}$) BSA at approximately 55^{o}C with vigorous shaking, and then incubated at 55^{o}C for additional 15 min to obtain a homogenous mixture. The final stock solution was immediately filtered in a sterile cabinet using 0.22 µm filter and stored at -20^{o}C until further use. An 8%($^{v}/_{v}$) ethanol/BSA conjugate (as stock solution - vehicle control) was also prepared at 60^{o}C using similar procedure.

For use in cytotoxicity experiments, 16 mM palmitate/BSA sock solution was warmed at 55^{o}C for approximately 10 min and then added to pre-warmed culture medium at 1:10 dilution to produce 1.6 mM palmitate as working solution. This procedure was repeated using 8%($^{v}/_{v}$) ethanol/BSA stock to make 0.8%($^{v}/_{v}$) ethanol-containing medium.

4.2.1.4 Cell Culture techniques

Culture media for human pancreatic 1.1B4 β-cells were prepared as described in Section 2.2.1.3.2. The 1.1B4 β-cells were subcultured as described in Section 2.2.3.2. Passage numbers of 1.1B4 β-cells used for experiments described in this chapter were between 34 and 40.

All culture media for human hepatoma HepG2 cells were prepared as described in Section 2.2.1.3.1. Subculturing of HepG2 cells was performed as described in Section 2.2.3.1 For HepG2 cells, passage numbers used were between 14 and 30.

4.2.1.5 Investigating glucotoxicity in 1.1B4 pancreatic β-cells

Exponentially growing β-cells were harvested and seeded at 7.0 x 10^4 cells/ml and 3.5 x 10^4 cells/ml in quadruplicate wells of 24-well plates and incubated at 37^{o}C. After approximately 28 h of culture, medium in each well was replaced with 1 ml glucose or mannitol containing-media (10%($^{v}/_{v}$) RPMI-1640 complete medium containing 11 mM glucose) in duplicate wells, using concentrations outlined in Table 4.1. The 1.1B4 human

β-cells were usually cultured in 10%($^{v}/_{v}$) RPMI-complete medium containing 11 mM glucose; hence, for glucotoxicity experiments, the right amount of glucose or mannitol was added to culture medium to achieve the desired treatment media, see Table 4.1. Cells were cultured at 37°C for 24 h, 48 h and 72 h prior to cell viability assessment.

Solution	**Effect**
5 mM glucose	Low glucose
11 mM glucose	Normoglycaemia
14 mM mannitol plus 11 m M glucose	Osmotic control for 25 mM glucose
25 mM glucose (14 mM glucose plus 11 m M glucose)	Glucotoxicity
29 mM mannitol plus 11 m M glucose	Osmotic control for 40 mM glucose
40 mM glucose (29 mM glucose plus 11 mM glucose)	Glucotoxicity

Table 4.1 List of solutions used in glucotoxicity experiments.

Cell viability was assessed using neutral red assay (as described in Section 2.2.5.3), as well as MTT assay described below. Assays were done in duplicate wells per treatment.

For MTT assay, 100 µl of 5 mg/ml MTT working solution was added to treatment-containing media in duplicate wells for each condition, 30 min before each time point. Cells were then incubated for 30 min at 37°C to enable viable cells to convert MTT to formazan crystals. The short incubation period was used to allow for the detection of only cells which were viable at that time of the assay. Afterwards medium was aspirated from each well and replaced with 1 ml DMSO (100%($^{v}/_{v}$)) at the time point, to extract formazan crystals from viable cells. The purple formazan extract in each well was transferred into 96-well plates (200 µl per well in quadruplicates) and absorbance determined at 570 nm.

4.2.1.6 Effect of replenishing high glucose medium on glucotoxicity in 1.1B4 pancreatic β-cells

Although prolonged exposure to high glucose is believed to induce cytotoxicity, this effect could be annulled by the depletion of glucose in culture medium due to increasing cellular

metabolic activities. Therefore, this experiment was conducted to investigate the added advantage of replenishing glucose medium on glucotoxicity.

Cells were seeded at 3.5 x 10^4 cells/ml in wells of 24-well plates and cultured at 37^{o}C for approximately 28 h. Cells (in quadruplicate wells) were then treated as described previously (Table 4.1). Glucotoxicity was assessed via neutral red uptake, after 24 h, 48 h and 72 h incubation at 37^{o}C. For each condition, the media in duplicate wells were replenished every 24 h. Cell viability was then assessed appropriately at the respective time points using neutral red assay described in Section 2.2.5.3.

4.2.1.7 Investigating the role of early and late apoptosis in glucotoxicity in 1.1B4 pancreatic β-cells

The 1.1B4 β-cells were seeded at 3.5 x 10^4 cells/ml per well in 24-well plates and cultured for approximately 28 h at 37^{o}C in a humidified incubator. Cells in quadruplicate wells were treated with mannitol- or glucose-containing medium as described above (4.2.1.5); with no change in culture medium at each time point. Cultured cells were subsequently prepared for flow cytometry analysis as described in Section 3.2.2.4.2.

4.2.1.8 Investigating glucotoxicity in HepG2 hepatoma cells.

Exponentially growing cells were harvested and seeded at 4.0 x 10^5 cells/ml or 2.0 x 10^5 cells/ml in duplicate wells of 24-well plates and cultured for approximately 28 h. Afterwards, cells were treated with 1 ml of 10%($^v/_v$) MEM Eagle complete medium with different treatments, in quadruplicate wells. The HepG2 cells were normally cultured in 10%($^v/_v$) MEM Eagle complete medium containing 5 mM glucose, which represented normoglycaemia; hence 35 mM glucose was added to this medium to make 40 mM glucose treatment medium (glucotoxicity) and 35 mM mannitol as osmotic control for 40 mM glucose. Cells were then incubated at 37^{o}C for 24 h, 48 h and 72 h. In duplicate wells containing cells at both cell densities, culture medium was replaced every 24 h to restore high glucose exposure to cells, and remove metabolic waste which have accumulated over culture period. At the respective time points, cell viability was assessed using neutral red assay as described in Section 2.2.5.3.

4.2.1.9 Investigating effect of palmitate on viability of 1.1B4 pancreatic β-cells

β-cells were harvested and seeded at 7 x 10^4 cells/ml in wells of a 24-well plate. After culturing for approximately 26 h at 37°C, cells were exposed to 1 ml 10%($^v/_v$) RPMI-1640 complete medium containing varying concentrations of palmitate/BSA and ethanol/BSA (outlined in Table 4.2) for 5 h or 20 h.

Palmitate/10%($^v/_v$) BSA	**Ethanol/10% BSA (negative control) (% refer to final concentration ($^v/_v$) of ethanol)**
0.1 mM	0.05%
0.2 mM	0.1%
0.4 mM	0.2%
0.8 mM	0.4%
1.6 mM	0.8%

Table 4.2 Concentrations of palmitate/BSA and their corresponding ethanol/BSA vehicle controls.

4.2.1.10 Investigating protection by phytochemicals against palmitate toxicity in 1.1B4 pancreatic β-cells

The cytoprotective activities of phytochemicals were evaluated in 1.1B4 cells, using palmitate as oxidant stressor. Cytoprotective concentrations of quercetin, curcumin and caffeic acid were chosen from previous cytoprotection data (Chapter 2) as being concentrations that produced minimal, medium and highest protection against *t*BHP-induced cytotoxicity, in both 5 h and 20 h conditions. Cell viability was assessed using neutral red assay, described in Section 2.2.5.3.

4.2.1.10.1 5 h co-exposure with phytochemicals

After the 26 h attachment period, culture medium was replaced with 10%($^v/_v$) RPMI-1640 complete medium (1 ml) containing either 1.6 mM palmitate/BSA or 0.8%($^v/_v$) ethanol/BSA control with varying concentrations of quercetin, curcumin and caffeic acid. Cells were then incubated at 37°C for 5 h.

4.2.1.10.2 20 h exposure conditions

After attaching to 24-well plates for approximately 26 h, cells were exposed to 1 ml of 10%($^{v}/_{v}$) RPMI-1640 complete medium containing varying concentration of quercetin, curcumin and caffeic acid for 20 h. Culture medium was then replaced with either 0.3 mM palmitate/BSA or 0.15%($^{v}/_{v}$) ethanol/BSA control and cells incubated further at 37^{o}C for 20 h.

4.2.1.11 Investigating Lipotoxicity in HepG2 hepatoma cells

Cells were harvested and seeded at 4.0 x 10^{5} cells/ml in wells of a 24-well plate and allowed to attach to 24-well plate for approximately 26 h. Cells were then incubated with varying concentrations of palmitate/BSA and ethanol/BSA in 10%($^{v}/_{v}$) MEM Eagle complete medium, using procedure described in Section 4.2.1.9.

Also protection against palmitate toxicity in HepG2 cells was evaluated using 10% MEM Eagle complete medium, as described in Section 4.2.1.10.

4.2.2 Images of treated cells

Images of cells obtained after exposure to palmitate or palmitate and phytochemicals are representative of cells in wells that correspond to respective treatment conditions. Although morphological changes are not obvious in all of the images presented, description of each image is made based on observations at the time of experiment.

4.2.3 Data analysis

4.2.3.1 Analysis of data obtained from glucotoxicity experiments

Percentage viability was determined by normalising mean absorbance of the neutral red assay for cells treated with 5 mM (glucose), 14 mM mannitol (plus 11 mM glucose) and 29 mM mannitol (plus 11 mM glucose) to mean absorbance of neutral red assay for cells treated with 11 mM glucose, and expressed as percentage for each exposure duration, i.e., 24 h, 48 h and 72 h. Also, mean absorbance of 25 mM glucose and 40 mM glucose

were normalised to corresponding mannitol controls, 14 mM (plus 11 mM glucose) and 29 mM (plus 11 mM glucose), respectively. Sample equations are shown below, using 5 mM glucose and 25 mM glucose:

$$\text{\% cell viability (at 5 mM glucose)} = \left[\frac{\text{mean absorbance at 5 mM glucose}}{\text{mean absorbance at control (11 mM glucose)}} \right] \text{X } 100\%$$

$$\text{\% cell viability (at 25 mM glucose)} = \left[\frac{\text{mean absorbance at 25 mM glucose}}{\text{mean absorbance at control (14 mM mannitol, plus 11-mM glucose)}} \right] \text{X } 100\%$$

4.2.3.2 Analysis of data obtained from lipotoxicity experiments

For palmitate toxicity studies, mean absorbance of neutral red assay for cells treated with palmitate (0.1 – 1.6 mM) was normalised to corresponding mean absorbance of neutral red assay for ethanol/BSA-treated cells to obtain percentage viability, as shown below (with 0.1 mM palmitate as an example):

$$\text{\% cell viability (at 0.1 mM palmitate)} = \left[\frac{\text{mean absorbance at 0.1 mM palmitate}}{\text{mean absorbance at control (0.05\% } (^{v}/_{v}) \text{ ethanol/BSA)}} \right] \text{X } 100\%$$

For protection studies, mean absorbance obtained from palmitate/BSA (0.3 mM or 1.6 mM) was normalised to mean absorbance obtained from each ethanol/BSA treatment (0.15%($^{v}/_{v}$) or 0.8%($^{v}/_{v}$)) as shown below:

$$\text{\% cell viability (at 0.02 mM quercetin)} = \left[\frac{\text{mean absorbance at quercetin + ethanol/BSA}}{\text{mean absorbance at control (DMSO + ethanol/BSA)}} \right] \text{X } 100\%$$

❖ For comparison between ethanol/BSA controls and corresponding palmitate concentrations, two-tailed Students' paired t-test was used.

Unless stated otherwise, statistical analysis was performed as outlined in Section 2.2.6.

4.3 Results

4.3.1 Investigating glucotoxicity in 1.1B4 β-cells

A number of experimental conditions were tested in an effort to develop a reproducible assay for glucotoxicity in 1.1B4 human β-cells. The variables tested initially were: glucose concentrations, exposure times, seeding density, and toxicity assay.

Glucose concentrations tested were 5 mM, 11 mM, 25 mM and 40 mM. The 5 mM glucose concentration was taken to represent low glucose, the 11 mM glucose to represent normoglycaemia (β-cells were normally cultured in 10%($^{v}/_{v}$) RPMI-1640 complete medium containing 11 mM glucose), the 25 mM glucose to represent glucotoxicity, and the 40mM glucose to also represent glucotoxicity. Osmotic controls for the 25 mM and 40 mM glucose concentrations were provided by use of 14 mM and 29 mM mannitol, in medium containing 11 mM glucose, respectively.

The exposure times tested were 24 h, 48 h and 72 h, at a low seeding density (3.5×10^4 cells/ml; 1 ml per well) and at high seeding density (7.0×10^4 cells/ml; 1 ml per well). The toxicity assays employed were morphology, MTT assay and NR assay. None of the treatments exerted a statistically significant effect relative to control, with confidence intervals within the same range across the dataset (Fig 4.3). This demonstrated that no glucotoxicity (i.e., loss in cell viability) could be observed within the experimental conditions employed.

The results of these studies informed other attempts to establish a reliable and reproducible glucotoxicity assay in 1.1B4 human β-cells, involving changing the culture medium, and assay for apoptosis or necrosis.

Changing the culture medium in an attempt to maintain high glucose concentrations throughout the 72 h exposure period did not elicit glucotoxicity in 1.1B4 human β-cells, except at 40 mM glucose after 72 h. However, similar effect was observed at 40 mM glucose after 72 h, with culture medium maintained (Table 4.3).

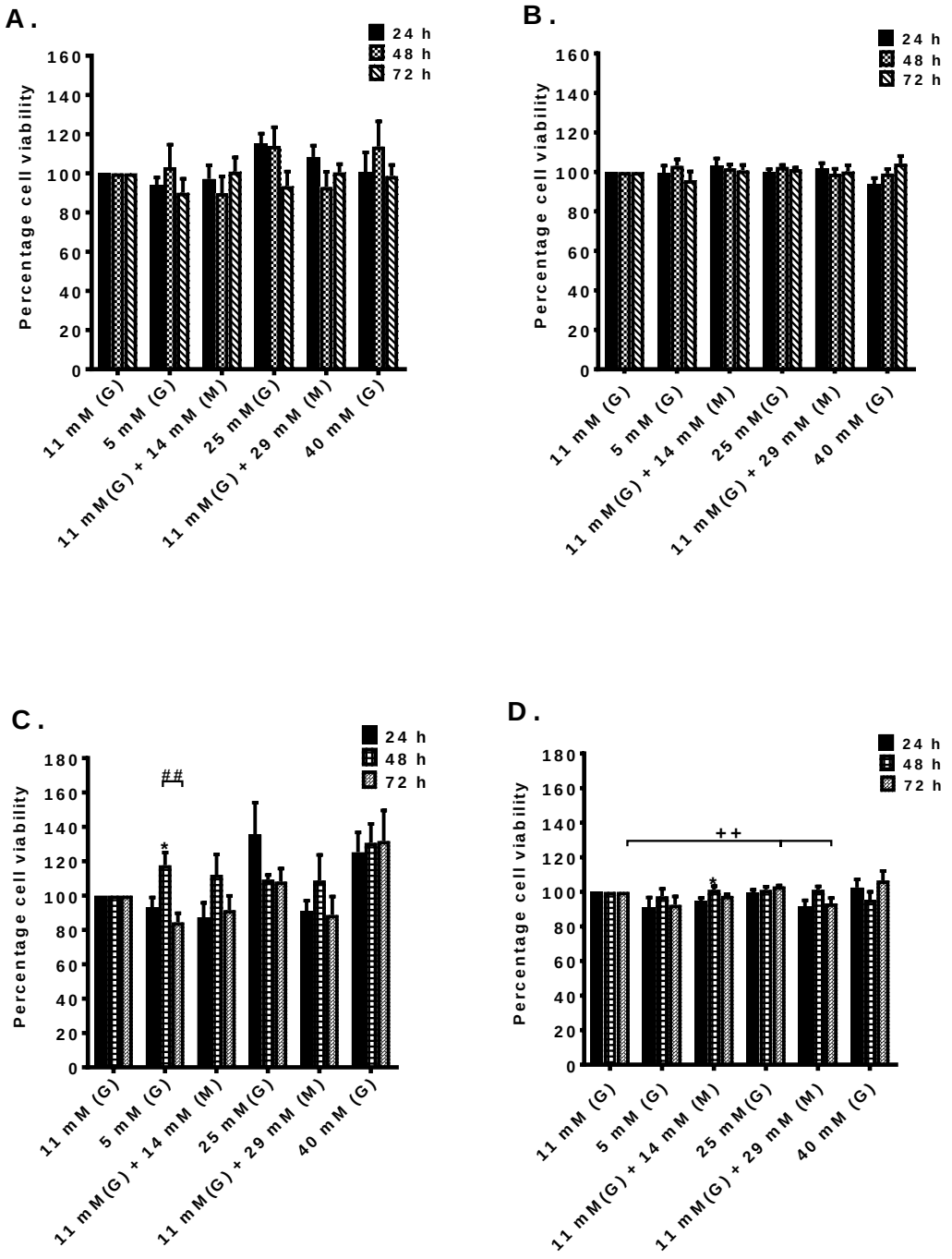

Figure 4.3 Effects of different glucose conditions on β-cell viability (seeded at high density) using MTT and neutral red viability assays. Approximately 28 h after plating at (A, B) 7.0 x10^4 cells/ml and (C, D) 3.5 x10^4 cells/ml, β-cells were treated with varying concentrations of glucose (G; 5 mM, 11 mM, 25 mM and 40 mM) as well as 14 mM mannitol (M) and 29 mM mannitol (M) (in 11mM glucose-containing 10%($^v/_v$) RPMI-1640 complete medium) as osmotic controls, and then cultured for 24 h, 48 h and 72 h. Cell viability was assessed using MTT assay (A, C) and neutral red viability assay (B, D) as described in Section 4.2.1.5. Each data point represents mean percentage viability from six independent experiments ± SEM. Statistical analysis was performed using one-way ANOVA and post hoc analysis by Bonferroni's multiple comparisons test. Where indicated, values were significantly different from 24 h exposure conditions and $P<0.05$ (*). Values were also significantly different from 48 h conditions at $P<0.01$ (##) and from 11 mM glucose at $P<0.01$ (++).

Exposure duration	5 (G)	11 mM G	14 (M) plus 11 (G)	25 (G) - 14 (G) plus 11 (G)	29 (M) plus 11 (G)	40 (G) - 29 (G) plus 11 (G)
	% cell viability (glucose-containing medium maintained)					
24 h	106.0±1.6	100.0±0.0	102.0±3.2	100.0±1.5	102.0±3.0	103.0±2.6
48 h	109.0±2.4	100.0±0.0	102.0±3.9	97.8±2.4	100.0±4.5	96.3±2.0
72 h	102.0±2.0	100.0±0.0	96.7±1.9	96.1±2.2	94.5±2.7	92.0±2.0*
	% cell viability (glucose-containing medium replaced every 24 h)					
24 h	112.0±3.1	100.0±0.0	102.0±2.3	107.0±6.0	97.6±4.2	95.5±4.7
48 h	111.0±3.2	100.0±0.0	102.0±2.2	94.4±3.2	102.0±4.1	92.6±1.4
72 h	103.0±5.9	100.0±0.0	96.8±3.0	93.4±2.2	95.6±4.4	88.6±3.2#

Table 4.3 Effect of different glucose conditions on β-cell viability under conditions of different culture media. Vaying concentrations of mannitol (M) were used as osmotic control for respective toxic concentrations of glucose (G). Each data point represents mean percentage viability from six independent experiments ± SEM. Statistical analysis was performed using Friedman's test and post hoc analysis by Dunn's multiple comparisons test. Where indicated, values were significantly different from 11mM glucose (medium maintained) at P<0.01 (*) and 11 mM glucose (culture medium replaced) at P<0.01 (#).

Effect of high glucose on early and late apoptosis was next analysed by flow cytometry (as described in Section 3.2.2.4.2) after 24 h, 48 h and 72 h exposure in an attempt to identify an alternative toxicity end-point. The FACS output presented in Appendix II was used to generate the distribution of cells shown in Fig 4.4. In particular, the data provided no evidence for either a time- or concentration-dependent increase in total apoptosis following exposure to high glucose levels (25 mM and 40 mM), and evidence for a small increase in necrosis score following 72 h exposure to 40 mM glucose was matched by similar increase in necrosis score in the 29 mM mannitol (plus 11 mM glucose) osmotic control. Taken together, the results of flow cytometry analysis have again failed to establish a reliable and reproducible assay for glucotoxicity in 1.1B4 human β-cells.

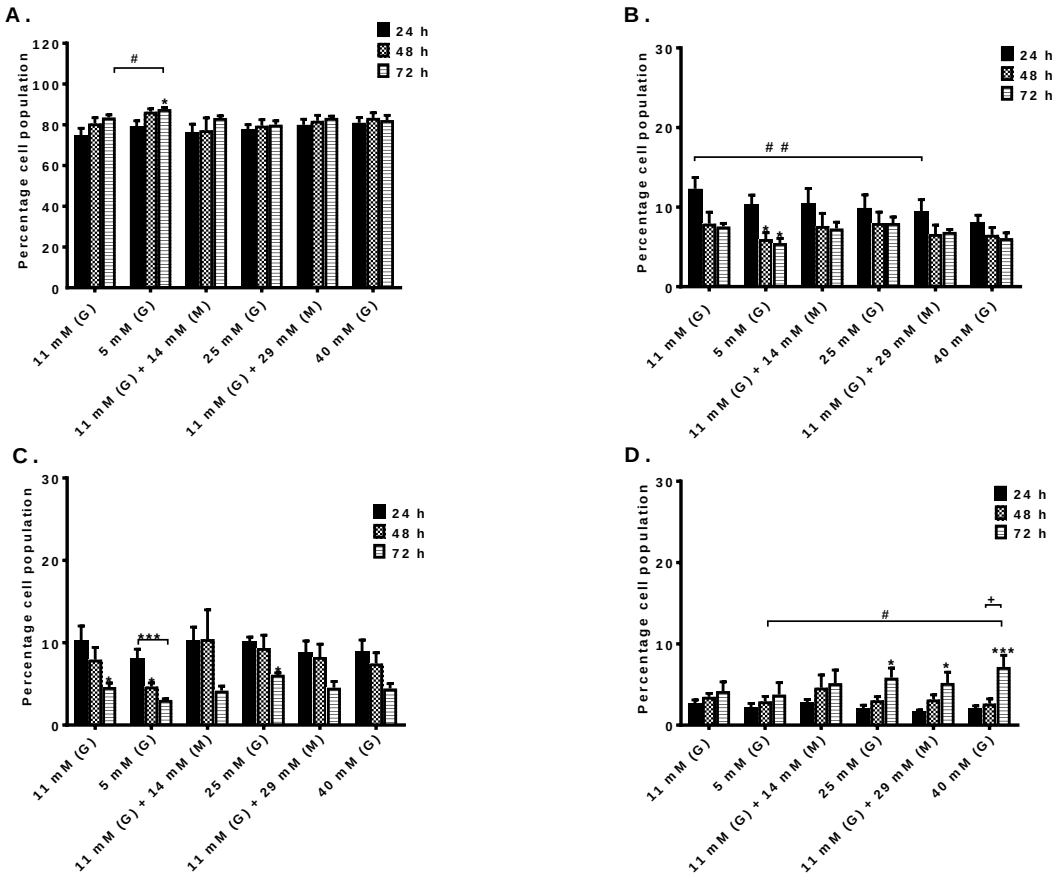

Figure 4.4 Effect of high glucose load on early and late apoptosis in 1.1B4 pancreatic β-cells following 24 h, 48 h and 72 h exposure. Figure shows proportion of live cells (A), early apoptotic cells (B), late apoptotic cells (C) and necrotic cells (D). Approximately 28 h after plating at 3.5 x 10^4cells/ml, β-cells were treated with varying concentrations of glucose (5 mM, 11 mM, 25 mM and 40 mM) as well as 14 mM mannitol and 29 mM mannitol (in 11 mM glucose-containing 10%($^v/_v$) RPMI-1640 complete medium) as osmotic controls. Each data point represents mean percentage viability from four independent experiments ± SEM. Statistical analysis was performed using one-way ANOVA and post hoc analysis by Dunnett's multiple comparisons test. Where indicated, values were significantly different from 24 h exposure at P<0.05 (*). Also, values were significantly different from 11 mM glucose at P <0.05 (#) and P<0.01 (##).

As presented in Fig 4.5, there was no significant effect under the experimental conditions used; therefore, glucotoxicity was not demonstrated in HepG2 cells.

Whilst this inability to establish an acceptable glucotoxicity assay will be commented on further in the 'Discussion' section of this chapter, the salient point is that the phytochemicals could not be tested for their protective action against cellular glucotoxicity in 1.1B4 β-cells.

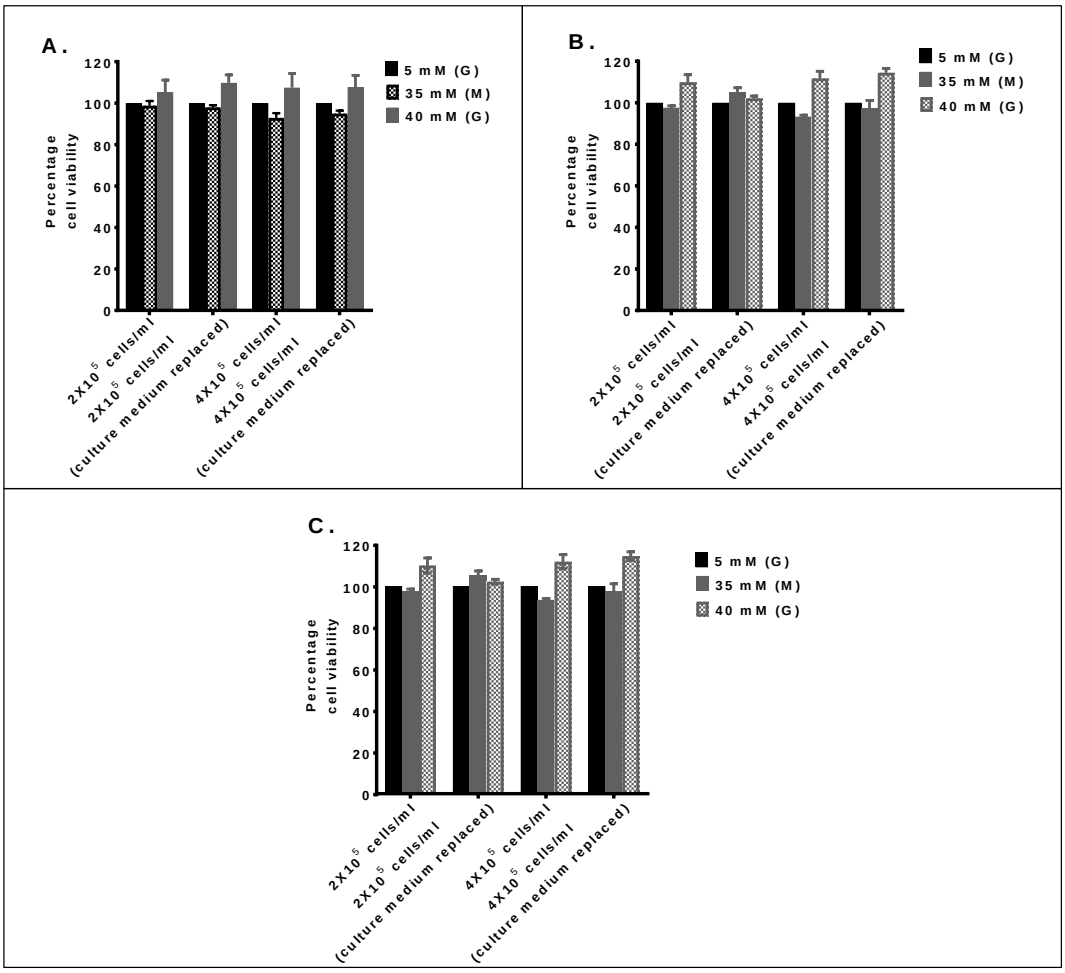

Figure 4.5 Effect of high glucose exposure on HepG2 cells using neutral red viability assay. Approximately 28 h after plating at 2.0 x10^5cells/ml and 4.0 x10^5cells/ml, HepG2 cells were treated with varying concentrations of glucose (5 mM and 40 mM) as well as 35 mM mannitol (in 5 mM glucose-containing 10%($^v/_v$) MEM Eagle complete medium) as osmotic controls, and cultured for 24 h (A), 48 h (B) and 72 h (C). For each time point, 100% viability was assumed for 5 mM glucose control. Each data point represents mean percentage viability from three independent experiments ± SEM.

4.3.2 Lipotoxicity in 1.1B4 and HepG2 cells

With the cytotoxic effect of *t*BHP in 1.1B4 and HepG2 cells established (Chapter 2), palmitate toxicity was investigated in keeping with the role of lipotoxicity in T2DM and in NASH (see review in Section 4.1.2). In both 5 h and 20 h conditions, control cells (treated with culture medium containing 10%($^v/_v$) FBS) were taken to be 100% viability. Relative to control cells, varying concentrations of ethanol/BSA controls (0.05 – 0.8%($^v/_v$)) did not cause cells (1.1B4 and HepG2) to appear rounded or separated from each other (data not shown). Also, 100% viability assumed for control cells was essentially retained after exposure to ethanol/BSA controls (data not shown).

4.3.2.1 Cytotoxic effects of sodium palmitate (5 h exposure)

4.3.2.1.1 1.1B4 β-cells

At concentrations above 0.4 mM, sodium palmitate caused cells to appear rounded and separated from each other (Figs 4.6B and C), relative to control (Fig 4.6A), after 5 h exposure. These morphological changes corresponded with minimal reduction in cell viability, which was recorded at concentrations below 0.8 mM palmitate (Fig 4.7). Approximately 44% cytotoxicity was recorded at 1.6 mM palmitate ($P<0.001$, $n = 6$).

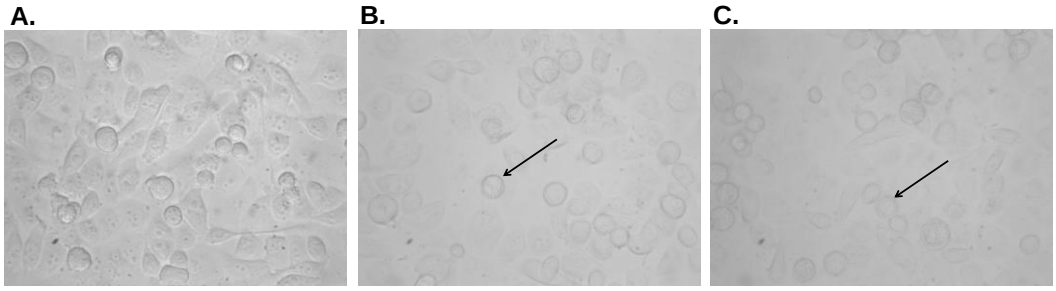

Figure 4.6 Representative images of 1.1B4 human pancreatic β-cells after 5 h exposure to varying concentrations of sodium palmitate. Images show β-cells after 5 h exposure to (A) control (10%($^{v}/_{v}$) RPMI-1640 complete medium). Cells were also treated with sodium palmitate at 0.8 mM (B) and 1.6 mM (C). Rounded cells have been indicated by black arrow. Images were obtained at 40X magnification using the CMEX-18PRO camera with the Olympus Ck2 microscope.

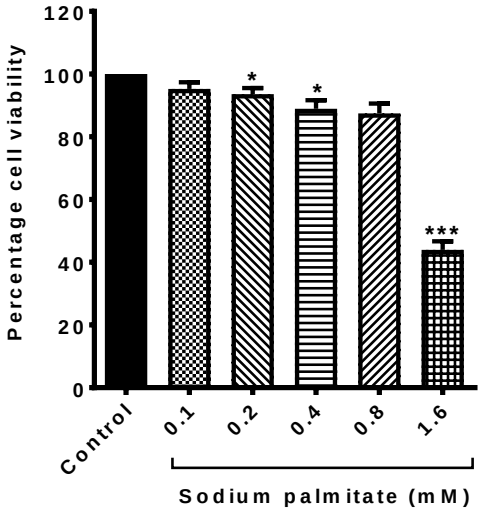

Figure 4.7 Cytotoxicity by sodium palmitate (5 h exposure) in 1.1B4 pancreatic β-cells. Cells were incubated with control (10%($^{v}/_{v}$) RPMI-1640 complete medium) and sodium palmitate (0.1 – 1.6 mM). Each data point represents percentage viability of duplicate wells from six independent experiments ± SEM. Mean absorbance from each treatment was normalised to corresponding mean absorbance of cells treated with ethanol control to obtain percentage viability. Statistical analysis was performed using Student's paired t-test when compared to respective ethanol/BSA controls (0.05 – 0.8% ($^{v}/_{v}$)) and significance denoted as $P<0.05$ (*) and $P<0.001$ (***).

4.3.2.1.2 HepG2 cells

HepG2 cells retained morphology of healthy cells after 5 h exposure to MEM complete medium (10%($^{v}/_{v}$) FBS) (Fig 4.8A). However, sodium palmitate caused cells to appear rounded and separated from each other in a concentration-dependent manner (Fig 4.8B and C), and this observation was in accordance with gradual reduction in cell viability (Fig 4.9). Significant toxicity of approximately 23% was recorded at 0.8 mM ($P<0.05$, n = 6), with an additional 10% increase in toxicity at 1.6 mM sodium palmitate ($P<0.01$, n = 6).

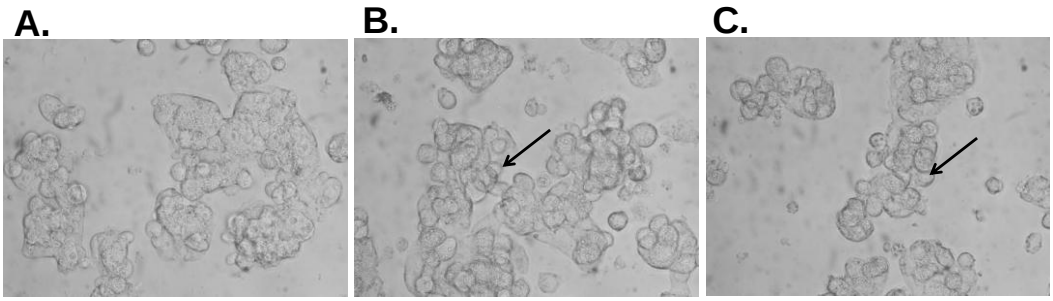

Figure 4.8 Representative images of human hepatoma HepG2 cells after 5 h exposure to varying concentrations of sodium palmitate. Images show HepG2 cells after 5 h exposure to 10%($^{v}/_{v}$) MEM complete medium (A) and sodium palmitate at 0.8 mM (B) and 1.6 mM (C). Cells were rounded and separated from each other with increasing concentration of sodium palmitate. Rounded cells have been indicated by black arrow. Images were obtained at 40X magnification using the CMEX-18PRO camera with the Olympus Ck2 microscope.

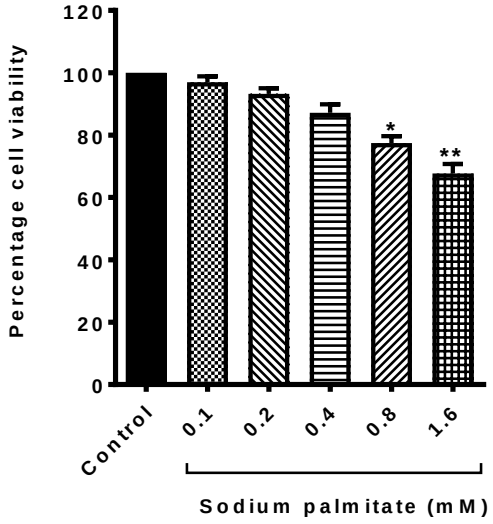

Figure 4.9 Cytotoxicity by sodium palmitate (5 h exposure) in HepG2 hepatoma cells. After culturing for 26 h, cells were treated with 10%($^{v}/_{v}$) MEM Eagle complete medium containing sodium palmitate (0.1 – 1.6 mM) for 5 h. Each data point represents percentage viability from duplicate wells of six independent experiments ± SEM. Statistical analysis was performed using paired Student's t-test when compared to respective ethanol/BSA controls. Where indicated, values were significantly different from corresponding ethanol controls at $P<0.05$ (*) and $P<0.01$ (**).

4.3.2.2 Cytotoxic effects of sodium palmitate (20 h exposure)

4.3.2.2.1 1.1B4 β-cells

Prolonged exposure (20 h) of β-cells to sodium palmitate resulted in 1.1B4 cells appearing rounded and separated from each other (Fig 4.10), corresponding to a concentration-dependent cytotoxicity. As presented in Fig 4.11 sodium palmitate caused a gradual decline in cell viability to 37.70 ±4.01% at 0.4 mM, producing approximately 100% cytotoxicity at 1.6 mM ($P<0.001$, $n = 6$). Furthermore, mean TC_{50} value of 0.30 ±0.06 mM sodium palmitate was estimated using GraphPad prism. When cells were incubated with 1.6 mM sodium palmitate (Fig 4.10C), high amount of debris was observed. This observation was also made when palmitate-containing medium was incubated at 37^{o}C without 1.1B4 cells (4.10D) and could result from instability of high amounts of sodium palmitate in aqueous solutions, over a longer period of time (20 h versus 5 h, lack of "debris" observed).

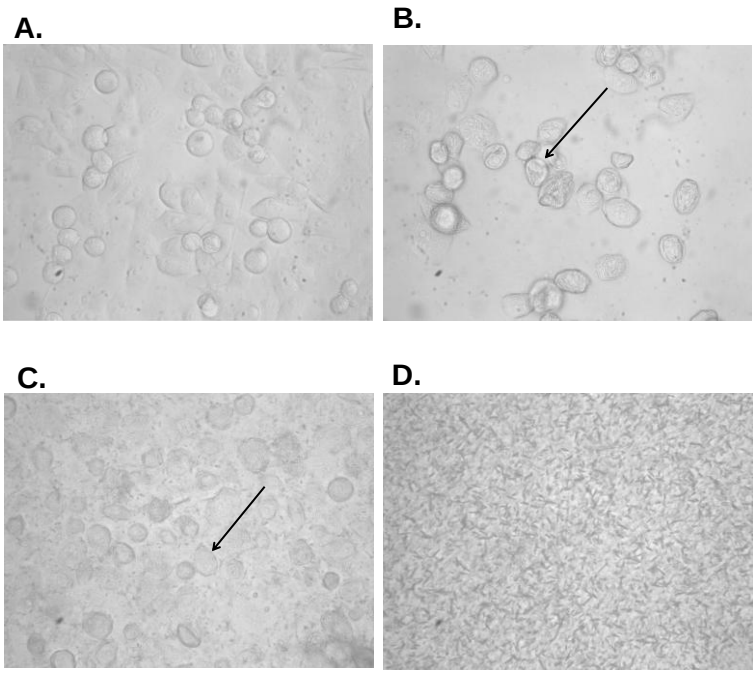

Figure 4.10 Representative images of human pancreatic 1.1B4 β-cells after 20 h exposure to varying concentrations of sodium palmitate. Images show β-cells after 20 h incubation with (A) control (10%($^{v}/_{v}$) RPMI-1640 complete medium) and palmitate at 0.4 mM (B) and 1.6 mM (C). Debris observed after 20 h incubation with 1.6 mM palmitate (D) was also observed in no-cell medium at 37^{o}C. Rounded cells have been indicated by black arrows. Images were obtained at 40X magnification using the CMEX-18PRO camera with the Olympus Ck2 microscope.

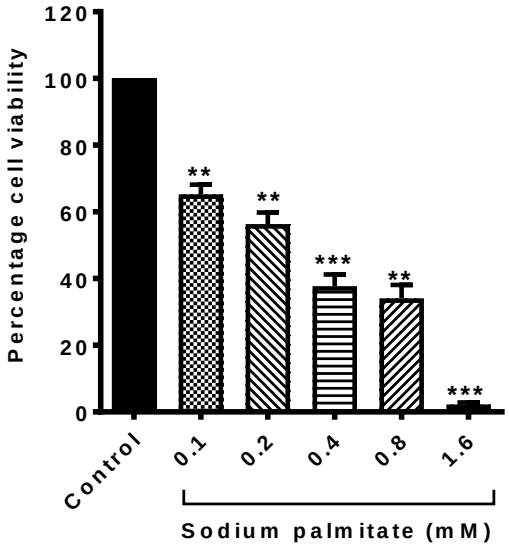

Figure 4.11 Cytotoxicity by sodium palmitate (20 h exposure) in 1.1B4 pancreatic β-cells. Cells were incubated with control (10%($^{v}/_{v}$) RPMI-1640 complete medium) and palmitate (0.1 – 1.6 mM). Each data point represents percentage viability of duplicate wells from six independent experiments ± SEM. Mean absorbance from each treatment was normalised to corresponding mean absorbance of cells treated with ethanol control to obtain percentage viability. Statistical analysis was performed using paired Student's t-test when compared to respective ethanol/BSA controls (0.05 – 0.8%($^{v}/_{v}$)) and significance denoted as P<0.01 (**) and P<0.001 (***).

4.3.2.2.2 HepG2 cells

As presented in Fig 4.12, HepG2 cells appeared rounded, separated from each other and detached from wells after 20 h exposure to increasing concentration of sodium palmitate (Figs 4.12B and C). In accordance with morphological changes, cell viability decreased significantly with increasing concentration of sodium palmitate, producing a drastic reduction in cell viability from approximately 50% at 0.4 mM to 20.99 ±4.70% at 0.8 mM (P<0.01, n = 6). Cell viability reduced further, to 5.36 ±1.28% at 1.6 mM sodium palmitate (P<0.001, n = 6; Fig 4.13). Mean TC50 value of 0.42 ±0.06 mM sodium palmitate was estimated after 20 h exposure in HepG2 cells.

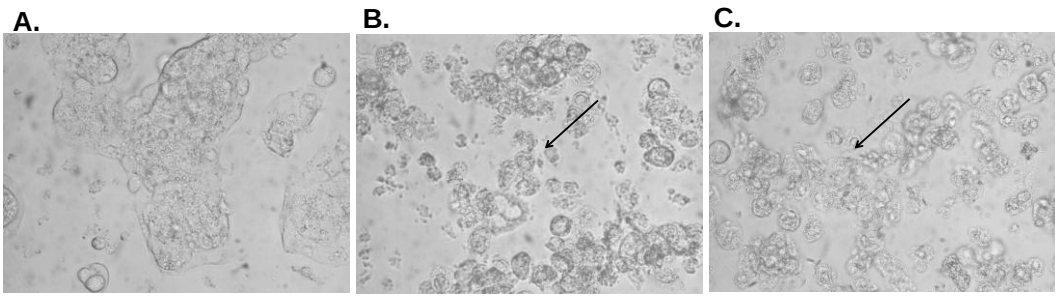

Figure 4.12 Representative images of human hepatoma HepG2 cells after 20 h exposure to varying concentrations of sodium palmitate. Images show HepG2 cells after 20 h exposure to 10%($^{v}/_{v}$) MEM complete medium (A) and sodium palmitate at 0.4mM (B) and 1.6 mM (C). Cells were rounded and separated from each other as indicated by black arrows. Images were obtained at 40X magnification using the CMEX-18PRO camera with the Olympus Ck2 microscope.

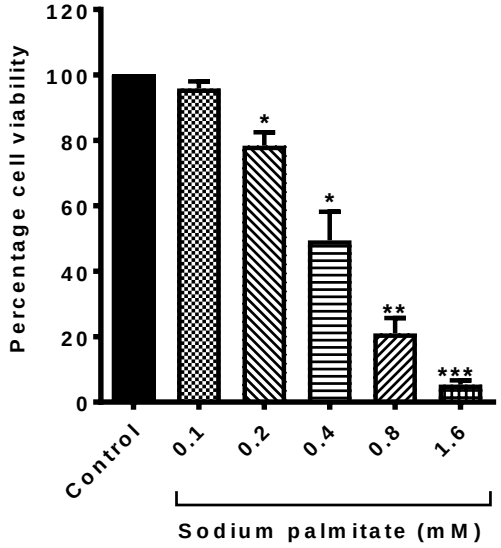

Figure 4.13 Cytotoxicity by sodium palmitate (20 h exposure) in HepG2 hepatoma cells. After culturing for 26 h, cells were treated with MEM complete medium (10%($^{v}/_{v}$) FBS) containing palmitate (0.1 – 1.6 mM) for 20 h. Each data point represents percentage viability from duplicate wells of six independent experiments ± SEM. Statistical analysis was performed using paired Student's t-test when compared to respective ethanol/BSA controls. Where indicated, values were significantly different from corresponding ethanol controls at $P<0.05$ (*), $P<0.01$ (**) and $P<0.001$ (***).

4.3.3 Effects of co-exposure to phytochemicals and sodium palmitate on 1.1B4 and HepG2 cells

The effects of phytochemicals on palmitate toxicity in 1.1B4 and HepG2 cells are presented in the following sections. Representative morphological data are shown in accordance with effects of phytochemicals and sodium palmitate (used alone or together)

on cell viability. Direct cytoprotective activities of quercetin, curcumin and caffeic acid were assessed after 5 h co-exposure with 1.6 mM palmitate, cells were co-treated with culture medium containing phytochemicals and 0.8%($^{v}/_{v}$) ethanol/BSA as control. For cells treated with DMSO and 0.8%($^{v}/_{v}$) ethanol/BSA alone, 100% viability was assumed.

4.3.3.1 Phytochemicals enhance palmitate toxicity in 1.1B4 cells

In 0.8%($^{v}/_{v}$) ethanol/BSA-containing medium, quercetin did not produce any significant effect on cell viability (Fig 4.14A), relative to DMSO-treated cells. However, 1.6 mM sodium palmitate alone caused approximately 28% toxicity ($P<0.05$, $n = 6$), and this effect was amplified in the presence of quercetin resulting in 49% viability at 0.33 mM quercetin (Fig 4.14A).

Relative to DMSO, curcumin (0.02 mM and 0.03 mM) showed no significant cytotoxicity although, 11% loss in viability was recorded at 0.07 mM curcumin (Fig 4.14B). Again, sodium palmitate (1.6 mM) alone was significantly cytotoxic, with additional 27% toxicity recorded in the presence of 0.07 mM curcumin ($P<0.01$, $n = 6$).

Caffeic acid was essentially non-cytotoxic after 5 h exposure (Fig 4.14C). While lipotoxicity recorded was consistent with Figs 4.14A and 4.14B, this effect was more pronounced in co-treated cells with approximately 18% added toxicity at 1.1 mM caffeic acid. Hence, caffeic acid also showed no direct cytoprotection against palmitate toxicity, but amplified cytotoxic effects.

Thus, under the experimental conditions, quercetin, curcumin and caffeic acid did not demonstrate direct cytoprotection against sodium palmitate but amplified palmitate toxicity. Furthermore, phytochemicals did not restore morphological intergrity of 1.1B4 cells in co-exposure conditions; 1.6 mM sodium palmitate alone caused cells to appear round and separated from each other (data not shown).

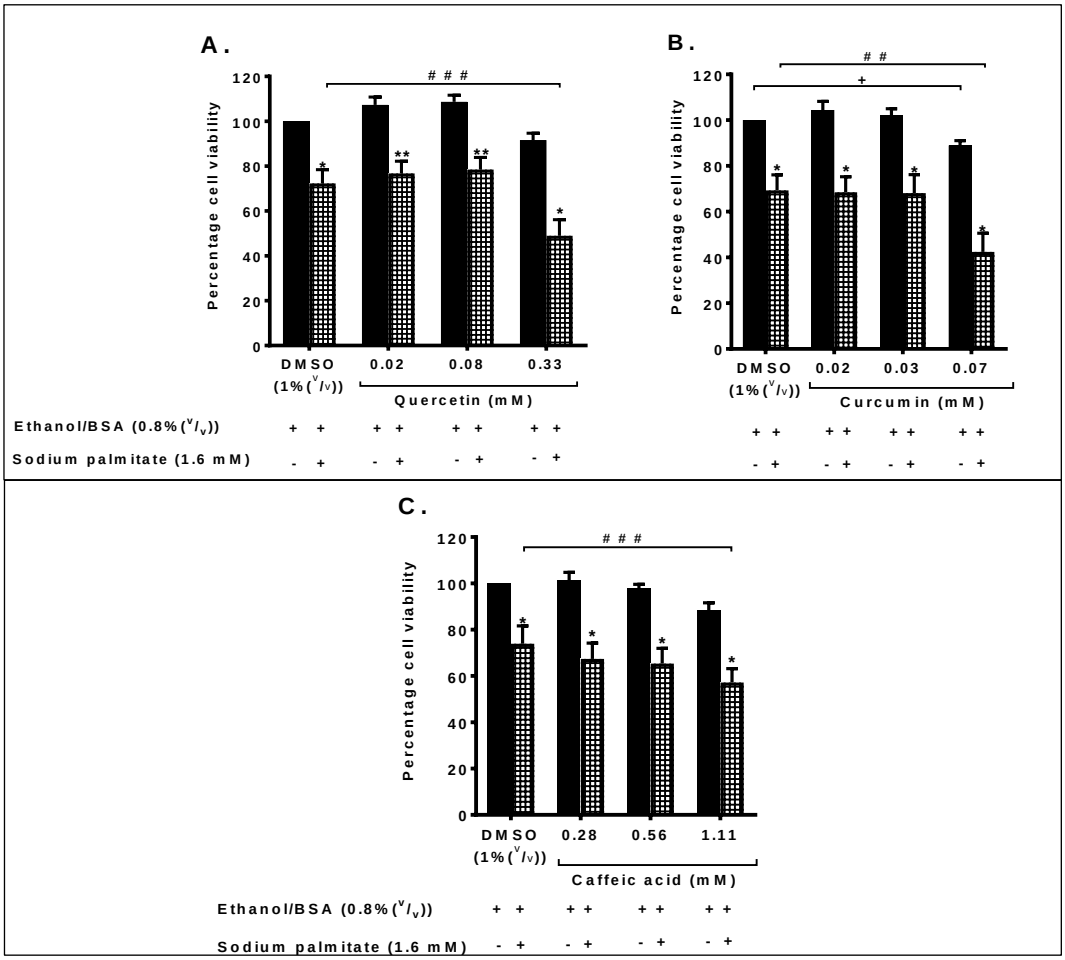

Figure 4.14 Cytotoxic effects of selected phytochemicals after 5 h co-exposure with sodium palmitate in 1.1B4 pancreatic β-cells. β-cells were incubated with varying concentrations of quercetin (A), curcumin (B) and caffeic acid (C) in 10%($^{v}/_{v}$) RPMI-1640 complete medium containing 0.8%($^{v}/_{v}$) ethanol/BSA or 1.6 mM sodium palmitate. DMSO (1%($^{v}/_{v}$)) and 0.8%($^{v}/_{v}$) ethanol/BSA were used as vehicle controls for selected phytochemicals and sodium palmitate respectively. Each data point represents percentage viability of duplicate wells from six independent experiments ± SEM. Statistical analysis was performed using Friedman test and post hoc by Dunn's multiple comparisons test. For comparison with DMSO and each phytochemical alone as control, paired Students' t-test was performed. Where indicated, values were significantly different from 1.6 mM sodium palmitate control at P< 0.01 (##) and P<0.001 (###). Statistical significance relative to individual phytochemical controls was denoted as P<0.05 (*) and P<0.01 (**). Also, values for curcumin were significantly different from DMSO at P<0.05 (+).

4.3.3.2 Effects of phytochemicals on palmitate toxicity (5 h-co-exposure) in HepG2 cells

Compared to DMSO-treated cells (Fig 4.15A), 5 h exposure to quercetin did not alter morphology of HepG2 cells (Fig 4.15B). This observation was in accordance with the lack of significant effect on cell viability (Fig 4.16). Cells appeared rounded and separated from each other after 5 h treatment with 1.6 mM sodium palmitate (Fig 4.15C),

corresponding to approximately 16% toxicity ($P<0.01$, Fig 4.16). Nevertheless, morphological changes caused by sodium palmitate were averted by co-exposure with quercetin, with significant effect at 0.33 mM quercetin (Fig 4.15D). Preservation of structural integrity of cells, by quercetin, was consistent with direct cytoprotective activities produced in a concentration-dependent manner, with significant increase in cell viability (approximately 10%) at 0.33 mM quercetin ($P<0.05$, $n = 6$).

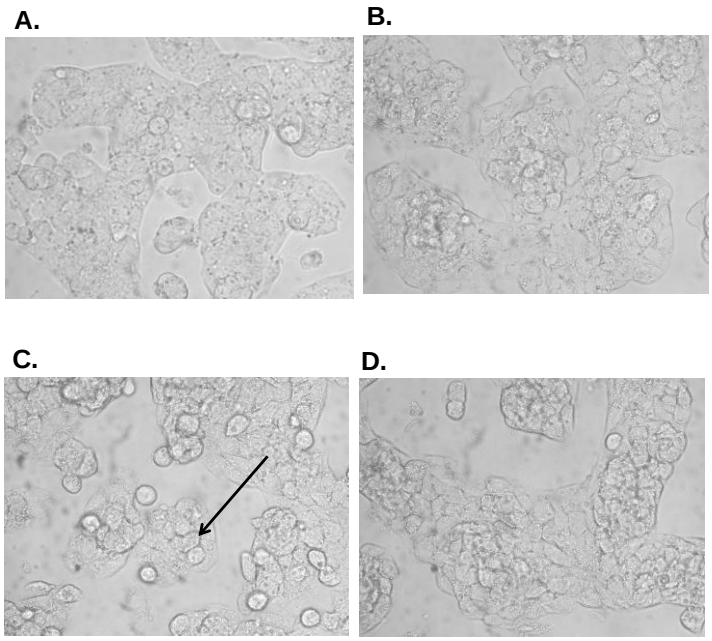

Figure 4.15 Representative images of human hepatoma HepG2 cells after 5 h co-exposure to quercetin and 1.6 mM sodium palmitate. Images show cells treated with 1%($^{v}/_{v}$) DMSO (A) and 0.33 mM quercetin (B) in 0.8%($^{v}/_{v}$) ethanol/BSA-containing media. HepG2 cells were also co-treated with 1.6 mM sodium palmitate and DMSO (C), and 0.33 mM quercetin (D). Effect of 1.6 mM sodium palmitate on morphology is indicated by black arrow. Images were obtained at 40X magnification using the CMEX-18PRO camera with the Olympus Ck2 microscope.

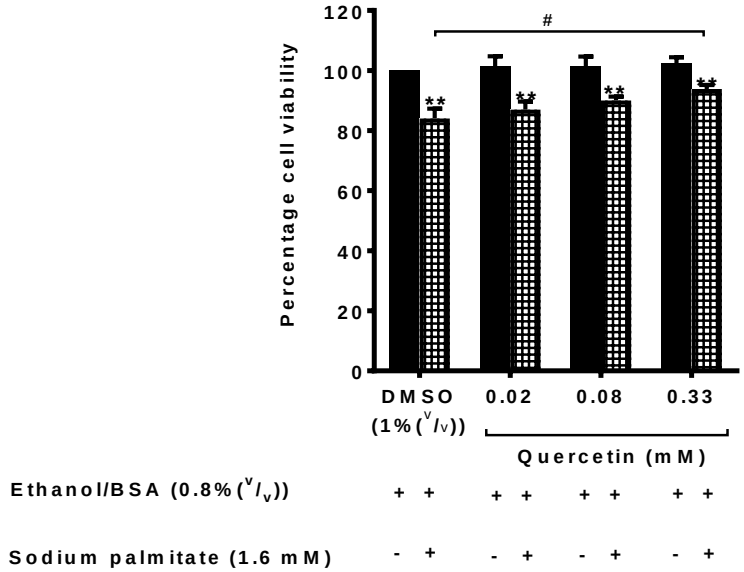

Figure 4.16 Protection by quercetin against sodium palmitate following 5 h co-exposure in HepG2 hepatoma cells. Cells were treated with DMSO (1%($^{v}/_{v}$) and 0.8%($^{v}/_{v}$) ethanol/BSA as vehicle controls for quercetin (and sodium palmitate respectively. Each data point represents mean absorbance from duplicate wells of six independent experiments ± SEM. Statistical analysis was performed using Friedman test and post hoc by Dunn's multiple comparisons test. Where indicated, values were significantly different from 1.6 mM sodium palmitate control at P<0.05 (#). For comparison with corresponding DMSO and quercetin controls, paired Students' t-test was performed, with significant effect at P<0.01 (**).

As observed previously, 1.6 mM sodium palmitate alone caused cells to appear distinctly rounded after 5 h exposure (Fig 4.17D), producing not greater than 20% cytotoxicity (Fig 4.18).

Curcumin showed no effect on HepG2 cell morphology and no toxicity after 5 h exposure, relative to DMSO (Fig 4.18A). However, cytotoxic effects observed after exposure to sodium palmitate alone persisted in the presence of curcumin, with additive effect at 0.07 mM curcumin (P<0.01, n = 6). This observation was consistent with no restoration of morphological abnormalities caused by sodium palmitate (Fig 4.17E).

Relative to DMSO, caffeic acid alone was without cytotoxic effect after 5 h exposure (Fig 4.17C). However, caffeic acid did not demonstrate direct cytoprotection against 1.6 mM sodium palmitate, and did not restore morphological intergrity of HepG2 cells (Fig 4.17F). The lack of direct cytoprotection by curcumin and caffeic acid (in HepG2 cells) was consistent with their inability to restore structural intergrity of 1.1B4 cells (data not shown).

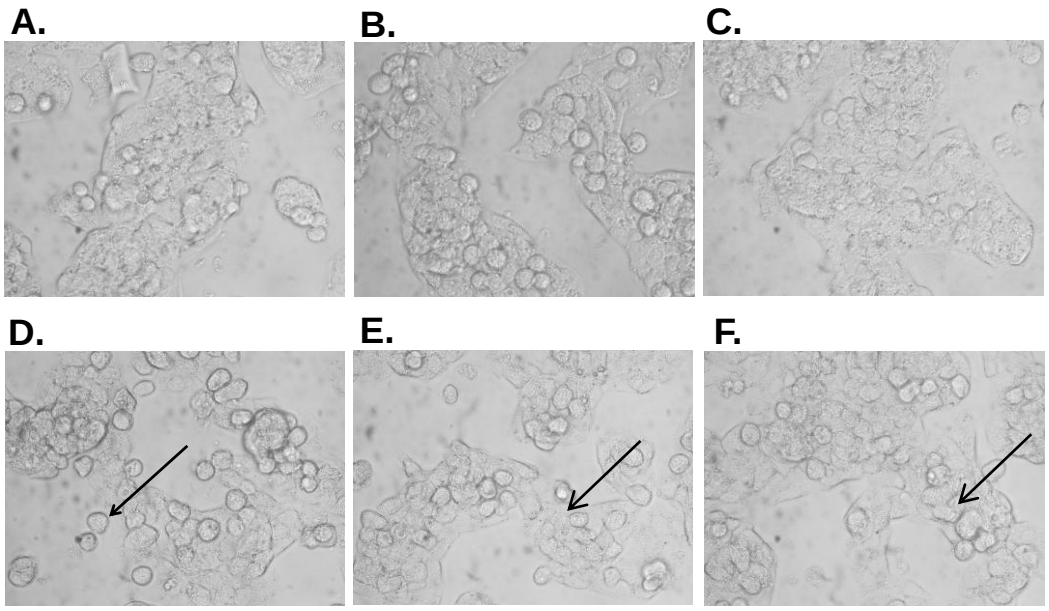

Figure 4.17 Representative images of human hepatoma HepG2 cells after 5 h co-exposure to curcumin and caffeic acid, and 1.6 mM sodium palmitate. Images show cells treated with 1%($^{v}/_{v}$) DMSO (A), 0.07 mM curcumin (B) and 1.1 mM caffeic acid (C) in 0.8%($^{v}/_{v}$) ethanol/BSA-containing media. HepG2 cells were also co-treated with 1.6 mM sodium palmitate and DMSO (D), 0.07 mM curcumin (E) and 1.11 mM caffeic acid (F). Effect of 1.6 mM sodium palmitate on morphology is indicated by black arrow. Images were obtained at 40X magnification using the CMEX-18PRO camera with the Olympus Ck2 microscope.

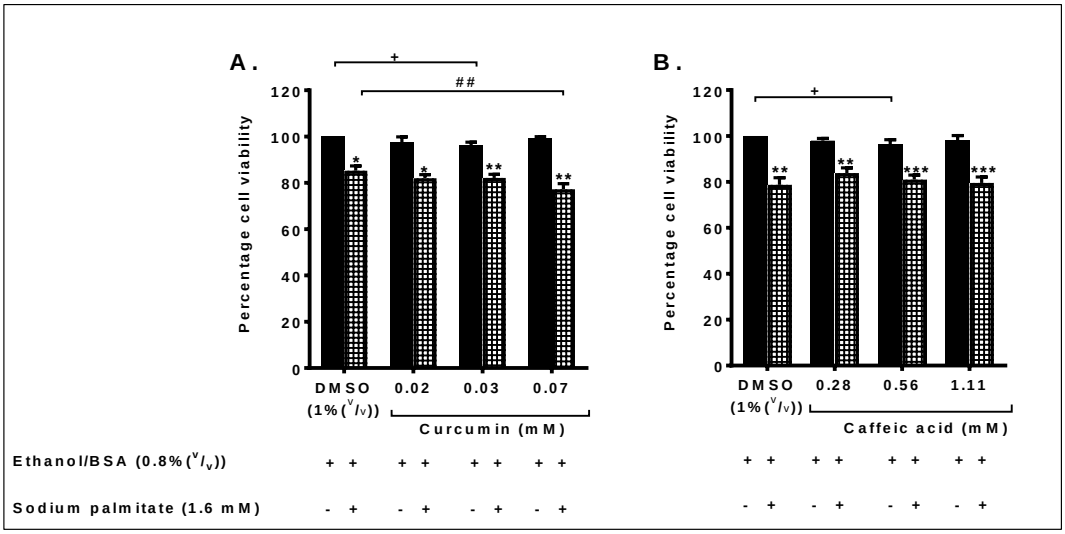

Figure 4.18 Effects of 5 h co-exposure with curcumin and cffeic acid, and sodium palmitate in HepG2 hepatoma cells. Cells were treated with DMSO (1%($^{v}/_{v}$)) and 0.8%($^{v}/_{v}$) ethanol/BSA as vehicle controls for curcumin (A) and caffeic acid (B), and sodium palmitate respectively. Each data point represents mean absorbance from duplicate wells of six independent experiments ± SEM. Statistical analysis was performed using Friedman test and post hoc by Dunn's multiple comparisons test. Where indicated, values were significantly different from DMSO at $P<0.05$ (+) and 1.6 mM sodium palmitate control at $P<0.01$ (##). For comparison with corresponding DMSO and phytochemical controls, paired Students' t-test was performed, with significant effect at $P<0.05$ (*) and $P<0.01$ (**).

4.3.4 Effects of pre-exposure to phytochemicals on lipotoxicity on 1.1B4 and HepG2 cells

The following data represent effects of pre-treatment with quercetin, curcumin and caffeic acid on palmitate toxicity in 1.1B4 and HepG2 cells. Cells were pre-treated with phytochemicals for 20 h prior to 20 h exposure to culture medium containing vehicle control (0.15%($^{v}/_{v}$) ethanol/BSA) or 0.30 mM palmitate.

4.3.4.1 Pre-treatment of 1.1B4 β-cells with phytochemicals enhances lipotoxicity

The 1.1B4 cells maintained their normal morphology following pre-exposure to DMSO (Fig 4.19A); however, quercetin alone caused cells to appear rounded in a concetration-dependent manner (Fig 4.19B), corresponding to approximately 32% cytotoxicity 0.33 mM quercetin ($P<0.01$, $n = 6$; Fig 4.21A). Pre-treatment with curcumin caused similar morphological changes (Fig 4.19C), leading to a concentration-dependent cytotoxicity with aproximately 30% decrease in cell viability at 0.03 mM curcumin (Fig 4.21B). Similar observation was made with caffeic acid (Fig 4.19D), which recorded approximately 20% cell viability at 0.56 mM caffeic acid (Fig 4.21C).

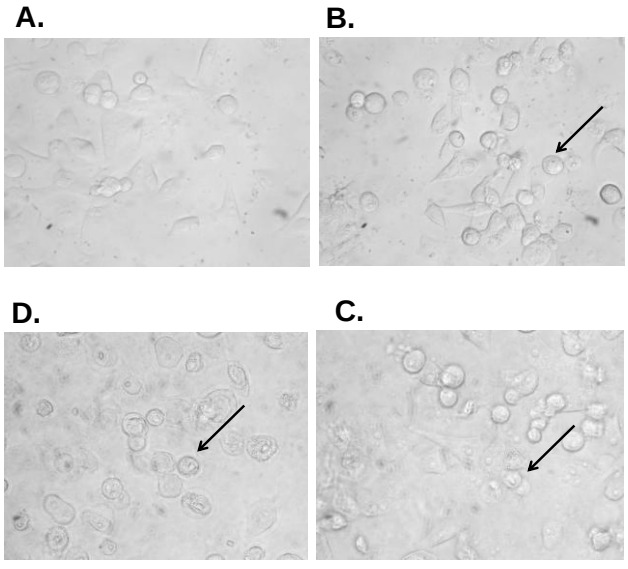

Figure 4.19 Representative images of human pancreatic 1.1B4 β-cells after 20 h pre-exposure to selected phytochemicals. Cells were pre-treated with 1%($^{v}/_{v}$) DMSO (A), 0.33 mM quercetin (B), 0.03 mM curcumin (C) and 0.56 mM caffeic acid (D) for 20 h and for 20 h with 0.15%($^{v}/_{v}$) ethanol/BSA-containing media. Rounded cells have been indicated by black arrows. Images were obtained at 40X magnification using the CMEX-18PRO camera with the Olympus Ck2 microscope.

As presented in Figs 4.20A, 20 h exposure to 0.3 mM sodium palmitate alone resulted in cell appearing rounded and separated from each other. This observation corresponded to approximately 50% cytotoxicity in 1.1B4 cells (Fig 4.21). However, these morphological changes were more distinct in pre-treated cells (Figs 4.21B - D).

In keeping with morphological observations, concentration-dependent toxicity was recorded by pre-treated cells, producing no greater than 35% cell viability at 0.17 mM quercetin (Fig 4.21A), 0.03 mM curcumin (Fig 4.21B) and 0.56 mM caffeic acid (Fig 4.21C). This indicates that selected phytochemicals did not exhibit indirect cytoprotection against sodium palmitate under experimental conditions used; rather additive cytotoxicity was observed.

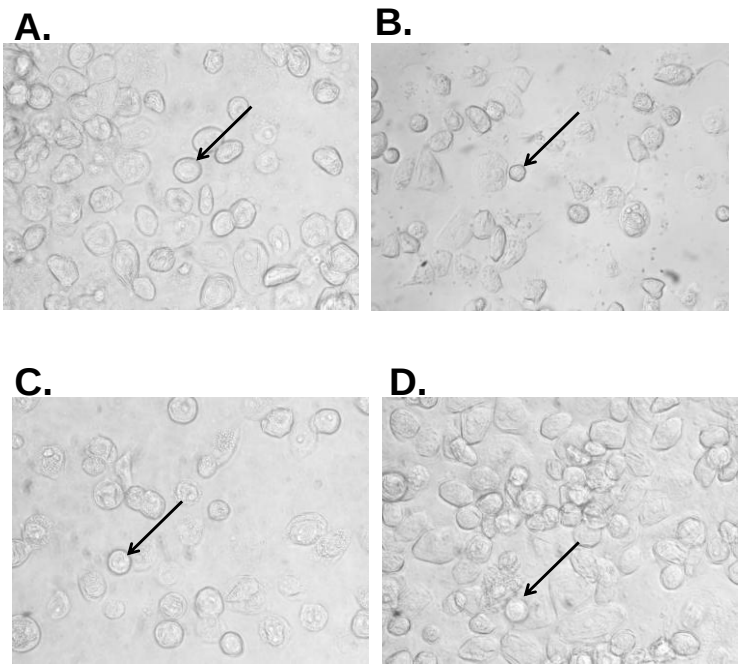

Figure 4.20 Representative images of human pancreatic 1.1B4 β-cells (pre-treated with selected phytochemicals) after 20 h exposure to 0.3 mM sodium palmitate. The 1.1B4 cells were pre-treated with DMSO (A), 0.33 mM quercetin (B), 0.03 mM curcumin (C) and 0.56 mM caffeic acid (D) in 0.3 mM sodium palmitate-containing media. Black arrows indicate cells appearing rounded and separated from each other. Images were obtained at 40X magnification using the CMEX-18PRO camera with the Olympus Ck2 microscope.

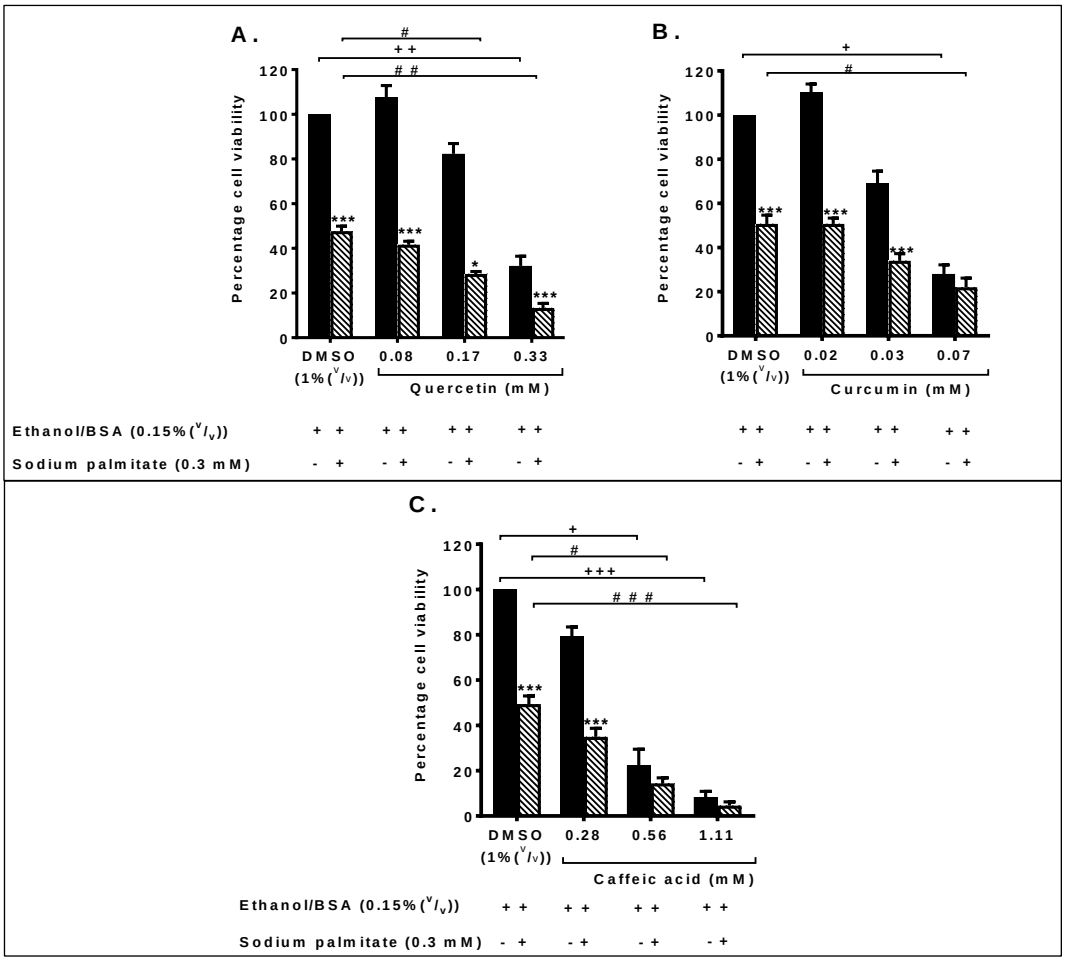

Figure 4.21 Cytotoxic effects following pre-treatment with selected phytochemicals on palmitate toxicity in 1.1B4 pancreatic β-cells. β-cells were pre-treated with vaying concentrations of quercetin (A), curcumin (B) and caffeic acid (C) for 20 h prior to 0.3 mM sodium palmitate exposure. DMSO (1%($^{v}/_{v}$)) and 0.15%($^{v}/_{v}$) ethanol/BSA were used as vehicle controls for selected phytochemicals and sodium palmitate respectively. Each data point represents percentage viability of duplicate wells from six independent experiments ± SEM. Statistical analysis was performed using Friedman test and post hoc by Dunn's multiple comparisons test. Where indicated, values were significantly different from respective DMSO control at P<0.05 (+), P<0.01 (++) and P<0.001 (+++). Values were also significantly different from 0.3 mM sodium palmitate control at P<0.05 (#), P<0.01 (##) and P<0.001 (###). For comparison with corresponding DMSO and phytochemical controls, paired Students' t-test was performed, with significant difference recorded at P<0.05 (*) and P<0.001 (***).

4.3.4.2 Pre-treatment with phytochemicals exacerbates lipotoxicity in HepG2 cells

Images presented in Fig 4.22 show the effect of phytochemicals, and sodium palmitate on HepG2 morphology. Although morphological changes by quercetin were not distinct (Fig 4.22B), relative to lack of effect DMSO (Fig 4.22A), pre-treatment resulted in a concentration-dependent decrease in cell viability, leading to approximately 20% reduction in viability at 0.33 mM quercetin (P<0.001, n = 6; Fig 4.23A). Following 20 h

pre-treatment with 0.03 mM curcumin cells appeared rounded and separated from each other (Fig 4.22C).

After 20 h exposure to sodium palmitate, HepG2 cells appeared rounded (Fig 4.22 D) but, this led to minimal cytotoxicity (approximately 6%, Fig 4.23). Palmitate toxicity was amplified by about 47% after pre-exposure to varying concentrations of quercetin ($P<0.01$, Fig 4.23A). Cell viability also decreased with increasing concentration of curcumin, leading to pronounced cytotoxicity after 20 h exposure to 0.3 mM sodium palmitate (Fig 4.23B). Relative to sodium palmitate, additive cytotoxicity of approximately 33% was recorded at 0.03 mM curcumin ($P<0.001$, $n = 6$).

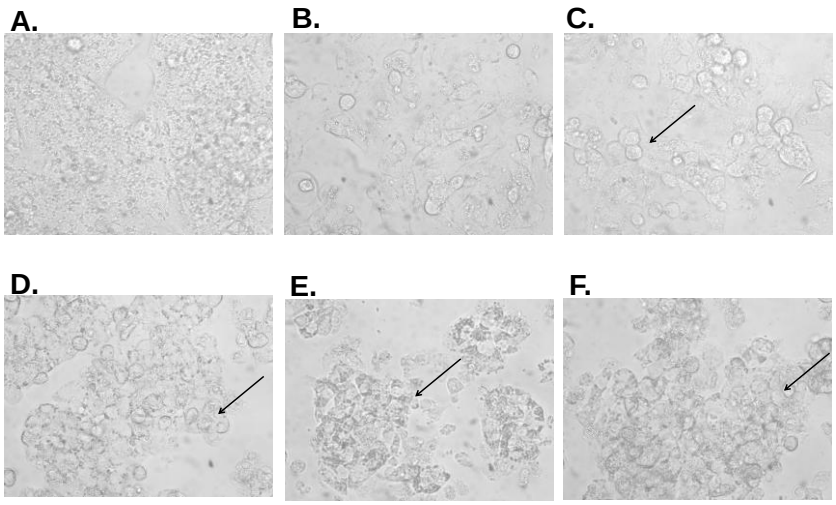

Figure 4.22 Representative images of human hepatoma HepG2 cells after 20 h pre-exposure to selected phytochemicals, and then 20 h treatment with sodium palmitate. Cells were pre-treated with 1%($^{v}/_{v}$) DMSO (A), 0.33 mM quercetin (B) and 0.03 mM curcumin (C) for 20 h, and for 20 h with 0.15%($^{v}/_{v}$) ethanol/BSA-containing media. Cells were then treated with 0.3 mM sodium palmitate after 20 h exposure with 1%($^{v}/_{v}$) DMSO (D), 0.33 mM quercetin (E) and 0.03 mM curcumin (F). Rounded cells have been indicated by black arrows. Images were obtained at 40X magnification using the CMEX-18PRO camera with the Olympus Ck2 microscope.

Pre-treatment with caffeic acid (0.28 – 1.11 mM) did not alter cell morphology (data not shown) and retained 100% viability. Exposure to 0.3 mM sodium palmitate alone caused approximately 4% toxicity, which was not significant in this set of experiments (Fig 4.23C). However, palmitate toxicity was exacerbated following pre-treatment with caffeic acid, producing approximately 30% toxicity at 1.11 mM caffeic acid ($P<0.001$, $n = 6$). Thus, quercetin, curcumin and caffeic acid lacked the inability to restore morphological

intergrity of HepG2 cells and did not demonstrate indirect cytoprotection against sodium palmitate, but exercebated cytotoxic effect under these experimental conditions.

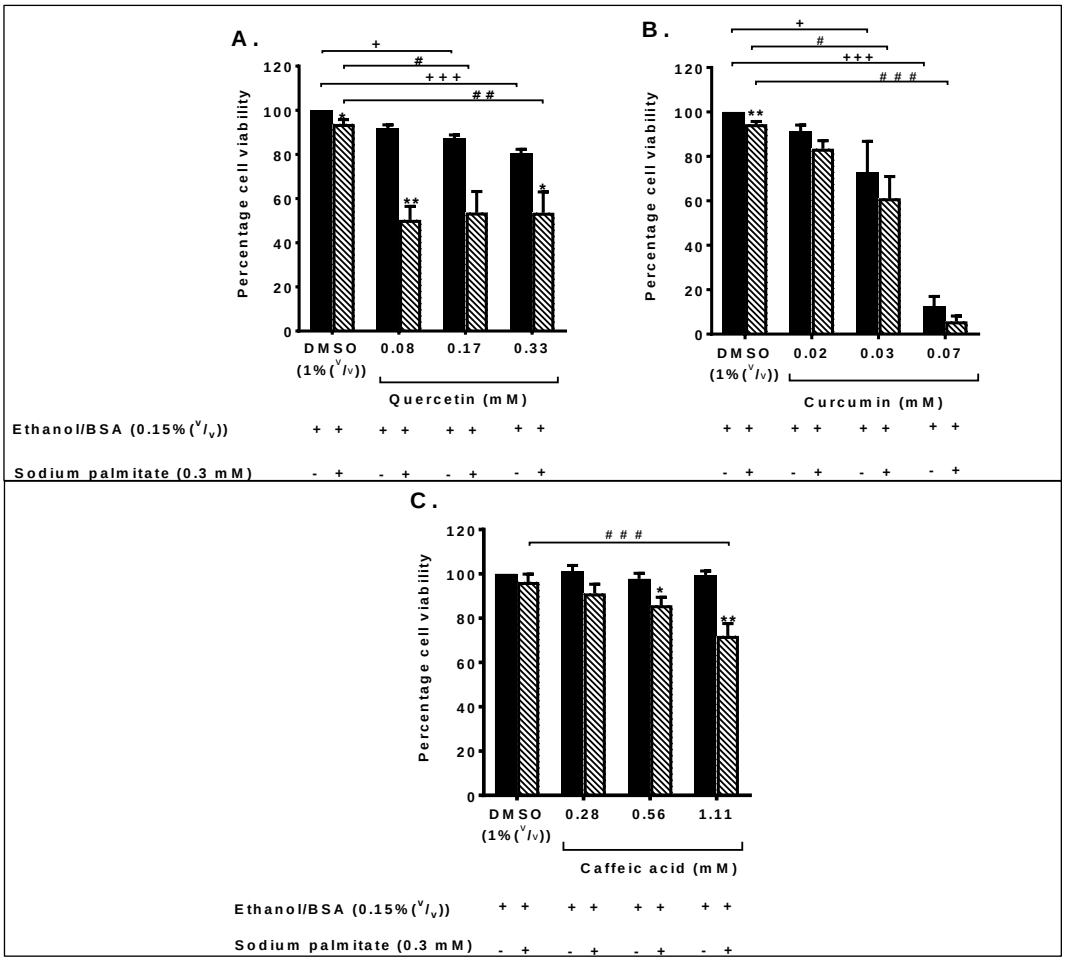

Figure 4.23 Cytotoxic effects by pre-treatment with selected phytochemicals, on palmitate toxicity in HepG2 hepatoma cells. Cells were pre-treated with varying concentrations of quercetin (A), curcumin (B) and caffeic acid (C). DMSO(1%($^{v}/_{v}$)) and 0.15%($^{v}/_{v}$) ethanol/BSA were used as vehicle controls for selected phytochemicals and sodium palmitate, respectively. Each data point represents percentage viability of duplicate wells from six independent experiments ± SEM. Statistical analysis was performed using Friedman test and post hoc by Dunn's multiple comparisons test. Where indicated, values were significantly different from DMSO control at P<0.05 (+), P<0.01 (++) and P<0.001 (+++). Values were also different from 0.3 mM sodium palmitate control at P<0.05 (#), P<0.01 (##) and P<0.001 (###). For comparison with corresponding DMSO and phytochemical controls, paired Students' t-test was performed, significance denoted as P<0.05 (*) and P<0.01 (**).

4.3.5 HepG2 cells cultured at high density are less vulnerable to palmitate toxicity

From Section 4.3.4.2, 0.3 mM sodium palmitate produced less than 7% toxicity in HepG2 cells. This level of toxicity was less than expected (estimated cytotoxicity of 50% at this concentration) and may have resulted from increased cell density during the 20 h culture

period prior to sodium palmitate exposure. To confirm this, the 20 h cytotoxicity experiment was repeated in HepG2 cells. HepG2 cells were pre-treated with 1%($^{v}/_{v}$) DMSO (vehicle control for phytochemicals) for 20 h, prior to palmitate exposure.

As presented in Fig 4.24(A), HepG2 cells appeared more confluent compared to Fig 4.12. Cells appeared rounded after 20 h exposure to sodium palmitate, above 0.4 mM, which caused cells to separate from each other (moderately) and to detach from 24-well plates (Figs 4.24B and C).

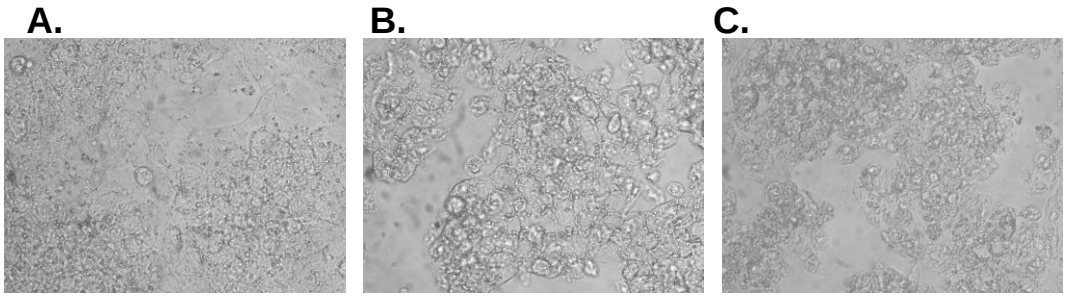

Figure 4.24 Representative images of confluent human hepatoma HepG2 cells after 20 h exposure to varying concentrations of sodium palmitate. Images show HepG2 cells after 20 h exposure to 10%($^{v}/_{v}$) MEM Eagle complete medium (A) and sodium palmitate at 0.4 mM (B) and 1.6 mM (C). Images were obtained at 40X magnification using the CMEX-18PRO camera with the Olympus Ck2 microscope.

Similar to Fig 4.13, cell viability decreased with increasing concentration of sodium palmitate, but significant effect occurred in a more gradual pattern (Fig 4.25). Nevertheless, 1.6 mM palmitate produced less than 7-fold decrease in toxicity following 20 h exposure to confluent cells, compared to less confluent cells (Fig 4.13). This confirms that minimal toxicity observed after 20 h exposure to 0.3 mM palmitate in pre-treated cells (Section 4.3.4.2) resulted from increased cell density. Thus, the palmitate-to-cell ratio was reduced as predicted. Results of lipotoxicity experiments are summarised in Table 4.4.

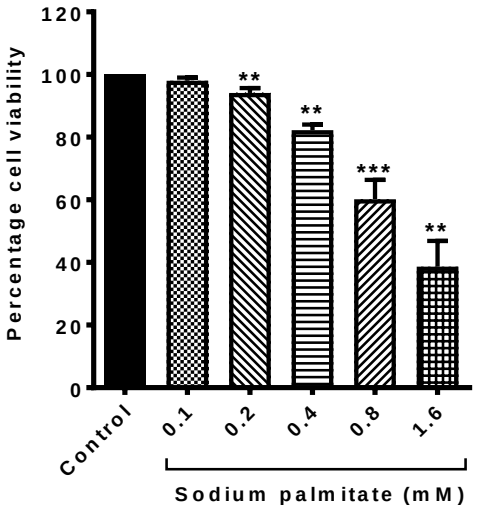

Figure 4.25 Cytotoxicity by sodium palmitate (20 h exposure) in confluent HepG2 hepatoma cells. After culturing for 26 h, cells were treated with 1%($^{v}/_{v}$) DMSO for 20 h and then 10%($^{v}/_{v}$) MEM Eagle complete medium containing sodium palmitate (0.1 – 1.6 mM) for 20 h. Each data point represents percentage viability from duplicate wells of six independent experiments ± SEM. Statistical analysis was performed using paired Student's t-test when compared to respective ethanol/BSA controls (0.05 – 0.8%($^{v}/_{v}$)). Where indicated, values were significantly different from corresponding ethanol controls at P<0.05 (*), P<0.01 (**) and P<0.001 (***).

Palmitate toxicity		
Cell type	**Exposure time**	**Cytotoxic effect**
1.1B4 β-cells	5 h	44% cytotoxicity at 1.6 mM
	20 h	Mean EC_{50}: 0.30mM (0.14, 0.45)
HepG2 cells	5 h	33% cytotoxicity at 1.6 mM
	20 h	Mean EC_{50}: 0.42 mM (0.26, 0.58)
Effects of phytochemicals on palmitate toxicity (1.1B4 cells)		
Palmitate and phytochemicals	**5 h co-exposure**	**20 h pre-exposure**
Quercetin	Additive cytotoxicity	Additive cytotoxicity
Curcumin	Additive cytotoxicity	Additive cytotoxicity
Caffeic acid	Additive cytotoxicity	Additive cytotoxicity
Effects of phytochemicals on palmitate toxicity (HepG2 cells)		
Palmitate and phytochemicals	**5 h co-exposure**	**20 h pre-exposure**
Quercetin	Cytoprotective activity	Additive cytotoxicity
Curcumin	Additive cytotoxicity	Additive cytotoxicity
Caffeic acid	No effect	Additive cytotoxicity

Table 4.4 Summary of results obtained from lipotoxicity experiments in 1.1B4 β-cells and HepG2 cells.

4.4 Discussion

Whilst the exact mechanisms and sequence of events are still being explored, it is believed that oxidative stress remains at the centre of glucotoxicity (in T2DM) and lipotoxicity (in NASH), resulting in apoptotic cell damage. Having established cytoprotective effects against *t*BHP-mediated oxidative stress, phytochemicals were investigated for cytoprotective activities against palmitate-induced cytotoxicity.

4.4.1 Absence of glucotoxicity in β-cells and HepG2 cells effects

The findings reported in this chapter indicate that continuous exposure (up to 72 h) to high glucose levels, 25 mM and 40 mM, did not demonstrate toxic effects in 1.1B4 pancreatic β-cells and HepG2 hepatoma cells. The lack of glucotoxicity was observed following assessment under various experimental conditions, including varying cell densities, exposure conditions and toxicity assays, all of which failed to provide a reproducible assay for glucotoxicity in 1.1B4 human β-cells. So far in this thesis, the neutral red assay has been established as a reliable measure of cell viability, which has produced results that were consistent with early and late apoptosis assays (Chapter 3). Similarly, the absence of reproducible loss in viability recorded by MTT assay (Figs 4.3A and C) and lack of increase in early or late apoptosis events after continuous exposure to high glucose (40 mM), relative to osmotic control (29 mM mannitol plus 11 mM glucose) (Fig 4.4B and C), were consistent in this study.

This raises the issue in defining viable and non-viable cells using different assays. While the MTT assay measures mitochondrial function as an indicator of cell viability, reduction of the soluble tetrazolium salt (MTT) to an insoluble formazan precipitate is catalysed by NADPH dehydrogenase-dependent (Slater et al., 1963) and NADPH-independent reaction (involving ROS) (Rdhanjal and Fry, 1997). Therefore, in an assay where MTT was exposed to β-cells in the presence of high glucose, perhaps reduction of MTT could result from interactions with high cellular ROS levels.

The early and late apoptosis assay (using annexin V and propidium iodide), on the other hand, assesses cell viability by measuring integrity of cell membrane, which can be influenced by caspase-mediated externalisation of phosphatidylserine (Fink and Cookson, 2005). However, this loss of plasma membrane integrity represents a much later event in terms of mechanism, since caspase activation is regulated by more upstream parameters such as activation of pro-apoptotic proteins (Bax and Bad) and inhibition of anti-apoptotic proteins (Kim et al., 2006).

The neutral red assay assesses viability by the ability of cells to take up and incorporate the neutral red dye in lysosomal matrix. Uptake of the neutral red dye does not occur in non-viable cells because these cells are unable to maintain pH gradient (Filman et al., 1975) required for retaining the dye, which becomes charged and binds to anionic and phosphate groups in lysosomal matrix of live cells (Winckler, 1974). Therefore, consistent results provided by these three toxicity assays confirm the proposal that glucotoxicity was not present in 1.1B4 cells under the experimental conditions used.

The lack of glucotoxicity reported in the current study contradicts a recent report by Vasu et al., (2013), that glucotoxicity in 1.1B4 cells was mediated by apoptosis, with 70% increase in caspase-3 activity and 40% decrease in Bcl2 expression after 72 h exposure to 25 mM glucose. Studies conducted with rodent pancreatic β-cells (Tanaka et al., 1999; Bhattacharya et al., 2013) and in humans (Sempoux et al., 2001; Butler et al., 2003) have reported alterations in insulin signalling and synthesis as well as upstream targets of apoptosis following chronic hyperglycaemia and this concept is extensively reviewed (Robertson et al., 2003; Bensellam et al., 2012). Nevertheless, insulin gene expression was damaged after six months of glucose exposure in rat HIT-15 pancreatic β-cells (Tanaka et al., 1999).

In the absence of further studies, two inferences can be made. Firstly, assays used in the current study to measure glucotoxicity may have been downstream of the cytotoxicity pathway, and hence the potential of cell viability assays to measure glucotoxicity needs to be explored further, perhaps focusing on insulin signalling. Secondly, 72 h exposure period was probably not long enough to cause scientifically relevant glucotoxicity.

Nevertheless, attempts to increase duration of glucotoxicity experiments could either lead to artefactual increase in cell death, as a result of seeding cells at low density, or increase in cell numbers since the 1.1B4 cells normally have a high growth rate (Section 3.3.2.1.

Again, the lack of glucotoxicity in HepG2 cells contradicts earlier reports of glucose-mediated apoptosis (Chandrasekaran et al., 2010). These authors reported increased caspase activity and DNA fragmentation, in addition to 30% loss of cell viability. However, the reasons for the contradictory findings of this study are currently not known.

4.4.2 Lipotoxicity by sodium palmitate

In the current study, cytotoxic effects of sodium palmitate, recorded in 1.1B4 β-cells, resulted in a concentration-dependent decrease in cell viability. After 5 h exposure, 1.6 mM sodium palmitate caused approximately 50% toxicity (Fig 4.7). Moreover, 20 h exposure to varying concentrations of sodium palmitate produced an estimated mean TC_{50} value of 0.30 ±0.06 mM, while sodium palmitate caused concentration-dependent toxicity after short-term (5 h) and long-term (20 h). These findings support earlier reports where 18 h exposure to palmitate resulted in decreased glucokinase activity and activated ER stress response, in addition to depletion of Ca^{2+} stores and DNA fragmentation in 1.1B4 β-cells (Vasu et al., 2013). In another study, chronic exposure to palmitate decreased glucose-stimulated insulin secretion via decreasing calcium/calmodulin dependent protein kinase II and extracellular signal-regulated kinase (ERK) and increasing palmitate esterification in murine MIN6 insulinoma cells (Watson et al., 2011).

Effects of sodium palmitate exposure in HepG2 cells produced similar results with 33% toxicity after short-term exposure to 1.6mM and mean TC_{50} value of 0.40 ±0.06 mM after 20 h treatment. It has been previously shown that exposure to high palmitate levels resulted in a time-dependent increase in ROS production and loss of mitochondrial membrane potential in human hepatoma HepG2/C3A cell line (Srivastava and Chan, 2007). A follow-up *in silico* sensitivity analysis identified GSH depletion due to palmitate-induced inhibition of GSH synthesis, decreased levels of cysteine transporters which then

limits cysteine uptake (Srivastava and Chan, 2008). These reports suggest the role of mitochondrial-mediated oxidative stress in palmitate toxicity. In addition, palmitate toxicity in the current study was confirmed via the neutral red assay.

Furthermore, recent studies in HepG2 and other human hepatoma cells identified activation of JNK pathway and increased Bax expression by treatment with 0.11 mM sodium palmitate, which also inhibited GSK-3β protein to cause lipoapoptosis after 48 h exposure (Cao et al., 2014). The observation of palmitate toxicity via the neutral red assay, in the current study, suggests a rapid onset of apoptotic cell death in 1.1B4 and HepG2 cells; which requires early intervention. Thus, therapeutic focus could be aimed at underlying mechanisms of lipoapoptosis following relatively shorter duration of exposure.

The mechanism of palmitate toxicity involves a complex pathway of events including ceramide synthesis, oxidative stress, ER stress, lysosomal and mitochondrial damage, leading to apoptosis (Li et al., 2008; Malhi and Gores, 2008), although the order of events is still unknown. Ceramide synthesis also results from cellular metabolism of palmitate, which occurs in a series of reactions involving palmitoyl-transferase and ceramide synthase (Nolan et al., 2006). It has been reported that ceramide plays a key role in signalling during ROS-mediated apoptosis (Cacicedo et al., 2005), by inhibiting pyruvate, malate and succinate oxidation resulting in elevated ROS production at complex I of the electron transport chain (Di Paola et al., 2000).

4.4.3 Effect of phytochemicals on palmitate toxicity

4.4.3.1 Direct exposure to palmitate and phytochemicals

Further investigations in HepG2 cells revealed concentration-dependent cytoprotection by quercetin during 5 h co-exposure with palmitate, with significant effect at 0.33 mM ($P<0.05$, $n = 6$). However, neither curcumin nor caffeic acid demonstrated protection in 5 h co-exposure conditions, while curcumin exacerbated lipotoxicity during co-exposure with palmitate ($P<0.01$, $n = 6$). The current report on additive cytotoxic effects of selected phytochemicals and sodium palmitate, and direct cytoprotection by quercetin is a new finding.

While direct cytoprotection by quercetin can be related to direct cytoprotective activity, as was reported in Chapter 2, it can be inferred that curcumin and caffeic acid lacked direct cytoprotective activities against palmitate (5 h co-exposure). In Chapter 2, quercetin was shown to be the most potent direct cytoprotective phytochemical compared to curcumin and caffeic acid. Therefore, given the minimal toxicity recorded by 5 h treatment with 1.6 mM sodium palmitate alone (<20%), one could argue that quercetin may exhibit enhanced direct cytoprotection against higher levels of sodium palmitate.

In 1.1B4 human β-cells, cytotoxicity was exacerbated in the presence of quercetin and caffeic acid, while curcumin induced toxicity in absence of palmitate as well. Again the reason for this observation is unknown.

4.4.3.2 Pre-treatment with phytochemicals exacerbates palmitate toxicity

In pre-exposure conditions, none of the phytochemicals showed protection against lipotoxicity; in fact, quercetin, curcumin and caffeic acid increased cytotoxicity in both HepG2 and 1.1B4 β-cells. Furthermore, phytochemicals also elicited cytotoxicity effects following 20 h treatment, and this was not dependent on sodium palmitate.

Although proposals for the exact mechanism for this effect are discussed in Chapter 6, perhaps additive cytotoxicity can be inferred. However, caffeic acid alone was not cytotoxic to HepG2 cells but potentiated sodium palmitate toxicity in pre-treated cells. This suggests the increased vulnerability of both cell types to sodium palmitate following prophylactic exposure to phytochemicals. A similar observation was made where resveratrol amplified palmitate toxicity via ER stress-dependent mechanism (Rojas et al., 2014), and this agrees with results of the current study since polyphenols were also evaluated against sodium palmitate. As reviewed by Malhi and Gores, (2008), lipotoxicity is a multi-faceted event which involves a series of mechanisms (also see Section 4.4.2). It is believed that phytochemicals screened against lipotoxicity are able to induce ROS-mediated cell damage against *t*BHP (see Chapter 2). Hence, one possible explanation for the additive effect could be as a result of phytochemical-induced exacerbation of oxidative stress during in lipotoxicity.

4.5 Conclusion

Under the experimental conditions used, a reproducible cell viability assay could not be developed for glucotoxicity assessment in both HepG2 hepatoma cells and 1.1B4 pancreatic β-cells. However, palmitate was found to be cytotoxic, in both cell types, following short-term (5 h) and long-term (20 h) exposure.

Among the phytochemicals evaluated against lipotoxicity, only quercetin demonstrated direct cytoprotection in HepG2 hepatoma cells, but not in 1.1B4 pancreatic β-cells. Moreover, quercetin did not exhibit indirect cytoprotection against lipotoxicity in HepG2 cells and 1.1B4 β-cells, as was also observed with curcumin and caffeic acid, which had neither direct nor indirect cytoprotective activities under these experimental conditions.

The findings presented in this chapter will be discussed further in the context of the findings relating to *t*BHP-mediated oxidative stress in the final chapter.

CHAPTER 5

Effect of selected phytochemicals on expression of cytoprotective enzyme in HepG2 and 1.1B4 cells

CHAPTER 5 - Effect of selected phytochemicals on cytoprotective enzyme expression in HepG2 and 1.1B4 cells

This chapter evaluates expression of cytoprotective enzymes following treatment with phytochemicals in HepG2 and 1.1B4 β-cells. In addition, an attempt is made to identify effects of cytoprotective compounds on expression of phospho-proteins in HepG2 cells, using a global proteomic approach.

5.1 Introduction

The effect of phytochemicals on the expression and activity of cytoprotective enzymes has gained interest in recent times, due to the ability of cytoprotective enzymes to avert cellular oxidative damage. According to Dinkova-Kostova and Talalay, (2010), ultimate antioxidants by are long-acting cytoprotective enzymes that catalyse a variety of chemical reactions as part of adaptation of cells to oxidative stress. Cytoprotective enzymes are normally present in cells at suboptimal levels requiring induction by indirect and bifunctional exogenous antioxidants, which upregulate enzyme expression and activity against oxidative damage (Dinkova-Kostova and Talalay, 2010). Indirect antioxidants have been defined as compounds that induce Phase II enzymes, while bifunctional antioxidants exhibit radical scavenging activities against ROS, as well as induce Phase II cytoprotective enzymes (Dinkova-Kostova and Talalay, 2010). The coordinate induction of Phase II enzymes by phenolic compounds accounts for their chemopreventive effects (Talalay et al., 1995). Pharmacological induction of cytoprotective enzymes, which are regulated by the Keap1/Nrf2 complex results in numerous benefits; examples are listed in Table 5.1.

Benefits of cytoprotective enzymes	Examples of targets
Upregulation of enzymes which detoxify electrophiles	Glutathione S-transferase (GST), epoxide hydrolase, NAD(P)H: quinone oxidoreductase EC 1.6.99.2 (NQO1)
Upregulation of enzymes that facilitate inactivation of oxidants	Superoxide dismutase, selenium-dependent glutathione peroxidase, catalase and glutathione peroxidase function of GSTs
Production of direct antioxidants	Carbon monoxide and bilirubin through heme oxygenase and biliverdin reductase
Averting iron overload	Increasing ferritin levels
Increasing activities of thioredoxin reductase, glutathione reductase and GCL, to trigger GSH synthesis and regeneration	

Table 5.1 Examples of the benefits of pharmacological induction of cytoprotective enzymes. As reviewed by Dinkova-Kostova and Talalay, (2010).

5.1.1 NQO1

NQO1 is ubiquitously present in plant, animal and microbial systems (Benson et al., 1980). NQO1 is a good representative marker for cytoprotection, since it is well distributed in mammalian tissues and its response to inducers is measurable in experimental conditions (Prochaska et al., 1992; Dinkova-Kostova and Talalay, 2010). NQO1 is a homodimer that exists in the cytosolic phase associated with one FAD attached to each monomer (Ross, 2004). Ernster and Navazio, (1958) initially discovered this cytoprotective enzyme as DT-diaphorase and two years later it was found to correspond to dicoumarol-inhibited vitamin K reductase (Märki and Martius, 1960).

Among the cytoprotective enzymes, NQO1 plays a crucial role in chemoprevention by detoxifying reactive intermediate species such as quinones, which are generated during oxidative metabolism of aromatic hydrocarbons (O'Brien, 1991), as well as radical

scavenging (Ross, 2004). Antioxidant activity of NQO1 requires NADPH or NADH as reducing cofactors in an obligatory two-electron reduction of various quinone species to hydroquinones, which are more stable and further metabolised to glucuronide and sulfate conjugates, prior to excretion (Iyanagi and Yamazaki, 1970; Faig et al., 2000; Bianchet et al., 2004).

Quinones are toxic oxidative metabolites of aromatic hydrocarbons which cause damage to DNA, cellular macromolecules (Bachur et al., 1979) and thiol groups, including GSH, leading to GSH depletion which exacerbates oxidative damage (Prochaska et al., 1985; Dinkova-Kostova and Talalay, 2010). Although reports suggest that electrophilic nature of quinones makes them suitable inducers of Nrf2 via interacting with Keap1 sensors (Magesh et al., 2012), quinones engage in one-electron reduction and other redox cycling activities to generate autooxidizable toxic semiquinone intermediates and other ROS (Dinkova-Kostova and Talalay, 2010). Thus, NQO1 acts as a regulator against quinone toxicity (Lind et al., 1982) as illustrated in Fig 5.1.

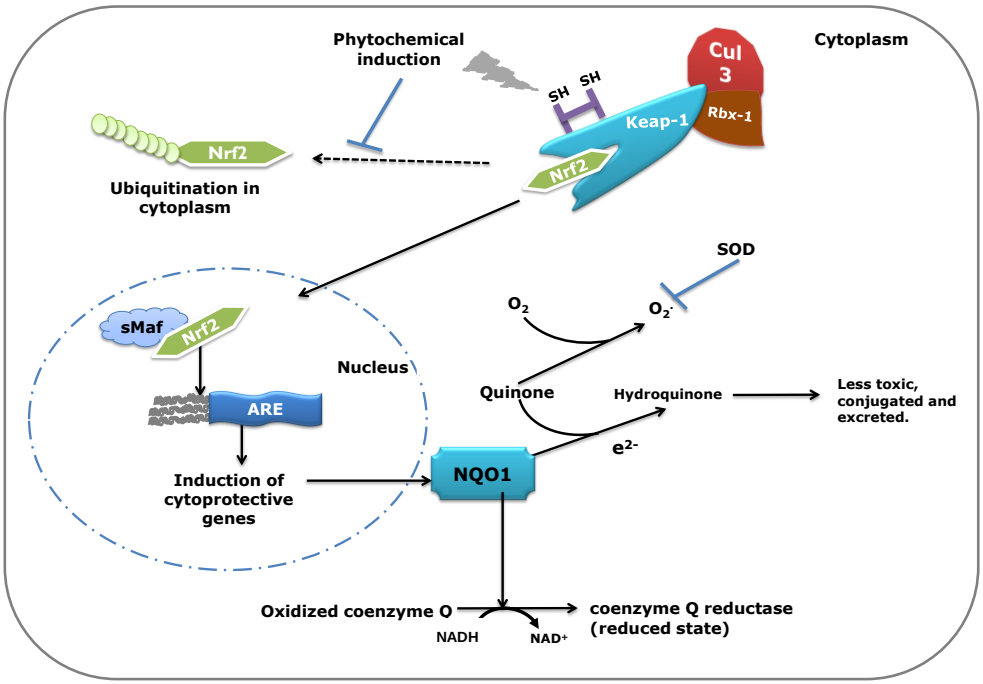

Figure 5.1 Keap1/Nrf2/ARE pathway induced by phytochemical treatment. During induction, Nrf2 escapes proteasomal degradation and subsequently activates upregulation of cytoprotective genes in the nucleus, including NQO1 (Dinkova-Kostova and Talalay, 2010).

It is reported that cytoprotective activities of NQO1 are also augmented by concomitantly acting with superoxide dismutase (Segura-Aguilar and Lind, 1989) and UDP-glyconosyl transferase (Lind, 1985), as reviewed (Cadenas, 1995). Thus, the ease of reactivity of *o*-quinones with oxygen molecules leads to increased superoxide levels which activate the antioxidant enzyme superoxide dismutase (Segura-Aguilar and Lind, 1989). An increase in glucuronide formation of quinol species in the presence of NQO1 has also been observed in rat liver microsomes (Lind, 1985). In addition to detoxification of quinones, NQO1 also indirectly supports cellular antioxidant system by maintaining antioxidant coenzyme Q reductase in its reduced state (Fig 5.1).

There is growing interest in the use of proteomics approach in comparative protein profiling, to identify biomarkers involved in disease and treatment conditions (Wang et al., 2009). According to Kultz, (2000), a minimal stress proteome is activated during redox signalling and may serve as target for phytochemicals, as part of their antioxidant activities. Due to the limitations of 2-dimensional gel electrophoresis, proteome fractionation is desired to produce reduced complexity and increased dynamic range of protein identification (Tooth et al., 2012). Differential detergent fractionation (DDF) is a commercialised (Abdolzade-Bavil et al., 2004), economical and robust alternative to ultracentrifugation (Ramsby et al., 1994) for separation of proteins. Also multidimensional column liquid chromatography is an efficient method used to enhance separation of complex peptide mixtures and this can shorten the duration of mass spectrometry and enhance structural analysis of proteins (Tooth et al., 2012). Mass spectrometry also provides high-throughput analysis and identification of phospho-proteins (Aebersold and Goodlett, 2001; Mann and Jensen, 2003).

5.1.3 Aim

The aim of this study was to evaluate the inductive effect of long-term exposure to phytochemicals on expression of NQO1 in HepG2- and 1.1B4 human β-cells. Subsequently, multidimensional separation of protein mixtures and high throughput protocols were used to identify effects of cytoprotective phytochemicals on the expression

phospho-proteins in HepG2 cells. The effects of phytochemicals on cellular proteins were investigated in the context of their role in mediating indirect cytoprotection against *t*BHP-induced damage, observed in Chapter 2.

5.2 Materials and methods

5.2.1 Materials

List of chemicals and their suppliers can be obtained from Appendix I. Also, the composition of solutions used in both Western blot and proteomics studies can be obtained from Appendix III and IV, respectively.

5.2.2 Methods

5.2.2.1 Cell treatment

Media were prepared as stated in Section 2.2.1.3. Cells were subcultured as described in Section 2.2.3. For HepG2 cells, passage numbers from 18 to 35 were used, while passage numbers for 1.1B4 cells ranged from 33 to 39.

Treatement of cells with EC_{50} concentrations of phytochemicals: HepG2 cells were cultured in wells of 24-well plates at seeding density of 1.2 x 10^6 cells/ml and allowed to attach to wells for approximately 28 h. After cells were attached, culture medium was replaced with 1 ml of 10%($^v/_v$) MEM Eagle complete medium containing phytochemicals and cultured for approximately 20 h, at which time, cells were prepared for SDS-PAGE analysis as described below. This same method was applied to cells treated with varying concentrations of quercetin (0.02 – 0.33 mM).

Optimisation of NQO1 expression: HepG2 cells were cultured in wells of 24-well plates from three different suppliers (Costar, Falcon and Sarstedt) at seeding density of 4.0 x 10^5 cells/ml and allowed to attach to wells for approximately 28 h. Different types of culture plates were used to assess the effect of plastic material (used to make plates) on basal expression of NQO1. In each plate type, cells were treated with MEM Eagle medium (with or without 10%($^v/_v$) FBS), 1%($^v/_v$) DMSO and quercetin (0.10 mM), in quadruplicate wells for approximately 20 h. Cells were then prepared for SDS-PAGE analysis as described below.

Treatment of 1.1B4 human β-cells: Cells were harvested as described in Section 2.2.3.2 and cultured in wells of 24-well plates at seeding density of 1.3 x 10^5 cells/ml. Cells were treated with quercetin (0.02 – 0.33 mM), curcumin (0.02 mM and 0.07 mM)

and caffeic acid (0.57 – 2.22 mM) in 1 ml of 10%($^{v}/_{v}$) RPMI-1640 complete medium in quadruplicate wells, and cultured for approximately 20 h. Cells were also treated with DMSO (1%($^{v}/_{v}$)) as vehicle control. Cells were prepared for SDS-PAGE analysis as described below.

5.2.2.2 Cell lysate preparation

Following treatment with phytochemicals, cells were kept on ice for cell lysis and sample collection. The culture medium was aspirated and cells washed with 400 µl ice-cold Dulbecco's PBS which was then aspirated and replaced with 200 µl lysis buffer, at pH 7.6 (see Appendix III for composition), per well. Cells were then homogenised using a pestle to aid cell lysis and release of cellular proteins into solution. The mixture from corresponding wells (per sample) was collected into 1.5 ml microfuge tubes and agitated at 45^{o} (to allow adequate turning of samples from one end of tube to the other, to facilitate lysis of cells) for approximately 20 min at 4^{o}C. Cell lysate was then kept at -80^{o}C at this stage until further use. For cytosolic fractions, cell lysates were centrifuged at 6000 rpm for 5 min and supernatant collected into labelled 1.5 ml microfuge tubes for storage at -80^{o}C. Labelled microfuge tubes containing 20 µl of the cell lysate were kept for protein quantification, while 500 µl was saved for Western blotting. At this stage, samples were frozen at -80^{o}C.

5.2.2.2.1 Protein quantification

Protein quantification was performed using Lowry assay, which is based on reduction of Cu^{2+} to Cu^{+} under alkaline conditions (Lowry et al., 1951). A 1 mg/ml solution of BSA was made up in distilled water and used to generate a standard curve within a range of concentrations (see Table 5.2). In separate 1.5 ml microfuge tubes, 20 µl of each sample was diluted with 180µl distilled water. Lowry AB solution was made up by adding 100 µl of 2%($^{w}/_{v}$) sodium-potassium tartrate and 100 µl of 1%($^{w}/_{v}$) copper sulphate as Lowry B solution to 20 ml of Lowry A solution (see Appendix III for composition); then, 1 ml of this Lowry AB solution was added to both standard and test samples. All samples were incubated at room temperature for 10 min, after which 100 µl of Folin reagent (made from

1:1 dilution with distilled water) was added to standard and test samples, with further incubation at room temperature for at least 45 min and no more than 3 h. Prior to detection, 200 µl of standard and test samples was pipetted into wells of a 96-well plate in triplicate and the resulting absorbance was determined at 750 nm using Spectra MAX 340pc plate reader. Protein content of samples was determined using BSA standard curve.

Tube label	BSA (µl)	Distilled water (µl)	Protein concentration (mg/ml)
0	0	200	0
1	10	190	0.05
2	20	180	0.1
3	30	170	0.15
4	40	160	0.2
5	50	150	0.25
6	60	140	0.3
7	70	130	0.35
8	80	120	0.4

Table 5.2 Concentrations of bovine serum albumin (BSA) in Lowry assay.

5.2.2.3 Sodium dodecyl sulphate polyacrylamide gel electrophoresis (SDS-PAGE)

The remaining cell samples were diluted with 20%($^{v}/_{v}$) solubilising buffer (from 6X stock, see Appendix III for composition) and could be stored at -20^{o}C for further use or loaded onto a gel for Western blot. Prior to loading on the gel, samples were denatured at 95^{o}C on a heating block for 5 min and then centrifuged at 13000 rpm for 1 min. Bio-Rad mini-PROTEAN TGX precast (4 – 20% polyacrylamide) gel was set up according to instruction from Bio-Rad, UK, in a Bio-Rad tank with 1X electrophoresis buffer (made from 10X stock, see Appendix III). A color pre-stained molecular weight marker (2 µl, from New England Biolabs, UK) was loaded into the first well of each gel to aid identification of molecular weight of desired proteins and also served as a guide to monitor progress of electrophoresis. The remaining wells were loaded with approximately 10 ug (amount of protein) of each sample and the gel was run at 175 V for 40 min.

5.2.2.4 Western blotting

After completion of electrophoresis, resolved proteins were transferred onto nitrocellulose membrane placed in a cassette, supported by filter paper and sponge pads, as shown in Fig 5.2. The nitrocellulose membrane, filter paper, cassette and sponges were conditioned in transfer buffer (see Appendix III) for approximately 15 min prior to use. The transfer set-up was then fitted into a tank (from Bio-Rad, UK) containing ice-pack and transfer buffer. Migration of resolved proteins from the gel to the nitrocellulose membrane occurred at a constant voltage of 100 V for 60 min.

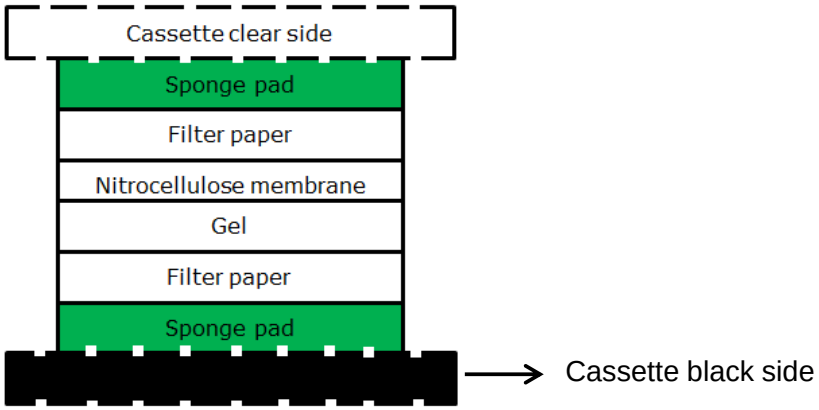

Figure 5.2 A model for assembly of protein transfer set-up in Western blotting. Figure shows sandwich layered with perforated cassette enclosing sponge pad, filter papers, gel and nitrocellulose membrane. During the transfer process, resolved proteins migrate from the cathode which is connected to the black side of the cassette, towards the anode at the clear side of the cassette.

After this time, effectiveness of protein transfer was confirmed by staining nitrocellulose membrane with approximately 2 ml of Ponceau Red Stain (Sigma, Dorset, UK), which was quickly washed with adequate amounts of distilled water and Tris-buffered Saline Tween 20 (TBST). Using the molecular weight marker as a guide, the nitrocellulose membrane was cut with stainless steel scalpel at marks corresponding to molecular weights of proteins of interest. Non-specific proteins were blocked at this stage for approximately 1 h at room temperature, using 5%($^{w}/_{v}$) non-fat milk in TBST, with gentle shaking at 37 revs/min. Primary antibody, NQO1, was diluted in TBST containing 5%($^{w}/_{v}$) non-fat milk at desired dilution (Table 5.3). The blot was incubated in a bag containing 5

ml of this antibody, and using Salter bag sealer and incubated overnight at 4°C with agitation at 70 revs/min.

Antibody	Specification	Supplier	Dilution
Quinone reductase (NQO1)	Goat polyclonal (ab2346)	Abcam, Cambridge, UK	1:1000 dilution
GAPDH	Mouse monoclonal	Sigma, Dorset, UK	1:5000

Table 5.3 Primary antibodies used in Western blotting.

Following overnight incubation, the blot was subjected to three quick washes using 20 ml TBST. Washing was repeated three times for 5 min and then repeated three times for 15 min to remove unbound primary antibody. The blot was then incubated with 1:10000 dilution of secondary antibody (made in 5% ($^{w}/_{v}$) non-fat milk in TBST; Table 5.4) and incubated at 37°C in the dark for 1 h. The solution containing secondary antibody was discarded and blot was washed, as described above, with final wash in distilled water prior to scanning.

Blots were scanned using an Odyssey® infrared fluorescent imaging scanner (LI-COR) and densitometric analysis by Odyssey® Image Studio version 3.1.

After scanning, blots were probed with glyceraldehyde 3-phosphate dehydrogenase (GADPH) as housekeeping protein (as described above), using desired concentration (Table 5.3). Blots were then washed three times using 20 ml TBST (quick washes) and washed again for 5 min (three times) using 20 ml TBST. Finally, washing was repeated three times for 15 min using equal volume of TBST before probing with secondary antibody (mentioned in Table 5.4.) as described above. Afterwards, secondary antibody was discarded and blots washed with TBST as described above. Blots were then scanned as mentioned above.

Antibody	Protein	Band colour and wavelength	Dilution
Polyclonal Donkey-anti Goat IgG (926-32214) LI-COR IRDye (LI-COR. Biosciences, UK)	NQO1	Green (800)	1:10000
Polyclonal Goat anti-rabbit 926-32211 (LI-COR)	GAPDH	Red (800)	1:10000

Table 5.4 Secondary antibodies used in Western blotting.

5.2.2.5 Protein quantification and identification using proteomics

Cell treatment: HepG2 cells were seeded at 1.2 x 10^6 cell/ml in wells of 24-well plate and initially allowed to attach for 28 h at 37°C. Culture medium was then replaced with medium containing 1%($^v/_v$) DMSO or phytochemicals (quercetin, curcumin and caffeic acid), and cells cultured for additional 20 h. Afterwards, culture medium was aspirated and cells were washed with 400 µl warm HBSS, which was also discarded. Cells were trypsinised using 100 µl 1x trypsin EDTA at 37°C for 5 min, after which 1 ml 10%($^v/_v$) MEM Eagle complete medium was used to stop trypsinisation reaction. Detached cells in a single cell suspension (from 16 wells for each treatment) were collected in a sterile 15 ml tube and centrifuged at 500 x g for 5 min. After discarding the supernatant, cell pellet was washed in 1 ml ice-cold PBS and centrifuged again at 500 x g for 5 min. Supernatant was discarded and the cell pellet was stored at -80°C in 1.5 ml microfuge tubes until subcellular fractionation was conducted using procedure illustrated in Fig 5.3.

5.2.2.5.1 Cell lysis and subcellular fractionation

Pelleted cells were recovered from frozen storage and kept on ice throughout the subcellular fractionation procedure. Prior to extraction, each pellet was visually calibrated using an equivalent volume of distilled water in a 1.5 ml microfuge tube and the required volume of respective buffer (Table 5.5) used to extract various subcellular fractions.

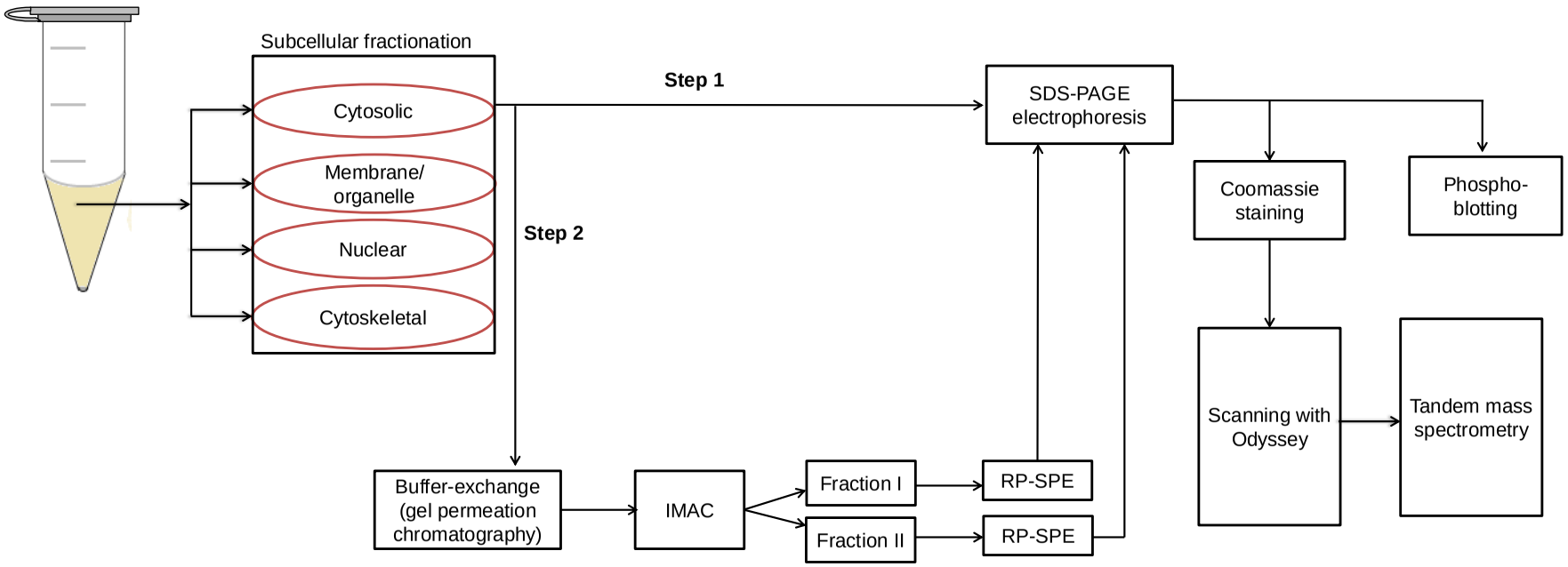

Figure 5.3 Scheme for proteomic assessment of HepG2 cells. Pelleted cells were sub-fractionated into different cellular compartments (cytosolic, membrane/organelle, nuclear and cytoskeletal fractions - Section 5.2.2.5.1). Proteins in each sub-cellular fraction were quantified, and then separated by SDS-PAGE electrophoresis (Section 5.2.2.5.2). Proteins transferred onto polyvinylidene difluoride membrane were then probed for phospho-proteins, while remaining proteins on the gel were stained with Coomassie blue. Bands on phospho-blot that correspond to phospho-proteins showing change in expression were identified for further analysis by tandem mass spectrometry (Section 5.2.2.5.6). Furthermore, proteins in cytosolic fractions were taken through chromatography (gel permeation – Section 5.2.2.5.3) and immobilised metal affinity chromatography (IMAC – Section 5.2.2.5.4) to obtain two fractions (fraction I – phospho-depleted proteins and fraction II – phospho-proteins). Proteins in both fractions were separated using reverse-phased solid phase extraction (RP-SPE) chromatography (Section 5.2.2.5.5) and proteins in the eluates obtained were then separated by SDS-PAGE electrophoresis (Section 5.2.2.5.2), then phospho-blotting of PVDF membrane and Coomassie staining of gel. Similarly, bands for phospho-proteins which showed change in protein expression were identified for analysis by tandem mass spectrometry (Section 5.2.2.5.6).

Treatment conditions	Pellet size (µl)	Buffer (I) µl	Buffer (II) µl	Buffer (III) µl	Buffer (IV) µl
Untreated	70	175	175	105	105
DMSO	60	150	150	90	90
Quercetin (0.04 mM)	60	150	150	90	90
Quercetin (0.33 mM)	70	175	175	105	105
Curcumin (0.07 mM)	60	150	150	90	90
Caffeic acid (2.22 mM)	60	150	150	90	90

Table 5.5 Volume of extraction buffers used for each sample during sub-cellular fractionation. Untreated samples refer to cells incubated in 10%($^{v}/_{v}$) MEM Eagle complete medium alone.

For each extraction stage, samples were resuspended by gently pipetting up and down four times and incubated on ice for the required time, agitated and incubated on ice again prior to centrifugation. Incubation time and centrifugation settings used are detailed in Table 5.6. Supernatant was collected in labelled microfuge tubes at each stage. Extraction steps were repeated for each subcellular fraction and supernantant could be stored at -20^{o}C at this stage.

Subcellular fraction	Buffer used	Incubation time	Cenfugation settings
Cytosolic	Cytosolic buffer I	10 min	2000 x g for 2 min
Membrane/organelle	Membrane/organelle buffer II	10 min	5000 x g for 2 min
Nuclear	Nuclear buffer III	5 min	10000 x g for 2 min
Cytoskeletal	Cytoskeletal buffer IV	5 min	10000 x g for 2 min

Table 5.6 Incubation times and centrifugation settings for subcellular fractionation.

Protein quantification: Subcellular fractions were quantified using bicinchoninic acid (BCA) protocol. Standard samples of 1 mg/ml BSA (0, 2.5, 5.0, 10, 20, 30 and 50 µl) were

pipetted into labelled microfuge tubes and made up to 100 µl with distilled water. Each test sample (5 µl) was also made up to 100 µl, with distilled water. To both test and standard samples, 1 ml BCA reagent was added. Solutions were vortexed and heated at 60^{o}C for 15 min. Using a negative control, the UV2101PC instrument was reset to auto-zero at 562 nm, then test samples and standards were analysed. Absorbance measured was then stipulated into a standard curve to obtain the amount of preoteins in each fraction.

5.2.2.5.2 SDS –PAGE analysis of subcellular fractions

Subcellular fractions were recovered from frozen storage and solubilized in 25 µl solubilising buffer (containing 0.01 g dithiothreitol in 750 µl distilled water and 250 µl of 4X NuPAGE sample buffer) by repeated pipetting. The samples were pulse-vortexed and heated at 90^{o}C for 5 min, both procedures being repeated before centrifuging samples at 15 x g for 3 min. In wells of a NuPage 4-12% Bis-Tris gel, 5 µl Novex Sharp Pre-stained molecular marker (Thermo-Fisher, UK) was run alongside the samples (40 µg for cytosolic fractions, 20 µg for nuclear fractions, 30 µg for membrane and organelle fractions and 20 µg for cytoskeletal fractions). The gel was run at 200 V for 45 min in running buffer. After electrophoresis, the separated proteins were transferred from the gel to a non-fluorescing polyvinylidene difluoride (PVDF) membrane (previously rehydrated in methanol and elution buffer) at 25 V for 15 min. The transfer conditions allowed transfer of approximately 15% of separated proteins onto the membrane (Tooth et al., 2012).

In terms of the transfer direction, the PVDF membrane (not necessarily non-fluorescing) was used as a filter to prevent contaminants of the filter paper from being transferred with separated proteins onto the desired membrane (non-fluorescing PVDF). The non-fluorescing PVDF membrane (containing approximately 15% proteins) was then rinsed in 50%($^{v}/_{v}$) methanol and subsequently in 100% methanol before drying in between filters papers. The gel was then fixed in 50%($^{v}/_{v}$) methanol for approximately 30 min with agitation, then stained with 50 ml colloidal G-250 (Coomassie blue) per gel (add four volumes of diluent to one volume of G-250 stain, see Appendix IV for composition) overnight with agitation. The stain was discarded and the gel rinsed in distilled water for

10 min with agitation and the water discarded. This was repeated twice with 30 min agitation. The gel was then soaked in distilled water and agitated for 4 - 8 h until components (on the gel) were well contrasted and background was clear. At this stage, the gel could be kept at 4°C in double distilled water until scanning was performed using Odyssey scanner at 84 µm resolution, focus at 0.0 mm and medium σ.

Gel drying: The gel was incubated in drying reagent (30%($^{v}/_{v}$) methanol, 65%($^{v}/_{v}$) distilled water and 5%($^{v}/_{v}$) polyethylene glycol) and agitated for 5 min. Cellophane film which was used to store the gel was also soaked in drying reagent for apprpximately 20 sec prior to use. Gel drying rack was rinsed with distilled water and set up for drying. The gel was set up between two cellophane films which were held in place by rack and clippers, then dried overnight at room temperature.

Phospho-blotting: The expression pattern of phospho-proteins on non-fluorescing PVDF membrane was investigated using pIMAGO-biotin kit. Detection of phospho-proteins was based on interaction between titanium (Ti) component of pIMAGO-biotin dendrimer (Ti-dendrimer) and phosphate groups on resolved proteins on PVDF membrane (Iliuk et al., 2012), see Fig 5.4.

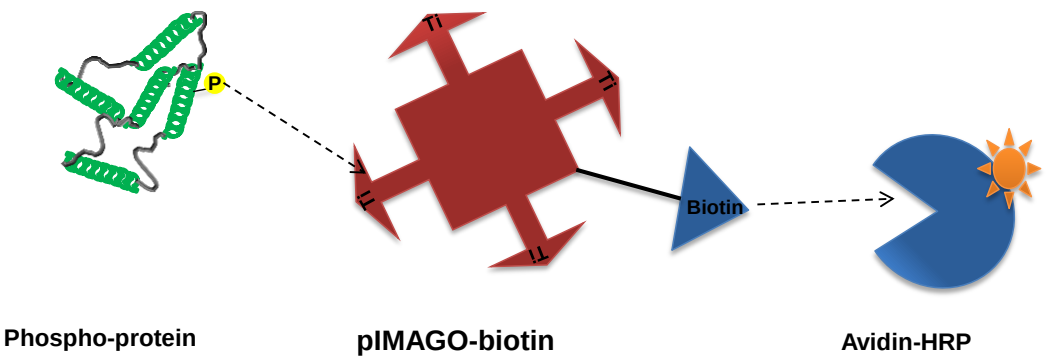

Figure 5.4 The underlying principles for detection of phospho-proteins with the pIMAGO kit. Figure shows dendrimer (globular nanopolymer) made active by Titanium ions for sensitive identification of phospho groups. Dendrimer is also conjugated with biotin (fluorophore), which aids detection by interacting with avidin Horseradish peroxide (avidin HRP) for detection.

Membranes were rehydrated in TBST for 3 min and non-specific targets were blocked with 50 ml (1X) pIMAGO blocking buffer (from 10X stock) for 5 h with agitation at room

temperature. Blocking buffer was discarded and membrane was incubated in 50 ml pIMAGO-biotin dendrimer overnight. Remaining dendrimer was collected and stored at 4^0C, while unbound dendrimer was discarded by rinsing with 100 ml TBST (quick rinse). The membrane was rinsed further with 50 ml TBST and agitated for 10 min; this was done three times. The membrane was then incubated at room temperature in 50 ml of avidin fluor 800 (100 µl and 450 µl TBST) as a secondary probe for 5 h. This was then collected and the membrane rinsed quickly in 100 ml TBST overnight. Prior to scanning, membrane was rinsed quickly in TBS (1X) after discarding TBST.

5.2.2.5.3 Buffer-exchange for Immobilized metal ion affinity chromatography (IMAC) using gel permeation chromatography

Gel permeation chromatography (GPC) separates proteins based on molecular size and shape, where smaller proteins diffuse through porous beads hence, they are eluted slowly (Fig 5.5) (Porath and Flodin, 1959; Cheung et al., 2012). Larger proteins however have minimal or no access to porous beads and so are eluted rapidly (Fig 5.5).

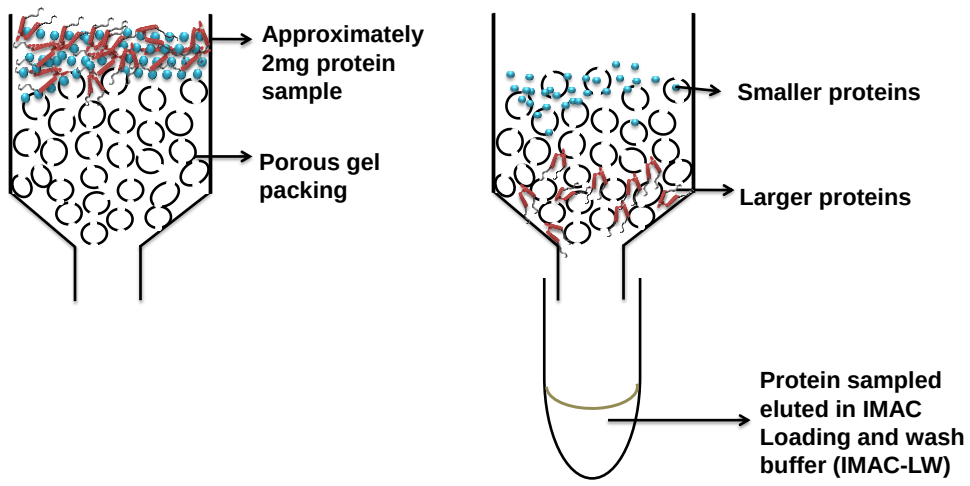

Figure 5.5 Schematic diagram for buffer-exchange gel permeation, showing cellular proteins eluted based on their sizes. Larger molecules are eluted ahead of smaller molecules, which interact with beads and hence slow their rate of elution.

Here, gel permeation liquid chromatography was used for buffer exchange to remove detergents used during subcellular fractionation, which could interfere with subsequent separation procedures. Sepharose (25 - 50 µm; 0.5 g) was weighed into each 6 ml fritted

polypropylene solid phase extraction tube (SPE tube) and sufficient IMAC-load wash (IMAC-LW) used to rehydrate the resin. A total of 10 bed mass volumes was used to wash resin, i.e. 10 ml using sequential additions and evacuated at -5 kPa only to finally leave the resin clear of buffer. For each cytosolic sample, 500 µl was pipetted gently on the resin and additional 1.25 ml of IMAC-LW evacuated to waste at -5 kPa vacuum. Exchanged samples (2.5 ml) were collected in labelled 5 ml tubes and subjected to immobilised metal affinity chromatography (IMAC), as described below.

5.2.2.5.4 Immobilised Metal ion Affinity chromatography (IMAC)

IMAC was performed to separate proteomes into phospho-enriched and phsopho-depleted categories, based on their interaction with Gallium resins. The use of IMAC was suggested based on the affinity exhibited by transition metals such as Cu^{2+} and Zn^{2+} towards tryptophan, histidine and cysteine in aqueous environment (Porath et al., 1975). Metal ions form complexes with chelating ligands which are contained in chromatographic sorbent used (Cheung et al., 2012). During IMAC, electrophilic groups on protein surfaces adsorb onto ligands on immobilized metal ions (Fig 5.6), subsequently, phospho-proteins are eluted selectively from IMAC using an elution buffer (IMAC-EL).

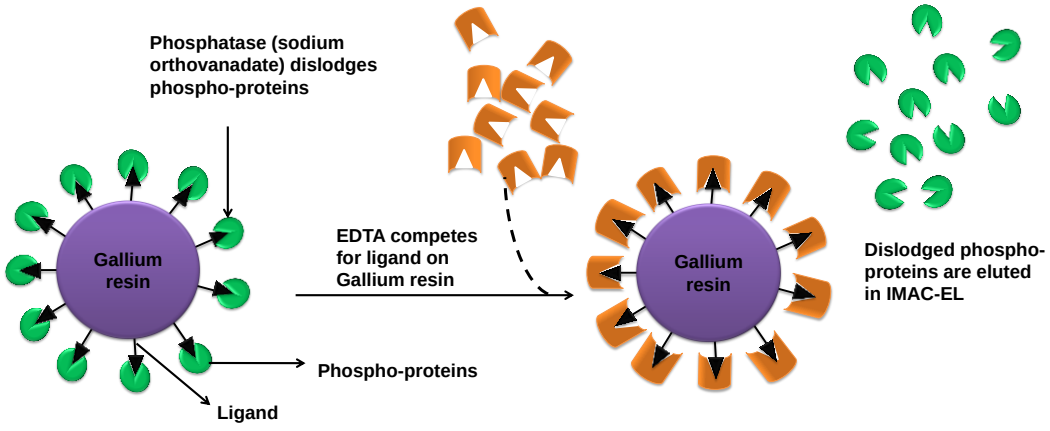

Figure 5.6 Schematic diagram showing binding of phospho-enriched proteins on ligands of gallium resin. Prior to elution, phospho-proteins are dislodged from the resin by phosphatase and EDTA, to aid elution in IMAC-EL.

Conditioning Gallium loaded IMAC resin: 1 – 10 ml resin bed volume (50%($^{w}/_{v}$) slurry) was transferred to 6 to 20 ml fritted SPE tubes and liquid phase evacuated to waste after

centrifugation at 1000 x g for 1 min. Resin was conditioned with 3-bed volumes of chelating buffer with agitation for 5 min and discarded after centrifugation, this step was repeated once. Also 3-bed volumes of 0.1 M gallium sulphate: (42 mg/ml in chelating buffer) was added with agitation for 5 min, centrifuged and then discarded as done before. Resin was washed twice with 3-bed volume of chelating buffer and subsequently with up to 10 bed-volume of distilled water, finally storing in 20%($^{v}/_{v}$) methanol. This could be refrigerated for use within one month.

Fritted polypropylene SPE tubes (6 ml) were labelled and loaded with 0.2 ml resin slurry (Bio-Rad, Profinity IMAC Gallium, suitable for up to 2 mg proteins). Slurry buffer was discarded and conditioned with 15-bed volumes (3 ml) of IMAC-LW buffer by sequential evacuation at -5 kPa, discarding flow-through fractions to waste. Samples (3 ml) were loaded in tubes containing resins, sealed and agitated at 45^{o}C (to allow adequate turning of samples from one end of tube to the other) for 5 min at room temperature before transferring samples to 4^{o}C. Samples were incubated overnight by keeping tubes horizontal, as this position enhanced interaction between samples and gallium resins. After overnight incubation, samples were agitated again at room temperature at 45^{o}C (to allow adequate turning of samples from one end of tube to the other) for 10 min and subjected to chromatography.

The un-retained fraction (I), which comprised predominantly of phospho-depleted proteomes, was recovered by evacuation at -5 kPa into labelled polypropylene SPE tubes. Additional 0.7 ml of IMAC-LW was added to each tube and agitated further for 10 min. Again un-retained material was evacuated as was done previously to obtain final liquid samples in labelled tubes. Resin was washed twice with 10-bed volume (2 ml) and agitated for 10 min before discarding flow through to waste. This step was essential to remove traces of un-retained fraction (I) to minimise contamination with the retained fraction (II).

The retained fraction (II), which comprised predominantly of phospho-enriched proteins, was desorbed using 10-bed volumes (2 ml) of eluent (IMAC-EL), which contained phosphatase (sodium orthovanadate) and a competitive agent (EDTA) to displace bound phospho-proteins. Samples were agitated for 30 min and eluted into labelled tubes at -5

kPa. This was repeated and the eluates added to the previous collection. Both fractions (I and II) were kept at 4°C at this time, prior to reversed-phase chromatography.

5.2.2.5.5 Reversed-phase chromatography

During reversed-phase chromatography, proteins are separated according to hydrophobicity by enabling hydrophobic ends of proteins to orient with the solid phase. Subsequently, proteins are eluted according to increasing hydrophobicity with the least hydrophobic eluting first in the lowest concentration of acetonitrile (Fig 5.7).

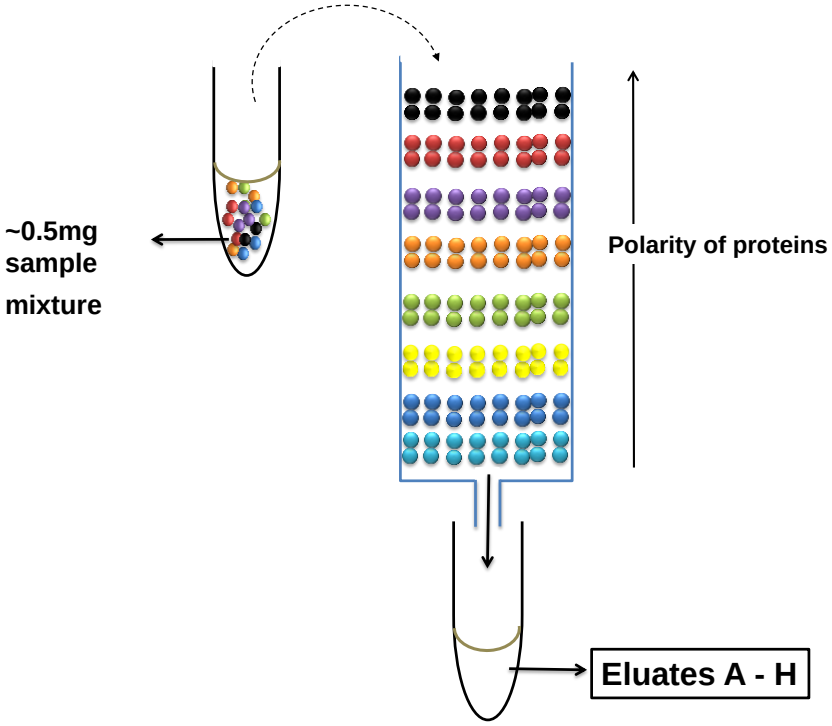

Figure 5.7 Elution of hydrophobic proteins in reverse-phase chromatography. Hydrophobic solid phase interacts with hydrophobic proteins and are subsequently eluted using acetonitrile, which desorbs hydrophobic proteins from solid phase.

Eluents containing appropriate amounts of acetonitrile and distilled water were used to desorb hydrophilic proteins from solid phase and subsequently eluted in labelled tubes (see Table 5.7 for composition of eluents used). Due to volatility of solvents used, this approach was employed as the final chromatographic procedure (Tooth et al., 2012).

Reversed-phase solid phase extraction (RP-SPE) cartridges (IST, 75 mg, 1000Å) were labelled and conditioned with 1 ml of 70%($^{v}/_{v}$) eluate (35 ml acetonitrile and 15 ml distilled water), then evacuated under vacuum at flow similar to 1 ml/min. This was followed with 1 ml ‘O% acetonitrile’ and flow through fractions diverted to remove traces of acetonitrile

from 70%($^{v}/_{v}$) eluent. Using 1 ml of eluents A - H, samples were eluted into labelled tubes to obtain 8 eluates separately for phospho-depleted proteomes (fraction I), and then for phospho-proteins (fraction II). Solid phase purified components were dried using vacuum-centrifuge and archived in air-tight vials at -80°C.

Dried protein residues were resuspended in sample buffer for electrophoresis and phospho-blotting as described in Section 5.2.2.5.2.

Eluent ($^{v}/_{v}$)	**100% acetonitrile (200 ml acetonitrile + 200 µl TFA)**	**0% acetonitrile (200 ml dH_2O + 200 µl TFA)**
Eluent A' 30%	6 ml	14 ml
Eluent B' 35%	7 ml	13 ml
Eluent C '40%	8 ml	12 ml
Eluent D '43%	8.6 ml	11.4 ml
Eluent E '45%	9 ml	11 ml
Eluent F '48%	9.6 ml	10.4 ml
Eluent G '50%	10 ml	10 ml
Eluent H '90%	18 ml	2 ml
'70%	35 ml	15 ml

Table 5.7 Composition of eluents used in reversed-phase chromatography.

5.2.2.5.6 Band identification and mass spectrometry analysis

Bands showing increased or decreased expression of phospho-proteins compared to control (untreated or 1%($^{v}/_{v}$) DMSO), were identified and aligned using Microsoft PowerPoint to facilitate excision of bands of interest.

Bands of interest identified on phospho-blots were then aligned for their positions on respective gels and excised in a filtered cabinet with the aid of a cutting mask guide, using a clean stainless steel scalpel. The volume of each polyacrylamide gel piece was estimated visually and transferred to wash buffer in pre-rinsed microfuge tubes containing about 10-times the volume of the gel pieces. The gel pieces were agitated with at least

two changes of wash buffer until Coomassie blue dye had been completely cleared and supernatant discarded after final wash.

The gel pieces were taken through a sequence of procedures, i.e., reduction and alkylation. Reduction of gel pieces was conducted by agitating in 10-volumes of 10 mM dithiothreitol (DTT) in the dark for 20 – 30 min at room temperature and then, supernatant was discarded. For alkylation, gel pieces were agitated again in 10-volumes of 20 mM iodoacetamide in the dark for 20 – 30 min at room temperature and then, the supernatant was also discarded. Gel pieces were then washed twice by agitating in 10-volumes of wash buffer for 5 – 20 min. Final wash with agitation was conducted in 10-volumes of 100% acetonitrile for 5 - 20 min and supernatant discarded.

Excised regions of polyacrylamide gels (PAGs) containing a standard or no protein were prepared simultaneously from each experimental PAG.

Proteolysis and peptide extraction: Polyacrylamide gel pieces were air-dried to dehydrate and then 25 – 50 µl of trypsin working solution (20 ug trypsin in 20 µl resuspension buffer, see Appendix IV) was added to swell gels overnight (samples were agitated at this stage) at 37^{o}C. After overnight incubation, supernatants were recovered into pre-rinsed microfuge tubes and gels agitated twice with 3-volumes of extraction reagent (0.1%($^{v}/_{v}$) formic acid in 70%($^{v}/_{v}$) aqueous acetonitrile) for approximately 30 min, pooling all of the supernatants into labelled microfuge tubes for each sample. Peptide extracts were evaporated to 50 µl or less and stored at -70^{o}C prior to tandem mass spectrometry analysis.

Tandem mass spectrometry sample processing: Extracts were submitted to external source (University of Leicester) for mass spectrometry analysis.

5.2.6 Statistical analysis

For multiple comparison of NQO1 expression by the various phytochemicals, statistical analysis was performed with one-way ANOVA and posthoc using Dunnett's test, with statistical significance set at $P<0.05$. Where confidence intervals of data were within the same range, statistical analysis was not performed.

Statistical analysis of NQO1 expression by quercetin, under different cell culture conditions, was performed using paired Students' 2-tailed t-test.

5.3 Results

5.3.1 Effect of phytochemicals on NQO1 expression in HepG2 cells

Effect of 20 h treatment with DMSO (1%($^{v}/_{v}$)) and the various phytochemicals on NQO1 expression is shown in Figure 5.8A. The blot suggests that after prolonged exposure in HepG2 cells, none of the phytochemicals increased expression of NQO1. This correlated positively with marginal increase in protein expression observed after 20 h exposure to quercetin and curcumin, while caffeic acid and sulforaphane also demonstrated no significant effect (Fig 5.8B).

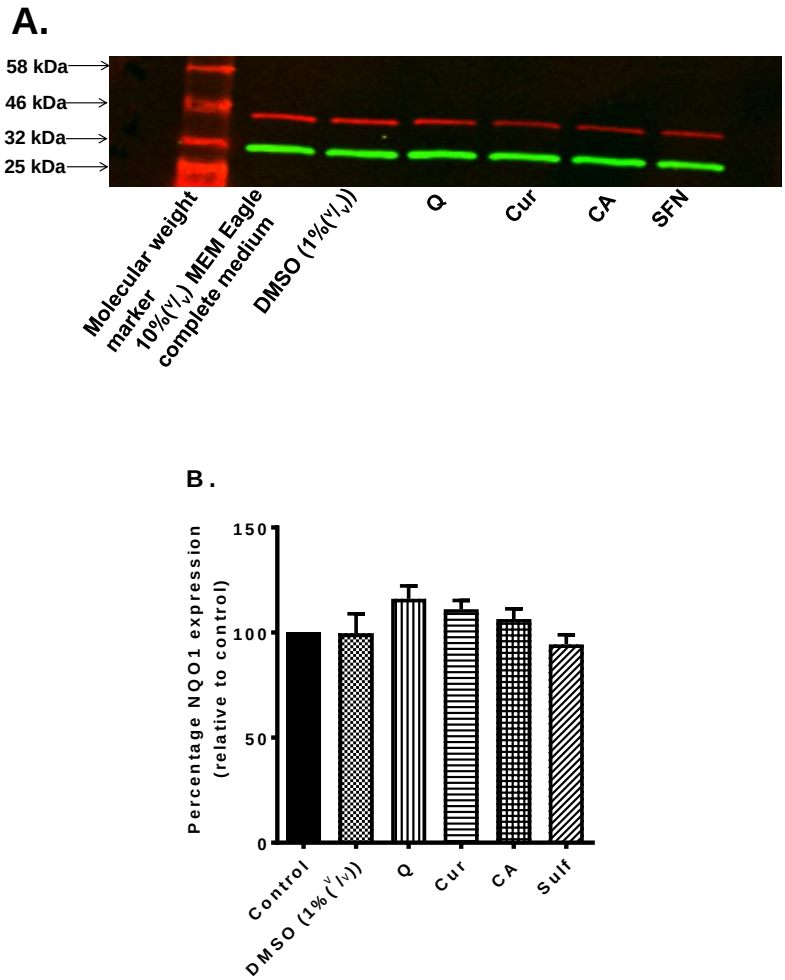

Figure 5.8 Effect of phytochemicals on NQO1 expression in cytosolic fractions HepG2 hepatoma cells. Cells seeded at 1.2 X 10^{6} cells/ml were lysed following 20 h treatment with 10%($^{v}/_{v}$) MEM Eagle complete medium, DMSO (1%($^{v}/_{v}$)), (Q) quercetin (0.10 mM), (Cur) curcumin (0.01 mM), (CA) caffeic acid (0.57 mM) and (SFN) sulforaphane (0.06 mM). Representative Western immunoblots (A) show expression of housekeeping protein GAPDH (43 kDa) in red and NQO1 (31 kDa) in green, while densitometric quantification of bands (B) were

determined by normalising GAPDH expression and presented as relative to percentage expression of untreated cells (10%($^{v}/_{v}$) MEM Eagle complete medium). Values are mean ± SEM for three independent experiments from cells of quadruplicate wells.

5.3.2 Optimising NQO1 expression in HepG2 cells

The following sets of data present the impact of serum on both basal and inductive expression of NQO1, as well as the effect of plastic components of culture plates on protein expression.

5.3.2.1 Basal expression of NQO1 in serum-containing and serum-free media

Basal expression of NQO1 of cells cultured in Costar plates was comparable to expression obtained with Falcon and Sarstedt plates, using MEM Eagle medium without serum as culture medium (Fig 5.9 and 5.11A). A similar observation was made when cells were cultured in MEM Eagle medium supplemented with 10%($^{v}/_{v}$) serum (10%($^{v}/_{v}$) MEM Eagle complete medium), where the type of culture plate used showed no significant effect on basal NQO1 expression (Fig 5.10 and 5.11B). Hence, the high basal expression of NQO1 levels observed in Fig 5.8 did not result from the use of serum or plastic material in the type of cell culture plate used.

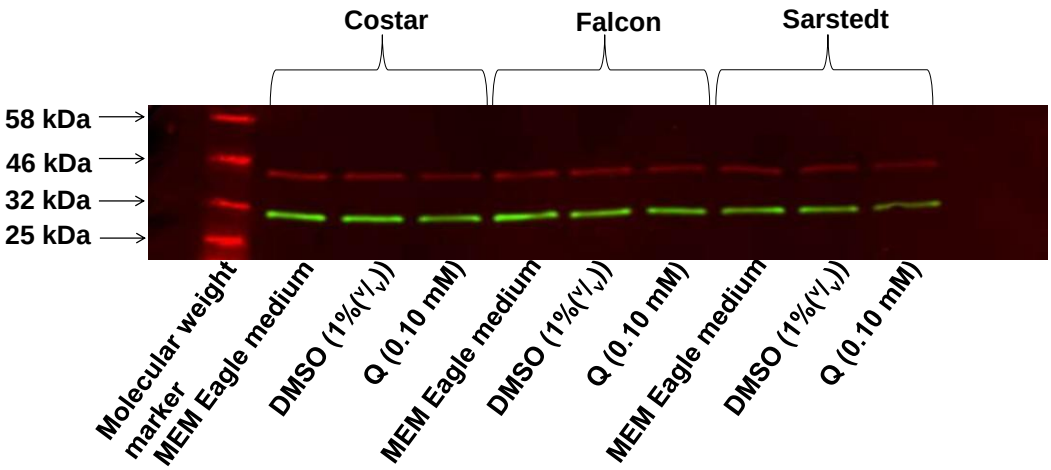

Figure 5.9 Representative western immunoblots of cytosolic fractions of HepG2 hepatoma cells in serum-free media. Cells were prepared for immunoblotting following 20 h treatment with 1%($^{v}/_{v}$) DMSO and quercetin in culture medium without serum. Blot represents scan from one experiment showing expression of housekeeping protein GAPDH (43 kDa) in red and NQO1 (31 kDa) in green.

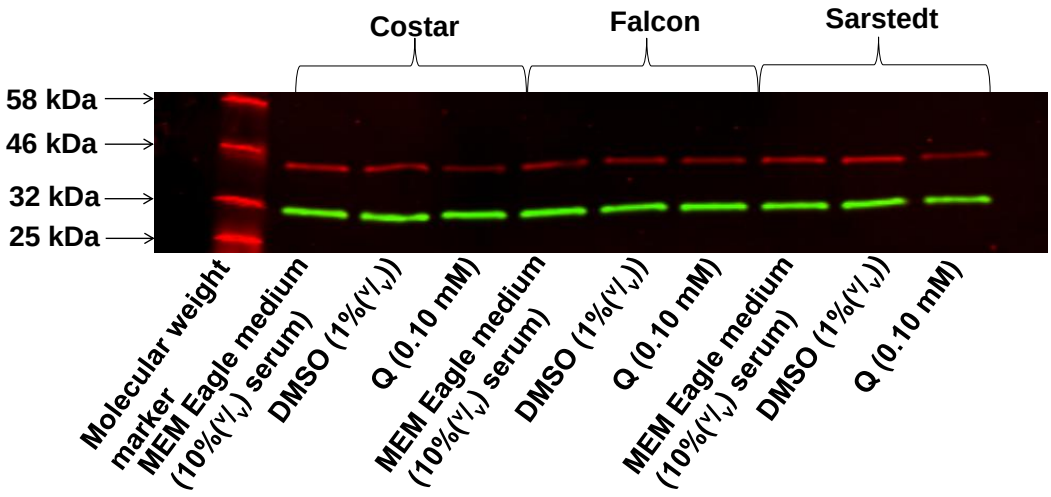

Figure 5.10 Representative western immunoblots of cytosolic fractions of HepG2 hepatoma cells in serum-containing media. Cells were prepared for immunoblotting following 20 h treatment with 1%($^{v}/_{v}$) DMSO and quercetin in culture medium with 10%($^{v}/_{v}$) serum. Blot represents scan from one experiment showing expression of housekeeping protein GAPDH (43kDa) in red and NQO1 (31kDa) in green.

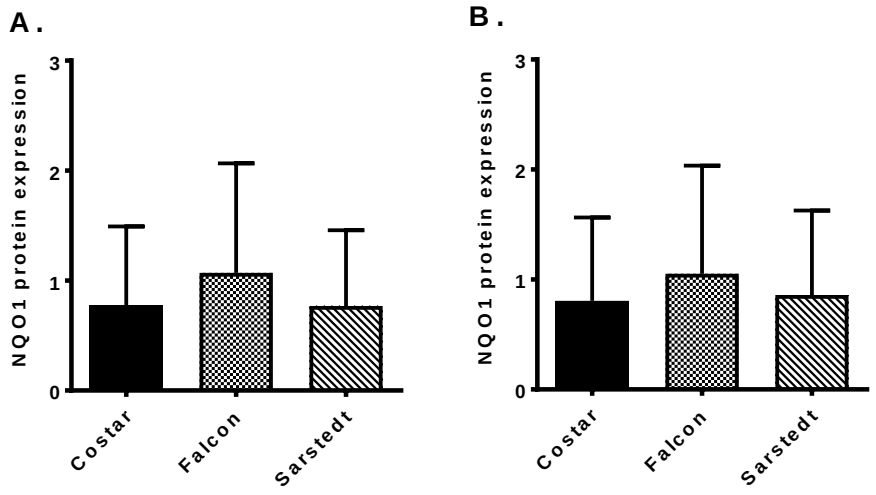

Figure 5.11 Densitometric quantification of western immunoblots obtained in cytosolic fractions of HepG2 cells. Cells seeded at 4.0 x 10^5 cells/ml were prepared for immunoblotting following 20 h culture in MEM Eagle medium without serum (A) or with 10%($^{v}/_{v}$) serum (B). Results obtained were normalised to GAPDH. Values are mean NQO1 expression ± SEM from cells obtained from quadruplicate wells of three independent experiments.

5.3.2.2 Effect of serum on inducible expression of NQO1 in HepG2 cells

The effect of cell culture conditions (serum and type of culture plate) on quercetin-induced NQO1 expression was evaluated in HepG2 cells at low-seeding density. In serum-free

medium (Fig 5.12A), there was no significant effect in NQO1 expression in cells cultured in Costar, Falcon and Sarstedt plates, following 20 h treatment with DMSO or quercetin.

Treatment with 1%($^{v}/_{v}$) DMSO in 10%($^{v}/_{v}$) MEM Eagle complete medium, produced marginal increase in protein expression in cells cultured with Costar plates, while significant increase to 204.1 ±18.05% was recorded in quercetin-treated cells ($P<0.05$, $n = 3$) (Fig 5.12B). Similar observation was made with cells cultured in Falcon plates, where DMSO caused marginal decline in protein expression but cells treated with quercetin showed an increase in NQO1 levels to 132 ±17.42% ($P<0.05$). However, there was no significant decrease in NQO1 expression when cells cultured in Sarstedt plates were subsequently treated with DMSO, as well as quercetin. Thus, inductive response of NQO1 was common to both Costar and Falcon plates, when cells were cultured in serum-containing medium.

Taken together, results obtained suggest that NQO1 induction was significantly increased in cells cultured in Costar plates than Falcon plates ($P<0.05$), following treatment with quercetin (0.1 mM) in 10%($^{v}/_{v}$) MEM Eagle complete medium. Hence, for subsequent studies on protein expression, cells were cultured under these conditions, i.e., cells were cultured in Costar plates and in 10%($^{v}/_{v}$) MEM Eagle complete medium.

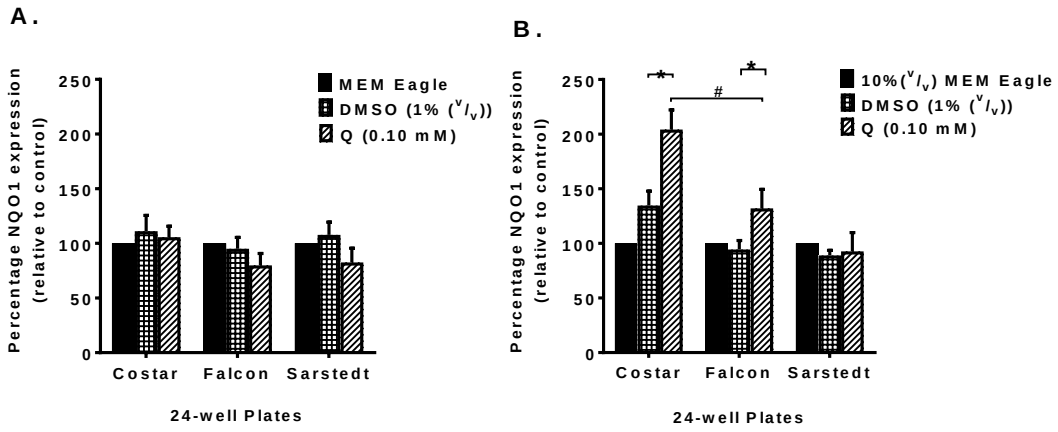

Figure 5.12 Densitometric quantification of western immunoblots obtained in cytosolic fractions of HepG2 hepatoma cells. Cells were prepared for immunoblotting following 20 h treatment with MEM Eagle complete medium without serum (A) or with 10%($^{v}/_{v}$) serum (B),1%($^{v}/_{v}$) DMSO and quercetin (0.1 mM). Results obtained were normalised to corresponding GAPDH expression and data normalised appropriate basal expression in Figs 5.9 and 5.10. Data were presented as relative to percentage expression of medium-treated cells. Values are mean ± SEM for three independent experiments from cells of quadruplicate wells. Statistical analysis was performed with Student's t-test. Where indicated, values were significantly different from corresponding DMSO controls at P<0.05 (*), and different from quercetin in Costar plates at P<0.05 (#).

5.3.3 Effect of phytochemicals on NQO1 expression in 1.1B4 β-cells

With evidence of indirect cytoprotective activities in 1.1B4 cells, selected phytochemicals were evaluated for their effect on NQO1 expression. The culture conditions used included the use of serum-containing media and Costar plates, since NQO1 expression was observed under these conditions. As presented in Fig 5.13A and B, basal expression of NQO1 was not detected h in 1.1B4 β-cells, and this was evident in cells treated with 1%($^{v}/_{v}$) DMSO for 20 h. Furthermore, there was no induction of NQO1 following treatment with cytoprotective concentrations of quercetin (0.02 – 0.33 mM), curcumin (0.02 mM and 0.07 mM) and caffeic acid (0.57 – 2.22 mM). Similar to previous observations, shown in Fig 5.8, basal expression of NQO1 was present in HepG2 cells, although treatment with higher concentrations of quercetin showed no significant increase (Fig 5.14). This suggests that NQO1 was not present or inducible in 1.1B4 human β-cells under the experimental conditions used.

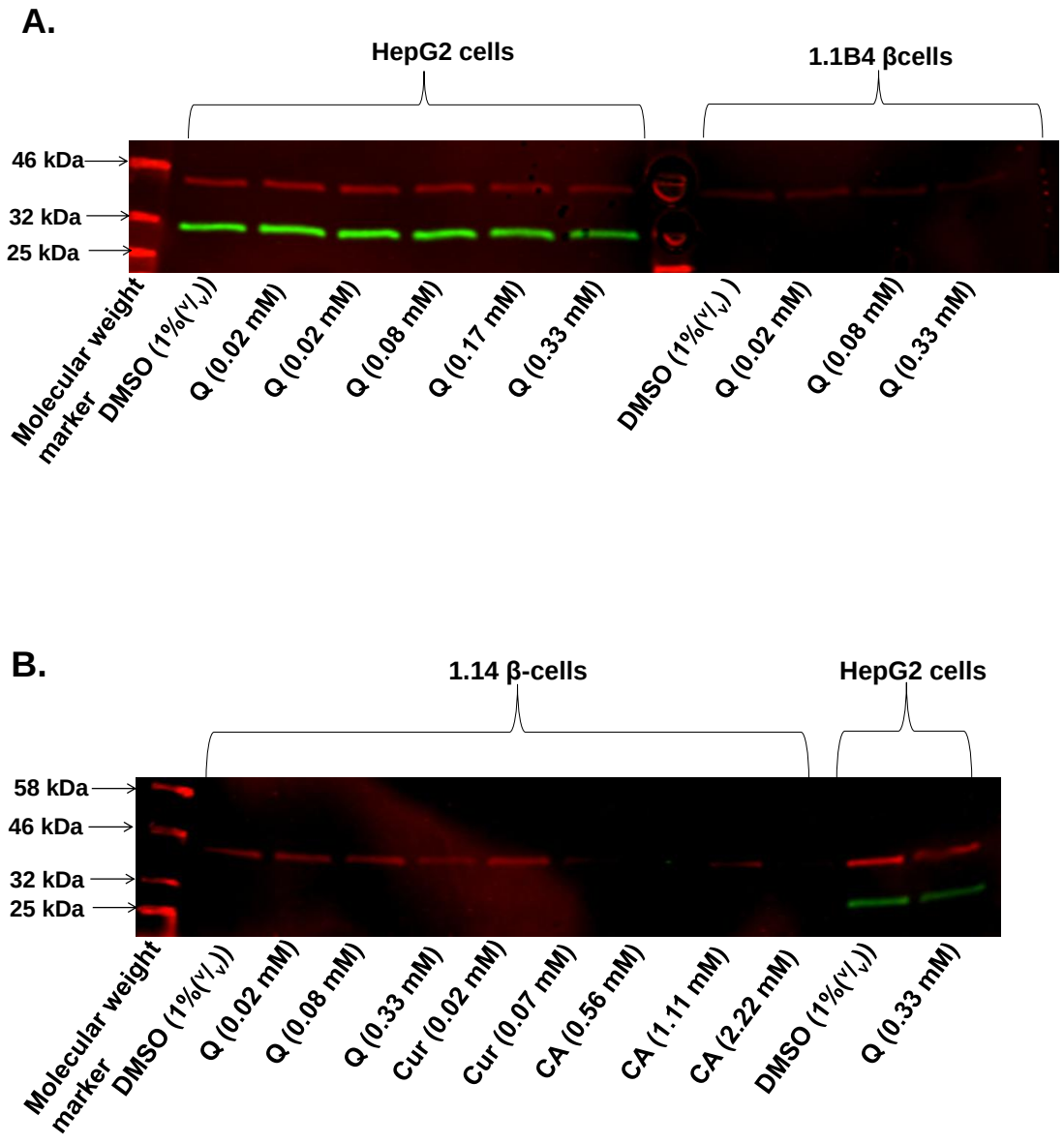

Figure 5.13 Representative western immunoblots of cell lysate preparations from 1.1B4 β-cells and cytosolic fractions of HepG2 hepatoma cells. Cells were prepared for immunoblotting following 20 h treatment with (A) 1%($^{v}/_{v}$) DMSO, and varying concentrations of quercetin in HepG2 cells and 1.1B4 β-cells. Also, NQO1 expression was evaluated in (B) 1.1B4 human β-cells treated with varying concentrations of quercetin, curcumin and caffeic acid and in HepG2 cells treated with DMSO (1%($^{v}/_{v}$) and quercetin (0.33 mM). Bands for HepG2 cells were obtained from the same sampleto serve as positive control, assessed alongside different samples for 1.1B4 β-cells. Blots represents scan from one experiment showing expression of housekeeping protein GAPDH (43 kDa) in red and desired protein NQO1 (31 kDa) in green.

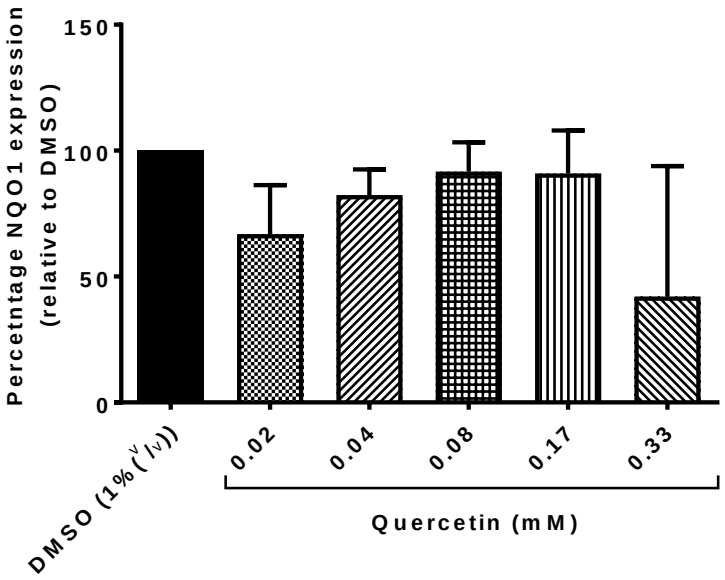

Figure 5.14 Densitometric quantification of western immunoblots obtained from cytosolic fractions of HepG2 cells, shown in Figure 5.13A. Results obtained were normalised to GAPDH. For HepG2 cells, data were obtained with the same sample. Due to the absence of NQO1 expression in 1.1B4 cells, no data was presented for these β-cells. Values are mean ± SEM for three independent experiments from cells of quadruplicate wells.

5.3.4 Global proteomic assessment of subcellular fractions of HepG2 cells treated with selected phytochemicals

Zhang et al., (2006), suggested that phytochemicals have multiple targets which could also account for their diverse pharmacological activities. Therefore, the effects of quercetin, curcumin and caffeic acid on expression of phospho-proteins in HepG2 cells were investigated, as shown in Fig 5.3.

5.3.4.1 Quantification of protein content in subcellular fractions

Following differential detergent fractionation, amount of proteins in the subcellular fractions was quantified using the BCA protocol. Observation of the protein quantities obtained from each fraction (presented in Fig 5.15) indicates a general trend of decreasing protein quantities from cytosolic to cytoskeletal fractions. This was expected since most cellular proteins are present in the cytosol.

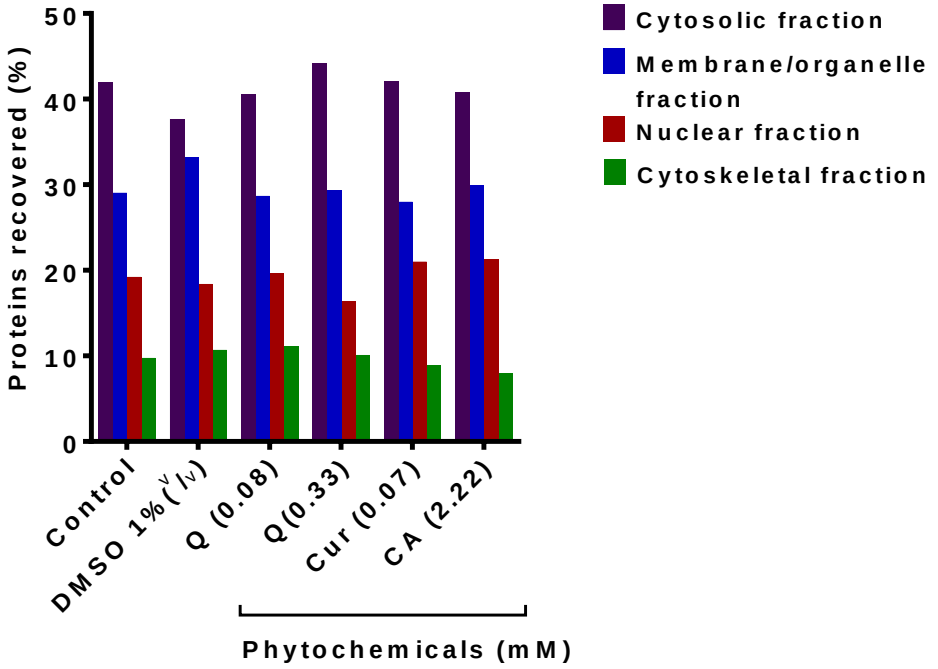

Figure 5.15 Distribution of proteins recovered in the various subcellular fractions of HepG2 hepatoma cells. Following 20 h treatment with control (10%($^{v}/_{v}$) MEM Eagle complete medium), DMSO (1%($^{v}/_{v}$)), quercetin (Q), curcumin (Cur) and caffeic acid (CA), proteins were quantified using the BCA protocol. Amount of protein obtained in mg/ml was normalised to total extracted protein for each sample as a percentage.

5.3.4.2 Phospho-blotting of subcellular fractions

After protein quantification, each of the fractions obtained was separated using SDS-PAGE electrophoresis (Fig 5.16A) and proteins on PVDF probed for expression of phospho-proteins (Fig 5.16B). As presented in Fig 5.16B, 20 h exposure to quercetin and caffeic acid resulted in increase in expression of phospho-proteins present in the cytosol, labelled (in red boxes) as II, III, IV and VI. Additionally, bands denoted as V and VII were identified as downregulated compared to untreated (10%($^{v}/_{v}$) MEM Eagle complete medium) and DMSO (1%$^{v}/_{v}$) controls. Expression of phospho-proteins at band corresponding to 110 kDa (I) was found to be present in all the samples hence, band A was marked as internal control. However, no difference in expression of nuclear, membrane/organelle or cytoskeletal fractions was observed (see Fig 5.17B). Due to lack of time, these samples were not submitted for tandem mass spectrometry, as the project drew to a close.

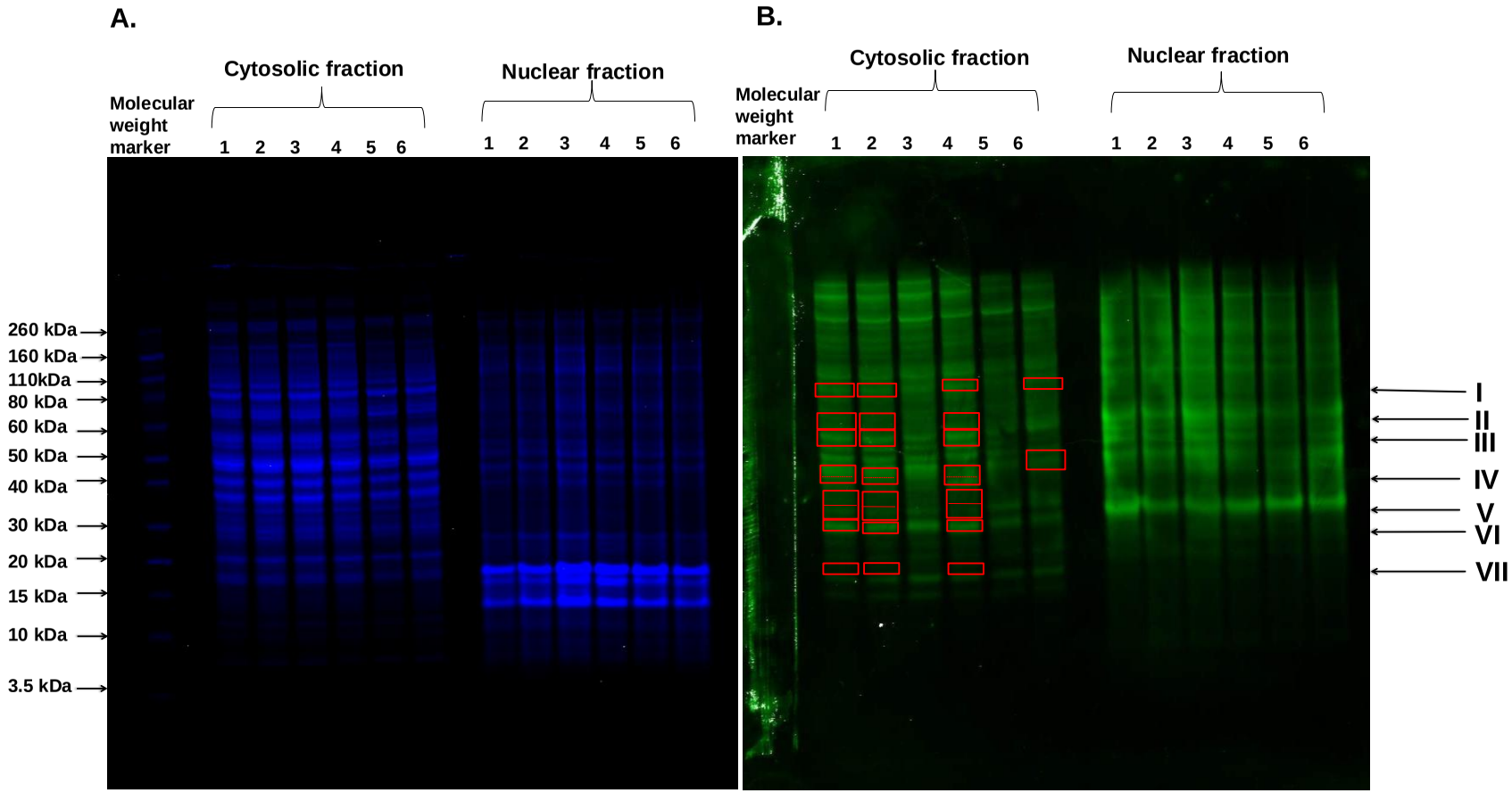

Figure 5.16 Representative comparative scans of cytosolic and nuclear fractions of HepG2 hepatoma cells from six different treatments. Figure shows SDS-PAGE analysis of with Coomassie blue G250-stained gel (A) and phospho-blot (B) following 20 h treatment with 10% ($^{v}/_{v}$) MEM Eagle complete medium (1), DMSO (1%($^{v}/_{v}$) (2), quercetin 0.04 mM (3), quercetin 0.33 mM (4), curcumin 0.07 mM (5) and caffeic acid 2.22 mM (6). Bands of interest of treated samples (4 and 6) on phospho-blot are enclosed in red squares, with corresponding bands of control samples (1 and 2).

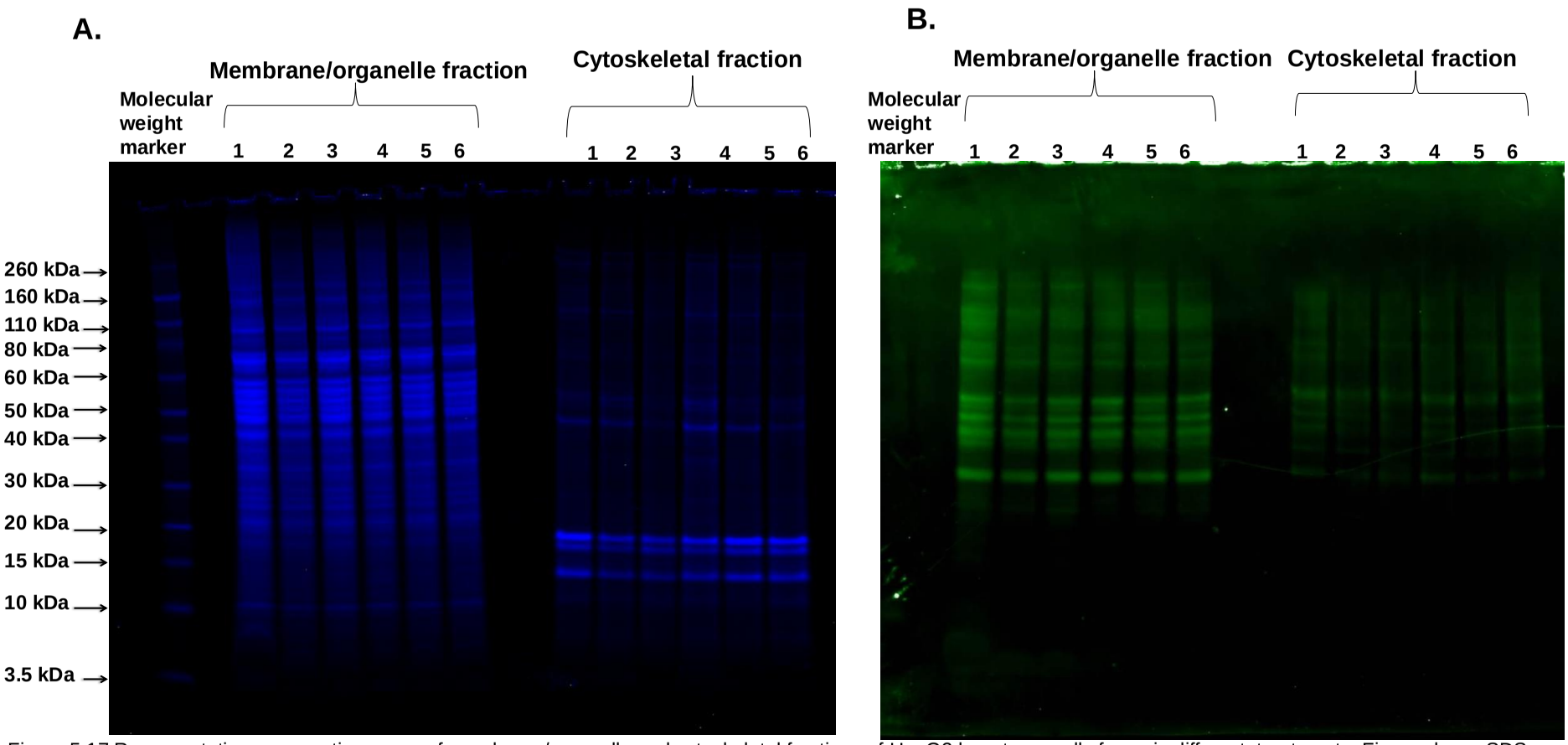

Figure 5.17 Representative comparative scans of membrane/organelle and cytoskeletal fractions of HepG2 hepatoma cells from six different treatments. Figure shows SDS-PAGE analysis of with Coomassie blue G250-stained gel (A) and phospho-blot (B) following 20 h treatment with 10% ($^{v}/_{v}$) MEM Eagle complete medium (1), DMSO (1% ($^{v}/_{v}$)) (2), quercetin 0.04 mM (3), quercetin 0.33 mM (4), curcumin 0.07 mM (5) and caffeic acid 2.22 mM (6).

5.3.4.2 Effect of phytochemicals on phospho-proteins in reversed-phase solid phase extracts

Following the observation of change in expression of cytosolic phospho-proteins (due to phytochemical treatment), multidimensional liquid chromatography was applied to the cytosolic fractions to reduce the complexity of these proteins (Step 2 in Fig 5.3) to approximately 6% (per residue) of each cytosolic fraction.

Observation of phospho-blots obtained from eluates of reversed-phase solid phase extraction, suggested that in eluate D (eluted with 43%($^{v}/_{v}$) acetonitrile, see Table 5.6) expression of three bands (labelled A, B and C) was enhanced by treatment with quercetin, curcumin and caffeic acid, relative to untreated (10%($^{v}/_{v}$) MEM Eagle complete medium) and DMSO (1%($^{v}/_{v}$)) controls (Figure 5.18).

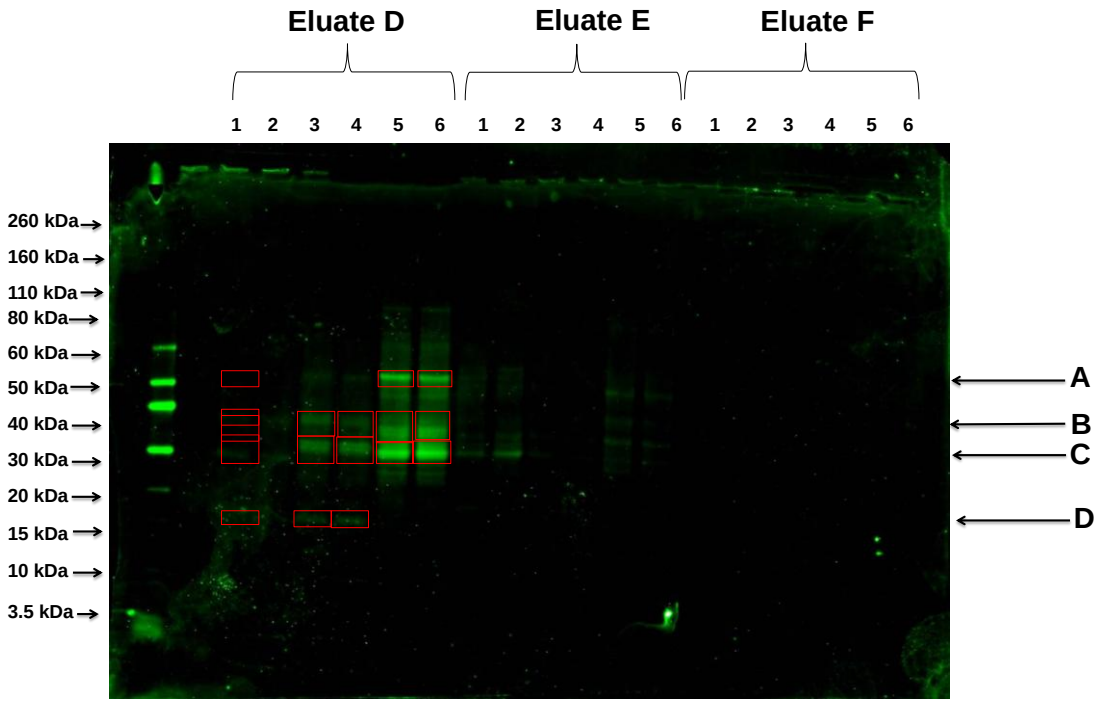

Figure 5.18 Representative comparative scan of cytosolic fractions (from reversed-phase extraction) of HepG2 hepatoma cells from six different treatments. Phospho-blots were obtained after SDS-PAGE analysis of reversed-phase solid phase extraction of cytosolic fractions of HepG2 cells, showing eluates D - F extracted with 43% - 48% acetonitrile. Figure shows cells treated with 10%($^{v}/_{v}$) MEM Eagle complete medium (1), 1%($^{v}/_{v}$) DMSO (2), quercetin 0.04 mM (3), quercetin 0.33 mM (4), curcumin 0.07 mM (5) and caffeic acid 2.22 mM (6). Bands of interest of treated samples (3 – 6) on phospho-blot are enclosed in red squares, with corresponding bands of control sample (1).

In addition, phosphoprotein expression, at band denoted as D, was intensified in cells treated with quercetin (0.04 mM and 0.33 mM) compared to controls. Hence these bands of interest, which are highlighted here by red boxes, were excised for tandem mass spectrometry. However, at the time of thesis submission, no meaningful data had been obtained.

5.4 Discussion

In the current study, EC_{50} values obtained for curcumin, caffeic acid and sulforaphane (from indirect cytoprotection data – Chapter 2) did not induce NQO1 expression in HepG2 hepatoma cells. However, at low cell-seeding density, quercetin (0.10 mM) produced an increase in NQO1 protein expression in HepG2 cells. The 1.1B4 β-cells lacked basal and inductive expression of NQO1 after 20 h treatment.

5.4.1 High basal expression of NQO1 in HepG2 cells

Following 20 h incubation, high basal expression of NQO1 was observed in HepG2 cells, irrespective of cell seeding density, and this could have influenced the lack of inductive expression by the various phytochemicals. The proposal that exogenous inducers activate cytoprotective enzymes has been based on rapid response of these enzymes to inducers, such as phytochemicals (Dinkova-Kostova and Talalay, 2010). The high basal expression of this cytoprotective enzyme in HepG2 cells suggests that these cells were well protected against quinone toxicity and oxidative damage. Thus, HepG2 cells (Section 2.3.2.1) were found to be less sensitive to *t*BHP-induced oxidative damage than the 1.1B4 cells (Section 2.3.3.1).

It may be expected that HepG2 cells, which were derived from the liver will possess good basal expression of antioxidant enzymes such as NQO1, due to their role in xenobiotic metabolism. One possible reason for lack of response to phytochemicals (inducers) could be overexpression of Nrf2 in HepG2 cells, which has been reported alongside GSTP1 in hepatocellular carcinoma (Ikeda et al., 2004). This agrees with the cellular model used which was derived from a similar origin. It is becoming more apparent that NQO1 and other Nrf2/ARE-targeted antioxidant proteins could be essential in cancer progression and have been linked to constitutive activation of Nrf2, as a result of mutation, referred to as the 'dark side of Nrf2' (Wang et al., 2008). Wang et al., (2008) made this observation due to its presence in cisplatin-, doxorubicin- and etoposide-resistant cancer cells. Thus, following transcriptional activation, Nrf2 protects all cells irrespective of their genetic makeup (Lau et al., 2008). Furthermore, increased expression of NQO1 is associated

with increase in expression of HO-1, GST and other cytoprotective enzymes, hence contributing towards enhanced protection in cancer cells, in favour of tumorigenesis and to some extent chemoresistance (Nioi and Hayes, 2004).

5.4.2 Lack of NQO1 induction in HepG2 cells by phytochemicals

The lack of NQO1 induction after 20 h exposure to curcumin, caffeic acid and sulforaphane was unexpected, since these phytochemicals are known inducers of the Keap1/Nrf2 complex, based on their interaction with Keap1 sensors (Dinkova-Kostova and Talalay, 1999; Dinkova-Kostova and Talalay, 2008). Nevertheless, compared to rat hepatoma cells, NQO1 was poorly induced by sulforaphane in human liver cells (Hanlon et al., 2009), and this report could be supported by results obtained in the current study.

At low cell-seeding density, NQO1 expression was upregulated following treatment with quercetin in serum-containing medium (only) in HepG2 cells, using Costar and Falcon 24-well plates ($P<0.05$, $n = 3$); not Sarstedt 24-well plates (Fig 5.12B). These results agree with those of a previous study in which, induction of NQO1 expression by increasing quercetin concentrations, was observed under similar experimental conditions (Abu Bakar et al., 2013). Results obtained here suggest that induction of NQO1 expression may be dependent on cell density, upregulation of NQO1 was observed in sparsely cultured (Fig 5.12B) but not in confluent cells (Figures 5.8).

This observation was also made during bioactivation of 2,5-bis[1-aziridinyl]-1,4 benzoquinone (DZQ) in HepG2 cells (Cordoba-Pedregosa et al., 2006). Perhaps, the presence of serum, which mimics albumin exposure from interstitial fluid (Smith and Staples, 1982) presented ambient culture conditions for optimal metabolic activities by HepG2 liver cells. These results confirm the hypothesis that long-term exposure to quercetin exhibits cytoprotective effects via upregulating cytoprotective enzymes, NQO1 in this case.

5.4.3 Lack of NQO1 expression in 1.1B4 β-cells

The absence of NQO1 basal expression in 1.1B4 human β-cells suggests for the first time that, NQO1 is not present in these β-cells. In spite of the controversial role of Nrf2 in β-cell function (Pi et al., 2010), lack of antioxidant enzymes such as NQO1 in these cells could present increased risk to oxidative damage, as seen previously following treatment with *t*BHP (Section 2.3.3.1). Furthermore, none of the cytoprotective phytochemicals used was able to induce upregulation of NQO1 after 20 h exposure. Induction of NQO1 was recently reported in rat RINm5F β-cells, against fructose and nitric oxide stress (Yagishita et al., 2014) while, elevated NQO1 levels have been reported in human primary pancreatic adenocarcinoma cells (Lewis et al., 2005). However in 1.1B4 human β-cells, presence of superoxide dismutase, catalase and glutathione peroxidase was reported by Vasu et al., (2013) not NQO1.

Due to challenges associated with reproducibility of Western blot data, a global proteomic approach was adapted to assess effect of cytoprotective compounds on cellular proteomes, in HepG2 hepatoma cells.

5.4.4 Global proteomic assessment following phytochemical treatment in HepG2 cells

Phosphorylation of proteins forms a key part of post-translational changes that influence cellular functions, including cell proliferation, signal transduction and apoptosis (Hunter, 2000). Following 20 h treatment with quercetin (0.04 mM and 0.33 mM), curcumin (0.07 mM) and caffeic acid (2.22 mM), cytosolic fractions showed increased and decreased expression of phospho-proteins (Fig 5.16). Consequently, complex cytosolic components were separated using IMAC and RP-SPE facilitated partial fractionation, an established method of proteomic assessment of human samples (Tooth et al., 2012).

Regarding the samples submitted to the University of Leicester (Fig 5.18), no meaningful data had been received at the time of thesis submission. However, observation of upregulation or downregulation of some phospho-proteins by phytochemicals could suggest that prolonged exposure to these phytochemicals enables their involvement in

protein activities in HepG2 cells. It is predicted that some of these bands could correspond to kinases or transcription factors involved in phosphorylation, or perhaps, stress response. Given more time, corresponding antibodies of the proteins could be purchased and investigated further for their expression (using Western blotting) or activities (using enzyme activity assays).

5.5 Conclusion

In spite of its high basal expression in HepG2 cells, NQO1 was upregulated by prolonged (20 h) treatment with quercetin. The current study has also highlighted the need for optimal culture conditions for investigating the effect of phytochemicals on expression of NQO1. However, 1.1B4 cells lacked both basal and inductive expression of NQO1 under the experimental conditions used.

CHAPTER 6

General discussion

CHAPTER 6 - General discussion

This chapter provides a brief introduction and summary of research findings obtained, highlighting the similarities or differences between the two cellular models. A mechanism for cytoprotective activities is proposed and key observations are discussed in the context of the results obtained, in addition to future studies.

The well-known 'antioxidant hypothesis' has caused a rapid surge in antioxidant products worldwide, with evidence that increased intake of fruits and vegetables reduces risks of diseases such as cancers and cardiovascular diseases (Spencer and Crozier, 2012). This hypothesis results from the understanding that reactive free radicals, mainly ROS, play a causative role in the pathogenesis of such disease conditions. The imbalance between cellular defence and ROS, forms the basis of the oxidative stress theory of disease. In the case of T2DM, chronic exposure to high glucose and lipid levels leads to glucolipotoxicity (Robertson and Harmon, 2007) while, elevated FFA levels lead to hepatic lipid accumulation and ultimately lipoapotosis in NASH, via a mechanism in part dependent on oxidative stress (Malhi and Gores, 2008). Thus, the evidence that phytochemicals possess antioxidant activities has shifted therapeutic focus to antioxidants of plant origin.

The present study was intended to evaluate selected phytochemicals - quercetin, curcumin, sulforaphane, rosmarinic acid and its principal metabolites - for radical scavenging activities against the $DPPH^{\cdot}$ free radical in a non-cellular assay. Subsequently, cytoprotective activities of the chosen phytochemicals were evaluated against two types of oxidant stressors – *t*BHP, a well-characterised experimental stressor, and sodium palmitate, which represented a more physiologically relevant stressor. Whilst effects of the chosen phytochemicals against sodium palmitate are novel findings, no further studies were conducted at high glucose exposure since no reproducible glucotoxic effect was observed using the various cytotoxicity assays. Cellular experiments were conducted with two main aims: (i) to investigate direct cytoprotection against oxidative damage and (ii) to investigate indirect cytoprotection elicited by potentially upregulating cytoprotective enzymes against subsequent oxidative damage.

6.1 Summary of results

Detailed discussion, in relation to existing literature, can be found in Chapters 2 – 5.

The present investigations commenced with evaluating reference phytochemicals (quercetin, curcumin and sulforaphane), rosmarinic acid and its principal metabolites for which there is evidence antioxidant potential. As reported in Chapter 2, radical scavenging activities against free radical $DPPH^{\cdot}$ revealed quercetin as comparable to rosmarinic acid, caffeic acid and danshensu, while being more potent than curcumin and ferulic acid. Sulforaphane and *m*-coumaric acid were not effective. When evaluated in HepG2 hepatoma cells, direct cytoprotection was observed as quercetin > rosmarinic acid = caffeic acid > curcumin, in decreasing rank order of cytoprotective potencies (elicited against 0.5 mM *t*BHP). However, curcumin demonstrated the most potent indirect cytoprotective activity relative to quercetin > rosmarinic acid = caffeic acid, in decreasing rank order. Indirect cytoprotective activity of sulforaphane led to approxiamately 50% cytoprotection at 0.07 mM sulforaphane.

It was rather unexpected that danshensu and ferulic acid did not emulate radical scavenging activities (previously observed in non-cellular assay) against *t*BHP in HepG2 cells, with rosmarinic acid and caffeic acid being less effective than quercetin. Hence, it was proposed that poor lipophilicity profiles of rosmarinic acid and its principal metabolites accounted for discrepancy between DPPH-scavenging and direct cytoprotective activities. Furthermore, co-treatment of HepG2 cells with quercetin and curcumin (used together at EC_{10} values) produced marked direct cytoprotective activities against *t*BHP, which was not exhibited by each of the phytochemicals (used separately) or together in pre-exposure conditions.

Subsequently, these findings led to assessment of cytoprotective activities of phytochemicals in human pancreatic 1.1B4 β-cells; which were found to be more vulnerable to *t*BHP-induced cytotoxicity than HepG2 cells, due to their low antioxidant capacity. However, direct and indirect cytoprotective activities by quercetin, against 0.5 mM *t*BHP, were comparable to HepG2 cells, being more potent than curcumin > caffeic acid. Both curcumin and caffeic acid exhibited direct cytoprotection against cytotoxicity

induced by 0.5 mM and 0.125 mM *t*BHP but showed indirect cytoprotection against 0.125 mM *t*BHP only. However, cytoprotective activities of curcumin and caffeic acid overlapped with their cytotoxic activities in 1.1B4 β-cells. Sulforaphane was not protective aginst 0.5 mM *t*BHP in 1.1B4 cells.

This study was then extended (Chapter 3) to evaluate the effect of cytoprotective compounds (quercetin, curcumin, sulforaphane and caffeic acid) and cytotoxic phytochemicals (curcumin and sulforaphane) on viability of HepG2 cells, within the context of 20 h pre-exposure conditions. Also, 'pro-proliferative effects' of quercetin, curcumin and caffeic acid in 1.1B4 cells were investigated using the neutral red assay as a measure of cell viability. It emerged that indirect cytoprotective activities in both cell types were independent of 'pro-proliferative effects'. Hence, it was proposed that pre-exposure experiments enabled phytochemicals to augment expression of cellular antioxidant enzymes against subsequent oxidative challenge, rather than by increasing cell number. Cytotoxic effects of curcumin and sulforaphane were also recorded after 2 h treatment in both cell types, caffeic acid in 1.1B4 cells. Moreover, FACS analysis of cells treated with curcumin, sulforaphane and caffeic acid showed cells were predominantly necrotic rather than apoptotic.

Extensive studies were performed to establish a cellular model of glucolipotoxicity and the results were presented in Chapter 4. In spite of several attempts to investigate cytotoxic effects of high glucose, using varying conditions such as: glucose concentrations, exposure times and media conditions, none of the cytotoxicity assays used - neutral red, MTT and apoptosis assays - were able to establish a reproducible method for measuring glucotoxicity in HepG2 hepatoma cells and human pancreatic 1.1B4 β-cells. However, concentration-dependent toxicity was recorded in both HepG2 and 1.1B4 β-cells after exposure to sodium palmitate for 5 h and 20 h, using the neutral red viability assay, with an estimated mean TC_{50} value of 0.3 mM after 20 h exposure. Furthermore, co-exposure to 1.6 mM sodium palmitate and quercetin led to a concentration-dependent protection in HepG2 cells, but not in 1.1B4 β-cells. In the 1.1B4

cells, curcumin and caffeic acid were also not effective against sodium palmitate but exacerbated lipotoxicity at high concentrations, while causing cytotoxicity in the absence of sodium palmitate. Nevertheless, lipotoxicity was not enhanced after co-exposure to caffeic acid in HepG2 cells, but was observed after co-exposure with curcumin; both phytochemicals lacked diret cytoprotective activities under the experimental conditions used. Following pre-treatment with quercetin, curcumin and caffeic acid, cytotoxic effect of sodium palmitate was exacerbated, with no evidence of indirect cytoprotection in both HepG2 and 1.1B4 β-cells.

Having presented an overview of the principal research findings, a number of more general topics can be discussed.

6.2 Proposed mechanisms of cytoprotection against *t*BHP-induced oxidative damage

Cytoprotection against *t*BHP was exhibited in two distinct ways, i.e. different exposure conditions, implying that fairly diverse activities may have resulted in direct and indirect cytoprotection. Here, in this section, two mechanisms are proposed in this respect.

6.2.1 Direct cytoprotection

As mentioned in Section 2.4.2, oxidative damage caused by *t*BHP is mainly through an increase in cellular ROS levels, via the Fenton reaction. Therefore, 5 h co-exposure experiments facilitated direct interaction between polyphenols (quercetin, curcumin, rosmarinic acid and caffeic acid) and cellular ROS. In both HepG2 and 1.1B4 cells, a similar order of direct cytoprotective activities was observed. Hence it can be inferred that, phytochemicals were not metabolised to inactive or less active compounds, although HepG2 cells are of hepatic origin and are therefore well-equipped with drug metabolising enzymes (Knasmüller et al., 2004). Therefore, it is proposed that direct cytoprotection resulted from radical scavenging of ROS and metal chelation (by catechol and hydroxyl groups of each phytochemical), as illustrated in Fig 6.1 with quercetin as an example.

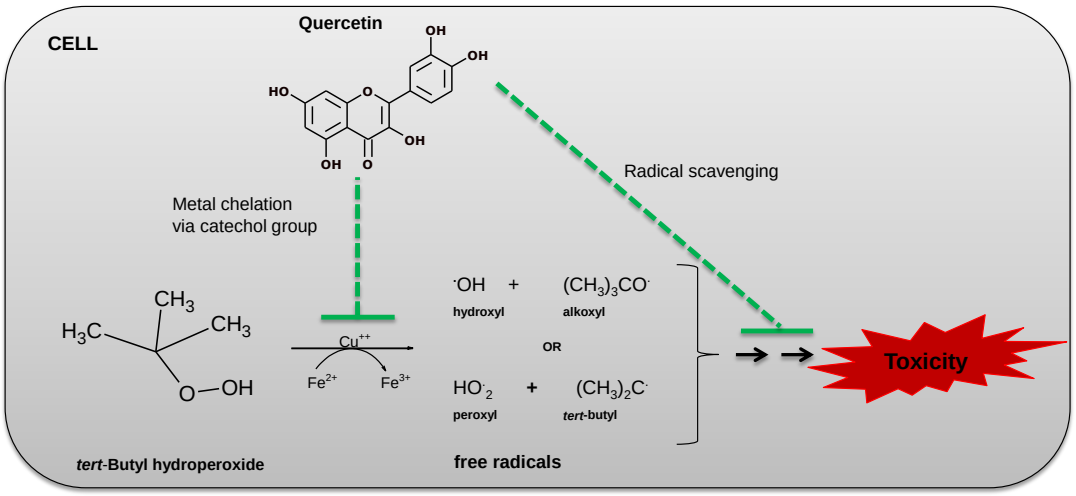

Figure 6.1 Proposed mechanism of direct cytoprotection against *t*BHP-induced oxidative damage in 5 h co-exposure experiment. This scheme shows quercetin as model polyphenolic compound, exerting metal chelating and radical scavenging activities, to prevent cytotoxicity, as reviewed by Vargas and Burd, (2010).

6.2.2 Indirect cytoprotection

Finally in Chapter 5, the ability of phytochemicals to up-regulate NQO1 was investigated in both HepG2 cells and 1.1B4 β-cells. The 1.1B4 cells lacked both basal and inductive expression of NQO1. Although basal expression was essentially high in HepG2 cells, quercetin upregulated NQO1 expression after 20 h treatment. This could have contributed towards indirect cytoprotective activity of quercetin, as illustrated in Fig 6.2.

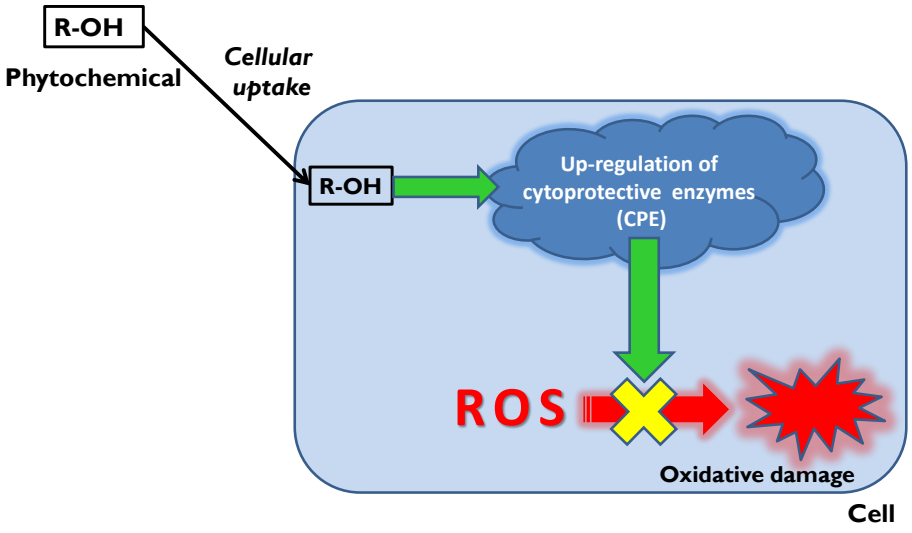

Figure 6.2 Proposed mechanism of indirect cytoprotection against *t*BHP-induced oxidative damage in 20 h pre-exposure experiment.

These observations were in accordance with the proposal that phytochemicals can induce adaptive stress response against oxidative damage potentially by cross tolerance (induced by increased tolerance to one form of stress following initial pre-conditioning by another form of stress) (Kultz, 2005).

6.2.2.1 Proposed mechanism for induction of NQO1 by quercetin

Pro-oxidant activities, reported after long-term exposure to concentrations above 100 µM quercetin (Vargas and Burd, 2010), have been linked to autoxidation or oxidation by superoxide anion to quercetin-semiquinone and hydrogen peroxide (MacGregor and Jurd, 1978; Metodiewa et al., 1999), due to redox liability of the catechol group (Fig 6.3). However, quercetin can be regenerated by radical scavenging activities of GSH to produce high levels of GSSG (Metodiewa et al., 1999). Semiquinone and quinone forms of the flavonoid lead to upregulation of NQO1, which was responsible for the two-electron reduction of semiquinones to quinones (O'Brien, 1991), Fig 6.3. The exact mechanism of NQO1 induction remains to be defined, however, it is probably mediated by stress signalling, by increased levels of toxic semiquinone and quinone species or ROS.

Furthermore, quinones are electrophilic species which engage in Michael addition reactions with cysteine rich Keap1 sensors, leading to induction of the Nrf2/ARE-regulated cytoprotective enzymes (Baird and Dinkova-Kostova, 2011). Moreover, it has been suggested that increased formation of GSSG, at the expense of cellular GSH levels (illustrated in Fig 6.3), is a more favoured factor for upregulation of NQO1 by flavonoids (Lee-Hilz et al., 2006). Thus, pre-exposure to pro-oxidant concentrations of quercetin could have led to adaptive stress response against *t*BHP-induced damage. This observation is a significant boost to the antioxidant properties of quercetin, as it confirms that modulation of the expression of cytoprotective enzymes, by quercetin, produces cytoprotection against oxidative stress.

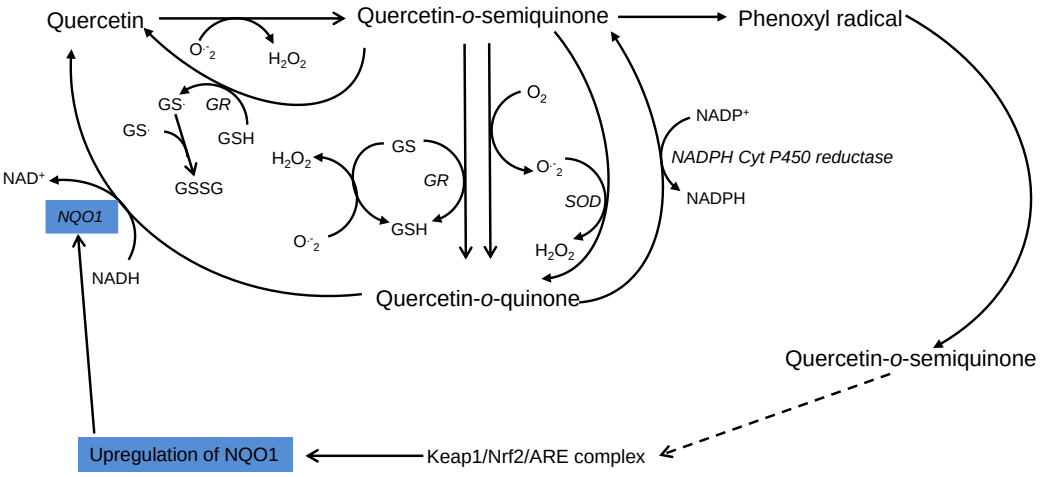

Figure 6.3 Oxidation of quercetin by superoxide anion to generate intermediate reactive species. This step-wise process could account for induction of NQO1 and then indirect cytoprotective activities. The potential regeneration of quercetin by NQO1 could result in continuous resupply of quercetin in situ with simultaneous changes of the level of cellular NADH (Metodiewa et al., 1999).

6.3 Importance of cellular access to phytochemicals

Cellular access to pharmacological agents is vital for the observance of pharmacological acitivities. In this project, it is proposed that poor cellular uptake of rosmarinic acid and its principal metabolites could be a limiting factor to their cytoprotective activities. Whilst the poor lipophilicity profiles of rosmarinic acid and its principal metabolites have been discussed in the context of their hepatoprotective activities against *t*BHP (Chapter 2), decreased cytoprotective activity was also observed with caffeic acid in subsequent studies (cytoprotection in 1.1B4 β-cells). Thus, poor cellular uptake could have markedly limited the pharmacological activities of rosmarinic acid and its principal metabolites, which were comparable to quercetin in the $DPPH^{\cdot}$ scavenging assay.

The importance of cell permeability in drug discovery can be inferred from research interest in the development of advanced drug formulations, such as the use of nanotechnology and liposomes, to enhance cellular access to drugs (Aggarwal et al., 2003). Poor lipid solubility of organic acids can hinder their pharmacological activities, as can be inferred from rosmarinic acid and its principal metabolites. Moreover, lipophilicity profiles of phenolic antioxidants is reported to influence their cytoprotective activities (Kaneko et al., 1994). Therefore, the use of such technologies could enhance the

pharmacological benefits of promising phytochemicals such as rosmarinic acid and its principal metabolites.

Additionally, structural modification of rosmarinic acid and its principal metabolites could promote their progress in the drug discovery process. Considering that their strong radical scavenging activities are mediated by polyhydroxyl groups, the carboxylic acid functional group on their chemical structures could be modified to improve their lipophilicity profiles, and ultimately cellular uptake.

As an aside, the high lipid solubility of *t*BHP (compared to hydrogen peroxide) formed the basis for its use as an oxidant stressor in cytoprotection experiments. Thus, *t*BHP generates ROS within the cell, to induce oxidative stress. However, it is not conclusively certain if, perhaps, this organic hydroperoxide may be generating ROS outside the cell, which then impact on the cell membrane to cause cell damage. If that were the case, then cytoprotection experiments were conducted in an aqueous environment so one would expect that phytochemicals with $DPPH^{\cdot}$ radical scavenging activity would be equally active against *t*BHP (co-exposure conditions). Thus, rosmarinic acid and its principal metabolites could elicit direct cytoprotective activities by averting extracellular ROS-mediated cell damage. In the same way, quercetin would be expected to act against both extracellular and intracellular ROS. Now quercetin was as potent as rosmarinic acid and its metabolites, against $DPPH^{\cdot}$ radicals so, if this idea of extracellular ROS generation was true, then these organic acids (rosmarinic acid and its principal metabolites) would be expected to exhibit similar direct cytoprotective activity as quercetin. But this was not the case since quercetin was most potent in co-exposure conditions.

Furthermore, the presence of serum in culture media (during co-exposure conditions) could not have contributed to poor cellular access to the organic acids since quercetin, positive control, is known to extensively bind to plasma proteins (Boulton et al., 1998). Thus, poor cellular uptake and decreased direct cytoprotective activities of rosmarinic acid and its principal metabolites could be largely influenced by their poor lipophilicity profiles.

6.4 Additive cytotoxic effects of phytochemicals and palmitate

Overall, pre-treatment with selected phytochemicals (quercetin, curcumin and caffeic acid) exacerbated palmitate toxicity in both HepG2 cells and 1.1B4 cells, although direct cytoprotection was observed after co-exposure of HepG2 cells with quercetin and sodium palmitate. This additive cytotoxic effect was particularly exhibited under conditions where phytochemicals demonstrated cytotoxicity on their own (this was more pronounced in 20 h conditions), and suggests that at least two different pathways were triggered to produce this additive effect. The exact mechanisms involved are currently not known, however a similar effect has been reported with the well-characterised polyphenol resveratrol (Rojas et al., 2014). In the absence of additional experimental data, a few reasons are proposed for further investigation.

One possible reason is the compounding effect of increased ROS in the presence of elevated cellular palmitate levels. It is reported that quercetin (Bishayee et al., 2013), curcumin (Syng-ai et al., 2004) and caffeic acid (Jaganathan, 2012) can induce high ROS generation on their own, which can exercebate peroxidation of lipid molecules present (including palmitate) and damage other cellular macromolecules. ROS could also facilitate ER stress to exercebate lipotoxicity.

The second reason, partly related to ROS generation by selected phytochemicals, is that mitochondrial damage could result from ROS-induced damage to mitochondrial DNA, leading to impaired β-oxidation of palmitate, promoting palmitate-induced ER stress as well as ceramide formation, and lysosomal damage, leading to additive cytotoxic effects. This proposal is supported by the apoptotic effect of curcumin due to altered mitochondrial membrane potential and calcium imbalance (Wang et al., 2011). Likewise, quercetin altered the expression of pro-apoptotic and anti-apoptotic proteins, causing mitochondrial damage and apoptosis (Granado-Serrano et al., 2006). Apoptosis by caffeic acid also occurred concomitantly with decreased mitochondrial membrane potential and production of high ROS levels (Jaganathan, 2012).

In the case of curcumin, lysosomal permeabilization following pre-treatment could have compromised structural and functional integrity of cells; curcumin induced release of lysosomal protease, Cathespin B, into the cytosol, triggered by high curcumin-mediated ROS levels (Chen et al., 2012). A link between lysosomal permeabilization and mitochondrial permeabilization has previously been established following the cytosolic presence of Cathespin B, leading to activation of caspases (Guicciardi et al., 2004).

The final explanation is that phytochemicals could have induced ER stress prior to treatment with sodium palmitate. Induction of the ER stress-apoptosis pathways by quercetin and curcumin (Kim et al., 2015) has recently been reported. Furthermore, quercetin potentiated the cytotoxic effect of cisplatin by inducing ER stress (Yang et al., 2015).

At this stage, a call for the most likely explanation to the additive effect observed is a difficult one, since further studies are clearly required to arrive at a potential mechanism. However, the most predominant reason could be that high ROS levels by selected phytochemicals accentuated ER stress, induced by sodium palmitate. Nevertheless, induction of ER stress could also be mediated by increased ROS levels, in pre-exposure conditions, and may well be the key trigger for additive effect observed.

6.5 Mis-match between *t*BHP and palmitate as cellular stressors in cytoprotection experiments

Having shown that quercetin, curcumin and caffeic acid exhibited indirect cytoprotection against *t*BHP, it was presumed that phytochemicals would demonstrate a similar response against sodium palmitate, due to the proposed causative role of oxidative stress in lipotoxicity. Therefore, the contrasting results obtained, i.e., additive cytotoxicity following treatment with selected phytochemicals and sodium palmitate was surprising and requires further studies on the mechanisms involved. Perhaps, these results highlight the differences in mechanisms of cytotoxicity elicited by *t*BHP and sodium palmitate.

It is proposed that the mitochondria is the target organelle for mediating *t*BHP-induced oxidative stress, leading to apoptotic cell death (Haidara et al., 2002; Prasad et al., 2007). *t*BHP-induced cytotoxicity could result from GSH depletion, and ROS-mediated damage to macromolecules and lipid peroxidation (Alia et al., 2005). Change in mitochondrial membrane potential and subsequent activation of pro-apoptotic proteins Bax and Bad, and caspases have also resulted from *t*BHP exposure (Haidara et al., 2002; Piret et al., 2004; Haidara et al., 2008).

The mechanism for palmitate metabolism, however, suggests a challenge in the use of antioxidants as cytoprotective compounds against lipotoxicity. Lipotoxicity can be mediated via damage to lysosomes, mitochondria and endoplasmic reticulum, as well as the formation of ceramides, leading to lipoapoptosis as reviewed by Malhi and Gores, (2008). Also, treatment with palmitate led to activation of pro-apoptotic protein Bax and lysosomal permeabilization, which occurred concomitantly with decreased expression of anti-apoptotic protein Bcl-$_X$L (Feldstein et al., 2003).

In view of these differences in mechanisms, one could ask – is *t*BHP a reputable experimental stressor for screening of cytoprotective compounds? In essence, the answer is – yes, because cytoprotective response by selected phytochemicals, in co-exposure conditions were generally reflective of their intrinsic antioxidant properties. Thus, preliminary screening of phytochemicals presents a major step in the drug discovery process, for characterisation of the pharmacological properties of such promising phytochemicals. On other hand, *t*BHP may not represent a good model for investigating the “oxidative stress theory of diseases” due to the complex interplay of pathways that may be involved in such diseases, as reported with palmitate-toxicity. Furthermore, there is also the likelihood that oxidative stress may result from underlying pathologies of chronic diseases. This could also highlight the challenges associated with targeting high lipid exposure for therapeutic purposes. Thus, the antioxidant theory for prevention and treatment of diseases may have, rather, been over-simplified.

6.6 Dietary phytochemicals, and *in vivo* situation

The high intake of fruits and vegetables as a major part of human diet can be credited to recent public health programs such as the “five a day program” which have achieved success in changing dietary habits in humans. This public health advice has been based on the proposal that antioxidants confer benefits in disease prevention and treatment. However, a systematic review by Bjelakovic et al., (2012) queries the basis for antioxidant supplements, due to findings from seventy eight trials reporting increased mortality in humans who recieved beta-carotene, vitamins A and E singularly or in combination with other antioxidant supplements. There was also no benefits on longetivity, following supplementation with vitamin C as well as lack of primary or secondary preventative effects against chronic diseases (Bjelakovic et al., 2012).

While the antioxidant benefits of dietary phytochemicals is widely promoted, it is important to note that phytochemicals exhibit other pharmacological activities such as anti-proliferative and apoptotic effects, boost insulin signalling and cell survival. Therefore, controversies on their antioxidant benefits should not negate potential health benefits of dietary phytochemicals.

It is also reported that phytochemicals can accumulate in mammalian tissues following continuous intake (Bieger et al., 2008). Although low plasma and tissue levels have been reported (Section 1.5), one can envisage that with continuous oral intake of fruits and vegetables, levels of dietary phytochemicals in tissues of the gut and liver could be relatively higher because of dilution in total blood volume blood. Thus, levels from ingestion of a plant extract could well be much higher than from ingestion of a meal containing the herbs; repeat dosing of extract or from meals could also increase ‘physiological’ levels.

This study recorded cytoprotective activities, of selected phytochemicals, in the high micromolar range compared to nanomolar levels reported in plasma and mamalian tissues levels after oral intake (reviewed in Section 1.5). However, our findings present an *in vitro* scenario on the effects of accummulated levels of dietary phytochemicals in

tissues, following prolonged exposure. Also, this study was intended to provide a rapid assessment of cytoprotective activities by selected phytochemicals within 48 h of exposure; hence, the use of high concentrations. Although, the levels of selected phytochemicals used in 1.1B4 cells may not be reminiscent of tissue distribution *in vivo*, the potential benefits of dietary phytochemicals in pancreatic tissues could be enhanced by the use of liposomes.

6.7 Data variability

Data variability observed in the current study could have been resulted from experimental conditions, such as culture media or FBS used. However, components of culture media used were maintained throughout the current study. Although FBS, which is mostly obtained from the beef industry, contains factors required for cell proliferation and attachment, it may include proteins and metabolites (Gstraunthaler et al., 2013). Also, variations between different batches of serum from different geographical source (mainly Brazil, Argentina, South Africa, Australia and Central America) could cause adulteration (Fujimoto, 2002; Jochems et al., 2002). The presence of endogenous antioxidants, (influenced by the diet of the mother cow) or albumin, which is also reported to exhibit radical scavenging activities, could also affect cell culture systems (Roche et al., 2008).

The use of different cell passages could also contribute to data variability. However, this was controlled by using cells within an acceptable range of passage numbers (based on our laboratory protocol). The type of plastic material of cell culture flasks and plates, as well as treatments by respective companies to induce the charge required for cell adhesion, could also contribute to data variability, although to a very minimal extent.

6.8 Proposals for future studies

An assessment of cellular uptake of rosmarinic acid and its principal metabolites (using HPLC) may confirm the effect of poor lipophilicity profiles on their cytoprotective activities.

With recent advances in drug delivery formulations, the role of apoptosis in mediating cytotoxicity by caffeic acid, curcumin and sulforaphane requires further evaluation. Furthermore, cytotoxic effects of these phytochemicals in proliferating versus non-proliferating cells could be evaluated, in order to define their anticancer potentials.

Cytoprotection studies in this study could be repeated in primary tissues, to determine cytoprotective activities of selected phytochemicals in non-proliferating cells.

The effects of glucotoxicity on insulin secretion and glucose metabolism in HepG2 and 1.1B4 cells need to be investigated. Additionally, effects of high glucose exposure on β-cell dysfunction requires further evaluation in other β-cell and hepatic cell models as well, to ascertain results obtained in this study.

In addition to palmitic acid, increase in saturated free fatty acids such as oleic acid have also been reported in NASH patients. Therefore, the cytotoxic effect of an oleic acid and palmitic acid cocktail in HepG2 cells could better mimic NASH in an *in vitro* model.

Further studies involving the effects of sodium palmitate and selected phytochemicals on expression of molecular markers (protein targets) of mitochondrial damage and ER stress could be done using Western blotting. The increase or decrease in activities of enzymes involved in lipid metabolism could also be evaluated using enzyme activity assays.

Effects of high glucose and high lipid exposure (together - glucolipotoxicity) on β-cell viability and function needs to be investigated in 1.1B4 β-cells.

Proteomic assessment on the effects of palmitate and *t*BHP in HepG2- and 1.1B4 β-cells could enable identification of biomarkers that mediate cytotoxic effects of both pro-oxidants. This could enhance our understanding of the contrasting results obtained.

In accordance with the apparent upregulation of NQO1 by quercetin, there is the need to investigate activation of other cytoprotective enzymes, such as HO- 1, in terms of protein expression (using Western blotting) and protein function (enzyme activity studies).

6.9 Conclusion

In conclusion, selected polyphenols - quercetin, rosmarinic acid, caffeic acid, danshensu, curcumin and ferulic acid possess good intrinsic antioxidant properties. However, direct and indirect cytoprotective activities against *t*BHP-induced oxidative damage were exhibited by quercetin, curcumin, rosmarinic acid and caffeic acid in human hepatoma HepG2 cells and human pancreatic 1.1B4 β-cells (rosmarinic acid not tested in 1.1B4 β-cells), sulforaphane showing indirect cytoprotection in HepG2 cells only. However, the lack of cytoprotection by danshensu and ferulic acid highlights the limitation posed by poor lipophilicity profiles of organic acids. Moreover caffeic acid, curcumin and sulforaphane were found to be necrotic in 1.1B4 β-cells and HepG2 cells (caffeic acid not tested in HepG2 cells).

In spite of their cytoprotective activities against *t*BHP (in 1.1B4 β-cells), quercetin, curcumin and caffeic acid amplified cytotoxicity by sodium palmitate in pre-treatment and co-treatment conditions. Although quercetin showed direct cytoprotection against sodium palmitate in HepG2 cells, curcumin and caffeic acid exacerbated cytotoxic effect of sodium palmitate in both exposure conditions; quercetin causing additive toxicity in pre-exposure conditions. Thus, the hypothesis that antioxidant compounds can protect against oxidative stress-mediated diseases such as NASH and T2DM is rather over-simplified, requiring further investigations.

APPENDICES

Appendix I

List of chemicals and their suppliers

The following chemicals were purchased from Sigma, Dorset, UK: 2,2-Diphenyl-1-picrylhydrazyl radical ($DPPH^{\cdot}$), MTT [3-(4,5-Dimethylthiazol-2-yl)-2,5-Diphenyltetrazolium Bromide], amphotericin B (250 µg/ml), Dulbecco's phosphate buffered saline (PBS), Minimum essential medium Eagle with Earle's salts (MEM), foetal bovine serum (FBS), Non-essential amino acid, neutral red dye, dimethylsulfoxide (DMSO), ethanol and sterile water. Trypsin-EDTA (1X), Hank's Balanced Salts Solution (HBSS), L-glutamine, RPMI-1640 medium, Trypsin-EDTA (10X), Penicillin (100 IU/ml) and Streptomycin (0.1 mg/l), benzonase, protease inhibitor cocktail, D-glucose, mannitol, bovine serum albumin (BSA <0.005% free fatty acids) and sodium palmitate were also purchased from Sigma, Dorset, UK.

Plant derived-chemicals used in the current study, and their suppliers are listed in the table below.

Phytochemicals	**Suppliers**	**Purity**
Quercetin dihydrate	Sigma, Dorset, UK	98%
Curcumin	Cayman chemicals, UK	≥96%
L-Sulforaphane	Cayman chemicals, UK	≥98%
Rosmarinic acid	Sigma, Dorset, UK	≥95%
Caffeic acid	Sigma, Dorset, UK	99%
Danshensu	Stratech, UK	≥98%
Ferulic acid	Sigma, Dorset, UK	99%
m-Coumaric acid	Sigma, Dorset, UK	99%

Table 1.1 Sources and purity of phytochemicals used in this study

Also, methanol was obtained from Fluka Chemicals, UK, while gentamicin sulfate (50 mg/ml) and No glucose RPMI-1640 medium were purchased from Lonza. The Expedeon pIMAGO-Biotin HRP Western kit was purchased from, Fisher Scientific, UK.

Instrumentation: Olympus Ck2 microscope (Japan), CMEX-18PRO camera, Nuaire class II cell culture cabinet, Mistral 2000 centrifuge and Bio-Rad TC10 automated cell

counter were used. Also, T175 cm^2 flasks (Greiner Bio-One Limited, UK), tissue-culture Costar® 24-well plates (Corning Incorporated New York, USA), Nunc 96-well plates (ThermoFisher Scientific UK), Multiskan Accent spectrophotometer (Thermo Electron Corporation, Basingstoke, UK), SANYO CO_2 incubator and Bio-Rad dual chambered cell counting slides were employed in this study.

APPENDIX II

FACS output

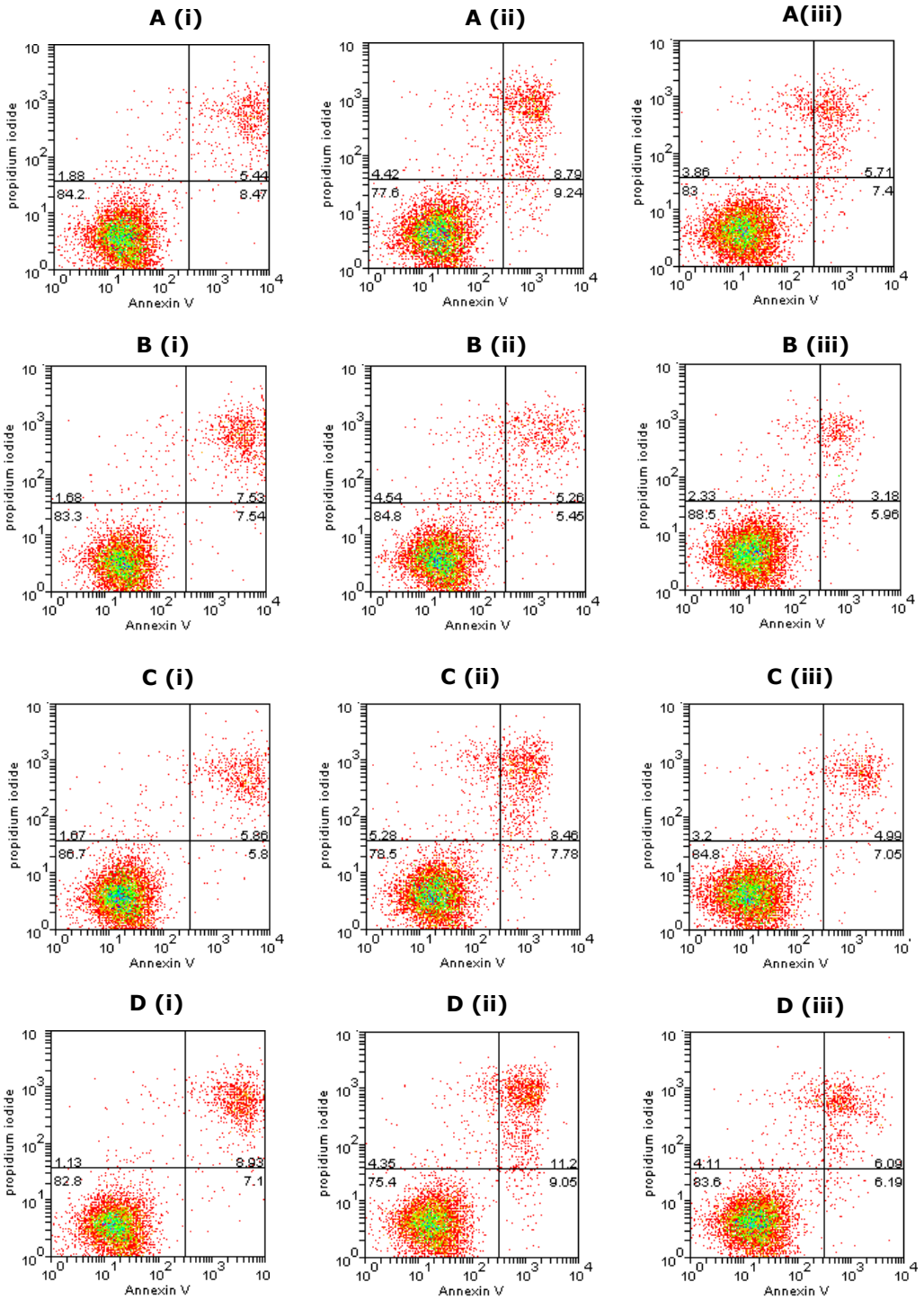

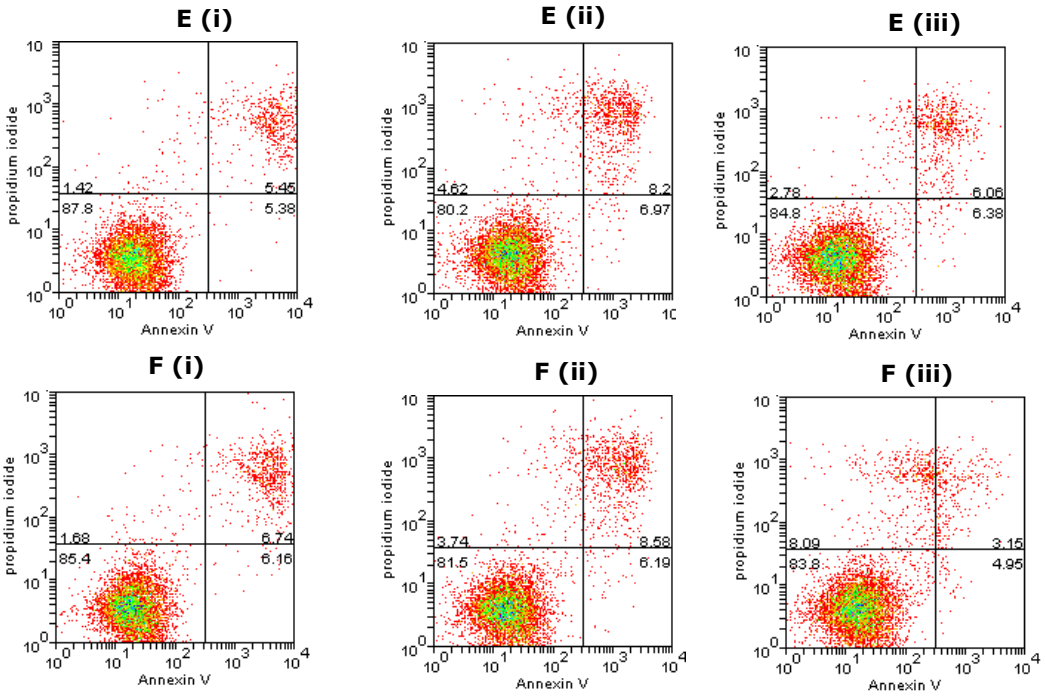

Figure 2 Flow cytometry analysis of early and late apoptosis in 1.1B4 β-cells after exposure to high glucose concentrations. Scans are representative of one experiment. Cultured cells were treated with (A) 10%($^{v}/_{v}$) RPMI-1640 complete medium (containing 11 mM glucose), (B) 10%($^{v}/_{v}$) RPMI-1640 complete medium (containing 5 mM glucose), (C) 14 mM mannitol (in 11 mM glucose containing medium), (D) 25 mM glucose, (E) 29 mM mannitol (in 11 mM glucose containing medium) (F) 40 mM glucose for 24 h (i), 48 h (ii) and 72 h (iii) prior to apoptosis assay. Scans show forward scatter (annexin V) and side scatter (propidium iodide) of gated cells categorised as annexin/PI negative (LL: lower left quadrant), annexin positive (early apoptotic, LR: lower right quadrant), annexin/PI positive (late apoptotic, UR: upper right quadrant) or PI positive (necrotic, UL: upper left quadrant).

Appendix III

SDS-PAGE and Western blotting solutions

Lowry A solution: 500 ml solution contained 2 g of NaOH, 1 g sodium dodecyl sulphate (SDS) and 10 g Na_2CO_3 made up to volume with distilled water. Final solution was stored at room temperature.

Lysis buffer: was made up of 20 mM Tris (12.1 g), 1 mM EGTA (1.9 g), 320 mM sucrose (51.7 g), 0.1% triton X100 (500 ul), 1 mM sodium fluoride (0.021 g) and 10 mM beta glycerophosphate (1.08 g) in distilled water. Final solution was buffered at pH 7.6 with 1.5 M HCl and made up to 500 ml with distilled water. This was stored at 4^{o}C.

10X electrophoresis buffer: 30.3 g Tris, 144 g glycine and 10 g sodium dodecyl sulphate (SDS) were made up to 1 litre with distilled water. Final solution was stored at room temperature.

Transfer buffer: was made up of 30.3 g Tris and 144 g glycine dissolved in 8 litres of distilled water. In addition, 2 litres of methanol was added and final solution was kept at 4^{o}C.

Tris Buffered Saline Tween 20 (TBST): comprised of 25 mM Tris (30.3 g) and 125 mM sodium chloride (73.12 g) dissolved in 1 litre distilled water. Solution was adjusted to pH 7.6 and made up to 10 litres with distilled water. To the final solution, 10 ml Tween 20 was added to achieve final concentration of 0.1%. The final solution was stored at room temperature.

Solubilisation buffer: For 6X buffer, 2.4 g sodium dodecyl sulphate (final 4%), 3 ml of 30% glycerol (final 5%), 3 ml beta mercaptoethanol (final 5%), 240 µl bromophenol blue (final 0.01%) and 2.50 µl of 1.5 M Tris HCl (final 0.0625 M) in a 50 ml tube was made up to 10 ml with distilled water. Dissolution of SDS was facilitated by warming at 37^{o}C for approximately 5 min. Final solution was stored at -20^{o}C.

Appendix IV

1. Solutions for proteomics

Subcellular fractionation

HEPES buffer (50 mM HEPES, 150 mM NaCl at pH 7.4): in 0.9 litres of distilled water, 11.9 g HEPES and 7.5 g NaCl were dissolved and pH adjusted using $NaOH_{(aq).}$ The final solution was made up to 1 litre and stored at 4°C.

Cytosolic buffer I: comprised of 0.01% (100 µg/ml) digitonin and 5 mM EDTA. This buffer was made by adding 10 mg digitonin and 0.186 g EDTA (disodium, dihydrate) to 100 ml 'HEPES buffer'. Also, 10µl protease-inhibitor-cocktail, 1µl benzonase (1 U/µl 1:250 in 50% glycerol TBS, 0.5mg/ml $MgCl_2$) and 1µl (5mg/ml MG132 in DMSO) proteasome-inhibitor were added to each ml of buffer. Cytosolic buffer was freshly prepared and kept on ice prior to use.

Membrane/Organelle buffer II: was made up of 1% NP40 (prepared by dissolving 1.0 g NP-40 in 100 ml HEPES buffer). Also 10 µl protease-inhibitor-cocktail, 1µl benzonase (1U/µ 1:250 in 50% glycerol TBS, 0.5 mg/ml $MgCl_2$) and 1 µl (5 mg/ml MG132 in DMSO) Proteasome-inhibitor were added to each mL of buffer. This buffer was freshly prepared and kept on ice prior to use.

Nuclear buffer III: comprised of 0.5% deoxycholate and 0.1% SDS (made by dissolving 0.25 g sodium deoxycholate and 0.10 g SDS in 100 ml HEPES buffer). Also, 10 µl protease-inhibitor-cocktail, 1 µl benzonase (1 U/µl 1:250 in 50% glycerol TBS, 0.5 mg/ml $MgCl_2$) and 1 µl (5 mg/ml MG132 in DMSO) proteasome-inhibitor were added to each ml of buffer. The nuclear Buffer was freshly prepared and kept on ice prior to use.

Cytoskeletal buffer IV: prepared from 0.5% deoxycholate and 1.0% SDS, by dissolving 0.25 g sodium deoxycholate and 1.0 g SDS in 100 ml HEPES buffer. To each ml of buffer, 10 µl protease-inhibitor-cocktail, 1 µl benzonase (1 U/µl 1:250 in 50% glycerol TBS, 0.5 mg/ml $MgCl_2$) and 1 µl (5 mg/ml MG132 in DMSO) proteasome-inhibitor were added to make the final solution. Buffer was freshly prepared and kept on ice prior to use.

BCA Reagent: 20 µl of 'Solution B' ($CuSO_4$ solution) was added to each ml of 'Solution A' and gently mix. This was prepared freshly prior to use.

SDS-PAGE analysis

X1-Sample buffer: 0.010 g/ml dithiothreitol (DTT) was initailly dissolved in 750 µl distilled water then, 250 µl NuPAGE (X4) was added to the solution, which was carefully mixed, to make final the solution.

Gel running buffer:, 50 ml Invitrogen (X20) MES running buffer was added to 950 ml distilled water to make 1 litre (required for 2 gels).

Colloidal G-250': 'G-250 diluent' was made by adding 118 ml (85%) phosphoric acid to 500 ml distilled water, then 100 g ammonium sulphate was added. When dissolved, solution was made up to 800 ml with distilled water and labelled. For Coomassie Blue G-250 stock, 1.2 g was dissolved in 200 ml methanol and label as 'X5 G-250'. Immediately before use, four volumes of G-250 diluent as added to one volume of X5 G-250 stain.

Gel-permeation chromatography

Anion-exchange Load and Wash buffer 'AE-LW': composed of 8 M Urea, 20 mM Tris (pH 10). 240 g Urea and 1.21 g TrisS-base were dissolved in 0.4 litre distilled water, and pH adjusted to 10.0 with HCl. Final volume was adjusted to 0.5l with distilled water.

Immobilised metal ion affinity chromatography (IMAC)

IMAC Load and Wash buffer 'IMAC-LW' (200mL) comprised of 4 M Urea, 0.5 M NaCl, 1 mM Na vanadate, 10 mM Na fluoride, 50 mM MES at pH 5.3. In addition, 60 g Urea, 2.44 g MES (not Na salt), 7.25 g NaCl, 2.5 ml (100 mM activated, I1310) sodium orthovanadate and 105 mg sodium fluoride were dissolved in 200 ml water. Using HCl, pH was adjusted to 5.3$\pm$ 0.1 (0.5 ml, 0.5 M) and final volume to 250 ml with distilled water.

IMAC Eluent 'IMAC-EL': was prepared using 4 M Urea, 200 mM phosphate at pH 8.3, 0.1 M EDTA, 1 mM sodium vanadate, 10 mM Na fluoride. Allowing 6 ml/1 ml loaded sample volume, the following solutions were prepared

a) X2 stock of 0.2 M EDTA and 0.4 M phosphate was prepared by adding 2.76 g $NaH_2PO_4.H_2O$, 3.72 g EDTA.2Na.2H_2O, 0.5 ml (100 mM activated) sodium orthovanadate, 42 mg sodium fluoride and 1.2 g sodium hydroxide to 40 ml water. Once dissolved pH was 7.7$\pm$ 0.1 and final volume made up with distilled water to 50 ml.
b) In 38 ml of X2 stock (1), 18 g Urea was dissolved to achieve final volume of 68 ml. This was adjusted to 75 ml with distilled water. Final pH was 8.0

Chelating buffer (50mM Na acetate and 0.3M NaCl at pH 4.0): 0.34 g sodium acetate trihydrate and 0.87 g NaCl were dissolved in 40 ml distilled water. pH was adjusted to 4.0 with acetic acid and final volume to 50 ml. This allowed 15 ml/ml IMAC resin.

2. Solutions for proteolysis in polyacrylamide gels pieces

Digestion buffer comprised of 0.2 M ammonium bicarbonate buffered at pH 8 and stored at room temperature for up to 1 week.

Wash buffer: was made of 0.1 M ammonium bicarbonate buffered at pH 8, 50% acetonitrile, 10 ml 0.2 M AmBic and 10 ml acetonitrile. Buffer was stored at room temperature for up to 1 week.

10 mM dithiothreitol (DTT): was freshly prepared prior to use by dissolving 7.7 mg DTT in 5 ml wash buffer

20 mM iodoacetamide: was also freshly made prior to use by dissolving 18.5mg iodoacetamide in 5 ml wash buffer

Resuspension buffer: 3 µl acetic acid added to 1 ml distilled water to make 50 mM acetic acid.

0.1 mg/ml Protease (Trypsin) one vial of use TPCK-treated Trypsin (e.g. Sigma TPCK-Bovine sequencing grade trypsin) was reconstituted in resuspension buffer prior to use. Stock was diluted in digestion buffer immediately before use to obtain 100ng trypsin to 10 µl gel piece (containing 1µg of protein).

Extraction Buffer: 0.1% formic acid in 70% acetonitrile was made up in distilled water.

REFERENCES

References

ABDOLZADE-BAVIL, A., HAYES, S., GORETZKI, L., KROGER, M., ANDERS, J. & HENDRIKS, R. 2004. Convenient and versatile subcellular extraction procedure, that facilitates classical protein expression profiling and functional protein analysis. *Proteomics,* 4**,** 1397-405.

ABDULL RAZIS, A. F., IORI, R. & IOANNIDES, C. 2011. The natural chemopreventive phytochemical R-sulforaphane is a far more potent inducer of the carcinogen-detoxifying enzyme systems in rat liver and lung than the S-isomer. *Int J Cancer,* 128**,** 2775-82.

ABU BAKAR, M. F. 2010. Chemopreventive and chemotherapeutic properties of selected fruits endemic to Borneo: Investigation on *Mangnifera pajang* and *Artocarpus odoratissimus*. *PhD Thesis, University of Nottingham*.

ABU BAKAR, M. F., MOHAMED, M., RAHMAT, A., BURR, S. A. & FRY, J. R. 2013. Cellular assessment of the extract of bambangan (Mangifera pajang) as a potential cytoprotective agent for the human hepatocellular HepG2 cell line. *Food Chem,* 136**,** 18-25.

ADAM, A., CRESPY, V., LEVRAT-VERNY, M.-A., LEENHARDT, F., LEUILLET, M., DEMIGNÉ, C. & RÉMÉSY, C. 2002. The bioavailability of ferulic acid is governed primarily by the food matrix rather than its metabolism in intestine and liver in rats. *The Journal of nutrition,* 132**,** 1962-1968.

AEBERSOLD, R. & GOODLETT, D. R. 2001. Mass spectrometry in proteomics. *Chem Rev,* 101**,** 269-95.

AGGARWAL, B. B., KUMAR, A. & BHARTI, A. C. 2003. Anticancer potential of curcumin: preclinical and clinical studies. *Anticancer research,* 23.

AGGARWAL, B. B., SUNDARAM, C., MALANI, N. & ICHIKAWA, H. 2007. Curcumin: the Indian solid gold. *Advances in experimental medicine and biology.,* 595**,** 1-75.

AGGARWAL, B. B. & SUNG, B. 2009. Pharmacological basis for the role of curcumin in chronic diseases: an age-old spice with modern targets. *Trends in pharmacological sciences,* 30**,** 85-94.

AGUIRRE, V., UCHIDA, T., YENUSH, L., DAVIS, R. & WHITE, M. F. 2000. The c-Jun NH(2)-terminal kinase promotes insulin resistance during association with insulin receptor substrate-1 and phosphorylation of Ser(307). *J Biol Chem,* 275**,** 9047-54.

AGUIRRE, V., WERNER, E. D., GIRAUD, J., LEE, Y. H., SHOELSON, S. E. & WHITE, M. F. 2002. Phosphorylation of Ser307 in insulin receptor substrate-1 blocks interactions with the insulin receptor and inhibits insulin action. *J Biol Chem,* 277**,** 1531-7.

AK, T. & GULCIN, I. 2008. Antioxidant and radical scavenging properties of curcumin. *Chem Biol Interact,* 174**,** 27-37.

AL-MUSAYEIB, N., PERVEEN, S., FATIMA, I., NASIR, M. & HUSSAIN, A. 2011. Antioxidant, anti-glycation and anti-inflammatory activities of phenolic constituents from Cordia sinensis. *Molecules,* 16**,** 10214-10226.

ALBERTS, B., JOHNSON, A., LEWIS, J., MARTIN, R., KEITH, R. & PETER, W. 2002. Electron-Transport Chains and Their Proton Pumps. *Molecular Biology of the Cell,* 4th edition**,** http://www.ncbi.nlm.nih.gov/books/NBK26904.

ALESSIO, H. M. & HAGERMAN, A. E. 2006. *Oxidative stress, exercise, and aging* [Online]. London; Hackensack, NJ: Imperial College Press ; Distributed by World Scientific Pub. Available: http://site.ebrary.com/id/10201215.

ALIA, M., RAMOS, S., MATEOS, R., BRAVO, L. & GOYA, L. 2005. Response of the antioxidant defense system to tert-butyl hydroperoxide and hydrogen peroxide in a human hepatoma cell line (HepG2). *J Biochem Mol Toxicol,* 19**,** 119-28.

ALÍA, M., RAMOS, S., MATEOS, R., GRANADO-SERRANO, A. B., BRAVO, L. & GOYA, L. 2006. Quercetin protects human hepatoma HepG2 against oxidative stress induced by tert-butyl hydroperoxide. *Toxicology and Applied Pharmacology,* 212**,** 110-118.

ALONSO-SALCES, R. M., SERRA, F., RENIERO, F. & HEBERGER, K. 2009. Botanical and geographical characterization of green coffee (Coffea arabica and Coffea canephora): chemometric evaluation of phenolic and methylxanthine contents. *J Agric Food Chem,* 57**,** 4224-35.

AMIC, D., DAVIDOVIC-AMIC, D., BESLO, D. & TRINAJSTIC, N. 2003. Structure-radical scavenging activity relationships of flavonoids. *Croatica Chemica Acta,* 76**,** 55-61.

AMMON, H. P. & WAHL, M. A. 1991. Pharmacology of Curcuma longa. *Planta Medica,* 57**,** 1-7.

ANAND, P., KUNNUMAKKARA, A. B., NEWMAN, R. A. & AGGARWAL, B. B. 2007. Bioavailability of curcumin: Problems and promises. *Molecular Pharmaceutics,* 4**,** 807-818.

ANDREE, H. A., REUTELINGSPERGER, C. P., HAUPTMANN, R., HEMKER, H. C., HERMENS, W. T. & WILLEMS, G. M. 1990. Binding of vascular anticoagulant alpha (VAC alpha) to planar phospholipid bilayers. *J Biol Chem,* 265**,** 4923-8.

ARAKI, E., OYADOMARI, S. & MORI, M. 2003. Endoplasmic reticulum stress and diabetes mellitus. *Intern Med,* 42**,** 7-14.

ARIVARASU, N. A., PRIYAMVADA, S. & MAHMOOD, R. 2013. Oral administration of caffeic acid ameliorates the effect of cisplatin on brush border membrane enzymes and antioxidant system in rat intestine. *Experimental and toxicologic pathology : official journal of the Gesellschaft fur Toxikologische Pathologie,* 65**,** 21-5.

ASAI, A. & MIYAZAWA, T. 2001. Dietary curcuminoids prevent high-fat diet-induced lipid accumulation in rat liver and epididymal adipose tissue. *Journal of Nutrition,* 131**,** 2932-2935.

ASAOKA, Y., TERAI, S., SAKAIDA, I. & NISHINA, H. 2013. The expanding role of fish models in understanding non-alcoholic fatty liver disease. *Disease Models and Mechanisms,* 6**,** 905-914.

ASGARY, S., NADERI, G., SARRAFZADEGAN, N., GHASSEMI, N., BOSHTAM, M., RAFIE, M. & AREFIAN, A. 1999. Anti-oxidant effect of flavonoids on hemoglobin glycosylation. *Pharm Acta Helv,* 73**,** 223-6.

AURA, A. M., O'LEARY, K. A., WILLIAMSON, G., OJALA, M., BAILEY, M., PUUPPONEN-PIMIÄ, R., NUUTILA, A. M., OKSMAN-CALDENTEY, K. M. & POUTANEN, K. 2002. Quercetin derivatives are deconjugated and converted to hydroxyphenylacetic acids but not methylated by human fecal flora in vitro. *Journal of Agricultural and Food Chemistry,* 50**,** 1725-30.

BABA, S., OSAKABE, N., NATSUME, M. & TERAO, J. 2004. Orally administered rosmarinic acid is present as the conjugated and/or methylated forms in plasma, and is degraded and metabolized to conjugated forms of caffeic acid, ferulic acid and m-coumaric acid. *LFS</cja:jid> Life Sciences,* 75**,** 165-178.

BABA, S., OSAKABE, N., NATSUME, M., YASUDA, A., MUTO, Y., HIYOSHI, K., TAKANO, H., YOSHIKAWA, T. & TERAO, J. 2005. Absorption, metabolism, degradation and urinary excretion of rosmarinic acid after intake of Perilla frutescens extract in humans. *European Journal of Nutrition,* 44**,** 1-9.

BACHUR, N. R., GORDON, S. L., GEE, M. V. & KON, H. 1979. NADPH cytochrome P-450 reductase activation of quinone anticancer agents to free radicals. *Proc Natl Acad Sci U S A,* 76**,** 954-7.

BACON, B. R., FARAHVASH, M. J., JANNEY, C. G. & NEUSCHWANDER-TETRI, B. A. 1994. Nonalcoholic steatohepatitis: an expanded clinical entity. *Gastroenterology,* 107**,** 1103-9.

BAHADORAN, Z., MIRMIRAN, P., HOSSEINPANAH, F., RAJAB, A., ASGHARI, G. & AZIZI, F. 2012. Broccoli sprouts powder could improve serum triglyceride and oxidized LDL/LDL-cholesterol ratio in type 2 diabetic patients: A randomized double-blind placebo-controlled clinical trial. *Diabetes Research and Clinical Practice,* 96**,** 348-354.

BAIRD, L. & DINKOVA-KOSTOVA, A. T. 2011. The cytoprotective role of the Keap1-Nrf2 pathway. *Arch Toxicol,* 85**,** 241-72.

BARCELO, S., GARDINER, J. M., GESCHER, A. & CHIPMAN, J. K. 1996. CYP2E1-mediated mechanism of anti-genotoxicity of the broccoli constituent sulforaphane. *Carcinogenesis,* 17**,** 277-82.

BAYNES, J. W. 1991. Role of oxidative stress in development of complications in diabetes. *Diabetes,* 40**,** 405-12.

BEL-RHLID, R., CRESPY, V., PAGE-ZOERKLER, N., NAGY, K., RAAB, T. & HANSEN, C. E. 2009. Hydrolysis of Rosmarinic Acid from Rosemary Extract with Esterases

and Lactobacillus johnsonii in Vitro and in a Gastrointestinal Model. *Journal of Agricultural and Food Chemistry,* 57**,** 7700-7705.

BENSELLAM, M., LAYBUTT, D. R. & JONAS, J. C. 2012. The molecular mechanisms of pancreatic beta-cell glucotoxicity: recent findings and future research directions. *Mol Cell Endocrinol,* 364**,** 1-27.

BENSON, A. M., HUNKELER, M. J. & TALALAY, P. 1980. Increase of NAD(P)H:quinone reductase by dietary antioxidants: possible role in protection against carcinogenesis and toxicity. *Proc Natl Acad Sci U S A,* 77**,** 5216-20.

BERHOW, M. A., AFFUM, A. O. & GYAN, B. A. 2012. Rosmarinic Acid Content in Antidiabetic Aqueous Extract of Ocimum canum Sims Grown in Ghana. *Journal of Medicinal Food,* 15**,** 611-620.

BHATTACHARYA, S., OKSBJERG, N., YOUNG, J. F. & JEPPESEN, P. B. 2013. Caffeic acid, naringenin and quercetin enhance glucose-stimulated insulin secretion and glucose sensitivity in INS-1E cells. *Diabetes Obes Metab*.

BIANCHET, M. A., FAIG, M. & AMZEL, L. M. 2004. Structure and mechanism of NAD[P]H:quinone acceptor oxidoreductases (NQO). *Methods Enzymol,* 382**,** 144-74.

BIEGER, J., CERMAK, R., BLANK, R., DE BOER, V. C., HOLLMAN, P. C., KAMPHUES, J. & WOLFFRAM, S. 2008. Tissue distribution of quercetin in pigs after long-term dietary supplementation. *The Journal of nutrition,* 138**,** 1417-20.

BISHAYEE, K., GHOSH, S., MUKHERJEE, A., SADHUKHAN, R., MONDAL, J. & KHUDA-BUKHSH, A. 2013. Quercetin induces cytochrome-c release and ROS accumulation to promote apoptosis and arrest the cell cycle in G2/M, in cervical carcinoma: signal cascade and drug-DNA interaction. *Cell proliferation,* 46**,** 153-163.

BJELAKOVIC, G., NIKOLOVA, D., GLUUD, L. L., SIMONETTI, R. G. & GLUUD, C. 2012. Antioxidant supplements for prevention of mortality in healthy participants and patients with various diseases. *Cochrane Database Syst Rev***,** CD007176.

BLOOM, D. A. & JAISWAL, A. K. 2003. Phosphorylation of Nrf2 at Ser40 by protein kinase C in response to antioxidants leads to the release of Nrf2 from INrf2, but is not required for Nrf2 stabilization/accumulation in the nucleus and transcriptional activation of antioxidant response element-mediated NAD(P)H:quinone oxidoreductase-1 gene expression. *J Biol Chem,* 278**,** 44675-82.

BONNER-WEIR, S. 2000. Islet growth and development in the adult. *Journal of Molecular Endocrinology,* 24**,** 297-302.

BONORA, E. 2008. Protection of pancreatic beta-cells: is it feasible? *Nutrition, Metabolism and Cardiovascular Diseases,* 18**,** 74-83.

BORS, W., HELLER, W., MICHEL, C. & SARAN, M. 1990. [36] Flavonoids as antioxidants: Determination of radical-scavenging efficiencies. *Methods in Enzymology.* Academic Press.

BOULTON, D. W., WALLE, U. K. & WALLE, T. 1998. Extensive binding of the bioflavonoid quercetin to human plasma proteins. *J Pharm Pharmacol,* 50**,** 243-9.

BOURNE, L. C. & RICE-EVANS, C. 1998. Bioavailability of ferulic acid. *Biochem Biophys Res Commun,* 253**,** 222-7.

BOVERIS, A. & CHANCE, B. 1973. The mitochondrial generation of hydrogen peroxide. General properties and effect of hyperbaric oxygen. *Biochem J,* 134**,** 707-16.

BOVERIS, A., COSTA, L. E. & CADENAS, E. 1999. The mitochondrial production of oxygen radicals and cellular aging

Understanding the process of aging: the roles of mitochondria, free radicals, and antioxidants, Marcel Dekker, Inc, New York, E. Cadenas, L. Packer (Eds.), pp. **,** 1-16.

BRIAUD, I., HARMON, J. S., KELPE, C. L., SEGU, V. B. & POITOUT, V. 2001. Lipotoxicity of the pancreatic beta-cell is associated with glucose-dependent esterification of fatty acids into neutral lipids. *Diabetes,* 50**,** 315-21.

BRISSOVA, M., FOWLER, M. J., NICHOLSON, W. E., CHU, A., HIRSHBERG, B., HARLAN, D. M. & POWERS, A. C. 2005. Assessment of human pancreatic islet architecture and composition by laser scanning confocal microscopy. *Journal of Histochemistry & Cytochemistry,* 53**,** 1087-1097.

BROSKOVÁ, Z., DRÁBIKOVÁ, K., SOTNÍKOVÁ, R., FIALOVÁ, S. & KNEZL, V. 2012. Effect of Plant Polyphenols on Ischemia-Reperfusion Injury of the Isolated rat Heart and Vessels. *Phytother. Res. Phytotherapy Research*, n/a.

BROWN, E. J., KHODR HICHAM, HIDER C. ROBERT & A., R.-E. C. 1998. Structural dependence of flavonoid interactions with Cu2+ ions: implications for their antioxidant properties. *Biochemical Journal,* 330**,** 1173-1178.

BROWNING, J. D. & HORTON, J. D. 2004. Molecular mediators of hepatic steatosis and liver injury. *J Clin Invest,* 114**,** 147-52.

BRUIX, J. & SHERMAN, M. 2011. Management of hepatocellular carcinoma: an update. *Hepatology,* 53**,** 1020-2.

BUTLER, A. E., JANSON, J., BONNER-WEIR, S., RITZEL, R., RIZZA, R. A. & BUTLER, P. C. 2003. Beta-cell deficit and increased beta-cell apoptosis in humans with type 2 diabetes. *Diabetes,* 52**,** 102-10.

CACICEDO, J. M., BENJACHAREOWONG, S., CHOU, E., RUDERMAN, N. B. & IDO, Y. 2005. Palmitate-induced apoptosis in cultured bovine retinal pericytes: roles of NAD(P)H oxidase, oxidant stress, and ceramide. *Diabetes,* 54**,** 1838-45.

CADENAS, E. 1995. Antioxidant and prooxidant functions of DT-diaphorase in quinone metabolism. *Biochem Pharmacol,* 49**,** 127-40.

CADENAS, E. & DAVIES, K. J. 2000. Mitochondrial free radical generation, oxidative stress, and aging. *Free Radic Biol Med,* 29**,** 222-30.

CAI, D., YUAN, M., FRANTZ, D. F., MELENDEZ, P. A., HANSEN, L., LEE, J. & SHOELSON, S. E. 2005. Local and systemic insulin resistance resulting from hepatic activation of IKK-beta and NF-kappaB. *Nat Med,* 11**,** 183-90.

CAI, Y.-Z., MEI, S., JIE, X., LUO, Q. & CORKE, H. 2006. Structure–radical scavenging activity relationships of phenolic compounds from traditional Chinese medicinal plants. *Life Sciences,* 78**,** 2872-2888.

CAMARASA, J., ESCUBEDO, E. & ADZET, T. 1988. Pharmacokinetics of caffeic acid in rats by a high-performance liquid chromatography method. *J Pharm Biomed Anal,* 6**,** 503-10.

CANNITO, S., TURATO, C., PATERNOSTRO, C., BIASIOLO, A., COLOMBATTO, S., CAMBIERI, I., QUARTA, S., NOVO, E., MORELLO, E. & VILLANO, G. 2015. Hypoxia up-regulates SERPINB3 through HIF-2α in human liver cancer cells. *Oncotarget,* 6**,** 2206.

CANO, M. D. V., REYES J M, PARK C Y, GAO X, MORI K, CHUCK R S & GEHLBACH P L 2008. Demonstration by redox fluorometry that sulforaphane protects retinal pigment epithelial cells against oxidative stress. *Invest Ophthalmol Vis Sci,* 49**,** 2606-12.

CAO, J., FENG, X. X., YAO, L., NING, B., YANG, Z. X., FANG, D. L. & SHEN, W. 2014. Saturated free fatty acid sodium palmitate-induced lipoapoptosis by targeting glycogen synthase kinase-3beta activation in human liver cells. *Dig Dis Sci,* 59**,** 346-57.

CAO, J., LIU, Y., JIA, L., ZHOU, H.-M., KONG, Y., YANG, G., JIANG, L.-P., LI, Q.-J. & ZHONG, L.-F. 2007. Curcumin induces apoptosis through mitochondrial hyperpolarization and mtDNA damage in human hepatoma G2 cells. *Free Radical Biology and Medicine,* 43**,** 968-975.

CASAGRANDE, F. & DARBON, J. M. 2001. Effects of structurally related flavonoids on cell cycle progression of human melanoma cells: regulation of cyclin-dependent kinases CDK2 and CDK1. *Biochem Pharmacol,* 61**,** 1205-15.

CASAS-GRAJALES, S. & MURIEL, P. 2015. Antioxidants in liver health. *World journal of gastrointestinal pharmacology and therapeutics,* 6**,** 59-72.

CHAN, J., GREGG, E. W., SARGENT, J. & HORTON, R. 2016. Reducing global diabetes burden by implementing solutions and identifying gaps: a Lancet Commission. *Lancet*.

CHANDRASEKARAN, K., SWAMINATHAN, K., CHATTERJEE, S. & DEY, A. 2010. Apoptosis in HepG2 cells exposed to high glucose. *Toxicol In Vitro,* 24**,** 387-96.

CHARLTON, M. 2004. Nonalcoholic fatty liver disease: a review of current understanding and future impact. *Clin Gastroenterol Hepatol,* 2**,** 1048-58.

CHEN, H., CARLSON, E. C., PELLET, L., MORITZ, J. T. & EPSTEIN, P. N. 2001. Overexpression of metallothionein in pancreatic β-cells reduces streptozotocin-induced DNA damage and diabetes. *Diabetes,* 50**,** 2040-2046.

CHEN, H., LI, X. & EPSTEIN, P. N. 2005. MnSOD and catalase transgenes demonstrate that protection of islets from oxidative stress does not alter cytokine toxicity. *Diabetes,* 54**,** 1437-1446.

CHEN, J. H. & HO, C.-T. 1997. Antioxidant activities of caffeic acid and its related hydroxycinnamic acid compounds. *Journal of Agricultural and Food Chemistry,* 45**,** 2374-2378.

CHEN, Q. Y., SHI, J. G., YAO, Q. H., JIAO, D. M., WANG, Y. Y., HU, H. Z., WU, Y. Q., SONG, J., YAN, J. & WU, L. J. 2012. Lysosomal membrane permeabilization is involved in curcumin-induced apoptosis of A549 lung carcinoma cells. *Mol Cell Biochem,* 359**,** 389-98.

CHEN, Y., YANG, Y., MILLER, M. L., SHEN, D., SHERTZER, H. G., STRINGER, K. F., WANG, B., SCHNEIDER, S. N., NEBERT, D. W. & DALTON, T. P. 2007. Hepatocyte-specific Gclc deletion leads to rapid onset of steatosis with mitochondrial injury and liver failure. *Hepatology,* 45**,** 1118-28.

CHENG, A. L., HSU, C. H., LIN, J. K., HSU, M. M., HO, Y. F., SHEN, T. S., KO, J. Y., LIN, J. T., LIN, B. R., MING-SHIANG, W., YU, H. S., JEE, S. H., CHEN, G. S., CHEN, T. M., CHEN, C. A., LAI, M. K., PU, Y. S., PAN, M. H., WANG, Y. J., TSAI, C. C. & HSIEH, C. Y. 2001. Phase I clinical trial of curcumin, a chemopreventive agent, in patients with high-risk or pre-malignant lesions. *Anticancer research,* 21.

CHESSON, A., PROVAN, G. J., RUSSELL, W. R., SCOBBIE, L., RICHARDSON, A. J. & STEWART, C. 1999. Hydroxycinnamic acids in the digestive tract of livestock and humans. *Journal of the Science of Food and Agriculture,* 79**,** 373-378.

CHEUNG, L., ZERVOU, S., MATTSSON, G., ABOUNA, S., ZHOU, L., IFANDI, V., PELENGARIS, S. & KHAN, M. 2010. c-Myc directly induces both impaired insulin secretion and loss of beta-cell mass, independently of hyperglycemia in vivo. *Islets,* 2**,** 37-45.

CHEUNG, R. C., WONG, J. H. & NG, T. B. 2012. Immobilized metal ion affinity chromatography: a review on its applications. *Appl Microbiol Biotechnol,* 96**,** 1411-20.

CHITKARA, D., NIKALAJE, S. K., MITTAL, A., CHAND, M. & KUMAR, N. 2012. Development of quercetin nanoformulation and in vivo evaluation using streptozotocin induced diabetic rat model. *Drug delivery and translational research,* 2**,** 112-123.

CHOE, E. & MIN, D. B. 2005. Chemistry and Reactions of Reactive Oxygen Species in Foods. *Journal of food science,* 70**,** R142-R159.

CHOE, E. & MIN, D. B. 2006. Chemistry and reactions of reactive oxygen species in foods. *Critical reviews in food science and nutrition,* 46**,** 1-22.

CHOE, E. & MIN, D. B. 2009. Mechanisms of Antioxidants in the Oxidation of Foods. *Comprehensive Reviews in Food Science and Food Safety,* 8**,** 345-358.

CHOUDHARY, M. I., NAHEED, N., ABBASKHAN, A., MUSHARRAF, S. G. & SIDDIQUI, H. 2008. Phenolic and other constituents of fresh water fern Salvinia molesta. *Phytochemistry,* 69**,** 1018-1023.

CHOUDHURY, R., SRAI, S. K., DEBNAM, E. & RICE-EVANS, C. A. 1999. Urinary excretion of hydroxycinnamates and flavonoids after oral and intravenous administration. *Free Radical Biology and Medicine,* 27**,** 278-286.

CHOUDHURY, S. T., DAS, N., GHOSH, S., GHOSH, D., CHAKRABORTY, S. & ALI, N. 2016. Vesicular (liposomal and nanoparticulated) delivery of curcumin: a comparative study on carbon tetrachloride–mediated oxidative hepatocellular damage in rat model. *International journal of nanomedicine,* 11**,** 2179.

CHOWDHRY, S., NAZMY, M. H., MEAKIN, P. J., DINKOVA-KOSTOVA, A. T., WALSH, S. V., TSUJITA, T., DILLON, J. F., ASHFORD, M. L. & HAYES, J. D. 2010. Loss of Nrf2 markedly exacerbates nonalcoholic steatohepatitis. *Free Radic Biol Med,* 48**,** 357-71.

CHU, Y. F., SUN, J., WU, X. & LIU, R. H. 2002. Antioxidant and antiproliferative activities of common vegetables. *J Agric Food Chem,* 50**,** 6910-6.

CLARKE, G., TING, K., WIART, C. & FRY, J. 2013. High Correlation of 2,2-diphenyl-1-picrylhydrazyl (DPPH) Radical Scavenging, Ferric Reducing Activity Potential and Total Phenolics Content Indicates Redundancy in Use of All Three Assays to

Screen for Antioxidant Activity of Extracts of Plants from the Malaysian Rainforest. *Antioxidants,* 2**,** 1-10.

CLARKE, J. D., HSU, A., RIEDL, K., BELLA, D., SCHWARTZ, S. J., STEVENS, J. F. & HO, E. 2011. Bioavailability and inter-conversion of sulforaphane and erucin in human subjects consuming broccoli sprouts or broccoli supplement in a cross-over study design. *Pharmacological Research,* 64**,** 456-463.

CLARKE, J. D., HSU, A., WILLIAMS, D. E., DASHWOOD, R. H., STEVENS, J. F., YAMAMOTO, M. & HO, E. 2011. Metabolism and tissue distribution of sulforaphane in Nrf2 knockout and wild-type mice. *Pharmaceutical research,* 28**,** 3171-9.

CLIFFORD, M. N. 1999. Chlorogenic acids and other cinnamates–nature, occurrence and dietary burden¹. *Journal of the Science of Food and Agriculture,* 79**,** 362-372.

CNOP, M., WELSH, N., JONAS, J. C., JORNS, A., LENZEN, S. & EIZIRIK, D. L. 2005. Mechanisms of pancreatic beta-cell death in type 1 and type 2 diabetes: many differences, few similarities. *Diabetes,* 54 Suppl 2**,** S97-107.

CONAWAY, C. C., GETAHUN, S. M., LIEBES, L. L., PUSATERI, D. J., TOPHAM, D. K. W., BOTERO-OMARY, M. & CHUNG, F. L. 2000. Disposition of glucosinolates and sulforaphane in humans after ingestion of steamed and fresh broccoli. *Nutrition and Cancer-an International Journal,* 38**,** 168-178.

COOPER, G. M. 2000. The Cell: A Molecular Approach. . *The Eukaryotic Cell Cycle,* 2nd edition.

CORDOBA-PEDREGOSA, M. C., VILLALBA, J. M., GONZALEZ-ARAGON, D., BELLO, R. I. & ALCAIN, F. J. 2006. Cellular density and cell type are the key factors in growth inhibition induced by 2,5bis [1-aziridinyl]-1,4 benzoquinone (DZQ). *Anticancer Res,* 26**,** 3535-40.

COUTEAU, D., MCCARTNEY, A. L., GIBSON, G. R., WILLIAMSON, G. & FAULDS, C. B. 2001. Isolation and characterization of human colonic bacteria able to hydrolyse chlorogenic acid. *Journal of Applied Microbiology,* 90**,** 873-881.

CRESPY, V., MORAND, C., BESSON, C., MANACH, C., DÉMIGNÉ, C. & RÉMÉSY, C. 2001. Comparison of the intestinal absorption of quercetin, phloretin and their glucosides in rats. *The Journal of nutrition,* 131**,** 2109-14.

CRUZ–CORREA, M., SHOSKES, D. A., SANCHEZ, P., ZHAO, R., HYLIND, L. M., WEXNER, S. D. & GIARDIELLO, F. M. 2006. Combination Treatment With Curcumin and Quercetin of Adenomas in Familial Adenomatous Polyposis. *Clinical Gastroenterology and Hepatology,* 4**,** 1035-1038.

D'ARCHIVIO, M., FILESI, C., DI BENEDETTO, R., GARGIULO, R., GIOVANNINI, C. & MASELLA, R. 2007. Polyphenols, dietary sources and bioavailability. *Annali-Istituto Superiore di Sanita,* 43**,** 348.

DALTON, T., PALMITER, R. D. & ANDREWS, G. K. 1994. Transcriptional induction of the mouse metallothionein-I gene in hydrogen peroxide-treated Hepa cells involves a composite major late transcription factor/antioxidant response element and metal response promoter elements. *Nucleic Acids Res,* 22**,** 5016-23.

DAY, A. J., GEE, J. M., DUPONT, M. S., JOHNSON, I. T. & WILLIAMSON, G. 2003. Absorption of quercetin-3-glucoside and quercetin-4-glucoside in the rat small intestine: the role of lactase phlorizin hydrolase and the sodium-dependent glucose transporter. *BCP</cja:jid> Biochemical Pharmacology,* 65**,** 1199-1206.

DAY, C. P. & JAMES, O. F. 1998. Steatohepatitis: a tale of two "hits"? *Gastroenterology,* 114**,** 842-5.

DAYOUB, R., VOGEL, A., SCHUETT, J., LUPKE, M., SPIEKER, S. M., KETTERN, N., HILDT, E., MELTER, M. & WEISS, T. S. 2013. Nrf2 activates augmenter of liver regeneration (ALR) via antioxidant response element and links oxidative stress to liver regeneration. *Mol Med,* 19**,** 237-44.

DE ALMEIDA, I. T., CORTEZ-PINTO, H., FIDALGO, G., RODRIGUES, D. & CAMILO, M. E. 2002. Plasma total and free fatty acids composition in human non-alcoholic steatohepatitis. *Clin Nutr,* 21**,** 219-23.

DE LA TOUR D, HALVORSEN T, DEMETERCO C, TYRBERG B, ITKIN-ANSARI P, LOY M, YOO S J, HAO E, BOSSIE S & LEVINE F 2001. Beta-cell differentiation from a human pancreatic cell line in vitro and in vivo. *Mol Endocrinol,* 15**,** 476-83.

DE OLIVEIRA, N. C. D., SARMENTO, M. S., NUNES, E. A., PORTO, C. M., ROSA, D. P., BONA, S. R., RODRIGUES, G., MARRONI, N. P., PEREIRA, P. & PICADA,

J. N. 2012. Rosmarinic acid as a protective agent against genotoxicity of ethanol in mice. *Food and Chemical Toxicology*.

DEL RIO, D., RODRIGUEZ-MATEOS, A., SPENCER, J. P., TOGNOLINI, M., BORGES, G. & CROZIER, A. 2013. Dietary (poly)phenolics in human health: structures, bioavailability, and evidence of protective effects against chronic diseases. *Antioxid Redox Signal,* 18**,** 1818-92.

DEMPE, J. S., SCHEERLE, R. K., PFEIFFER, E. & METZLER, M. 2013. Metabolism and permeability of curcumin in cultured Caco-2 cells. *Molecular Nutrition & Food Research,* 57**,** 1543-9.

DI PAOLA, M., COCCO, T. & LORUSSO, M. 2000. Ceramide interaction with the respiratory chain of heart mitochondria. *Biochemistry,* 39**,** 6660-8.

DINKOVA-KOSTOVA, A. T. & TALALAY, P. 1999. Relation of structure of curcumin analogs to their potencies as inducers of Phase 2 detoxification enzymes. *Carcinogenesis,* 20**,** 911-4.

DINKOVA-KOSTOVA, A. T. & TALALAY, P. 2008. Direct and indirect antioxidant properties of inducers of cytoprotective proteins. *Molecular Nutrition & Food Research,* 52**,** S128-S138.

DINKOVA-KOSTOVA, A. T. & TALALAY, P. 2010. NAD(P)H:quinone acceptor oxidoreductase 1 (NQO1), a multifunctional antioxidant enzyme and exceptionally versatile cytoprotector. *YABBI Archives of Biochemistry and Biophysics,* 501**,** 116-123.

DINKOVA-KOSTOVA, A. T. & WANG, X. J. 2011. Induction of the Keap1/Nrf2/ARE pathway by oxidizable diphenols. *Chem Biol Interact,* 192**,** 101-6.

DROGE, W. 2002. Free radicals in the physiological control of cell function. *Physiol Rev,* 82**,** 47-95.

DUARTE, V. M., HAN, E., VEENA, M. S., SALVADO, A., SUH, J. D., LIANG, L. J., FAULL, K. F., SRIVATSAN, E. S. & WANG, M. B. 2010. Curcumin enhances the effect of cisplatin in suppression of head and neck squamous cell carcinoma via inhibition of IKKbeta protein of the NFkappaB pathway. *Mol Cancer Ther,* 9**,** 2665-75.

DUMONT, A., HEHNER, S. P., HOFMANN, T. G., UEFFING, M., DROGE, W. & SCHMITZ, M. L. 1999. Hydrogen peroxide-induced apoptosis is CD95-independent, requires the release of mitochondria-derived reactive oxygen species and the activation of NF-kappaB. *Oncogene,* 18**,** 747-57.

DUVOIX, A., BLASIUS, R., DELHALLE, S., SCHNEKENBURGER, M., MORCEAU, F., HENRY, E., DICATO, M. & DIEDERICH, M. 2005. Chemopreventive and therapeutic effects of curcumin. *Cancer Lett,* 223**,** 181-90.

EDWARDS, R. L., LYON, T., LITWIN, S. E., RABOVSKY, A., SYMONS, J. D. & JALILI, T. 2007. Quercetin reduces blood pressure in hypertensive subjects. *J Nutr,* 137**,** 2405-11.

EGERT, S., WOLFFRAM, S., BOSY-WESTPHAL, A., BOESCH-SAADATMANDI, C., WAGNER, A. E., FRANK, J., RIMBACH, G. & MUELLER, M. J. 2008. Daily quercetin supplementation dose-dependently increases plasma quercetin concentrations in healthy humans. *The Journal of nutrition,* 138**,** 1615-21.

EIZIRIK, D. L., PIPELEERS, D. G., LING, Z., WELSH, N., HELLERSTRÖM, C. & ANDERSSON, A. 1994. Major species differences between humans and rodents in the susceptibility to pancreatic beta-cell injury. *Proceedings of the National Academy of Sciences,* 91**,** 9253-9256.

EL-GOGARY, R. I., RUBIO, N., WANG, J. T.-W., AL-JAMAL, W. T., BOURGOGNON, M., KAFA, H., NAEEM, M., KLIPPSTEIN, R., ABBATE, V. & LEROUX, F. D. R. 2014. Polyethylene glycol conjugated polymeric nanocapsules for targeted delivery of quercetin to folate-expressing cancer cells in vitro and in vivo. *ACS nano,* 8**,** 1384-1401.

ERKAN, N., AYRANCI, G. & AYRANCI, E. 2008. Antioxidant activities of rosemary (Rosmarinus Officinalis L.) extract, blackseed (Nigella sativa L.) essential oil, carnosic acid, rosmarinic acid and sesamol. *Food Chemistry,* 110**,** 76-82.

FADOK, V. A., VOELKER, D. R., CAMPBELL, P. A., COHEN, J. J., BRATTON, D. L. & HENSON, P. M. 1992. Exposure of phosphatidylserine on the surface of apoptotic lymphocytes triggers specific recognition and removal by macrophages. *J Immunol,* 148**,** 2207-16.

FAIG, M., BIANCHET, M. A., TALALAY, P., CHEN, S., WINSKI, S., ROSS, D. & AMZEL, L. M. 2000. Structures of recombinant human and mouse NAD(P)H:quinone oxidoreductases: species comparison and structural changes with substrate binding and release. *Proc Natl Acad Sci U S A,* 97**,** 3177-82.

FAN, D., ZHOU, X., ZHAO, C., CHEN, H., ZHAO, Y. & GONG, X. 2011. Anti-inflammatory, antiviral and quantitative study of quercetin-3-O-beta-D-glucuronide in Polygonum perfoliatum L. *Fitoterapia,* 82**,** 805-10.

FAN, J. G., SAIBARA, T., CHITTURI, S., KIM, B. I., SUNG, J. J. & CHUTAPUTTI, A. 2007. What are the risk factors and settings for non-alcoholic fatty liver disease in Asia-Pacific? *J Gastroenterol Hepatol,* 22**,** 794-800.

FAUSTO, N. & WEBBER, E. M. 1993. Control of liver growth. *Crit Rev Eukaryot Gene Expr,* 3**,** 117-35.

FAUTZ, R., HUSEIN, B. & HECHENBERGER, C. 1991. Application of the neutral red assay (NR assay) to monolayer cultures of primary hepatocytes: rapid colorimetric viability determination for the unscheduled DNA synthesis test (UDS). *Mutation Research/Environmental Mutagenesis and Related Subjects,* 253**,** 173-179.

FELDSTEIN, A. E., CANBAY, A., ANGULO, P., TANIAI, M., BURGART, L. J., LINDOR, K. D. & GORES, G. J. 2003. Hepatocyte apoptosis and fas expression are prominent features of human nonalcoholic steatohepatitis. *Gastroenterology,* 125**,** 437-43.

FERNANDO, P. M., PIAO, M. J., KANG, K. A., RYU, Y. S., HEWAGE, S. R., CHAE, S. W. & HYUN, J. W. 2016. Rosmarinic Acid Attenuates Cell Damage against UVB Radiation-Induced Oxidative Stress via Enhancing Antioxidant Effects in Human HaCaT Cells. *Biomol Ther (Seoul),* 24**,** 75-84.

FERRY, D. R., SMITH, A., MALKHANDI, J., FYFE, D. W., DETAKATS, P. G., ANDERSON, D., BAKER, J. & KERR, D. J. 1996. Phase I clinical trial of the flavonoid quercetin: pharmacokinetics and evidence for in vivo tyrosine kinase inhibition. *Clinical cancer research : an official journal of the American Association for Cancer Research,* 2**,** 659-68.

FETONI, A. R., MANCUSO, C., ERAMO, S. L. M., RALLI, M., PIACENTINI, R., BARONE, E., PALUDETTI, G. & TROIANI, D. 2010. In vivo protective effect of ferulic acid against noise-induced hearing loss in the guinea-pig. *Neuroscience,* 169**,** 1575-1588.

FILMAN, D. J., BRAWN, R. J. & DANDLIKER, W. B. 1975. Intracellular supravital stain delocalization as an assay for antibody-dependent complement-mediated cell damage. *J Immunol Methods,* 6**,** 189-207.

FINEGOOD, D. T., SCAGLIA, L. & BONNER-WEIR, S. 1995. Dynamics of β-cell Mass in the Growing Rat Pancreas: Estimation With a Simple Mathematical Model. *Diabetes,* 44**,** 249-256.

FINK, S. L. & COOKSON, B. T. 2005. Apoptosis, pyroptosis, and necrosis: mechanistic description of dead and dying eukaryotic cells. *Infect Immun,* 73**,** 1907-16.

FOTI, M. C., DAQUINO, C. & GERACI, C. 2004. Electron-transfer reaction of cinnamic acids and their methyl esters with the DPPH(*) radical in alcoholic solutions. *J Org Chem,* 69**,** 2309-14.

FOURQUET, S., GUEROIS, R., BIARD, D. & TOLEDANO, M. B. 2010. Activation of NRF2 by nitrosative agents and H2O2 involves KEAP1 disulfide formation. *J Biol Chem,* 285**,** 8463-71.

FRIDLYAND, L. E. & PHILIPSON, L. H. 2004. Does the glucose-dependent insulin secretion mechanism itself cause oxidative stress in pancreatic beta-cells? *Diabetes,* 53**,** 1942-8.

FUJIMOTO, B. 2002. Fetal bovine serum—supply vs. demand. *Art to Science,* 21**,** 1-4.

GALATI, G., MORIDANI, M. Y., CHAN, T. S. & O'BRIEN, P. J. 2001. Peroxidative metabolism of apigenin and naringenin versus luteolin and quercetin: glutathione oxidation and conjugation. *Free Radical Biology and Medicine,* 30**,** 370-382.

GALLUZZI, L., VITALE, I., ABRAMS, J. M., ALNEMRI, E. S., BAEHRECKE, E. H., BLAGOSKLONNY, M. V., DAWSON, T. M., DAWSON, V. L., EL-DEIRY, W. S., FULDA, S., GOTTLIEB, E., GREEN, D. R., HENGARTNER, M. O., KEPP, O., KNIGHT, R. A., KUMAR, S., LIPTON, S. A., LU, X., MADEO, F., MALORNI, W., MEHLEN, P., NUNEZ, G., PETER, M. E., PIACENTINI, M., RUBINSZTEIN, D.

C., SHI, Y., SIMON, H. U., VANDENABEELE, P., WHITE, E., YUAN, J., ZHIVOTOVSKY, B., MELINO, G. & KROEMER, G. 2012. Molecular definitions of cell death subroutines: recommendations of the Nomenclature Committee on Cell Death 2012. *Cell Death Differ,* 19**,** 107-20.

GÁLVEZ, M. C., BARROSO, C. G. & PÉREZ-BUSTAMANTE, J. A. 1994. Analysis of polyphenolic compounds of different vinegar samples. *Zeitschrift für Lebensmittel-Untersuchung und Forschung,* 199**,** 29-31.

GANDHI, G. R., VANLALHRUAIA, P., STALIN, A., IRUDAYARAJ, S. S., IGNACIMUTHU, S. & PAULRAJ, M. G. 2014. Polyphenols-rich Cyamopsis tetragonoloba (L.) Taub. beans show hypoglycemic and β-cells protective effects in type 2 diabetic rats. *Food and Chemical Toxicology,* 66**,** 358-365.

GAO, L., WEI, H., ZHAO, H., XIAO, S. & ZHENG, R. 2005. Antiapoptotic and antioxidant effects of rosmarinic acid in astrocytes. *Die Pharmazie-An International Journal of Pharmaceutical Sciences,* 60**,** 62-65.

GAO, Y., MIYAZAKI, J. & HART, G. W. 2003. The transcription factor PDX-1 is post-translationally modified by O-linked N-acetylglucosamine and this modification is correlated with its DNA binding activity and insulin secretion in min6 beta-cells. *Arch Biochem Biophys,* 415**,** 155-63.

GARCEA, G., JONES, D. J. L., SINGH, R., DENNISON, A. R., FARMER, P. B., SHARMA, R. A., STEWARD, W. P., GESCHER, A. J. & BERRY, D. P. 2004. Detection of curcumin and its metabolites in hepatic tissue and portal blood of patients following oral administration. *British Journal of Cancer,* 90**,** 1011-1015.

GIUGLIANO, D., CERIELLO, A. & ESPOSITO, K. 2008. Glucose metabolism and hyperglycemia. *Am J Clin Nutr,* 87**,** 217S-222S.

GO, H., HWANG, H.-J. & NAM, T.-J. 2011. Polysaccharides from Capsosiphon fulvescens Stimulate the Growth of IEC-6 Cells by Activating the MAPK Signaling Pathway. *Marine Biotechnology,* 13**,** 433-440.

GOMEZ-RUIZ, J. A., LEAKE, D. S. & AMES, J. M. 2007. In vitro antioxidant activity of coffee compounds and their metabolites. *J Agric Food Chem,* 55**,** 6962-9.

GONTHIER, M. P., REMESY, C., SCALBERT, A., CHEYNIER, V., SOUQUET, J. M., POUTANEN, K. & AURA, A. M. 2006. Microbial metabolism of caffeic acid and its esters chlorogenic and caftaric acids by human faecal microbiota in vitro. *Biomedicine & Pharmacotherapy,* 60**,** 536-540.

GONTHIER, M. P., VERNY, M. A., BESSON, C., REMESY, C. & SCALBERT, A. 2003. Chlorogenic acid bioavailability largely depends on its metabolism by the gut microflora in rats. *J Nutr,* 133**,** 1853-9.

GONZALEZ-VALLINAS, M., REGLERO, G. & RAMIREZ DE MOLINA, A. 2015. Rosemary (Rosmarinus officinalis L.) Extract as a Potential Complementary Agent in Anticancer Therapy. *Nutr Cancer,* 67**,** 1221-9.

GOODWIN, B. L., RUTHVEN, C. R. & SANDLER, M. 1994. Gut flora and the origin of some urinary aromatic phenolic compounds. *Biochem Pharmacol,* 47**,** 2294-7.

GRADOLATTO, A., CANIVENC-LAVIER, M. C., BASLY, J. P., SIESS, M. H. & TEYSSIER, C. 2004. Metabolism of apigenin by rat liver phase I and phase ii enzymes and by isolated perfused rat liver. *Drug metabolism and disposition: the biological fate of chemicals,* 32**,** 58-65.

GRAF, E. 1992. Antioxidant potential of ferulic acid. *Free Radical Biology and Medicine,* 13**,** 435-448.

GRANADO-SERRANO, A. B., MARTÍN, M. A., BRAVO, L., GOYA, L. & RAMOS, S. 2006. Quercetin induces apoptosis via caspase activation, regulation of Bcl-2, and inhibition of PI-3-kinase/Akt and ERK pathways in a human hepatoma cell line (HepG2). *The Journal of nutrition,* 136**,** 2715-2721.

GREMLICH, S., BONNY, C., WAEBER, G. & THORENS, B. 1997. Fatty acids decrease IDX-1 expression in rat pancreatic islets and reduce GLUT2, glucokinase, insulin, and somatostatin levels. *J Biol Chem,* 272**,** 30261-9.

GRYNKIEWICZ, G. & SLIFIRSKI, P. 2012. Curcumin and curcuminoids in quest for medicinal status. *Acta biochimica Polonica,* 59**,** 201-12.

GSTRAUNTHALER, G., LINDL, T. & VAN DER VALK, J. 2013. A plea to reduce or replace fetal bovine serum in cell culture media. *Cytotechnology,* 65**,** 791-793.

GUERRERO-BELTRÁN, C. E., CALDERÓN-OLIVER, M., PEDRAZA-CHAVERRI, J. & CHIRINO, Y. I. 2012. Protective effect of sulforaphane against oxidative stress:

recent advances. *Experimental and toxicologic pathology : official journal of the Gesellschaft fur Toxikologische Pathologie,* 64**,** 503-8.

GUERRIERO, E., SORICE, A., CAPONE, F., COSTANTINI, S., PALLADINO, P., D'ISCHIA, M. & CASTELLO, G. 2011. Effects of Lipoic Acid, Caffeic Acid and a Synthesized Lipoyl-Caffeic Conjugate on Human Hepatoma Cell Lines. *Molecules,* 16**,** 6365-6377.

GUICCIARDI, M. E., LEIST, M. & GORES, G. J. 2004. Lysosomes in cell death. *Oncogene,* 23**,** 2881-90.

GUO, J., SUN, K., WANG, C. S., FANG, S. P., HORIE, Y., YANG, J. Y., LUI, Y. Y., WANG, F., LUI, L. Y., FAN, J. Y., HIBI, T. & HAN, J. Y. 2008. Protective effects of dihydroxyl-phenyl lactic acid and salvianolic acid B on LPS-induced mesenteric microcirculatory disturbance in rats. *Shock,* 29**,** 205-211.

GUPTA, S. C., PRASAD, S., KIM, J. H., PATCHVA, S., WEBB, L. J., PRIYADARSINI, I. K. & AGGARWAL, B. B. 2011. Multitargeting by curcumin as revealed by molecular interaction studies. *Nat Prod Rep,* 28**,** 1937-55.

HAIDARA, K., MARION, M., GASCON-BARRÉ, M., DENIZEAU, F. & AVERILL-BATES, D. A. 2008. Implication of caspases and subcellular compartments in tert-butylhydroperoxide induced apoptosis. *Toxicology and Applied Pharmacology,* 229**,** 65-76.

HAIDARA, K., MOREL, I., ABALÉA, V., GASCON BARRÉ, M. & DENIZEAU, F. 2002. Mechanism of tert-butylhydroperoxide induced apoptosis in rat hepatocytes: involvement of mitochondria and endoplasmic reticulum. *Biochimica et Biophysica Acta (BBA) - Molecular Cell Research,* 1542**,** 173-185.

HAJAGHAMOHAMMADI, A.-A., ZIAEE, A. & RAFIEI, R. 2008. The efficacy of silymarin in decreasing transaminase activities in non-alcoholic fatty liver disease: A randomized controlled clinical trial. *Hepatitis Monthly,* 8**,** 191.

HAJIANI, E. & HASHEMI, S. J. 2009. Comparison of therapeutic effects of silymarin and vitamin e in nonalcoholic fatty liver disease: results of an open-labele, prospective, randomized study. *Jundishapur Journal of Natural Pharmaceutical Products,* 4**,** 8-14.

HALKIER, B. A. & GERSHENZON, J. 2006. Biology and biochemistry of glucosinolates. *Annu Rev Plant Biol,* 57**,** 303-33.

HAMAGUCHI, T., ONO, K., MURASE, A. & YAMADA, M. 2009. Phenolic compounds prevent Alzheimer's pathology through different effects on the amyloid-beta aggregation pathway. *Am J Pathol,* 175**,** 2557-65.

HAMED, A. R. M. 2009. Investigation of multiple cytoprotective actions of individual phytochemicals and plant extracts. *Unpublished PhD thesis, University of Nottingham*.

HAN, J. M., LEE, Y. J., LEE, S. Y., KIM, E. M., MOON, Y., KIM, H. W. & HWANG, O. 2007. Protective effect of sulforaphane against dopaminergic cell death. *The Journal of pharmacology and experimental therapeutics,* 321**,** 249-56.

HAN, J. Y., HORIE, Y., FAN, J. Y., SUN, K., GUO, J., MIURA, S. & HIBI, T. 2009. Potential of 3,4-dihydroxy-phenyl lactic acid for ameliorating ischemia-reperfusion-induced microvascular disturbance in rat mesentery. *American Journal of Physiology-Gastrointestinal and Liver Physiology,* 296**,** G36-G44.

HANLON, N., POYNTON, C. L., COLDHAM, N., SAUER, M. J. & IOANNIDES, C. 2009. The aliphatic isothiocyanates erucin and sulforaphane do not effectively up-regulate NAD(P)H:quinone oxidoreductase (NQO1) in human liver compared with rat. *Mol Nutr Food Res,* 53**,** 836-44.

HARMON, J. S., STEIN, R. & ROBERTSON, R. P. 2005. Oxidative stress-mediated, post-translational loss of MafA protein as a contributing mechanism to loss of insulin gene expression in glucotoxic beta cells. *J Biol Chem,* 280**,** 11107-13.

HARNLY, J. M., DOHERTY, R. F., BEECHER, G. R., HOLDEN, J. M., HAYTOWITZ, D. B., BHAGWAT, S. & GEBHARDT, S. 2006. Flavonoid content of U.S. fruits, vegetables, and nuts. *Journal of Agricultural and Food Chemistry,* 54**,** 9966-77.

HARRIS, K. E. & JEFFERY, E. H. 2008. Sulforaphane and erucin increase MRP1 and MRP2 in human carcinoma cell lines. *The Journal of Nutritional Biochemistry,* 19**,** 246-254.

HARWOOD, M., DANIELEWSKA-NIKIEL, B., BORZELLECA, J. F., FLAMM, G. W., WILLIAMS, G. M. & LINES, T. C. 2007. A critical review of the data related to the

safety of quercetin and lack of evidence of in vivo toxicity, including lack of genotoxic/carcinogenic properties. *FCT Food and Chemical Toxicology,* 45**,** 2179-2205.

HAUKELAND, J. W., DAMAS, J. K., KONOPSKI, Z., LOBERG, E. M., HAALAND, T., GOVERUD, I., TORJESEN, P. A., BIRKELAND, K., BJORO, K. & AUKRUST, P. 2006. Systemic inflammation in nonalcoholic fatty liver disease is characterized by elevated levels of CCL2. *J Hepatol,* 44**,** 1167-74.

HAUPTMANN, N., GRIMSBY, J., SHIH, J. C. & CADENAS, E. 1996. The metabolism of tyramine by monoamine oxidase A/B causes oxidative damage to mitochondrial DNA. *Arch Biochem Biophys,* 335**,** 295-304.

HENQUIN, J. C. 2000. Triggering and amplifying pathways of regulation of insulin secretion by glucose. *Diabetes,* 49**,** 1751-60.

HEX, N., BARTLETT, C., WRIGHT, D., TAYLOR, M. & VARLEY, D. 2012. Estimating the current and future costs of Type 1 and Type 2 diabetes in the UK, including direct health costs and indirect societal and productivity costs. *Diabet Med,* 29**,** 855-62.

HIGGINS, L. G. & HAYES, J. D. 2011. The cap'n'collar transcription factor Nrf2 mediates both intrinsic resistance to environmental stressors and an adaptive response elicited by chemopreventive agents that determines susceptibility to electrophilic xenobiotics. *Chem Biol Interact,* 192**,** 37-45.

HOEHLE, S. I., PFEIFFER, E. & METZLER, M. 2007. Glucuronidation of curcuminoids by human microsomal and recombinant UDP-glucuronosyltransferases. *MNFR Molecular Nutrition & Food Research,* 51**,** 932-938.

HOEHLE, S. I., PFEIFFER, E., SÓLYOM, A. M. & METZLER, M. 2006. Metabolism of curcuminoids in tissue slices and subcellular fractions from rat liver. *Journal of Agricultural and Food Chemistry,* 54**,** 756-64.

HONDA, H., IKEJIMA, K., HIROSE, M., YOSHIKAWA, M., LANG, T., ENOMOTO, N., KITAMURA, T., TAKEI, Y. & SATO, N. 2002. Leptin is required for fibrogenic responses induced by thioacetamide in the murine liver. *Hepatology,* 36**,** 12-21.

HONG, F., SEKHAR, K. R., FREEMAN, M. L. & LIEBLER, D. C. 2005. Specific patterns of electrophile adduction trigger Keap1 ubiquitination and Nrf2 activation. *J Biol Chem,* 280**,** 31768-75.

HOTAMISLIGIL, G. S., PERALDI, P., BUDAVARI, A., ELLIS, R., WHITE, M. F. & SPIEGELMAN, B. M. 1996. IRS-1-mediated inhibition of insulin receptor tyrosine kinase activity in TNF-alpha- and obesity-induced insulin resistance. *Science,* 271**,** 665-8.

HUANG, H. C., NGUYEN, T. & PICKETT, C. B. 2002. Phosphorylation of Nrf2 at Ser-40 by protein kinase C regulates antioxidant response element-mediated transcription. *J Biol Chem,* 277**,** 42769-74.

HUNTER, T. 2000. Signaling--2000 and beyond. *Cell,* 100**,** 113-27.

HWANG, E. S. & JEFFERY, E. H. 2005. Induction of quinone reductase by sulforaphane and sulforaphane N-acetylcysteine conjugate in murine hepatoma cells. *Journal of Medicinal Food,* 8**,** 198-203.

IHARA, Y., TOYOKUNI, S., ICHIDA, K. & ODAKA, H. 1999. Hyperglycemia causes oxidative stress in pancreatic beta-cells of GK rats, a model of type 2 diabetes. *Diabetes,* 48**,** 927.

IKEDA, H., NISHI, S. & SAKAI, M. 2004. Transcription factor Nrf2/MafK regulates rat placental glutathione S-transferase gene during hepatocarcinogenesis. *Biochemical Journal,* 380**,** 515-521.

ILIUK, A., LIU, X. S., XUE, L., LIU, X. & TAO, W. A. 2012. Chemical visualization of phosphoproteomes on membrane. *Mol Cell Proteomics,* 11**,** 629-39.

INNAMORATO, N. G., ROJO, A. I., GARCÍA-YAGÜE, A. J., YAMAMOTO, M., DE CEBALLOS, M. L. & CUADRADO, A. 2008. The transcription factor Nrf2 is a therapeutic target against brain inflammation. *Journal of immunology (Baltimore, Md. : 1950),* 181**,** 680-9.

INOGUCHI, T., LI, P., UMEDA, F., YU, H. Y., KAKIMOTO, M., IMAMURA, M., AOKI, T., ETOH, T., HASHIMOTO, T., NARUSE, M., SANO, H., UTSUMI, H. & NAWATA, H. 2000. High glucose level and free fatty acid stimulate reactive oxygen species production through protein kinase C--dependent activation of NAD(P)H oxidase in cultured vascular cells. *Diabetes,* 49**,** 1939-45.

INTERNATIONAL DIABETES FEDERATION 2015. International Diabetes Federation, Brussels *IDF diabetes* 7th edition**,** http://www.diabetesatlas.org (accessed March 30, 2016).

IODICE, S., GANDINI, S., MAISONNEUVE, P. & LOWENFELS, A. B. 2008. Tobacco and the risk of pancreatic cancer: a review and meta-analysis. *Langenbecks Arch Surg,* 393**,** 535-45.

IRESON, C., ORR, S., JONES, D. J., VERSCHOYLE, R., LIM, C. K., LUO, J. L., HOWELLS, L., PLUMMER, S., JUKES, R., WILLIAMS, M., STEWARD, W. P. & GESCHER, A. 2001. Characterization of metabolites of the chemopreventive agent curcumin in human and rat hepatocytes and in the rat in vivo, and evaluation of their ability to inhibit phorbol ester-induced prostaglandin E2 production. *Cancer research,* 61**,** 1058-64.

IRESON, C. R., JONES, D. J. L., ORR, S., COUGHTRIE, M. W. H., BOOCOCK, D. J., WILLIAMS, M. L., FARMER, P. B., STEWARD, W. P. & GESCHER, A. J. 2002. Metabolism of the cancer chemopreventive agent curcumin in human and rat intestine. *Cancer Epidemiology Biomarkers & Prevention,* 11**,** 105-111.

ISHII, T., ITOH, K., TAKAHASHI, S., SATO, H., YANAGAWA, T., KATOH, Y., BANNAI, S. & YAMAMOTO, M. 2000. Transcription factor Nrf2 coordinately regulates a group of oxidative stress-inducible genes in macrophages. *J Biol Chem,* 275**,** 16023-9.

ITOH, K., CHIBA, T., TAKAHASHI, S., ISHII, T., IGARASHI, K., KATOH, Y., OYAKE, T., HAYASHI, N., SATOH, K., HATAYAMA, I., YAMAMOTO, M. & NABESHIMA, Y. 1997. An Nrf2/small Maf heterodimer mediates the induction of phase II detoxifying enzyme genes through antioxidant response elements. *Biochem Biophys Res Commun,* 236**,** 313-22.

ITOH, K., IGARASHI, K., HAYASHI, N., NISHIZAWA, M. & YAMAMOTO, M. 1995. Cloning and characterization of a novel erythroid cell-derived CNC family transcription factor heterodimerizing with the small Maf family proteins. *Mol Cell Biol,* 15**,** 4184-93.

IYANAGI, T. & YAMAZAKI, I. 1970. One-electron-transfer reactions in biochemical systems V. Difference in the mechanism of quinone reduction by the NADH dehydrogenase and the NAD(P)H dehydrogenase (DT-diaphorase). *Biochim. Biophys. Acta,* 216**,** 288-294.

JACOB, R. A. 1996. Three eras of vitamin C discovery. *Subcell Biochem,* 25**,** 1-16.

JACQUEMINET, S., BRIAUD, I., ROUAULT, C., REACH, G. & POITOUT, V. 2000. Inhibition of insulin gene expression by long-term exposure of pancreatic beta cells to palmitate is dependent on the presence of a stimulatory glucose concentration. *Metabolism,* 49**,** 532-6.

JAGANATHAN, S. K. 2012. Growth inhibition by caffeic acid, one of the phenolic constituents of honey, in HCT 15 colon cancer cells. *ScientificWorldJournal,* 2012**,** 372345.

JAGANATHAN, S. K., MANDAL, S. M., JANA, S. K., DAS, S. & MANDAL, M. 2010. Studies on the phenolic profiling, anti-oxidant and cytotoxic activity of Indian honey: in vitro evaluation. *Natural Product Research,* 24**,** 1295-1306.

JANATPOUR, K., PAGLIERONI, T. G., SCHULLER, L., FOLEY, K., RIZZARDO, T. & HOLLAND, P. V. 2002. Interpretation of atypical patterns encountered when using a flow cytometry-based method to detect residual leukocytes in leukoreduced red blood cell components. *Cytometry,* 50**,** 254-60.

JANJIC, D., MAECHLER, P., SEKINE, N., BARTLEY, C., ANNEN, A. S. & WOLHEIM, C. B. 1999. Free radical modulation of insulin release in INS-1 cells exposed to alloxan. *Biochem Pharmacol,* 57**,** 639-48.

JEMAL, A., BRAY, F., CENTER, M. M., FERLAY, J., WARD, E. & FORMAN, D. 2011. Global cancer statistics. *CA Cancer J Clin,* 61**,** 69-90.

JENSEN, M. V., JOSEPH, J. W., RONNEBAUM, S. M., BURGESS, S. C., SHERRY, A. D. & NEWGARD, C. B. 2008. Metabolic cycling in control of glucose-stimulated insulin secretion. *Am J Physiol Endocrinol Metab,* 295**,** E1287-97.

JIANG, H., HA, T. & WEI, D. 2001. [A study on the mechanism of the biological roles of danshensu on fibroblast]. *Zhonghua shao shang za zhi = Zhonghua shaoshang zazhi = Chinese journal of burns,* 17**,** 36-8.

JOCHEMS, C. E., VAN DER VALK, J. B., STAFLEU, F. R. & BAUMANS, V. 2002. The use of fetal bovine serum: ethical or scientific problem? *ATLA-NOTTINGHAM-,* 30**,** 219-228.

JOHNSON, P. J. 2013. How do mechanisms of hepatocarcinogenesis (HBV, HCV, and NASH) affect our understanding and approach to HCC? *Am Soc Clin Oncol Educ Book*.

JOU, J., CHOI, S. S. & DIEHL, A. M. 2008. Mechanisms of disease progression in nonalcoholic fatty liver disease. *Semin Liver Dis,* 28**,** 370-9.

JOVANOVIC, S. V., BOONE, C. W., STEENKEN, S., TRINOGA, M. & KASKEY, R. B. 2001. How curcumin works preferentially with water soluble antioxidants. *J Am Chem Soc,* 123**,** 3064-8.

JOVANOVIC, S. V., STEENKEN, S., BOONE, C. W. & SIMIC, M. G. 1999. H-Atom Transfer Is A Preferred Antioxidant Mechanism of Curcumin. *Journal of the American Chemical Society,* 121**,** 9677-9681.

JUNG, E. H., KIM, S. R., HWANG, I. K. & HA, T. Y. 2007. Hypoglycemic effects of a phenolic acid fraction of rice bran and ferulic acid in C57BL/KsJ-db/db mice. *J Agric Food Chem,* 55**,** 9800-4.

JUNG, U. J., LEE, M.-K., PARK, Y. B., JEON, S.-M. & CHOI, M.-S. 2006. Antihyperglycemic and antioxidant properties of caffeic acid in db/db mice. *Journal of Pharmacology and Experimental Therapeutics,* 318**,** 476-483.

KAHN, S. E. 2003. The relative contributions of insulin resistance and beta-cell dysfunction to the pathophysiology of Type 2 diabetes. *Diabetologia,* 46**,** 3-19.

KAHN, S. E., COOPER, M. E. & DEL PRATO, S. 2014. Pathophysiology and treatment of type 2 diabetes: perspectives on the past, present, and future. *The Lancet,* 383**,** 1068-1083.

KAISER, N., CORCOS, A. P., SAREL, I. & CERASI, E. 1991. Monolayer culture of adult rat pancreatic islets on extracellular matrix: modulation of B-cell function by chronic exposure to high glucose. *Endocrinology,* 129**,** 2067-76.

KAJIMOTO, Y., MATSUOKA, T., KANETO, H., WATADA, H., FUJITANI, Y., KISHIMOTO, M., SAKAMOTO, K., MATSUHISA, M., KAWAMORI, R., YAMASAKI, Y. & HORI, M. 1999. Induction of glycation suppresses glucokinase gene expression in HIT-T15 cells. *Diabetologia,* 42**,** 1417-24.

KANEKO, T., KAJI, K. & MATSUO, M. 1994. Protection of linoleic acid hydroperoxide-induced cytotoxicity by phenolic antioxidants. *Free Radical Biology and Medicine,* 16**,** 405-409.

KANETO, H., KAJIMOTO, Y., MIYAGAWA, J., MATSUOKA, T., FUJITANI, Y., UMAYAHARA, Y., HANAFUSA, T., MATSUZAWA, Y., YAMASAKI, Y. & HORI, M. 1999. Beneficial effects of antioxidants in diabetes: possible protection of pancreatic beta-cells against glucose toxicity. *Diabetes,* 48**,** 2398-406.

KANETO, H., SHARMA, A., SUZUMA, K., LAYBUTT, D. R., XU, G., BONNER-WEIR, S. & WEIR, G. C. 2002. Induction of c-Myc expression suppresses insulin gene transcription by inhibiting NeuroD/BETA2-mediated transcriptional activation. *J Biol Chem,* 277**,** 12998-3006.

KANETO, H., SUZUMA, K., SHARMA, A., BONNER-WEIR, S., KING, G. L. & WEIR, G. C. 2002. Involvement of protein kinase C beta 2 in c-myc induction by high glucose in pancreatic beta-cells. *J Biol Chem,* 277**,** 3680-5.

KANETO, H., XU, G., FUJII, N., KIM, S., BONNER-WEIR, S. & WEIR, G. C. 2002. Involvement of c-Jun N-terminal kinase in oxidative stress-mediated suppression of insulin gene expression. *J Biol Chem,* 277**,** 30010-8.

KANG, C. & KIM, E. 2010. Synergistic effect of curcumin and insulin on muscle cell glucose metabolism. *Food and Chemical Toxicology Food and Chemical Toxicology,* 48**,** 2366-2373.

KANG, L. I., MARS, W. M. & MICHALOPOULOS, G. K. 2012. Signals and cells involved in regulating liver regeneration. *Cells,* 1**,** 1261-92.

KANSKI, J., AKSENOVA, M., STOYANOVA, A. & BUTTERFIELD, D. A. 2002. Ferulic acid antioxidant protection against hydroxyl and peroxyl radical oxidation in synaptosomal and neuronal cell culture systems in vitro: structure-activity studies. *J Nutr Biochem,* 13**,** 273-281.

KARADAG, A., OZCELIK, B. & SANER, S. 2009. Review of methods to determine antioxidant capacities. *Food Analytical Methods,* 2**,** 41-60.

KARSLIOGLU, E., KLEINBERGER, J. W., SALIM, F. G., COX, A. E., TAKANE, K. K., SCOTT, D. K. & STEWART, A. F. 2011. cMyc is a principal upstream driver of beta-cell proliferation in rat insulinoma cell lines and is an effective mediator of human beta-cell replication. *Mol Endocrinol,* 25**,** 1760-72.

KARTHIK, D., VISWANATHAN, P. & ANURADHA, C. V. 2011. Administration of rosmarinic acid reduces cardiopathology and blood pressure through inhibition of p22phox NADPH oxidase in fructose-fed hypertensive rats. *Journal of Cardiovascular Pharmacology,* 58**,** 514.

KASONO, K., YASU, T., KAKEHASHI, A., KINOSHITA, N., TAMEMOTO, H., NAMAI, K., OHNO, R., UEBA, H., KUROKI, M. & ISHIKAWA, S. 2004. Nicorandil improves diabetes and rat islet beta-cell damage induced by streptozotocin in vivo and in vitro. *European journal of endocrinology,* 151**,** 277-285.

KEISARI, Y., BRAUN, L. & FLESCHER, E. 1983. The oxidative burst and related phenomena in mouse macrophages elicited by different sterile inflammatory stimuli. *Immunobiology,* 165**,** 78-89.

KEPPLER, D., LEIER, I. & JEDLITSCHKY, G. 1997. Transport of glutathione conjugates and glucuronides by the multidrug resistance proteins MRP1 and MRP2. *Biol Chem,* 378**,** 787-91.

KERN, S. M., BENNETT, R. N., NEEDS, P. W., MELLON, F. A., KROON, P. A. & GARCIA-CONESA, M. T. 2003. Characterization of metabolites of hydroxycinnamates in the in vitro model of human small intestinal epithelium caco-2 cells. *Journal of Agricultural and Food Chemistry,* 51**,** 7884-7891.

KERR, J. F., WYLLIE, A. H. & CURRIE, A. R. 1972. Apoptosis: a basic biological phenomenon with wide-ranging implications in tissue kinetics. *Br J Cancer,* 26**,** 239-57.

KIBITI, C. M. & AFOLAYAN, A. J. 2015. Herbal therapy: A review of emerging pharmacological tools in the management of diabetes mellitus in Africa. *Pharmacognosy Magazine,* 11**,** S258-74.

KIM, B., KIM, H. S., JUNG, E. J., LEE, J. Y., K TSANG, B., LIM, J. M. & SONG, Y. S. 2015. Curcumin induces ER stress-mediated apoptosis through selective generation of reactive oxygen species in cervical cancer cells. *Mol Carcinog*.

KIM, H., RAFIUDDIN-SHAH, M., TU, H.-C., JEFFERS, J. R., ZAMBETTI, G. P., HSIEH, J. J. D. & CHENG, E. H. Y. 2006. Hierarchical regulation of mitochondrion-dependent apoptosis by BCL-2 subfamilies. *Nat Cell Biol,* 8**,** 1348-1358.

KIM, H. G., LEE, J. H., LEE, S. J., OH, J. H., SHIN, E., JANG, Y. P. & LEE, Y. J. 2012. The increased cellular uptake and biliary excretion of curcumin by quercetin: a possible role of albumin binding interaction. *Drug Metab Dispos,* 40**,** 1452-5.

KIM, J. A., KANG, Y. S., KIM, Y. O., LEE, S. H. & LEE, Y. S. 1998. Role of Ca2+ influx in the tert-butyl hydroperoxide-induced apoptosis of HepG2 human hepatoblastoma cells. *Exp Mol Med,* 30**,** 137-44.

KIM, J. K., KIM, Y. J., FILLMORE, J. J., CHEN, Y., MOORE, I., LEE, J., YUAN, M., LI, Z. W., KARIN, M., PERRET, P., SHOELSON, S. E. & SHULMAN, G. I. 2001. Prevention of fat-induced insulin resistance by salicylate. *J Clin Invest,* 108**,** 437-46.

KIM, M. K., JUNG, H. S., YOON, C. S., KO, J. H., CHUN, H. J., KIM, T. K., KWON, M. J., LEE, S. H., KOH, K. S., RHEE, B. D. & PARK, J. H. 2010. EGCG and quercetin protected INS-1 cells in oxidative stress via different mechanisms. *Front Biosci (Elite Ed),* 2**,** 810-7.

KIM, S. J., GERSHOV, D., MA, X., BROT, N. & ELKON, K. B. 2002. I-PLA(2) activation during apoptosis promotes the exposure of membrane lysophosphatidylcholine leading to binding by natural immunoglobulin M antibodies and complement activation. *J Exp Med,* 196**,** 655-65.

KIM, Y., CHOI, Y., HAM, H., JEONG, H.-S. & LEE, J. 2013. Protective effects of oligomeric and polymeric procyanidin fractions from defatted grape seeds on tert-butyl hydroperoxide-induced oxidative damage in HepG2 cells. *Food Chemistry,* 137**,** 136-141.

KLIP, A. & PAQUET, M. R. 1990. Glucose transport and glucose transporters in muscle and their metabolic regulation. *Diabetes Care,* 13**,** 228-43.

KNASMÜLLER, S., MERSCH-SUNDERMANN, V., KEVEKORDES, S., DARROUDI, F., HUBER, W. W., HOELZL, C., BICHLER, J. & MAJER, B. J. 2004. Use of human-

derived liver cell lines for the detection of environmental and dietary genotoxicants; current state of knowledge. *Toxicology,* 198**,** 315-328.

KNEKT, P., JARVINEN, R., REUNANEN, A. & MAATELA, J. 1996. Flavonoid intake and coronary mortality in Finland: a cohort study. *BMJ,* 312**,** 478-81.

KOEK, G. H., LIEDORP, P. R. & BAST, A. 2011. The role of oxidative stress in non-alcoholic steatohepatitis. *Clinica Chimica Acta,* 412**,** 1297-1305.

KOLODZIEJCZYK, J., OLAS, B., SALUK-JUSZCZAK, J. & WACHOWICZ, B. 2011. Antioxidative properties of curcumin in the protection of blood platelets against oxidative stress in vitro. *Platelets,* 22**,** 270-6.

KONISHI, H., TANAKA, M., TAKEMURA, Y., MATSUZAKI, H., ONO, Y., KIKKAWA, U. & NISHIZUKA, Y. 1997. Activation of protein kinase C by tyrosine phosphorylation in response to H2O2. *Proc Natl Acad Sci U S A,* 94**,** 11233-7.

KONISHI, Y., HITOMI, Y., YOSHIDA, M. & YOSHIOKA, E. 2005. Pharmacokinetic study of caffeic and rosmarinic acids in rats after oral administration. *Journal of Agricultural and Food Chemistry,* 53**,** 4740-6.

KONISHI, Y. & KOBAYASHI, S. 2004. Microbial metabolites of ingested caffeic acid are absorbed by the monocarboxylic acid transporter (MCT) in intestinal caco-2 cell monolayers. *Journal of Agricultural and Food Chemistry,* 52**,** 6418-6424.

KOOPMAN, G., REUTELINGSPERGER, C. P., KUIJTEN, G. A., KEEHNEN, R. M., PALS, S. T. & VAN OERS, M. H. 1994. Annexin V for flow cytometric detection of phosphatidylserine expression on B cells undergoing apoptosis. *Blood,* 84**,** 1415-20.

KORUK, M., TAYSI, S., SAVAS, M. C., YILMAZ, O., AKCAY, F. & KARAKOK, M. 2004. Oxidative stress and enzymatic antioxidant status in patients with nonalcoholic steatohepatitis. *Ann Clin Lab Sci,* 34**,** 57-62.

KOWLURU, R. A. & KANWAR, M. 2007. Effects of curcumin on retinal oxidative stress and inflammation in diabetes. *Nutr Metab (Lond),* 4**,** 8.

KROON, P. A., FAULDS, C. B., RYDEN, P., ROBERTSON, J. A. & WILLIAMSON, G. 1997. Release of covalently bound ferulic acid from fiber in the human colon. *Journal of Agricultural and Food Chemistry,* 45**,** 661-667.

KUCERA, O. & CERVINKOVA, Z. 2014. Experimental models of non-alcoholic fatty liver disease in rats. *World J Gastroenterol,* 20**,** 8364-76.

KULKARNI, R. N., MIZRACHI, E. B., OCANA, A. G. & STEWART, A. F. 2012. Human beta-cell proliferation and intracellular signaling: driving in the dark without a road map. *Diabetes,* 61**,** 2205-13.

KULTZ, D. 2005. Molecular and evolutionary basis of the cellular stress response. *Annu Rev Physiol,* 67**,** 225-57.

KUNNUMAKKARA, A. B., DIAGARADJANE, P., ANAND, P., KUZHUVELIL, H. B., DEORUKHKAR, A., GELOVANI, J., GUHA, S., KRISHNAN, S. & AGGARWAL, B. B. 2009. Curcumin sensitizes human colorectal cancer to capecitabine by modulation of cyclin D1, COX-2, MMP-9, VEGF and CXCR4 expression in an orthotopic mouse model. *International Journal of Cancer,* 125**,** 2187-2197.

KUO, M., ZILBERFARB, V., GANGNEUX, N., CHRISTEFF, N. & ISSAD, T. 2008. O-GlcNAc modification of FoxO1 increases its transcriptional activity: a role in the glucotoxicity phenomenon? *Biochimie,* 90**,** 679-85.

KURISU, M., NAKASONE, R., MIYAMAE, Y., MATSUURA, D., KANATANI, H., YANO, S. & SHIGEMORI, H. 2013. Induction of hepatocyte growth factor production in human dermal fibroblasts by caffeic acid derivatives. *Biol Pharm Bull,* 36**,** 2018-21.

KUZU, N., BAHCECIOGLU, I. H., DAGLI, A. F., OZERCAN, I. H., USTUNDAG, B. & SAHIN, K. 2008. Epigallocatechin gallate attenuates experimental non-alcoholic steatohepatitis induced by high fat diet. *J Gastroenterol Hepatol,* 23**,** e465-70.

LAFAY, S., MORAND, C., MANACH, C., BESSON, C. & SCALBERT, A. 2006. Absorption and metabolism of caffeic acid and chlorogenic acid in the small intestine of rats. *British Journal of Nutrition,* 96**,** 39-46.

LAI, R. H., MILLER, M. J. & JEFFERY, E. 2010. Glucoraphanin hydrolysis by microbiota in the rat cecum results in sulforaphane absorption. *Food & function,* 1**,** 161-6.

LAMSON, D. W. & BRIGNALL, M. S. 2000. Antioxidants and cancer, part 3: quercetin. *Altern Med Rev,* 5**,** 196-208.

LANDER, H. M., HAJJAR, D. P., HEMPSTEAD, B. L., MIRZA, U. A., CHAIT, B. T., CAMPBELL, S. & QUILLIAM, L. A. 1997. A molecular redox switch on p21(ras). Structural basis for the nitric oxide-p21(ras) interaction. *J Biol Chem,* 272**,** 4323-6.

LAO, C. D., RUFFIN, M. T. T., NORMOLLE, D., HEATH, D. D., MURRAY, S. I., BAILEY, J. M., BOGGS, M. E., CROWELL, J., ROCK, C. L. & BRENNER, D. E. 2006. Dose escalation of a curcuminoid formulation. *BMC complementary and alternative medicine,* 6.

LAPIDOT, T., WALKER, M. D. & KANNER, J. 2002. Antioxidant and prooxidant effects of phenolics on pancreatic beta-cells in vitro. *J Agric Food Chem,* 50**,** 7220-5.

LAU, A., VILLENEUVE, N. F., SUN, Z., WONG, P. K. & ZHANG, D. D. 2008. Dual roles of Nrf2 in cancer. *Pharmacological Research,* 58**,** 262-270.

LEE-HILZ, Y. Y., BOERBOOM, A. M., WESTPHAL, A. H., BERKEL, W. J., AARTS, J. M. & RIETJENS, I. M. 2006. Pro-oxidant activity of flavonoids induces EpRE-mediated gene expression. *Chem Res Toxicol,* 19**,** 1499-505.

LEE, C. H., OLSON, P. & EVANS, R. M. 2003. Minireview: lipid metabolism, metabolic diseases, and peroxisome proliferator-activated receptors. *Endocrinology,* 144**,** 2201-7.

LEE, J., JUNG, E., KOH, J., KIM, Y. S. & PARK, D. 2008. Effect of rosmarinic acid on atopic dermatitis. *The Journal of Dermatology,* 35**,** 768-771.

LEE, J. H., PARK, K. H., LEE, M. H., KIM, H. T., SEO, W. D., KIM, J. Y., BAEK, I. Y., JANG, D. S. & HA, T. J. 2013. Identification, characterisation, and quantification of phenolic compounds in the antioxidant activity-containing fraction from the seeds of Korean perilla (Perilla frutescens) cultivars. *Food Chemistry,* 136**,** 843-852.

LELOUP, C., MAGNAN, C., BENANI, A., BONNET, E., ALQUIER, T., OFFER, G., CARRIERE, A., PERIQUET, A., FERNANDEZ, Y., KTORZA, A., CASTEILLA, L. & PENICAUD, L. 2006. Mitochondrial reactive oxygen species are required for hypothalamic glucose sensing. *Diabetes,* 55**,** 2084-90.

LELOUP, C., TOURREL-CUZIN, C., MAGNAN, C., KARACA, M., CASTEL, J., CARNEIRO, L., COLOMBANI, A. L., KTORZA, A., CASTEILLA, L. & PENICAUD, L. 2009. Mitochondrial reactive oxygen species are obligatory signals for glucose-induced insulin secretion. *Diabetes,* 58**,** 673-81.

LENZEN, S. 2008. The mechanisms of alloxan- and streptozotocin-induced diabetes. *Diabetologia,* 51**,** 216-226.

LENZEN, S., DRINKGERN, J. & TIEDGE, M. 1996. Low antioxidant enzyme gene expression in pancreatic islets compared with various other mouse tissues. *Free Radic Biol Med,* 20**,** 463-6.

LEWIS, A. M., OUGH, M., HINKHOUSE, M. M., TSAO, M. S., OBERLEY, L. W. & CULLEN, J. J. 2005. Targeting NAD(P)H:quinone oxidoreductase (NQO1) in pancreatic cancer. *Mol Carcinog,* 43**,** 215-24.

LI, F., CHEN, X., XU, B. & ZHOU, H. 2015. Curcumin induces p53-independent necrosis in H1299 cells via a mitochondria-associated pathway. *Mol Med Rep,* 12**,** 7806-14.

LI, H., XIE, Y. H., YANG, Q., WANG, S. W., ZHANG, B. L., WANG, J. B., CAO, W., BI, L. L., SUN, J. Y., MIAO, S., HU, J., ZHOU, X. X. & QIU, P. C. 2012. Cardioprotective Effect of Paeonol and Danshensu Combination on Isoproterenol-Induced Myocardial Injury in Rats. *Plos One,* 7.

LI, J.-M., WANG, W., FAN, C.-Y., WANG, M.-X., ZHANG, X., HU, Q.-H. & KONG, L.-D. 2013. Quercetin preserves β-cell mass and function in fructose-induced hyperinsulinemia through modulating pancreatic Akt/FoxO1 activation. *Evidence-Based Complementary and Alternative Medicine,* 2013.

LI, L., BRAITEH, F. S. & KURZROCK, R. 2005. Liposome-encapsulated curcumin: in vitro and in vivo effects on proliferation, apoptosis, signaling, and angiogenesis. *Cancer,* 104**,** 1322-31.

LI, N., FRIGERIO, F. & MAECHLER, P. 2008. The sensitivity of pancreatic b-cells to mitochondrial injuries triggered by lipotoxicity and oxidative stress. *Biochem. Soc. Trans Biochemical Society Transactions,* 36**,** 930-4. doi 10.1042/BST0360930.

LI, W., WANG, S., FENG, J., XIAO, Y., XUE, X., ZHANG, H., WANG, Y. & LIANG, X. 2009. Structure elucidation and NMR assignments for curcuminoids from the

rhizomes of Curcuma longa. *MRC Magnetic Resonance in Chemistry,* 47**,** 902-908.

LI, X., SHANG, L., WU, Y., ABBAS, S., LI, D., NETTER, P., OUZZINE, M., WANG, H. & MAGDALOU, J. 2011. Identification of the human UDP-glucuronosyltransferase isoforms involved in the glucuronidation of the phytochemical ferulic acid. *Drug Metab Pharmacokinet,* 26**,** 341-50.

LIMA, C. F., FERNANDES-FERREIRA M. & PEREIRA-WILSON C. 2006. Phenolic compounds protect HepG2 cells from oxidative damage: Relevance of glutathione levels. *Life Sciences,* 79**,** 2056-2068.

LIMA, C. F., VALENTAO, P. C. R., ANDRADE, P. B., SEABRA, R. M., FERNANDES-FERREIRA, M. & PEREIRA-WILSON, C. 2007. Water and methanolic extracts of Salvia officinalis protect HepG2 cells from t-BHP induced oxidative damage. *Chemico-Biological Interactions,* 167**,** 107-115.

LIND, C. 1985. Formation of benzo[a]pyrene-3,6-quinol mono- and diglucuronides in rat liver microsomes. *Arch Biochem Biophys,* 240**,** 226-35.

LIND, C., HOCHSTEIN, P. & ERNSTER, L. 1982. DT-diaphorase as a quinone reductase: a cellular control device against semiquinone and superoxide radical formation. *Arch Biochem Biophys,* 216**,** 178-85.

LIU, R. H. 2004. Potential synergy of phytochemicals in cancer prevention: mechanism of action. *J Nutr,* 134**,** 3479S-3485S.

LIU, Y., FISKUM, G. & SCHUBERT, D. 2002. Generation of reactive oxygen species by the mitochondrial electron transport chain. *J Neurochem,* 80**,** 780-7.

LIU, Y. H., MO, S. L., BI, H. C., HU, B. F., LI, C. G., WANG, Y. T., HUANG, L., HUANG, M., DUAN, W., LIU, J. P., WEI, M. Q. & ZHOU, S. F. 2011. Regulation of human pregnane X receptor and its target gene cytochrome P450 3A4 by Chinese herbal compounds and a molecular docking study. *Xenobiotica,* 41**,** 259-280.

LOWRY, O. H., ROSEBROUGH, N. J., FARR, A. L. & RANDALL, R. J. 1951. Protein measurement with the Folin phenol reagent. *J Biol Chem,* 193**,** 265-75.

LU, J. M., LIN, P. H., YAO, Q. & CHEN, C. 2010. Chemical and molecular mechanisms of antioxidants: experimental approaches and model systems. *J Cell Mol Med,* 14**,** 840-60.

LUDWIG, J., VIGGIANO, T. R., MCGILL, D. B. & OH, B. J. 1980. Nonalcoholic steatohepatitis: Mayo Clinic experiences with a hitherto unnamed disease. *Mayo Clin Proc,* 55**,** 434-8.

MACFARLANE, W. M., CHAPMAN, J. C., SHEPHERD, R. M., HASHMI, M. N., KAMIMURA, N., COSGROVE, K. E., O'BRIEN, R. E., BARNES, P. D., HART, A. W., DOCHERTY, H. M., LINDLEY, K. J., AYNSLEY-GREEN, A., JAMES, R. F., DOCHERTY, K. & DUNNE, M. J. 1999. Engineering a glucose-responsive human insulin-secreting cell line from islets of Langerhans isolated from a patient with persistent hyperinsulinemic hypoglycemia of infancy. *J Biol Chem,* 274**,** 34059-66.

MACGREGOR, J. T. & JURD, L. 1978. Mutagenicity of plant flavonoids: structural requirements for mutagenic activity in Salmonella typhimurium. *Mutat Res,* 54**,** 297-309.

MADAN, A., GRAHAM, R. A., CARROLL, K. M., MUDRA, D. R., BURTON, L. A., KRUEGER, L. A., DOWNEY, A. D., CZERWINSKI, M., FORSTER, J. & RIBADENEIRA, M. D. 2003. Effects of prototypical microsomal enzyme inducers on cytochrome P450 expression in cultured human hepatocytes. *Drug Metabolism and Disposition,* 31**,** 421-431.

MAECHLER, P. & WOLLHEIM, C. B. 1999. Mitochondrial glutamate acts as a messenger in glucose-induced insulin exocytosis. *Nature,* 402**,** 685-9.

MAGALHÃES, L. M., SEGUNDO, M. A., REIS, S. & LIMA, J. L. 2008. Methodological aspects about in vitro evaluation of antioxidant properties. *Anal Chim Acta,* 613**,** 1-19.

MAGALHÃES, L. M., SEGUNDO, M. A., SIQUET, C., REIS, S. & LIMA, J. L. 2007. Multi-syringe flow injection system for the determination of the scavenging capacity of the diphenylpicrylhydrazyl radical in methanol and ethanolic media. *Microchimica Acta,* 157**,** 113-118.

MAGEE, C. J., GHANEH, P. & NEOPTOLEMOS, J. P. 2002. Surgical and medical therapy for pancreatic carcinoma. *Best Pract Res Clin Gastroenterol,* 16**,** 435-55.

MAGESH, S., CHEN, Y. & HU, L. 2012. Small molecule modulators of Keap1-Nrf2-ARE pathway as potential preventive and therapeutic agents. *Med Res Rev,* 32**,** 687-726.

MAGRUDER, J. T., ELAHI, D. & ANDERSEN, D. K. 2011. Diabetes and pancreatic cancer: chicken or egg? *Pancreas,* 40**,** 339-51.

MALHI, H. & GORES, G. J. 2008. Molecular mechanisms of lipotoxicity in nonalcoholic fatty liver disease. *Semin Liver Dis,* 28**,** 360-9.

MALUMBRES, M. & BARBACID, M. 2009. Cell cycle, CDKs and cancer: a changing paradigm. *Nat Rev Cancer,* 9**,** 153-166.

MANCO, M., MARCELLINI, M., DEVITO, R., COMPARCOLA, D., SARTORELLI, M. R. & NOBILI, V. 2008. Metabolic syndrome and liver histology in paediatric non-alcoholic steatohepatitis. *Int J Obes (Lond),* 32**,** 381-7.

MANCUSO, C. & SANTANGELO, R. 2014. Ferulic acid: Pharmacological and toxicological aspects. *Food and Chemical Toxicology,* 65**,** 185-195.

MANN, M. & JENSEN, O. N. 2003. Proteomic analysis of post-translational modifications. *Nat Biotechnol,* 21**,** 255-61.

MARINI, M. G., CHAN, K., CASULA, L., KAN, Y. W., CAO, A. & MOI, P. 1997. hMAF, a small human transcription factor that heterodimerizes specifically with Nrf1 and Nrf2. *J Biol Chem,* 272**,** 16490-7.

MÄRKI, F. & MARTIUS, C. 1960. Vitamin K reductase preparation and properties. *Biochem. Soc. Trans Biochemical Society Transactions Z.,,* 333**,** 111-135.

MARRA, F., GASTALDELLI, A., SVEGLIATI BARONI, G., TELL, G. & TIRIBELLI, C. 2008. Molecular basis and mechanisms of progression of non-alcoholic steatohepatitis. *Trends in molecular medicine,* 14**,** 72-81.

MATEOS, R., GOYA, L. & BRAVO, L. 2006. Uptake and metabolism of hydroxycinnamic acids (chlorogenic, caffeic, and ferulic acids) by HepG2 cells as a model of the human liver. *Journal of Agricultural and Food Chemistry,* 54**,** 8724-8732.

MATTEUCCI, C., GRELLI, S., DE SMAELE, E., FONTANA, C. & MASTINO, A. 1999. Identification of nuclei from apoptotic, necrotic, and viable lymphoid cells by using multiparameter flow cytometry. *Cytometry,* 35**,** 145-53.

MCCLUSKEY, J. T., HAMID, M., GUO-PARKE, H., MCCLENAGHAN, N. H., GOMIS, R. & FLATT, P. R. 2011. Development and functional characterization of insulin-releasing human pancreatic beta cell lines produced by electrofusion. *J Biol Chem,* 286**,** 21982-92.

MCNALLY, S. J., HARRISON, E. M., ROSS, J. A., GARDEN, O. J. & WIGMORE, S. J. 2007. Curcumin induces heme oxygenase 1 through generation of reactive oxygen species, p38 activation and phosphatase inhibition. *International Journal of Molecular Medicine,* 19**,** 165-172.

MEGHANA, K., SANJEEV, G. & RAMESH, B. 2007. Curcumin prevents streptozotocin-induced islet damage by scavenging free radicals: A prophylactic and protective role. *European Journal of Pharmacology,* 577**,** 183-191.

METODIEWA, D., JAISWAL, A. K., CENAS, N., DICKANCAITE, E. & SEGURA-AGUILAR, J. 1999. Quercetin may act as a cytotoxic prooxidant after its metabolic activation to semiquinone and quinoidal product. *Free Radic Biol Med,* 26**,** 107-16.

METZLER, M., PFEIFFER, E., SCHULZ, S. I. & DEMPE, J. S. 2013. Curcumin uptake and metabolism. *BioFactors (Oxford, England),* 39.

MICHALOPOULOS, G. K. 1990. Liver regeneration: molecular mechanisms of growth control. *FASEB J,* 4**,** 176-87.

MINCU, I. & IONESCU-TIRGOVISTE, C. 1980. Half-life and hypoglycemic effect of intravenous insulin in patients with diabetic ketoacidosis. *Med Interne,* 18**,** 287-92.

MIZUKAMI, H., TAKAHASHI, K., INABA, W., TSUBOI, K., OSONOI, S., YOSHIDA, T. & YAGIHASHI, S. 2014. Involvement of Oxidative Stress-Induced DNA Damage, Endoplasmic Reticulum Stress, and Autophagy Deficits in the Decline of beta-Cell Mass in Japanese Type 2 Diabetic Patients. *Diabetes Care*.

MONTELLA, L., PALMIERI, G., ADDEO, R. & DEL PRETE, S. 2016. Hepatocellular carcinoma: Will novel targeted drugs really impact the next future? *World J Gastroenterol,* 22**,** 6114-26.

MOORE, J., YIN, J.-J. & YU, L. 2006. Novel fluorometric assay for hydroxyl radical scavenging capacity (HOSC) estimation. *Journal of Agricultural and Food Chemistry,* 54**,** 617-626.

MORALES-GONZALEZ, J. A., MADRIGAL-SANTILLAN, E., MORALES-GONZALEZ, A., BAUTISTA, M., GAYOSSO-ISLAS, E. & SANCHEZ-MORENO, C. 2015. What is Known Regarding the Participation of Factor Nrf-2 in Liver Regeneration? *Cells,* 4**,** 169-77.

MORIDANI, M. Y., SCOBIE, H., JAMSHIDZADEH, A., SALEHI, P. & O'BRIEN, P. J. 2001. Caffeic acid, chlorogenic acid, and dihydrocaffeic acid metabolism: Glutathione conjugate formation. *Drug Metabolism and Disposition,* 29**,** 1432-1439.

MOTOHASHI, H., O'CONNOR, T., KATSUOKA, F., ENGEL, J. D. & YAMAMOTO, M. 2002. Integration and diversity of the regulatory network composed of Maf and CNC families of transcription factors. *Gene,* 294**,** 1-12.

MOTOHASHI, H. & YAMAMOTO, M. 2004. Nrf2–Keap1 defines a physiologically important stress response mechanism. *Trends in molecular medicine,* 10**,** 549-557.

MULLEN, W., ROUANET, J. M., AUGER, C., TEISSEDRE, P. L., CALDWELL, S. T., HARTLEY, R. C., LEAN, M. E., EDWARDS, C. A. & CROZIER, A. 2008. Bioavailability of [2-(14)C]quercetin-4'-glucoside in rats. *J Agric Food Chem,* 56**,** 12127-37.

MUROTA, K. & TERAO, J. 2003. Antioxidative flavonoid quercetin: implication of its intestinal absorption and metabolism. *Archives of Biochemistry and Biophysics Archives of Biochemistry and Biophysics,* 417**,** 12-17.

NABAVI, S. F., RUSSO, G. L., DAGLIA, M. & NABAVI, S. M. 2015. Role of quercetin as an alternative for obesity treatment: You are what you eat! *Food Chemistry,* 179**,** 305-310.

NAIT, C. M., AL AHMAD, A., PELUSO, J., MULLER, C. D. & UBEAUD, G. 2009. Quercetin and naringenin transport across human intestinal Caco-2 cells. *J Pharm Pharmacol,* 61**,** 1473-83.

NAKAZAWA, T. & OHSAWA, K. 1998. Metabolism of rosmarinic acid in rats. *Journal of Natural Products,* 61**,** 993-996.

NAKAZAWA, T. & OHSAWA, K. 2000. Metabolites of orally administered Perilla frutescens extract in rats and humans. *Biol Pharm Bull,* 23**,** 122-7.

NARA, K., MIYOSHI, T., HONMA, T. & KOGA, H. 2006. Antioxidative activity of bound-form phenolics in potato peel. *Bioscience Biotechnology and Biochemistry,* 70**,** 1489-1491.

NARDINI, M., PISU, P., GENTILI, V., NATELLA, F., DI, M., PICCOLELLA, F. & SCACCINI, C. 1998. Effect of caffeic acid on tert-butyl hydroperoxide-induced oxidative stress in U937. *Free Radical Biology and Medicine,* 25**,** 1098-1105.

NATELLA, F., NARDINI, M., DI FELICE, M. & SCACCINI, C. 1999. Benzoic and Cinnamic Acid Derivatives as Antioxidants: Structure−Activity Relation. *Journal of Agricultural and Food Chemistry,* 47**,** 1453-1459.

NÉMETH, K., PLUMB, G. W., BERRIN, J.-G., JUGE, N., JACOB, R., NAIM, H. Y., WILLIAMSON, G., SWALLOW, D. M. & KROON, P. A. 2003. Deglycosylation by small intestinal epithelial cell b-glucosidases is a critical step in the absorption and metabolism of dietary flavonoid glycosides in humans. *Eur J Nutr European Journal of Nutrition : Zeitschrift für Ernährungswissenschaft,* 42**,** 29-42.

NENADIS, N. & TSIMIDOU, M. 2002. Observations on the estimation of scavenging activity of phenolic compounds using rapid 1,1-diphenyl-2-picrylhydrazyl (DPPH•) tests. *Journal of the American Oil Chemists' Society,* 79**,** 1191-1195.

NEWGARD, C. B. & MCGARRY, J. D. 1995. Metabolic coupling factors in pancreatic beta-cell signal transduction. *Annu Rev Biochem,* 64**,** 689-719.

NEWSHOLME, P., HABER, E., HIRABARA, S., REBELATO, E., PROCOPIO, J., MORGAN, D., OLIVEIRA-EMILIO, H., CARPINELLI, A. & CURI, R. 2007. Diabetes associated cell stress and dysfunction: role of mitochondrial and non-mitochondrial ROS production and activity. *The Journal of physiology,* 583**,** 9-24.

NGO, S. N., WILLIAMS, D. B. & HEAD, R. J. 2011. Rosemary and cancer prevention: preclinical perspectives. *Crit Rev Food Sci Nutr,* 51**,** 946-54.

NIMMI, O. & GEORGE, P. 2012. Evaluation of the antioxidant potential of a newly developed polyherbal formulation for antiobesity. *Int. J. Pharm. Pharm. Sci,* 4**,** 505-510.

NIOI, P. & HAYES, J. D. 2004. Contribution of NAD(P)H:quinone oxidoreductase 1 to protection against carcinogenesis, and regulation of its gene by the Nrf2 basic-region leucine zipper and the arylhydrocarbon receptor basic helix-loop-helix transcription factors. *Mutat Res,* 555**,** 149-71.

NISHIKAWA, T., EDELSTEIN, D., DU, X. L., YAMAGISHI, S., MATSUMURA, T., KANEDA, Y., YOREK, M. A., BEEBE, D., OATES, P. J., HAMMES, H. P., GIARDINO, I. & BROWNLEE, M. 2000. Normalizing mitochondrial superoxide production blocks three pathways of hyperglycaemic damage. *Nature,* 404**,** 787-90.

NISHIZAWA, M., IZUHARA, R., KANEKO, K. & FUJIMOTO, Y. 1987. 3-Caffeoyl-4-sinapoylquinic acid, a novel lipoxygenase inhibitor from Gardeniae fructus. *Chemical and pharmaceutical bulletin,* 35**,** 2133-2135.

NITURE, S. K., JAIN, A. K. & JAISWAL, A. K. 2009. Antioxidant-induced modification of INrf2 cysteine 151 and PKC-delta-mediated phosphorylation of Nrf2 serine 40 are both required for stabilization and nuclear translocation of Nrf2 and increased drug resistance. *J Cell Sci,* 122**,** 4452-64.

NOLAN, C. J., LEAHY, J. L., DELGHINGARO-AUGUSTO, V., MOIBI, J., SONI, K., PEYOT, M. L., FORTIER, M., GUAY, C., LAMONTAGNE, J., BARBEAU, A., PRZYBYTKOWSKI, E., JOLY, E., MASIELLO, P., WANG, S., MITCHELL, G. A. & PRENTKI, M. 2006. Beta cell compensation for insulin resistance in Zucker fatty rats: increased lipolysis and fatty acid signalling. *Diabetologia,* 49**,** 2120-30.

O'BRIEN, P. J. 1991. Molecular mechanisms of quinone cytotoxicity. *Chemico-Biological Interactions,* 80**,** 1-41.

O'LEARY, K. A., DAY, A. J., NEEDS, P. W., MELLON, F. A., OBRIEN, N. M. & WILLIAMSON, G. 2003. Metabolism of quercetin-7- and quercetin-3-glucuronides by an in vitro hepatic model: the role of human b-glucuronidase, sulfotransferase, catechol- O-methyltransferase and multi-resistant protein 2 (MRP2) in flavonoid metabolism. *BCP</cja:jid> Biochemical Pharmacology,* 65**,** 479-491.

OKITA, M., HAYASHI, M., SASAGAWA, T., TAKAGI, K., SUZUKI, K., KINOYAMA, S., ITO, T. & YAMADA, G. 2001. Effect of a moderately energy-restricted diet on obese patients with fatty liver. *Nutrition,* 17**,** 542-7.

OKUTAN, H., OZCELIK, N., YILMAZ, H. R. & UZ, E. 2005. Effects of caffeic acid phenethyl ester on lipid peroxidation and antioxidant enzymes in diabetic rat heart. *Clinical Biochemistry,* 38**,** 191-196.

OMENN, G. S., GOODMAN, G. E., THORNQUIST, M. D., BALMES, J., CULLEN, M. R., GLASS, A., KEOGH, J. P., MEYSKENS, F. L., VALANIS, B., WILLIAMS, J. H., BARNHART, S. & HAMMAR, S. 1996. Effects of a combination of beta carotene and vitamin A on lung cancer and cardiovascular disease. *N Engl J Med,* 334**,** 1150-5.

OSAKABE, N., YASUDA, A., NATSUME, M. & YOSHIKAWA, T. 2004. Rosmarinic acid inhibits epidermal inflammatory responses: anticarcinogenic effect of Perilla frutescens extract in the murine two-stage skin model. *Carcinogenesis,* 25**,** 549-557.

OU, S. & KWOK, K. C. 2004. Ferulic acid: pharmaceutical functions, preparation and applications in foods. *Journal of the Science of Food and Agriculture,* 84**,** 1261-1269.

OVERMAN, A., CHUANG, C. C. & MCINTOSH, M. 2011. Quercetin attenuates inflammation in human macrophages and adipocytes exposed to macrophage-conditioned media. *Int J Obes (Lond),* 35**,** 1165-72.

PAN, M. H., HUANG, T. M. & LIN, J. K. 1999. Biotransformation of curcumin through reduction and glucuronidation in mice. *Drug metabolism and disposition: the biological fate of chemicals,* 27**,** 486-94.

PANCHATCHARAM, M., MIRIYALA, S., GAYATHRI, V. S. & SUGUNA, L. 2006. Curcumin improves wound healing by modulating collagen and decreasing reactive oxygen species. *Mol Cell Biochem,* 290**,** 87-96.

PANG, C., ZHENG, Z., SHI, L., SHENG, Y., WEI, H., WANG, Z. & JI, L. 2016. Caffeic acid prevents acetaminophen-induced liver injury by activating the Keap1-Nrf2 antioxidative defense system. *Free Radical Biology and Medicine,* 91**,** 236-246.

PARK, H. Y., NAM, M. H., LEE, H. S., JUN, W., HENDRICH, S. & LEE, K. W. 2010. Isolation of caffeic acid from Perilla frutescens and its role in enhancing gamma-glutamylcysteine synthetase activity and glutathione level. *Food Chemistry,* 119**,** 724-730.

PARK, S. Y., KIM, G. Y., BAE, S. J., YOO, Y. H. & CHOI, Y. H. 2007. Induction of apoptosis by isothiocyanate sulforaphane in human cervical carcinoma HeLa and hepatocarcinoma HepG2 cells through activation of caspase-3. *Oncol Rep,* 18**,** 181-7.

PAYTON, F., SANDUSKY, P. & ALWORTH, W. L. 2007. NMR study of the solution structure of curcumin. *Journal of Natural Products,* 70**,** 143-6.

PEROCCO, P., BRONZETTI, G., CANISTRO, D., VALGIMIGLI, L., SAPONE, A., AFFATATO, A., PEDULLI, G. F., POZZETTI, L., BROCCOLI, M., IORI, R., BARILLARI, J., SBLENDORIO, V., LEGATOR, M. S., PAOLINI, M. & ABDEL-RAHMAN, S. Z. 2006. Glucoraphanin, the bioprecursor of the widely extolled chemopreventive agent sulforaphane found in broccoli, induces Phase-I xenobiotic metabolizing enzymes and increases free radical generation in rat liver. *Mutation Research-Fundamental and Molecular Mechanisms of Mutagenesis,* 595**,** 125-136.

PESSAYRE, D., FROMENTY, B. & MANSOURI, A. 2004. Mitochondrial injury in steatohepatitis. *Eur J Gastroenterol Hepatol,* 16**,** 1095-105.

PESSAYRE, D., MANSOURI, A. & FROMENTY, B. 2002. Nonalcoholic steatosis and steatohepatitis. V. Mitochondrial dysfunction in steatohepatitis. *Am J Physiol Gastrointest Liver Physiol,* 282**,** G193-9.

PETERSEN, M. & SIMMONDS, M. S. J. 2003. Rosmarinic acid. *Phytochemistry,* 62**,** 121-125.

PETRI, N., TANNERGREN, C., HOLST, B., MELLON, F. A., BAO, Y., PLUMB, G. W., BACON, J., O'LEARY, K. A., KROON, P. A., KNUTSON, L., FORSELL, P., ERIKSSON, T., LENNERNAS, H. & WILLIAMSON, G. 2003. Absorption/metabolism of sulforaphane and quercetin, and regulation of phase II enzymes, in human jejunum in vivo. *Drug metabolism and disposition: the biological fate of chemicals,* 31**,** 805-13.

PFEIFFER, E., HOEHLE, S. I., WALCH, S. G., RIESS, A., SÓLYOM, A. M. & METZLER, M. 2007. Curcuminoids form reactive glucuronides in vitro. *Journal of Agricultural and Food Chemistry,* 55**,** 538-44.

PFEIFFER, E., HÖHLE, S., SOLYOM, A. M. & METZLER, M. 2003. Studies on the stability of turmeric constituents. *JFOE</cja:jid> Journal of Food Engineering,* 56**,** 257-259.

PHAM, N. A., JACOBBERGER, J. W., SCHIMMER, A. D., CAO, P., GRONDA, M. & HEDLEY, D. W. 2004. The dietary isothiocyanate sulforaphane targets pathways of apoptosis, cell cycle arrest, and oxidative stress in human pancreatic cancer cells and inhibits tumor growth in severe combined immunodeficient mice. *Mol Cancer Ther,* 3**,** 1239-48.

PI, J., BAI, Y., ZHANG, Q., WONG, V., FLOERING, L. M., DANIEL, K., REECE, J. M., DEENEY, J. T., ANDERSEN, M. E., CORKEY, B. E. & COLLINS, S. 2007. Reactive oxygen species as a signal in glucose-stimulated insulin secretion. *Diabetes,* 56**,** 1783-91.

PI, J., ZHANG, Q., FU, J., WOODS, C. G., HOU, Y., CORKEY, B. E., COLLINS, S. & ANDERSEN, M. E. 2010. ROS signaling, oxidative stress and Nrf2 in pancreatic beta-cell function. *Toxicol Appl Pharmacol,* 244**,** 77-83.

PIAO, C. S., GAO, S., LEE, G.-H., PARK, B.-H., CHAE, S. W., CHAE, H.-J. & KIM, S. H. 2010. Sulforaphane protects ischemic injury of hearts through antioxidant pathway and mitochondrial K ATP channels. *Pharmacological Research,* 61**,** 342-348.

PIAZZON, A., VRHOVSEK, U., MASUERO, D., MATTIVI, F., MANDOJ, F. & NARDINI, M. 2012. Antioxidant Activity of Phenolic Acids and Their Metabolites: Synthesis and Antioxidant Properties of the Sulfate Derivatives of Ferulic and Caffeic Acids

and of the Acyl Glucuronide of Ferulic Acid. *Journal of Agricultural and Food Chemistry,* 60**,** 12312-12323.

PIRET, J.-P., ARNOULD, T., FUKS, B., CHATELAIN, P., REMACLE, J. & MICHIELS, C. 2004. Mitochondria permeability transition-dependent tert-butyl hydroperoxide-induced apoptosis in hepatoma HepG2 cells. *Biochemical Pharmacology,* 67**,** 611-620.

PISKULA, M. K. & TERAO, J. 1998. Accumulation of (−)-epicatechin metabolites in rat plasma after oral administration and distribution of conjugation enzymes in rat tissues. *The Journal of nutrition,* 128**,** 1172-1178.

PISONERO-VAQUERO, S., MARTINEZ-FERRERAS, A., GARCIA-MEDIAVILLA, M. V., MARTINEZ-FLOREZ, S., FERNANDEZ, A., BENET, M., OLCOZ, J. L., JOVER, R., GONZALEZ-GALLEGO, J. & SANCHEZ-CAMPOS, S. 2015. Quercetin ameliorates dysregulation of lipid metabolism genes via the PI3K/AKT pathway in a diet-induced mouse model of nonalcoholic fatty liver disease. *Mol Nutr Food Res,* 59**,** 879-93.

PLEDGIE-TRACY, A., SOBOLEWSKI, M. D. & DAVIDSON, N. E. 2007. Sulforaphane induces cell type-specific apoptosis in human breast cancer cell lines. *Mol Cancer Ther,* 6**,** 1013-21.

POITOUT, V. & ROBERTSON, R. P. 2002. Minireview: Secondary beta-cell failure in type 2 diabetes--a convergence of glucotoxicity and lipotoxicity. *Endocrinology,* 143**,** 339-42.

POQUET, L., CLIFFORD, M. N. & WILLIAMSON, G. 2008. Transport and metabolism of ferulic acid through the colonic epithelium. *Drug Metab Dispos,* 36**,** 190-7.

PORATH, J., CARLSSON, J., OLSSON, I. & BELFRAGE, G. 1975. Metal chelate affinity chromatography, a new approach to protein fractionation. *Nature,* 258**,** 598-9.

PORATH, J. & FLODIN, P. 1959. Gel filtration: a method for desalting and group separation. *Nature,* 183**,** 1657-9.

PRABHAKAR, P. K., PRASAD, R., ALI, S. & DOBLE, M. 2013. Synergistic interaction of ferulic acid with commercial hypoglycemic drugs in streptozotocin induced diabetic rats. *Phytomedicine,* 20**,** 488-94.

PRASAD, D. K., M.S., R., SAWHNEY, R. C., ILAVAZHAGAN, G. & BANERJEE, P. K. 2007. Mechanism of tert-butylhydroperoxide induced cytotoxicity in U-937 macrophages by alteration of mitochondrial function and generation of ROS. *Toxicology in Vitro,* 21**,** 846-854.

PREZIOSI, G., OBEN, J. A. & FUSAI, G. 2014. Obesity and pancreatic cancer. *Surgical Oncology,* 23**,** 61-71.

PROCHASKA, H. J., DE LONG, M. J. & TALALAY, P. 1985. On the mechanisms of induction of cancer-protective enzymes: a unifying proposal. *Proc Natl Acad Sci U S A,* 82**,** 8232-6.

PROCHASKA, H. J., SANTAMARIA, A. B. & TALALAY, P. 1992. Rapid detection of inducers of enzymes that protect against carcinogens. *Proc Natl Acad Sci U S A,* 89**,** 2394-8.

RACHAKONDA, G., XIONG, Y., SEKHAR, K. R., STAMER, S. L., LIEBLER, D. C. & FREEMAN, M. L. 2008. Covalent modification at Cys151 dissociates the electrophile sensor Keap1 from the ubiquitin ligase CUL3. *Chem Res Toxicol,* 21**,** 705-10.

RAHMAN, B., SCHNEIDER, H. P., BROER, A., DEITMER, J. W. & BROER, S. 1999. Helix 8 and helix 10 are involved in substrate recognition in the rat monocarboxylate transporter MCT1. *Biochemistry,* 38**,** 11577-84.

RAJENDRA, P. N., KARTHIKEYAN A., KARTHIKEYAN S. & REDDY B. V. 2011. Inhibitory effect of caffeic acid on cancer cell proliferation by oxidative mechanism in human HT-1080 fibrosarcoma cell line. *Mol Cell Biochem,* 349**,** 11-9.

RAMSBY, M. L., MAKOWSKI, G. S. & KHAIRALLAH, E. A. 1994. Differential detergent fractionation of isolated hepatocytes: biochemical, immunochemical and two-dimensional gel electrophoresis characterization of cytoskeletal and noncytoskeletal compartments. *Electrophoresis,* 15**,** 265-77.

RAO M U., SREENIVASULU, M., CHENGAIAH B., REDDY, K. J. & CHETTY, C. M. 2010. Herbal medicines for diabetes mellitus: a review. *Int J PharmTech Res,* 2**,** 1883-1892.

RAVINDRANATH, V. & CHANDRASEKHARA, N. 1980. Absorption and tissue distribution of curcumin in rats. *Toxicology,* 16**,** 259-65.

RDHANJAL, P. & FRY, J. R. 1997. Determinants of MTT reduction in rat hepatocytes. *Biomarkers,* 2**,** 111-6.

REPETTO, G., DEL PESO, A. & ZURITA, J. L. 2008. Neutral red uptake assay for the estimation of cell viability/cytotoxicity. *Nat. Protocols,* 3**,** 1125-1131.

RHO, M. C., AH LEE, K., MI KIM, S., SIK LEE, C., JEONG JANG, M., KOOK KIM, Y., SUN LEE, H., HYUN CHOI, Y., YONG RHIM, B. & KIM, K. 2007. Sensitization of vascular smooth muscle cell to TNF-alpha-mediated death in the presence of palmitate. *Toxicol Appl Pharmacol,* 220**,** 311-9.

RIBOLI, E. & NORAT, T. 2003. Epidemiologic evidence of the protective effect of fruit and vegetables on cancer risk. *Am J Clin Nutr,* 78**,** 559S-569S.

RICE-EVANS, C. A., MILLER, N. J. & PAGANGA, G. 1996. Structure-antioxidant activity relationships of flavonoids and phenolic acids. *Free Radical Biology and Medicine,* 20**,** 933-956.

RIVERA, L., MORON, R., SANCHEZ, M., ZARZUELO, A. & GALISTEO, M. 2008. Quercetin ameliorates metabolic syndrome and improves the inflammatory status in obese Zucker rats. *Obesity (Silver Spring),* 16**,** 2081-7.

ROBERTSON, R. P., HARMON, J., TRAN, P. O., TANAKA, Y. & TAKAHASHI, H. 2003. Glucose toxicity in beta-cells: type 2 diabetes, good radicals gone bad, and the glutathione connection. *Diabetes,* 52**,** 581-7.

ROBERTSON, R. P. & HARMON, J. S. 2007. Pancreatic islet beta-cell and oxidative stress: the importance of glutathione peroxidase. *FEBS Lett,* 581**,** 3743-8.

ROCHE, M., RONDEAU, P., SINGH, N. R., TARNUS, E. & BOURDON, E. 2008. The antioxidant properties of serum albumin. *FEBS Letters,* 582**,** 1783-1787.

ROJAS, C., PAN-CASTILLO, B., VALLS, C., PUJADAS, G., GARCIA-VALLVE, S., AROLA, L. & MULERO, M. 2014. Resveratrol enhances palmitate-induced ER stress and apoptosis in cancer cells. *Plos One,* 9**,** e113929.

ROSENDAHL, A. H., PERKS, C. M., ZENG, L., MARKKULA, A., SIMONSSON, M., ROSE, C., INGVAR, C., HOLLY, J. M. & JERNSTROM, H. 2015. Caffeine and Caffeic Acid Inhibit Growth and Modify Estrogen Receptor and Insulin-like Growth Factor I Receptor Levels in Human Breast Cancer. *Clin Cancer Res,* 21**,** 1877-87.

ROSS, D. 2004. Quinone reductases multitasking in the metabolic world. *Drug Metab Rev,* 36**,** 639-54.

ROTHWELL, J. A., MEDINA-REMÓN, A., PÉREZ-JIMÉNEZ, J., NEVEU, V., KNAZE, V., SLIMANI, N. & SCALBERT, A. 2015. Effects of food processing on polyphenol contents: A systematic analysis using Phenol-Explorer data. *MNFR Molecular Nutrition & Food Research,* 59**,** 160-170.

RUBIO, L., SERRA, A., MACIA, A., BORRAS, X., ROMERO, M. P. & MOTILVA, M. J. 2012. Validation of determination of plasma metabolites derived from thyme bioactive compounds by improved liquid chromatography coupled to tandem mass spectrometry. *Journal of Chromatography B-Analytical Technologies in the Biomedical and Life Sciences,* 905**,** 75-84.

SAKURABA, H., MIZUKAMI, H., YAGIHASHI, N., WADA, R., HANYU, C. & YAGIHASHI, S. 2002. Reduced beta-cell mass and expression of oxidative stress-related DNA damage in the islet of Japanese Type II diabetic patients. *Diabetologia,* 45**,** 85-96.

SALIMEI, P. S., MARFÈ, G., DI RENZO, L., DI STEFANO, C., GIGANTI, M. G., FILOMENI, G. & CIRIOLO, M. R. 2007. The interference of rosmarinic acid in the DNA fragmentation induced by osmotic shock. *Frontiers in Bioscience,* 12**,** 1308-1317.

SALLA, S., SUNKARA, R., OGUTU, S., WALKER, L. T. & VERGHESE, M. 2016. Antioxidant activity of papaya seed extracts against H 2 O 2 induced oxidative stress in HepG2 cells. *LWT-Food Science and Technology,* 66**,** 293-297.

SALTIEL, A. R. & KAHN, C. R. 2001. Insulin signalling and the regulation of glucose and lipid metabolism. *Nature,* 414**,** 799-806.

SÁNCHEZ-CAMPILLO, M., GABALDON, J. A., CASTILLO, J., BENAVENTE-GARCÍA, O., DEL BAÑO, M. J., ALCARAZ, M., VICENTE, V., ALVAREZ, N. & LOZANO, J.

A. 2009. Rosmarinic acid, a photo-protective agent against UV and other ionizing radiations. *Food and Chemical Toxicology,* 47**,** 386-392.

SANTOS, S. A., FREIRE, C. S., DOMINGUES, M. R. M., SILVESTRE, A. J. & NETO, C. P. 2011. Characterization of phenolic components in polar extracts of Eucalyptus globulus Labill. bark by high-performance liquid chromatography–mass spectrometry. *Journal of Agricultural and Food Chemistry,* 59**,** 9386-9393.

SAULNIER, L., VIGOUROUX, J. & THIBAULT, J.-F. 1995. Isolation and partial characterization of feruloylated oligosaccharides from maize bran. *Carbohydrate Research,* 272**,** 241-253.

SCHAFER, Z. T. & KORNBLUTH, S. 2006. The apoptosome: physiological, developmental, and pathological modes of regulation. *Dev Cell,* 10**,** 549-61.

SCHWABE, R. F. & BRENNER, D. A. 2007. Nuclear factor-kappaB in the liver: friend or foe? *Gastroenterology,* 132**,** 2601-4.

SEGURA-AGUILAR, J. & LIND, C. 1989. On the mechanism of the Mn3(+)-induced neurotoxicity of dopamine:prevention of quinone-derived oxygen toxicity by DT diaphorase and superoxide dismutase. *Chem Biol Interact,* 72**,** 309-24.

SEMPOUX, C., GUIOT, Y., DUBOIS, D., MOULIN, P. & RAHIER, J. 2001. Human type 2 diabetes: morphological evidence for abnormal beta-cell function. *Diabetes,* 50 Suppl 1**,** S172-7.

SERMEUS, A., GENIN, M., MAINCENT, A., FRANSOLET, M., NOTTE, A., LECLERE, L., RIQUIER, H., ARNOULD, T. & MICHIELS, C. 2012. Hypoxia-induced modulation of apoptosis and BCL-2 family proteins in different cancer cell types.

SERVIDDIO, G., BELLANTI, F., TAMBORRA, R., ROLLO, T., CAPITANIO, N., ROMANO, A. D., SASTRE, J., VENDEMIALE, G. & ALTOMARE, E. 2008. Uncoupling protein-2 (UCP2) induces mitochondrial proton leak and increases susceptibility of non-alcoholic steatohepatitis (NASH) liver to ischaemia-reperfusion injury. *Gut,* 57**,** 957-65.

SHARMA, R. A., EUDEN, S. A., PLATTON, S. L., COOKE, D. N., SHAFAYAT, A., HEWITT, H. R., MARCZYLO, T. H., MORGAN, B., HEMINGWAY, D., PLUMMER, S. M., PIRMOHAMED, M., GESCHER, A. J. & STEWARD, W. P. 2004. Phase I clinical trial of oral curcumin: biomarkers of systemic activity and compliance. *Clinical cancer research : an official journal of the American Association for Cancer Research,* 10**,** 6847-54.

SHARMA, R. A., GESCHER, A. J. & STEWARD, W. P. 2005. Curcumin: The story so far. *European Journal of Cancer European Journal of Cancer,* 41**,** 1955-1968.

SHARMA, R. A., STEWARD, W. P. & GESCHER, A. J. 2007. Pharmacokinetics and pharmacodynamics of curcumin. *Advances in experimental medicine and biology,* 595**,** 453-70.

SHARMA, S., KULKARNI, S. K. & CHOPRA, K. 2006. Curcumin, the active principle of turmeric (Curcuma longa), ameliorates diabetic nephropathy in rats. *Clin Exp Pharmacol Physiol,* 33**,** 940-5.

SHIFFLET, A. & WU, G. Y. 2009. Non-alcoholic steatohepatitis: an overview. *J Formos Med Assoc,* 108**,** 4-12.

SHIMABUKURO, M., OHNEDA, M., LEE, Y. & UNGER, R. H. 1997. Role of nitric oxide in obesity-induced beta cell disease. *J Clin Invest,* 100**,** 290-5.

SHIMOJI, Y., TAMURA, Y., NAKAMURA, Y., NANDA, K., NISHIDAI, S., NISHIKAWA, Y., ISHIHARA, N., UENAKAI, K. & OHIGASHI, H. 2002. Isolation and identification of DPPH radical scavenging compounds in Kurosu (Japanese unpolished rice vinegar). *Journal of Agricultural and Food Chemistry,* 50**,** 6501-6503.

SHIOTA, G. & TSUCHIYA, H. 2006. Pathophysiology of NASH: insulin resistance, free fatty acids and oxidative stress. *Journal of Clinical Biochemistry and Nutrition,* 38**,** 127-132.

SHOBA, G., JOY, D., JOSEPH, T., MAJEED, M., RAJENDRAN, R. & SRINIVAS, P. S. 1998. Influence of piperine on the pharmacokinetics of curcumin in animals and human volunteers. *Planta Medica,* 64**,** 353-6.

SILBERBERG, M., MORAND, C., MANACH, C., SCALBERT, A. & REMESY, C. 2005. Co-administration of quercetin and catechin in rats alters their absorption but not their metabolism. *Life Sci,* 77**,** 3156-67.

SIMIC, A., MANOJLOVIC, D., SEGAN, D. & TODOROVIC, M. 2007. Electrochemical behavior and antioxidant and prooxidant activity of natural phenolics. *Molecules (Basel, Switzerland),* 12**,** 2327-40.

SINGAL, A. K., JAMPANA, S. C. & WEINMAN, S. A. 2011. Antioxidants as therapeutic agents for liver disease. *Liver Int,* 31**,** 1432-48.

SINGH, K. K. 2006. *Oxidative stress, disease and cancer,* London; Hackensack, NJ, Imperial College Press ; Distributed by World Scientific Pub.

SINGH, S. V., SRIVASTAVA, S. K., CHOI, S., LEW, K. L., ANTOSIEWICZ, J., XIAO, D., ZENG, Y., WATKINS, S. C., JOHNSON, C. S. & TRUMP, D. L. 2005. Sulforaphane-induced cell death in human prostate cancer cells is initiated by reactive oxygen species. *Journal of Biological Chemistry,* 280**,** 19911-19924.

SINGHAL, A., JAIN, H., SINGHAL, V., ELIAS, E. J. & SHOWKAT, A. 2011. Colon-targeted quercetin delivery using natural polymer to enhance its bioavailability. *Pharmacognosy Res,* 3**,** 35.

SIROTA, R., GIBSON, D. & KOHEN, R. 2015. The role of the catecholic and the electrophilic moieties of caffeic acid in Nrf2/Keap1 pathway activation in ovarian carcinoma cell lines. *Redox Biol,* 4**,** 48-59.

SLATER, A. F., STEFAN, C., NOBEL, I., VAN DEN DOBBELSTEEN, D. J. & ORRENIUS, S. 1995. Signalling mechanisms and oxidative stress in apoptosis. *Toxicol Lett,* 82-83**,** 149-53.

SLATER, T. F., SAWYER, B. & STRAEULI, U. 1963. STUDIES ON SUCCINATE-TETRAZOLIUM REDUCTASE SYSTEMS. III. POINTS OF COUPLING OF FOUR DIFFERENT TETRAZOLIUM SALTS. *Biochim Biophys Acta,* 77**,** 383-93.

SMITH, E. B. & STAPLES, E. M. 1982. Plasma protein concentrations in interstitial fluid from human aortas. *Proc R Soc Lond B Biol Sci,* 217**,** 59-75.

SOLDEVILA, G., BUSCEMA, M., MARINI, V., SUTTON, R., JAMES, R. F., BLOOM, S. R., ROBERTSON, R. P., MIRAKIAN, R., PUJOL-BORRELL, R. & BOTTAZZO, G. F. 1991. Transfection with SV40 gene of human pancreatic endocrine cells. *J Autoimmun,* 4**,** 381-96.

SONG, M. Y., KIM, E. K., MOON, W. S., PARK, J. W., KIM, H. J., SO, H. S., PARK, R., KWON, K. B. & PARK, B. H. 2009. Sulforaphane protects against cytokine- and streptozotocin-induced beta-cell damage by suppressing the NF-kappaB pathway. *Toxicol Appl Pharmacol,* 235**,** 57-67.

SORIANO, F. X., LEVEILLE, F., PAPADIA, S., HIGGINS, L. G., VARLEY, J., BAXTER, P., HAYES, J. D. & HARDINGHAM, G. E. 2008. Induction of sulfiredoxin expression and reduction of peroxiredoxin hyperoxidation by the neuroprotective Nrf2 activator 3H-1,2-dithiole-3-thione. *J Neurochem,* 107**,** 533-43.

SPENCER, J. P., ABD-EL-MOHSEN, M. M. & RICE-EVANS, C. 2004. Cellular uptake and metabolism of flavonoids and their metabolites: implications for their bioactivity. *Arch Biochem Biophys,* 423**,** 148-61.

SPENCER, J. P., KUHNLE, G. G., WILLIAMS, R. J. & RICE-EVANS, C. 2003. Intracellular metabolism and bioactivity of quercetin and its in vivo metabolites. *The Biochemical journal,* 372**,** 173-81.

SPENCER, J. P. E. & CROZIER, A. 2012. *Flavonoids and related compounds: bioavailability and function*, CRC Press.

SRINIVASAN, M., RUKKUMANI, R., RAM SUDHEER, A. & MENON, V. P. 2005. Ferulic acid, a natural protector against carbon tetrachloride-induced toxicity. *Fundam Clin Pharmacol,* 19**,** 491-6.

SRIVASTAVA, R. K., TANG, S. N., ZHU, W., MEEKER, D. & SHANKAR, S. 2011. Sulforaphane synergizes with quercetin to inhibit self-renewal capacity of pancreatic cancer stem cells. *Front Biosci (Elite Ed),* 3**,** 515-28.

SRIVASTAVA, S. & CHAN, C. 2007. Hydrogen peroxide and hydroxyl radicals mediate palmitate-induced cytotoxicity to hepatoma cells: relation to mitochondrial permeability transition. *Free Radic Res,* 41**,** 38-49.

SRIVASTAVA, S. & CHAN, C. 2008. Application of metabolic flux analysis to identify the mechanisms of free fatty acid toxicity to human hepatoma cell line. *Biotechnol Bioeng,* 99**,** 399-410.

STEIN, L. L., DONG, M. H. & LOOMBA, R. 2009. Insulin sensitizers in nonalcoholic fatty liver disease and steatohepatitis: Current status. *Adv Ther,* 26**,** 893-907.

STEINER, D. J., KIM, A., MILLER, K. & HARA, M. 2010. Pancreatic islet plasticity: interspecies comparison of islet architecture and composition. *Islets,* 2**,** 135-145.

STEPHENS, N. G., PARSONS, A., SCHOFIELD, P. M., KELLY, F., CHEESEMAN, K. & MITCHINSON, M. J. 1996. Randomised controlled trial of vitamin E in patients with coronary disease: Cambridge Heart Antioxidant Study (CHAOS). *Lancet,* 347**,** 781-6.

STOEWSAND, G. 1995. Bioactive organosulfur phytochemicals in Brassica oleracea vegetables—a review. *Food and Chemical Toxicology,* 33**,** 537-543.

SUN, J., CHU, Y. F., WU, X. & LIU, R. H. 2002. Antioxidant and antiproliferative activities of common fruits. *J Agric Food Chem,* 50**,** 7449-54.

SURAPANENI, K. M. & JAINU, M. 2014. Pioglitazone, quercetin and hydroxy citric acid effect on hepatic biomarkers in Non Alcoholic Steatohepatitis. *Pharmacognosy Res,* 6**,** 153-62.

SYNG-AI, C., KUMARI, A. L. & KHAR, A. 2004. Effect of curcumin on normal and tumor cells: Role of glutathione and bcl-2. *Molecular Cancer Therapeutics,* 3**,** 1101-1108.

TAKATORI, A., ISHII, Y., ITAGAKI, S., KYUWA, S. & YOSHIKAWA, Y. 2004. Amelioration of the beta-cell dysfunction in diabetic APA hamsters by antioxidants and AGE inhibitor treatments. *Diabetes Metab Res Rev,* 20**,** 211-8.

TALALAY, P. 2000. Chemoprotection against cancer by induction of phase 2 enzymes. *BioFactors (Oxford, England),* 12**,** 1-4.

TALALAY, P., FAHEY, J. W., HOLTZCLAW, W. D., PRESTERA, T. & ZHANG, Y. 1995. Chemoprotection against cancer by phase 2 enzyme induction. *Toxicol Lett,* 82-83**,** 173-9.

TANAKA, Y., GLEASON, C. E., TRAN, P. O., HARMON, J. S. & ROBERTSON, R. P. 1999. Prevention of glucose toxicity in HIT-T15 cells and Zucker diabetic fatty rats by antioxidants. *Proc Natl Acad Sci U S A,* 96**,** 10857-62.

TANAKA, Y., TRAN, P. O., HARMON, J. & ROBERTSON, R. P. 2002. A role for glutathione peroxidase in protecting pancreatic beta cells against oxidative stress in a model of glucose toxicity. *Proc Natl Acad Sci U S A,* 99**,** 12363-8.

TANG, C., KOULAJIAN, K., SCHUIKI, I., ZHANG, L., DESAI, T., IVOVIC, A., WANG, P., ROBSON-DOUCETTE, C., WHEELER, M. & MINASSIAN, B. 2012. Glucose-induced beta cell dysfunction in vivo in rats: link between oxidative stress and endoplasmic reticulum stress. *Diabetologia,* 55**,** 1366-1379.

TANG, Y. Q., WANG, M. H., LE, X. Y., MENG, J. N., HUANG, L., YU, P., CHEN, J. & WU, P. 2011. Antioxidant and cardioprotective effects of Danshensu (3-(3, 4-dihydroxyphenyl)-2-hydroxy-propanoic acid from Salvia miltiorrhiza) on isoproterenol-induced myocardial hypertrophy in rats. *Phytomedicine,* 18**,** 1024-1030.

TANIGAWA, S., FUJII, M. & HOU, D.-X. 2007. Action of Nrf2 and Keap1 in ARE-mediated NQO1 expression by quercetin. *Free Radical Biology and Medicine,* 42**,** 1690-1703.

TAO, L., WANG, S., ZHAO, Y., SHENG, X., WANG, A., ZHENG, S. & LU, Y. 2014. Phenolcarboxylic acids from medicinal herbs exert anticancer effects through disruption of COX-2 activity. *Phytomedicine,* 21**,** 1473-82.

TERAO, J., PISKULA, M. & YAO, Q. 1994. Protective Effect of Epicatechin, Epicatechin Gallate, and Quercetin on Lipid Peroxidation in Phospholipid Bilayers. *Archives of Biochemistry and Biophysics,* 308**,** 278-284.

THIMMULAPPA, R. K., MAI, K. H., SRISUMA, S., KENSLER, T. W., YAMAMOTO, M. & BISWAL, S. 2002. Identification of Nrf2-regulated genes induced by the chemopreventive agent sulforaphane by oligonucleotide microarray. *Cancer Res,* 62**,** 5196-203.

THOUNAOJAM, M. C., JADEJA, R. N., DEVKAR, R. V. & RAMACHANDRAN, A. V. 2012. Non-alcoholic steatohepatitis: an overview including treatments with herbals as alternative therapeutics. *Journal of Applied Biomedicine,* 10**,** 119-136.

TIAN, Q., ROSSELOT, R. A. & SCHWARTZ, S. J. 2005. Quantitative determination of intact glucosinolates in broccoli, broccoli sprouts, Brussels sprouts, and cauliflower by high-performance liquid chromatography–electrospray ionization–tandem mass spectrometry. *Analytical Biochemistry,* 343**,** 93-99.

TØNNESEN, H. H., KARLSEN, J., MOSTAD, A., SAMUELSSON, B., ENZELL, C. R. & BERG, J.-E. 1982. Structural Studies of Curcuminoids. I. The Crystal Structure of Curcumin. *Acta Chem. Scand. Acta Chemica Scandinavica,* 36b**,** 475-479.

TOOTH, D. J., GOPALA KRISHNA, V. & LAYFIELD, R. 2012. An economical high-throughput protocol for multidimensional fractionation of proteins. *Int J Proteomics,* 2012**,** 735132.

USTA, M., WORTELBOER, H. M., VERVOORT, J., BOERSMA, M. G., RIETJENS, I. M., VAN BLADEREN, P. J. & CNUBBEN, N. H. 2007. Human glutathione S-transferase-mediated glutathione conjugation of curcumin and efflux of these conjugates in Caco-2 cells. *Chemical research in toxicology,* 20**,** 1895-902.

VAN DER WOUDE, H., BOERSMA, M. G., VERVOORT, J. & RIETJENS, I. M. 2004. Identification of 14 quercetin phase II mono- and mixed conjugates and their formation by rat and human phase II in vitro model systems. *Chemical research in toxicology,* 17**,** 1520-30.

VAN DEURSEN, D., JANSEN, H. & VERHOEVEN, A. J. 2008. Glucose increases hepatic lipase expression in HepG2 liver cells through upregulation of upstream stimulatory factors 1 and 2. *Diabetologia,* 51**,** 2078-87.

VAREED, S. K., KAKARALA, M., RUFFIN, M. T., CROWELL, J. A., NORMOLLE, D. P., DJURIC, Z. & BRENNER, D. E. 2008. Pharmacokinetics of curcumin conjugate metabolites in healthy human subjects. *Cancer epidemiology, biomarkers & prevention : a publication of the American Association for Cancer Research, cosponsored by the American Society of Preventive Oncology,* 17**,** 1411-7.

VARGAS, A. J. & BURD, R. 2010. Hormesis and synergy: pathways and mechanisms of quercetin in cancer prevention and management. *Nutrition reviews,* 68**,** 418-28.

VASU, S., MCCLENAGHAN, N. H., MCCLUSKEY, J. T. & FLATT, P. R. 2013. Effects of lipotoxicity on a novel insulin-secreting human pancreatic beta-cell line, 1.1B4. *Biol Chem,* 394**,** 909-18.

VESSAL, M., HEMMATI, M. & VASEI, M. 2003. Antidiabetic effects of quercetin in streptozocin-induced diabetic rats. *Comparative Biochemistry and Physiology Part C: Toxicology & Pharmacology,* 135**,** 357-364.

WALGREN, R. A., KARNAKY, K. J., JR., LINDENMAYER, G. E. & WALLE, T. 2000. Efflux of dietary flavonoid quercetin 4'-beta-glucoside across human intestinal Caco-2 cell monolayers by apical multidrug resistance-associated protein-2. *The Journal of pharmacology and experimental therapeutics,* 294**,** 830-6.

WALGREN, R. A., WALLE, U. K. & WALLE, T. 1998. Transport of Quercetin and Its Glucosides across Human Intestinal Epithelial Caco-2 Cells. *BCP</cja:jid> Biochemical Pharmacology,* 55**,** 1721-1727.

WALLE, T., BROWNING, A. M., STEED, L. L., REED, S. G. & WALLE, U. K. 2005. Flavonoid glucosides are hydrolyzed and thus activated in the oral cavity in humans. *The Journal of nutrition,* 135**,** 48-52.

WANG, H., LIN, W., SHEN, G. X., KHOR, T. O., NOMEIR, A. A. & KONG, A. N. 2011. Development and Validation of an LC-MS-MS Method for the Simultaneous Determination of Sulforaphane and its Metabolites in Rat Plasma and its Application in Pharmacokinetic Studies. *Journal of Chromatographic Science,* 49**,** 801-806.

WANG, M., RUAN, Y., CHEN, Q., LI, S., WANG, Q. & CAI, J. 2011. Curcumin induced HepG2 cell apoptosis-associated mitochondrial membrane potential and intracellular free Ca2+ concentration. *European Journal of Pharmacology,* 650**,** 41-47.

WANG, P., BOUWMAN, F. G. & MARIMAN, E. C. 2009. Generally detected proteins in comparative proteomics--a matter of cellular stress response? *Proteomics,* 9**,** 2955-66.

WANG, X. J., HAYES, J. D., HIGGINS, L. G., WOLF, C. R. & DINKOVA-KOSTOVA, A. T. 2010. Activation of the NRF2 signaling pathway by copper-mediated redox cycling of para- and ortho-hydroquinones. *Chem Biol,* 17**,** 75-85.

WANG, X. J., SUN, Z., VILLENEUVE, N. F., ZHANG, S., ZHAO, F., LI, Y., CHEN, W., YI, X., ZHENG, W., WONDRAK, G. T., WONG, P. K. & ZHANG, D. D. 2008. Nrf2 enhances resistance of cancer cells to chemotherapeutic drugs, the dark side of Nrf2. *Carcinogenesis,* 29**,** 1235-43.

WANG, Y.-J., PAN, M.-H., CHENG, A.-L., LIN, L.-I., HO, Y.-S., HSIEH, C.-Y. & LIN, J.-K. 1997. Stability of curcumin in buffer solutions and characterization of its degradation products. *PBA</cja:jid> Journal of Pharmaceutical and Biomedical Analysis,* 15**,** 1867-1876.

WANG, Z., ZHANG, Y., BANERJEE, S., LI, Y. & SARKAR, F. H. 2006. Notch-1 down-regulation by curcumin is associated with the inhibition of cell growth and the induction of apoptosis in pancreatic cancer cells. *Cancer,* 106**,** 2503-2513.

WARREN, C. A., PAULHILL, K. J., DAVIDSON, L. A., LUPTON, J. R., TADDEO, S. S., HONG, M. Y., CARROLL, R. J., CHAPKIN, R. S. & TURNER, N. D. 2009. Quercetin may suppress rat aberrant crypt foci formation by suppressing inflammatory mediators that influence proliferation and apoptosis. *The Journal of nutrition,* 139**,** 101-105.

WARSHAW, A. L. & FERNANDEZ-DEL CASTILLO, C. 1992. Pancreatic carcinoma. *N Engl J Med,* 326**,** 455-65.

WATSON, M. L., MACRAE, K., MARLEY, A. E. & HUNDAL, H. S. 2011. Chronic effects of palmitate overload on nutrient-induced insulin secretion and autocrine signalling in pancreatic MIN6 beta cells. *Plos One,* 6**,** e25975.

WEYER, C., BOGARDUS, C., MOTT, D. M. & PRATLEY, R. E. 1999. The natural history of insulin secretory dysfunction and insulin resistance in the pathogenesis of type 2 diabetes mellitus. *J Clin Invest,* 104**,** 787-794.

WILKENING, S., STAHL, F. & BADER, A. 2003. Comparison of primary human hepatocytes and hepatoma cell line Hepg2 with regard to their biotransformation properties. *Drug Metabolism and Disposition,* 31**,** 1035-1042.

WILKINS, R. C., KUTZNER, B. C., TRUONG, M., SANCHEZ-DARDON, J. & MCLEAN, J. R. 2002. Analysis of radiation-induced apoptosis in human lymphocytes: flow cytometry using Annexin V and propidium iodide versus the neutral comet assay. *Cytometry,* 48**,** 14-9.

WINCKLER, J. 1974. [Vital staining of lysosomes and other cell organelles of the rat with neutral red (author's transl)]. *Prog Histochem Cytochem,* 6**,** 1-91.

WOLF, G. 2005. The discovery of the antioxidant function of vitamin E: the contribution of Henry A. Mattill. *J Nutr,* 135**,** 363-6.

WOLLHEIM, C. B. & MAECHLER, P. 2002. Beta-cell mitochondria and insulin secretion: messenger role of nucleotides and metabolites. *Diabetes,* 51 Suppl 1**,** S37-42.

WONG, C. C., AKIYAMA, Y., ABE, T., LIPPIAT, J. D., ORFILA, C. & WILLIAMSON, G. 2012. Carrier-mediated transport of quercetin conjugates: involvement of organic anion transporters and organic anion transporting polypeptides. *Biochemical Pharmacology,* 84**,** 564-70.

WONG, C. C., MEINL, W., GLATT, H.-R., BARRON, D., STALMACH, A., STEILING, H., CROZIER, A. & WILLIAMSON, G. 2010. In vitro and in vivo conjugation of dietary hydroxycinnamic acids by UDP-glucuronosyltransferases and sulfotransferases in humans. *The Journal of Nutritional Biochemistry,* 21**,** 1060-1068.

WYLLIE, A. H. 1992. Apoptosis and the regulation of cell numbers in normal and neoplastic tissues: an overview. *Cancer Metastasis Rev,* 11**,** 95-103.

XAVIER, C. P., LIMA, C. F., FERNANDES-FERREIRA, M. & PEREIRA-WILSON, C. 2009. Salvia fruticosa, Salvia officinalis, and rosmarinic acid induce apoptosis and inhibit proliferation of human colorectal cell lines: the role in MAPK/ERK pathway. *Nutr Cancer,* 61**,** 564-71.

XING, H. C., LI, L. J., XU, K. J., SHEN, T., CHEN, Y. B., CHEN, Y., FU, S. Z., SHENG, J. F., CHEN, C. L., WANG, J. G., YAN, D., DAI, F. W. & SHA, X. Y. 2005. Effects of Salvia miltiorrhiza on intestinal microflora in rats with ischemia/reperfusion liver injury. . *Hepatobiliary Pancreat Dis Int,* 4**,** 274-280.

YAGISHITA, Y., FUKUTOMI, T., SUGAWARA, A., KAWAMURA, H., TAKAHASHI, T., PI, J., URUNO, A. & YAMAMOTO, M. 2014. Nrf2 protects pancreatic beta-cells from oxidative and nitrosative stress in diabetic model mice. *Diabetes,* 63**,** 605-18.

YAMAMOTO, N., MOON, J.-H., TSUSHIDA, T., NAGAO, A. & TERAO, J. 1999. Inhibitory Effect of Quercetin Metabolites and Their Related Derivatives on Copper Ion-Induced Lipid Peroxidation in Human Low-Density Lipoprotein. *YABBI</cja:jid> Archives of Biochemistry and Biophysics,* 372**,** 347-354.

YANG, K.-Y., LIN, L.-C., TSENG, T.-Y., WANG, S.-C. & TSAI, T.-H. 2007. Oral bioavailability of curcumin in rat and the herbal analysis from Curcuma longa by LC–MS/MS. *Journal of chromatography B,* 853**,** 183-189.

YANG, S.-Y., HONG, C.-O., LEE, G. P., KIM, C.-T. & LEE, K.-W. 2013. The hepatoprotection of caffeic acid and rosmarinic acid, major compounds of Perilla frutescens, against t-BHP-induced oxidative liver damage. *Food and Chemical Toxicology,* 55**,** 92-99.

YANG, Z., LIU, Y., LIAO, J., GONG, C., SUN, C., ZHOU, X., WEI, X., ZHANG, T., GAO, Q. & MA, D. 2015. Quercetin induces endoplasmic reticulum stress to enhance cDDP cytotoxicity in ovarian cancer: involvement of STAT3 signaling. *FEBS Journal,* 282**,** 1111-1125.

YEO, T. P., HRUBAN, R. H., LEACH, S. D., WILENTZ, R. E., SOHN, T. A., KERN, S. E., IACOBUZIO-DONAHUE, C. A., MAITRA, A., GOGGINS, M., CANTO, M. I., ABRAMS, R. A., LAHERU, D., JAFFEE, E. M., HIDALGO, M. & YEO, C. J. 2002. Pancreatic cancer. *Current Problems in Cancer,* 26**,** 176-275.

YOO, K. S., LEE, E. J. & PATIL, B. S. 2010. Quantification of quercetin glycosides in 6 onion cultivars and comparisons of hydrolysis-HPLC and spectrophotometric methods in measuring total quercetin concentrations. *Journal of food science,* 75**,** 160-5.

YOUL, E., BARDY, G., MAGOUS, R., CROS, G., SEJALON, F., VIRSOLVY, A., RICHARD, S., QUIGNARD, J., GROSS, R. & PETIT, P. 2010. Quercetin potentiates insulin secretion and protects INS-1 pancreatic β-cells against oxidative damage via the ERK1/2 pathway. *British Journal of Pharmacology,* 161**,** 799-814.

YOUN, J., LEE, K. H., WON, J., HUH, S. J., YUN, H. S., CHO, W. G. & PAIK, D. J. 2003. Beneficial effects of rosmarinic acid on suppression of collagen induced arthritis. *The Journal of rheumatology,* 30**,** 1203-1207.

YU, B. B., DAI, L. L., LI, X., LI, D. & JIANG, Z. H. 2009. [Effect of danshensu on activation of JNK pathway in hepatic stellate cells(HSCs) induced by IL-1 beta]. *Zhonghua gan zang bing za zhi = Zhonghua ganzangbing zazhi = Chinese journal of hepatology,* 17**,** 451-4.

YUAN, M., KONSTANTOPOULOS, N., LEE, J., HANSEN, L., LI, Z. W., KARIN, M. & SHOELSON, S. E. 2001. Reversal of obesity- and diet-induced insulin resistance with salicylates or targeted disruption of Ikkbeta. *Science,* 293**,** 1673-7.

YUSUF, S., DAGENAIS, G., POGUE, J., BOSCH, J. & SLEIGHT, P. 2000. Vitamin E supplementation and cardiovascular events in high-risk patients. The Heart Outcomes Prevention Evaluation Study Investigators. *N Engl J Med,* 342**,** 154-60.

ZALZMAN, M., ANKER-KITAI, L. & EFRAT, S. 2005. Differentiation of human liver-derived, insulin-producing cells toward the beta-cell phenotype. *Diabetes,* 54**,** 2568-75.

ZHANG, D. D., LO, S. C., CROSS, J. V., TEMPLETON, D. J. & HANNINK, M. 2004. Keap1 is a redox-regulated substrate adaptor protein for a Cul3-dependent ubiquitin ligase complex. *Mol Cell Biol,* 24**,** 10941-53.

ZHANG, D. D., LO, S. C., SUN, Z., HABIB, G. M., LIEBERMAN, M. W. & HANNINK, M. 2005. Ubiquitination of Keap1, a BTB-Kelch substrate adaptor protein for Cul3, targets Keap1 for degradation by a proteasome-independent pathway. *J Biol Chem,* 280**,** 30091-9.

ZHANG, H. Y., YANG, D. P. & TANG, G. Y. 2006. Multipotent antioxidants: from screening to design. *Drug Discov Today,* 11**,** 749-54.

ZHANG, L., WU, T., CHEN, J.-M., YANG, L.-L., SONG, H.-Y. & JI, G. 2012. Danshensu inhibits acetaldehyde-induced proliferation and activation of hepatic stellate cell-T6. *Zhong xi yi jie he xue bao = Journal of Chinese integrative medicine,* 10**,** 1155-61.

ZHANG, W. & LIU, H. T. 2002. MAPK signal pathways in the regulation of cell proliferation in mammalian cells. *Cell Res,* 12**,** 9-18.

ZHANG, Y. J., WU, L., ZHANG, Q. L., LI, J., YIN, F. X. & YUAN, Y. 2011. Pharmacokinetics of phenolic compounds of Danshen extract in rat blood and brain by microdialysis sampling. *Journal of Ethnopharmacology,* 136**,** 129-136.

ZHANG, Z. C., XU, M., SUN, S. F., QIAO, X., WANG, B. R., HAN, J. & GUO, D. A. 2008. Metabolic analysis of four phenolic acids in rat by liquid chromatography-tandem

mass spectrometry. *Journal of Chromatography B-Analytical Technologies in the Biomedical and Life Sciences,* 871**,** 7-14.

ZHAO, G. R., ZHANG, H. M., YE, T. X., XIANG, Z. J., YUAN, Y. J., GUO, Z. X. & ZHAO, L. B. 2008. Characterization of the radical scavenging and antioxidant activities of danshensu and salvianolic acid B. *Food and Chemical Toxicology,* 46**,** 73-81.

ZHAO, S. G., LI, Q., LIU, Z. X., WANG, J. J., WANG, X. X., QIN, M. & WEN, Q. S. 2011. Curcumin Attenuates Insulin Resistance in Hepatocytes by Inducing Nrf2 Nuclear Translocation. *Hepato-Gastroenterology,* 58**,** 2106-2111.

ZHAO, X., SUN, G., ZHANG, J., STRONG, R., DASH, P. K., KAN, Y. W., GROTTA, J. C. & ARONOWSKI, J. 2007. Transcription factor Nrf2 protects the brain from damage produced by intracerebral hemorrhage. *Stroke; a journal of cerebral circulation,* 38**,** 3280-6.

ZHAO, Z., EGASHIRA, Y. & SANADA, H. 2003. Ferulic acid sugar esters are recovered in rat plasma and urine mainly as the sulfoglucuronide of ferulic acid. *The Journal of nutrition,* 133**,** 1355-1361.

ZHAO, Z., EGASHIRA, Y. & SANADA, H. 2004. Ferulic acid is quickly absorbed from rat stomach as the free form and then conjugated mainly in liver. *J Nutr,* 134**,** 3083-8.

ZHAO, Z. & MOGHADASIAN, M. H. 2008. Chemistry, natural sources, dietary intake and pharmacokinetic properties of ferulic acid: A review. *Food Chemistry,* 109**,** 691-702.

ZHAO, Z., ZHAO, C., ZHANG, X. H., ZHENG, F., CAI, W., VLASSARA, H. & MA, Z. A. 2009. Advanced glycation end products inhibit glucose-stimulated insulin secretion through nitric oxide-dependent inhibition of cytochrome c oxidase and adenosine triphosphate synthesis. *Endocrinology,* 150**,** 2569-76.

ZHOU, L., CHOW, M. & ZOU, Z. 2006. Improved quality control method for Danshen products-consideration of both hydrophilic and lipophilic active components. *J Pharm Biomed Anal***,** 744-750.

ZHOU, Y., FANG, S. H., YE, Y. L., CHU, L. S., ZHANG, W. P., WANG, M. L. & WEI, E. Q. 2006. Caffeic acid ameliorates early and delayed brain injuries after focal cerebral ischemia in rats. *Acta Pharmacologica Sinica,* 27**,** 1103-1110.

ZHU, D. F., ZHAO, X. P. & CHENG, Y. Y. 2006. [Transport mechanism of danshensu across Caco-2 monolayer model]. *Zhongguo Zhong yao za zhi = Zhongguo zhongyao zazhi = China journal of Chinese materia medica,* 31**,** 1517-21.

ZOU, Y., HU, M., LEE, J., NAMBIAR, S. M., GARCIA, V., BAO, Q., CHAN, J. Y. & DAI, G. 2015. Nrf2 is essential for timely M phase entry of replicating hepatocytes during liver regeneration. *Am J Physiol Gastrointest Liver Physiol,* 308**,** G262-8.